Regulation of P-glycoprotein at the Blood-Brain Barrier

Dissertation

submitted to the

Combined Faculties for the Natural Sciences and for Mathematics

of the Ruperto-Carola University of Heidelberg, Germany

for the degree of

Doctor of Natural Sciences

presented by

Anika Maria Sophie Hartz, Pharmacist

born in Karlsruhe

2005

Regulation of P-glycoprotein at the Blood-Brain Barrier

Dissertation

submitted to the

Combined Faculties for the Natural Sciences and for Mathematics

of the Ruperto-Carola University of Heidelberg, Germany

for the degree of

Doctor of Natural Sciences

presented by

Anika Maria Sophie Hartz, Pharmacist

born in Karlsruhe

Oral examination: 24. June 2005

Regulation of P-glycoprotein at the Blood-Brain Barrier

Referees: **Prof. Dr. Gert Fricker**
Dr. David S. Miller

Dedicated to my family and Björn

Acknowledgements

I cordially thank my thesis supervisor, **Prof. Dr. Gert Fricker**, for the interesting research project that I thoroughly enjoyed working on. Thank you so much for this once in a lifetime opportunity to conduct my thesis work at NIEHS. It was an inspiring and encouraging time of my life. This experience along with the possibility to work in an excellent research environment will have a great impact on my future scientific career.

My profound gratitude also goes to **Dr. David S. Miller** for the opportunity to work in his laboratory at NIEHS. I am also very thankful for the research stay at MDIBL in Maine and the numerous possibilities to attend international scientific meetings to present my work. David, thank you so much for supporting me over the course of my thesis, for all your suggestions, guidance, encouragement and generosity. I greatly appreciate your mentoring and all the time you spent advising me. Thank you for sharing your knowledge and expertise as well as extraordinary scientific ideas with me.
I greatly enjoy working with you!

My gratitude and thanks to the members of my defense committee **Prof. Dr. Jürgen Reichling** and **Prof. Dr. Ulrich Hilgenfeldt**.

I would like to thank **Dr. John Pritchard** for his warm “Welcome” to North Carolina, his great support during the time of my thesis and his interest in my research.

My sincere gratitude and appreciation goes to **Jo Anne Johnson** for her expertise and skillful work throughout our collaboration.

A huge “thank you” goes to **Destiny Sykes** for her daily assistance and for providing a cordial atmosphere in the lab. Dusty, thank you so much for sincerely caring for me and giving me support all the time.

Thanks to all current and former colleagues:
Dr. Amy Aslamkhan, **Dr. Scott Barros**, **Dr. Sinya Benyajati**, **Dr. Kelly Bleasby**, **Dr. David Bourdet**, **Dr. Daniel Bow**, **Dr. Chris Breen**, **Dr. Lauretta Chan**, **Dr. Shannon Dallas**, **Dr. Neetu Dembla Rajpal**, **Laura Hall**, **Dr. Simon Lowes**, **Dr. Anusorn Lungkaphin**, **Nicki McClelland**, **Dr. Jennifer Perry**, **Dr. Chutima Srimaroeng**, **Dr. Deborah Thompson**, **Ramsey Walden**, **Kristin Wilson** and **Dr. Xiao-Ping Yang**. I also want to acknowledge **Jeff Reece** for providing help with the confocal microscope and **Mark Rafferty** for computer support. Thanks to **Barbara Morse** and **Leona Maghan** for their kind assistance with general and special needs.

Thanks to the **University of Heidelberg** for the scholarship *“Stipendium nach dem Landesgraduiertenförderungsgesetz (LGFG)”* from October 2002 until March 2005.

Special thanks go to my parents **Ingrid and Dieter Hartz** for providing the personal foundation and bedrock on which my personal life and career is built. Foremost, I am grateful for your patience, understanding and support during all this time.

Last, but by no means least, I thank **Dr. Björn Bauer** for launching with me on this journey of a lifetime. I benefit every day from taking the road “less traveled by”.

Abstract

Anika Maria Sophie Hartz, Pharmacist, Oral Examination: 24. June 2005

Regulation of P-glycoprotein at the Blood-Brain Barrier

Supervisor: Prof. Dr. Gert Fricker
Co-Supervisor: Dr. David S. Miller

Over 1 billion people worldwide suffer from some type of central nervous system (CNS) disorder (WHO, *The World Health Report*, 2001). This includes depression, epilepsy, multiple sclerosis, brain tumors, Alzheimer's and Parkinson's disease, as well as infections of the brain such as meningitis and HIV encephalitis. Consequently, there is a strong demand for effective treatments. However, pharmacotherapy of CNS disorders is greatly impaired by poor blood-to-brain transport of a large number of therapeutic drugs. The structure responsible for the low CNS penetration of drugs is the blood-brain barrier. An important element of barrier function is the ATP-driven efflux transporter, P-glycoprotein (P-gp) that denies CNS entry to a myriad of therapeutics. Thus, a better understanding of the mechanisms regulating P-gp expression and transport function might provide new strategies to improve drug delivery to the brain and increase drug levels in the CNS. Therefore, the objective of this thesis was to study regulation of P-glycoprotein at the blood-brain barrier.

P-glycoprotein transport function was assessed by measuring accumulation of the fluorescent, P-gp-specific substrate, NBD-cyclosporine A (NBD-CSA), in the lumens of isolated rat brain capillaries using confocal microscopy and quantitative image analysis. Exposing capillaries to the hormone endothelin-1 (ET-1) rapidly and reversibly reduced luminal NBD-CSA accumulation. Importantly, ET-1 did not affect tight junctions. Sarafotoxin, an ET_B receptor agonist, also reduced P-gp-mediated transport; the effects of ET-1 and sarafotoxin were blocked by an ET_B receptor antagonist, but not by an ET_A receptor antagonist. Immunostaining localized the ET_B receptor to the luminal and abluminal membranes of brain capillaries. NBD-CSA transport was also reduced by the NO donor, sodium nitroprusside (SNP), and by the protein kinase C (PKC) activator, PMA. Inhibition of NO synthase (NOS) or PKC blocked the effect of ET-1; PKC inhibition blocked the effects of SNP and PMA. Thus, P-glycoprotein function at the blood-brain barrier is regulated in the short-term by ET-1 acting through an ET_B receptor, NOS, NO and PKC (Hartz et al., 2004).

Transcriptional regulation of P-glycoprotein by the ligand-activated transcription factor, pregnane X receptor (PXR), was also demonstrated. PXR was shown for the first time to be expressed in isolated rat brain capillaries by RT-PCR, Western blot analysis and immunostaining. Six-hour exposure of isolated capillaries to the PXR ligands, PCN or dexamethasone, significantly increased expression of P-gp in the plasma membrane. Consistent with this, P-gp immunostaining demonstrated significantly increased immunoreactivity at the luminal membrane of capillaries. Increased P-gp-mediated NBD-CSA transport into capillary lumens was also detected. No such increases in P-gp expression were found when capillaries were exposed to ligands that activate human PXR (hyperforin, paclitaxel), but do not activate rodent PXR. Importantly, an increase in P-glycoprotein expression and transport function was also found in capillaries isolated from rats injected with PCN and dexamethasone (Bauer et al., 2004).

Zusammenfassung

Anika Maria Sophie Hartz, Apothekerin, Tag der mündlichen Prüfung: 24. Juni 2005

Regulation von P-glycoprotein in der Blut-Hirn-Schranke

Referent: Prof. Dr. Gert Fricker
Koreferent: Dr. David S. Miller

Mehr als 1 Milliarde Menschen weltweit leidet an Erkrankungen des Zentralnervensystems (ZNS) (WHO, *The World Health Report*, 2001). Hierzu zählen Depressionen, Epilepsie, Multiple Sklerose, Gehirntumore, Alzheimer-Demenz, Parkinson-Syndrom, sowie Infektionen des Gehirns (Hirnhautentzündung, HIV Enzephalopathie). Die medikamentöse Therapie von ZNS-Erkrankungen ist wegen der schlechten Hirngängigkeit vieler Arzneistoffe jedoch stark eingeschränkt. Verantwortlich für dieses Problem ist das Endothel der Kapillaren im Gehirn, die sogenannte Blut-Hirn-Schranke. Einen wesentlichen Anteil an der Schrankenfunktion hat der Efflux-Transporter P-glycoprotein (P-gp), der einerseits das Gehirn vor Toxinen schützt, andererseits aber auch zahlreiche Arzneistoffe daran hindert, in das ZNS zu gelangen. Ein Forschungsansatz um die Hirngängigkeit von Pharmaka zu erhöhen und somit die Therapie von ZNS-Erkrankungen zu verbesseren besteht darin, die Regulation von P-glycoprotein aufzuklären. Daher steht im Mittelpunkt dieser Arbeit die Regulation der P-glycoprotein Expression und Transportfunktion in der Blut-Hirn-Schranke.
Zunächst wurde die Kurzzeitregulation der P-glycoprotein Transportfunktion untersucht. Hierzu wurden isolierte Gehirnkapillaren der Ratte mit dem fluoreszierenden P-gp-Substrat NBD-Cyclosporin A (NBD-CSA) inkubiert. Die Anreicherung der NBD-CSA Fluoreszenz im Kapillarlumen wurde mittels konfokaler Lasermikroskopie und quantitativer Bildanalyse ermittelt. Inkubation der Kapillaren mit dem Hormon Endothelin-1 (ET-1) verringerte die luminale NBD-CSA-Fluoreszenz innerhalb von Minuten; dieser Effekt war reversibel wenn ET-1 entfernt wurde. Die Abnahme der luminalen NBD-CSA Fluoreszenz wurde ausschließlich durch einen Effekt auf P-gp hervorgerufen, da ET-1 keinen Einfluss auf die Tight Junctions hatte. Neben ET-1 verringerte auch Sarafotoxin, ein ET_B-Rezeptor-Agonist, den P-gp-vermittelten NBD-CSA-Transport. Sowohl der Effekt von ET-1 als auch der von Sarafotoxin wurden durch einen ET_B-Rezeptor-Antagonisten aufgehoben, nicht aber durch einen ET_A-Rezeptor-Antagonisten. Die Expression des ET_B-Rezeptors wurde durch Immunfärbung in der luminalen und abluminalen Kapillarmembran nachgewiesen. Der NBD-CSA Transport wurde auch durch Natriumnitroprussid (NNP), einem NO-Donor, sowie durch PMA, einem Aktivator der Proteinkinase C (PKC), verringert. Durch Inhibition der NO Synthase oder der PKC wurde der Effekt von ET-1 vollständig aufgehoben. Inhibition der PKC hemmte die Effekte von NNP und PMA. Diese Ergebnisse zeigen, dass die P-glycoprotein Transportfunktion in der Blut-Hirn-Schranke durch ET-1 reguliert wird. Die durch ET-1 vermittelte Kurzzeitregulation von P-gp verläuft über den ET_B-Rezeptor, NOS, NO und PKC (Hartz et al., 2004).

Im zweiten Teil der Arbeit wurde die transkriptionelle Regulation von P-glycoprotein durch den Nuklearrezeptor PXR (Pregnane X Rezeptor) untersucht. Zum ersten Mal konnte mit Hilfe von RT-PCR, Western Blot und Immunfärbung gezeigt werden, dass PXR in isolierten Gehirnkapillaren von Ratten exprimiert ist. Inkubation isolierter Kapillaren mit den PXR Liganden PCN oder Dexamethason über einen Zeitraum von 6 Stunden erhöhte die Expression von P-gp in der luminalen Kapillarmembran signifikant. Dies wurde über quantitative Immunfärbung und Western Blots gezeigt; auch der NBD-CSA-Transport durch P-gp war erhöht. Wurden die Kapillaren mit Liganden (Hyperforin, Paclitaxel) inkubiert, die nur den humanen PXR aktivieren nicht aber den von Ratten, so war P-gp nicht verstärkt exprimiert. Auch *in vivo* Versuche mit Ratten, denen PCN und Dexamethason injiziert wurde, ergaben, dass die P-gp Expression und Transportfunktion in Gehirnkapillaren stark erhöht war. P-gp war ausserdem auch in Leber und Niere induziert (Bauer et al., 2004).

This thesis was financially supported by a scholarship from the University of Heidelberg *("Stipendium nach dem Landesgraduiertenförderungsgesetz (LGFG)")*.

REFEREED PUBLICATIONS

Hartz, A.M.S.; Bauer, B.; Fricker, G. and Miller, D.S.
"Rapid regulation of P-glycoprotein at the blood-brain barrier by endothelin-1"
Molecular Pharmacology **66**(3):387-394 (2004)

Bauer, B.; **Hartz, A.M.S.**; Fricker, G. and Miller, D.S.
"Pregnane X receptor up-regulation of P-glycoprotein expression and transport function at the blood-brain barrier"
Molecular Pharmacology **66**(3):413-419 (2004)
This article was among the top ten articles viewed by the readership of Molecular Pharmacology during the month of September 2004

REVIEWS

Hartz, A.M.S.; Bauer, B.; Baehr, C.H.; Miller, D.S. and Fricker, G.
"Drug delivery across the blood-brain barrier"
Current Topics in Pharmacology **1**(3): (2005), (in press)

Bauer, B.; **Hartz, A.M.S.**; Fricker, G. and Miller, D.S.
"Modulation of P-glycoprotein transport function at the blood-brain barrier"
Experimental Biology and Medicine **230**(2):118-27 (2005)

PUBLISHED ABSTRACTS

Hartz, A.M.S.; Bauer, B.; Fricker, G. and Miller, D.S.
"Inflammatory mediators alter P-glycoprotein function and expression at the blood-brain barrier"
Naunyn-Schmiedeberg's Archives of Pharmacology, **371**, Suppl. 1 (2005)

Bauer, B.; **Hartz, A.M.S.**; Fricker, G. and Miller, D.S.
"Nuclear receptors regulate transport and metabolism at the blood-brain barrier"
Naunyn-Schmiedeberg's Archives of Pharmacology, **371**, Suppl. 1 (2005)

Hartz, A.M.S.; Bauer, B.; Fricker, G. and Miller, D.S**.**
"Mediators of inflammation alter P-glycoprotein function at the blood-brain barrier"
The AAPS Journal **6**(Suppl. 1):M1083 (2004)

Bauer, B.; **Hartz, A.M.S.**; Fricker, G. and Miller, D.S.
"Ligands of the pregnane X receptor (PXR) upregulate expression of the multidrug resistance associated protein 2 (Mrp2) at the blood-brain barrier"
The AAPS Journal **6**(Suppl. 1):M1081 (2004)

Bauer, B.; **Hartz, A.M.S.**; Fricker, G. and Miller, D.S.
"Pregnane X receptor (PXR) upregulates P-glycoprotein and Mrp2 in blood-brain barrier, liver and kidney in vivo"
Drug Metabolism Reviews **36**(Suppl. 1):303 (2004**)**

Bauer, B.; **Hartz, A.M.S.**; Fricker, G. and Miller, D.S.
"Ligands of the nuclear xenobiotic receptor, PXR, upregulate P-glycoprotein at the blood-brain barrier"
FASEB Journal **18**(4):A676-A676, Suppl. S (2004)

Hartz, A.M.S.; Bauer, B.; Fricker, G. and Miller, D.S.
"Rapid regulation of P-glycoprotein at the blood-brain barrier: the role of endothelin-1"
FASEB Journal **18**(4):A676-A677, Suppl. S (2004)

Hartz, A.M.S.; Bauer, B.; Miller, D.S. and Fricker, G.
"Short-term regulation of P-glycoprotein at the blood-brain barrier: the role of endothelin-1"
Naunyn-Schmiedeberg's Archives of Pharmacology, **369**(2), Suppl. 1 (2004)

Hartz, A.; Bauer, B.; Fricker, G. and Miller, D.S.
"Long-term effects of zinc on Mrp2 function in killifish (fundulus heteroclitus) brain capillaries"
The Bulletin **42**:124 (2003)

INVITED LECTURES

"Signaling by inflammatory mediators rapidly downregulates P-glycoprotein transport function at the blood-brain barrier" (May 03, 2005)
7th Blood-Brain Barrier Expert Meeting, Bad Herrenalb, Germany

"Inflammatory mediators alter P-glycoprotein function and expression at the blood-brain barrier" (March 16, 2005)
46th Annual Meeting of the German Society for Pharmacology and Toxicology (DGPT), Mainz, Germany

"Short-term regulation of P-glycoprotein at the blood-brain barrier" (May 18, 2004)
6th Blood-Brain Barrier Expert Meeting, Bad Herrenalb, Germany

"Short-term regulation of P-glycoprotein at the blood-brain barrier: role of endothelin-1" (March 10, 2004)
45th Annual Meeting of the German Society for Pharmacology and Toxicology (DGPT), Mainz, Germany

HONORS & AWARDS

NIH Fellows Award for Research Excellence, FARE2005, for scientific merit, originality, experimental setup, overall quality and presentation of the submitted abstract:
"Rapid and reversible modulation of P-glycoprotein at the blood-brain barrier by endothelin-1"

1st Poster Prize for Poster:
"Rapid regulation of P-glycoprotein at the blood-brain barrier: role of endothelin-1"
Hartz, A.M.S.; Bauer, B.; Fricker, G. and Miller, D.S.
Poster session "Crossing the Barriers: Mechanisms of Transport"
Gordon Research Conference "Barriers of the CNS", Tilton, NH, USA (June 30, 2004)

Table of Contents

Abbreviations

Å	Ångström (10^{-10} m)
ABC	ATP-Binding Cassette
ABD	ATP Binding Domain
AMP	Adenosine Mono Phosphate
aPKC	atypical Isoform of Protein Kinase C
BCRP	Breast Cancer Resistance Protein
BIM	Bisindolylmaleimide I
BSEP	Bile Salt Export Pump
CNS	Central Nervous System
CNT	Concentrative Nucleoside Transporter
Da	Dalton
DBD	DNA Binding Domain
ENT	Equilibrative Nucleoside Transporter
ET-1	Endothelin-1
ET_A receptor	Endothelin A Receptor
ET_B receptor	Endothelin B Receptor
GLUT	Glucose Transport Facilitator
JAM	Junctional Adhesion Molecule
LBD	Ligand Binding Domain
L-NMMA	N^G-Monomethyl-L-Arginine
MAGI	Membrane-Associated Guanylate Kinase Inverted Protein
MDR1	Multidrug Resistance Gene 1
MRP	Multidrug Resistance-Associated Protein
NBD-CSA	[N-ε(4-nitrobenzofurazan-7-yl)-D-Lys^8]-cyclosporine A
NOS	Nitric Oxide Synthase
OAT	Organic Anion Transporter
OATP	Organic Anion Transporting Polypeptide
OCT	Organic Cation Transporter
PCN	5-Pregnen-3β-ol-20-one-16α-carbonitrile
PCR	Polymerase Chain Reaction
P-gp	P-glycoprotein
PKC	Protein Kinase C
PMA	Phorbol-12-Myristate-13-Acetate
PXR	Pregnane X Receptor
RT	Reverse Transcription
RXR	Retinoid X Receptor
SEM	Standard Error of the Mean
SNP	Sodium Nitroprusside
TAP	Transporter Associated with Antigen Processing
TEM	Transmission Electron Microscopy
TMD	Transmembrane Domain
XRE	Xenobiotic Response Element
ZO	Zonula Occludens

1 Introduction

Over 1 billion people worldwide suffer from some type of central nervous system (CNS) disorder, e.g. depression, schizophrenia, stroke, epilepsy, multiple sclerosis, bacterial and viral infections (e.g. meningitis, HIV encephalitis), brain tumors, Alzheimer's disease and Parkinson's syndrome (Kermani and McGuire, 2002; WHO, 2001). This is more than twice as many people as those with diseases of the cardiovascular system. Nevertheless, the world wide market for CNS drugs is only half the size – around US$ 33 billion vs. US$ 70 billion (Pardridge, 2002). Since there are so many sufferers, there is also a strong demand for effective treatments. However, pharmacotherapy of CNS disorders is greatly impaired by the blood-brain barrier. The molecular basis of the selective, functionally active barrier is a group of ATP-driven efflux transporters; the most prominent of which is P-glycoprotein (P-gp). Acting as a "first line of defense", P-glycoprotein limits xenobiotics including a large number of drugs from penetrating into the brain. One potentially useful strategy to improve drug delivery to the brain and thus increase drug levels in the CNS is to manipulate P-gp protein expression and transport function. Therefore, a better understanding of the mechanisms that regulate P-glycoprotein at the blood-brain barrier holds the promise of improving drug therapy of CNS disorders.

The introduction following is in three parts:

1.1 The Blood-Brain Barrier
The first part gives a brief historical background and summarizes current knowledge on blood-brain barrier research.

1.2. P-glycoprotein at the Blood-Brain Barrier
The second part is focused on the efflux transporter P-glycoprotein, its structure, expression, physiological function and its importance for the blood-brain barrier.

1.3. Regulation of P-glycoprotein
The third part summarizes current knowledge on functional and transcriptional regulation of P-glycoprotein, with a focus on the blood-brain barrier.

1.1 The Blood-Brain Barrier

1.1.1 The Blood-Brain Barrier – Historical Background

Today's understanding of the blood-brain barrier is the result of 120 years of intensive research (Figure 1.1). The first experiments go back to Paul Ehrlich, who in 1885 observed that water soluble dyes injected into the peripheral circulation did not stain the brain (Ehrlich, 1885). Ehrlich interpreted these findings as a lack of dye affinity of the nervous system and did not believe that the brain capillaries could selectively exclude the dyes. However, experiments by Ehrlich's student, Edwin E. Goldmann, revealed that the same dyes injected into the subarachnoid space stained the brain, but not peripheral tissues (Goldmann, 1909; Goldmann, 1913). The concept of a vascular blood-brain barrier was born and it was Lewandowsky, who coined the term blood-brain barrier (***"Bluthirnschranke"***, Figure 1.1) (Lewandowsky, 1900).

Several years later, in 1923, Spatz hypothesized that the brain capillary endothelium had to be the structure responsible for barrier function; this started a discussion that would last for decades (Spatz, 1933). In 1946, August Krogh questioned how nutrients could reach the brain if the blood-brain barrier was impermeable. He therefore suggested a dynamic barrier involving active transport (Krogh, 1946). It took over 20 more years until Reese and Karnovsky (Reese and Karnovsky, 1967) and Brightman and Reese (Brightman and Reese, 1969; Reese and Karnovsky, 1967) using electron microscopy localized the barrier to the brain capillary endothelial cells and found tight junctions to be the responsible anatomical structure for barrier function (Figure 1.1). In 1969, Saikotos et al. reported the isolation of brain capillaries (Siakotos, 1969). Betz et al. isolated brain capillary endothelial cells and successfully established an *in vitro* blood-brain barrier model system (Betz et al., 1980). Since then, various *in vivo, ex vivo* and *in vitro* blood-brain barrier models have been used in basic research and industrial drug screening, mainly with the goal of improved drug delivery to the brain (Abbott et al., 1992; Audus et al., 1990; Goldstein et al., 1984; Miller et al., 2000; Pardridge et al., 1985; Pardridge et al., 1990b). More recently, understanding underlying molecular mechanisms of blood-brain barrier development, function and regulation have been the focus of an increasing number of research efforts (Grant et al., 1998; Risau and Wolburg, 1990; Staddon et al., 1995). However, even today, well into the genomics and proteomics eras, overcoming the blood-brain barrier to treat disorders of the central nervous system is still a challenge.

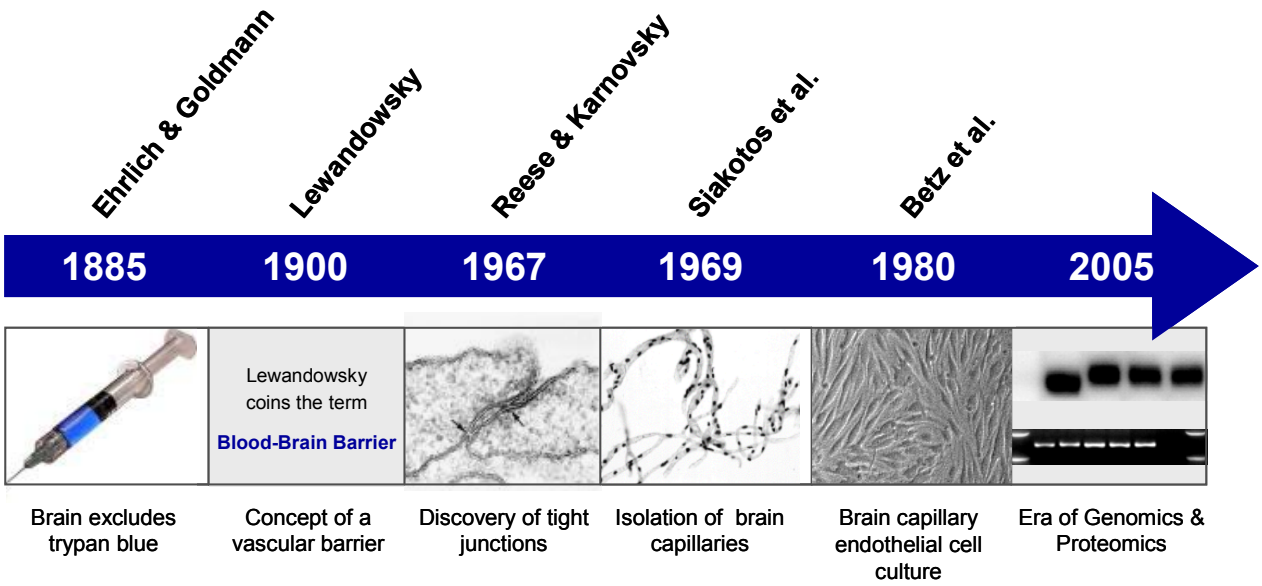

Figure 1.1
Time-line of blood-brain barrier research

1.1.2 The Blood-Brain Barrier – Physiological Function

The blood-brain barrier is the brain capillary endothelium between the blood and the brain. Its major functions are protection of CNS and maintenance of CNS homeostasis. The blood-brain barrier prevents entry to the brain of endogenous and exogenous potentially neurotoxic compounds including a large number of CNS drugs (Banks, 1999). However, rather than being a simple physical and mechanical obstacle, the blood-brain barrier is a highly active, dynamic and selective interface. As such, it regulates the exchange of compounds between blood and brain (Begley and Brightman, 2003). For example, the barrier is responsible for supplying the brain with glucose, amino acids and other nutrients, and at the same time for the disposal of metabolic wastes from the CNS. Thus, one essential physiological function of the blood-brain barrier is to control cerebral homoeostasis and to maintain a constant osmotic pressure for proper CNS function (Drewes, 1999). All these characteristics combined make the blood-brain barrier both an extremely complex organ, and a fascinating subject for research.

1.1.3 The Blood-Brain Barrier – A Microvascular Network

Brain capillaries (cerebral microvessels) are the structural basis of the blood-brain barrier. With a diameter as small as 3-7 µm, brain capillaries are the smallest vessels of the vascular system (Figure 1.2C) (Rodriguez-Baeza et al., 2003). The human blood-brain barrier is comprised of about 100 billion capillaries forming a highly branched microvascular network (Figure 1.2A, (Zlokovic and Apuzzo, 1998)). Because of the high capillary density in the brain, single capillaries are only about 40 µm apart from each other, a distance short enough for small molecules to diffuse within 1 second (Figure 1.2B, (Rodriguez-Baeza et al., 2003)). In addition, this ensures that every neuron is perfused by its own capillary to guarantee efficient nutrient supply. Despite the huge number of brain capillaries, they occupy only about 0.1% of the brain volume, or 1 ml in an adult human brain of 1200-1400 g (Pardridge, 2003b). The total length of the capillary network in an adult human brain is 600-650 km (370-400 mls) with a surface area of about 20 m^2 (215 ft^2), which makes the blood-brain barrier the third largest drug exchange surface area after intestine and lung (Pardridge, 2003a).

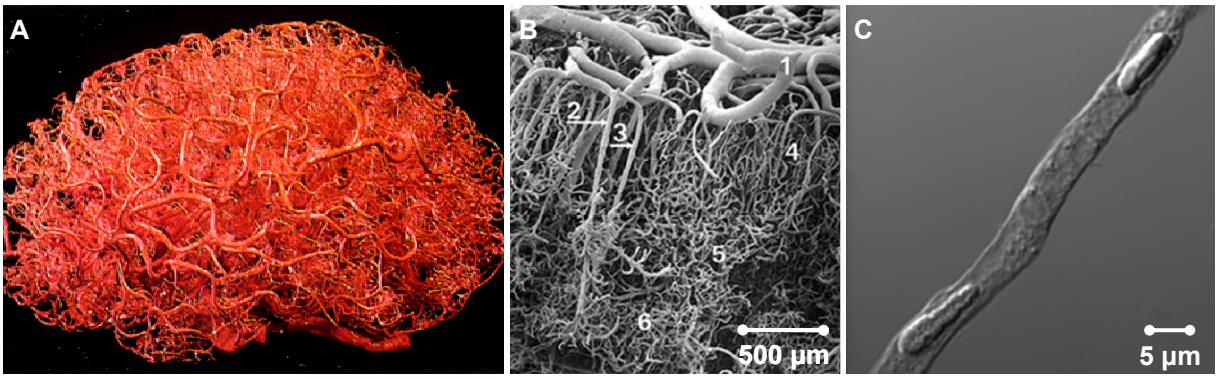

Figure 1.2
The blood-brain barrier – A microvascular network

A: Latex mold of the microvascular network of an adult human brain, from (Zlokovic and Apuzzo, 1998)
B: Scanning electron micrograph showing human cerebral cortex:
(1) pial vessels, (2) long and (3) middle cortical arteries, (4) superficial, (5) middle and (6) deep capillary zone, from (Rodriguez-Baeza et al., 2003)
C: Differential interference contrast image of an isolated rat brain capillary (Hartz et al., unpublished data)

1.1.4 The Blood-Brain Barrier – Morphology of Brain Capillaries

The cerebral microvessels of the blood-brain barrier are constituted by endothelial cells, the smallest unit of brain capillaries. Brain capillary endothelial cells are polarized cells, with an apical membrane facing the blood (luminal membrane) and a basolateral membrane facing the brain tissue (abluminal membrane) (Betz et al., 1980). Morphologically, brain capillary endothelial cells are long and spindle-shaped. However, they are very flat and thin, too, with only about 300 nm of cytoplasmic space in between the luminal and abluminal membranes (Pardridge, 2003b). Brain capillaries are surrounded by a basement membrane, which is complex in structure, composed of collagens and proteins, and that provides external support for the endothelial cells (Goldstein and Betz, 1983). At the basement membrane, pericytes, astrocytes and neurons are in contact with the endothelial cell (Figure 1.3). Today, this four-cell structure termed “Neurovascular Unit” is thought to be responsible for the regulation of blood flow and barrier function (Begley, 2004b). One important characteristic of the functional barrier are the so-called tight junctions. They seal the inter-endothelial space and create a tight, non-fenestrated capillary endothelium that restricts free diffusional exchange of solutes (Nag, 2003). In addition, cerebral endothelial cells show low pinocytotic activity and have no intercellular clefts. However, capillary endothelial cells contain a large number of mitochondria to meet the energy demand for active processes like metabolism and ATP-driven efflux transport (Goldstein and Betz, 1983).

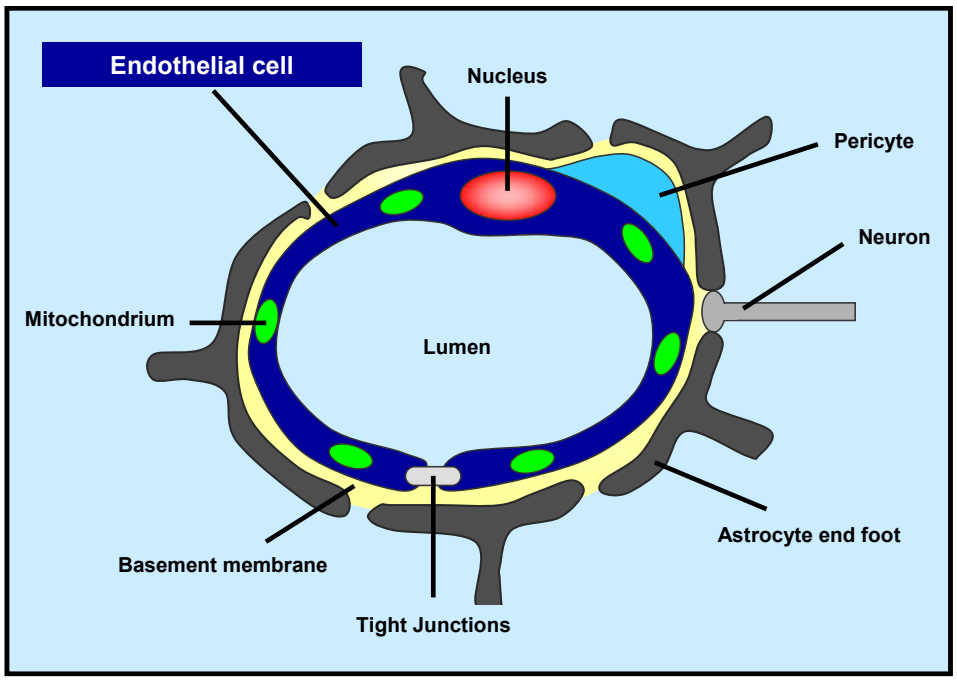

Figure 1.3
Morphology of brain capillaries

Brain endothelial cells are surrounded by a basement membrane. Astrocytic end feet, pericytes and neurons share this basement membrane. The interendothelial space is sealed by tight junctions.

1.1.5 The Blood-Brain Barrier – Tight Junctions

It wasn't until the studies of Reese and Karnovsky in 1967 (Reese and Karnovsky, 1967) and Brightman and Reese in 1969 (Brightman and Reese, 1969; Reese and Karnovsky, 1967) that tight junctions were identified as a crucial element of blood-brain barrier function. Tight junctions are cell-cell contacts between adjacent cerebral endothelial cells. They seal neighboring cells, thereby prevent paracellular diffusion and only allow restricted passage of water, ions and molecules smaller 0.2 nm. On a molecular level, tight junctions are highly complex and specialized contact zones linked to the cytoskeleton (Figure 1.4) (Matter and Balda, 2003b). In 1984, Nagy et al. demonstrated that brain capillary endothelial cells possess the most intricate and extended tight junctional complex in the cardiovascular system (Nagy et al., 1984).
Tight junctions are composed of transmembrane proteins like occludin, claudins and **j**unctional **a**dhesion **m**olecules (JAMs) and a so-called cytoplasmic "plaque" of submembranous adaptor and regulatory proteins (Vorbrodt and Dobrogowska, 2003; Vorbrodt and Dobrogowska, 2004). The adaptor proteins include **z**onula **o**ccludens (ZO) proteins, cingulin and **m**embrane-**a**ssociated **g**uanylate kinase **i**nverted (MAGI) proteins. They create a link between the junctional transmembrane proteins and actin filaments of the cytoskeleton (Matter and Balda, 2003b). The regulatory proteins include G proteins, **a**typical isoforms of **p**rotein **k**inase **C** (aPKC), and symplektin, all of which are involved in signaling to and from tight junctions (Matter and Balda, 2003b; Wolburg and Lippoldt, 2002). On the one hand, the complex junctional composition and structure guarantees a tight barrier. But on the other hand it also allows rapid modulation of barrier properties while retaining structural integrity and thus, protection of the CNS (Kniesel and Wolburg, 2000). However, under pathological conditions tight junctions can be disrupted leading to severe brain damage and impaired neuronal function (Huber et al., 2001).

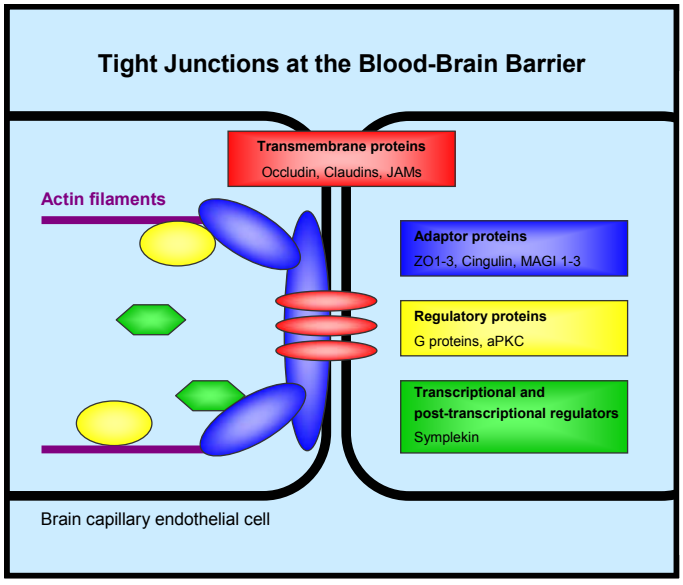

Figure 1.4
Tight junctions at the blood-brain barrier

Major components of tight junctions at the blood-brain barrier include transmembrane proteins as well as adaptor and regulatory proteins: occludin, claudins, junctional adhesion proteins (JAMs), zonula occludens (ZO), cingulin, membrane-associated guanylate kinase inverted (MAGI) proteins, G proteins, atypical protein kinase C (aPKC) and symplekin (adapted from (Matter and Balda, 2003b)).

1.1.6 The Blood-Brain Barrier – Drug Transporters

Over the past decade, it has become clear that the blood-brain barrier is a complex, dynamic structure with selective, active components. The molecular basis of the functional barrier is a number of multispecific, xenobiotic drug efflux transporters. Conventionally, transporters are grouped into families based on molecular and functional similarities. At present, mRNA for 15 drug transporters from several families has been detected in brain capillaries or brain capillary endothelial cell lines (Omidi et al., 2003; Zhang et al., 2000; Zhang et al., 2004a). This includes the **m**ulti**d**rug **r**esistance protein (MDR), **m**ultidrug **r**esistance-associated **p**rotein (MRP), **o**rganic **a**nion **t**ransporter (OAT), **o**rganic **a**nion **t**ransporting **p**olypeptide (OATP), **o**rganic **c**ation **t**ransporter (OCT), **c**oncentrative **n**ucleoside **t**ransporter (CNT), and **e**quilibrative **n**ucleoside **t**ransporter (ENT) subfamilies. However, it is very likely that this inventory of transporters is incomplete. About 15% of the genes expressed at the blood-brain barrier are expected to encode for transporters, and it is estimated that only about 50% of these are known (Pardridge, 2003b). Indeed, there have repeatedly been reports that cannot be fully explained by the transporters known so-far to be expressed at the blood-brain barrier (Lee et al., 2005). Therefore, it is anticipated that a blood-brain barrier genomics program will identify several new transporters (Pardridge, 2001).

Of the 15 transporters detected at the mRNA level, seven have been immunolocalized within brain capillary endothelial cells (Figure 1.5, (Bauer et al., 2005). Five ATP-driven drug export pumps, P-glycoprotein (P-gp), **b**reast **c**ancer **r**esistance **p**rotein (BCRP), Mrp1, Mrp2, and Mrp4 are on the luminal plasma membrane (blood side). Together, these transporters can handle a wide range of anionic (Mrp1, Mrp2 and Mrp4), cationic (P-glycoprotein and BCRP), and uncharged (all five) xenobiotics. Therefore, acting as a “first line of defense”, they limit xenobiotics including a large number of drugs from penetrating into the brain and likely also remove metabolic wastes from CNS to blood.

Also on the luminal membrane is Oatp2 (Figure 1.5), another organic anion transporter that handles steroid and drug conjugates, certain opioid peptides, and the cardiac glycoside, digoxin (Gao et al., 1999). Oatp2 could drive concentrative efflux from the cells if energetically coupled to the electrical potential difference across the luminal membrane. Clearly, also Oatp2 could contribute to the selective component of the blood-brain barrier.

Xenobiotic transporters are also present on the basolateral plasma membrane (brain side) of brain capillary endothelial cells. These include Mrp1, Mrp4, Oatp2 and Oat3 (Cisternino et al., 2003; Gao et al., 1999; Ohtsuki et al., 2002; Zhang et al., 2004a). The role of these transporters on the basolateral membrane is not well understood. However, when coupled to the appropriate ion gradients, both Oat3 and Oatp2 are capable of driving organic anions into endothelial cells. Thus, basal Oatp2 and Oat3 could pair with luminal Mrp1, Mrp2, Mrp4 and Oatp2 to drive anionic xenobiotics across the endothelium from the CNS into blood.

In addition, recently rat Oatp14 and human OATP-A have been detected at the blood-brain barrier by Northern and Western blotting, and immunolocalization techniques, respectively (Gao et al., 2000; Sugiyama et al., 2003b). While Oatp14 might be involved in thyroid hormone transport, the function of OATP-A is unclear (Tohyama et al., 2004).

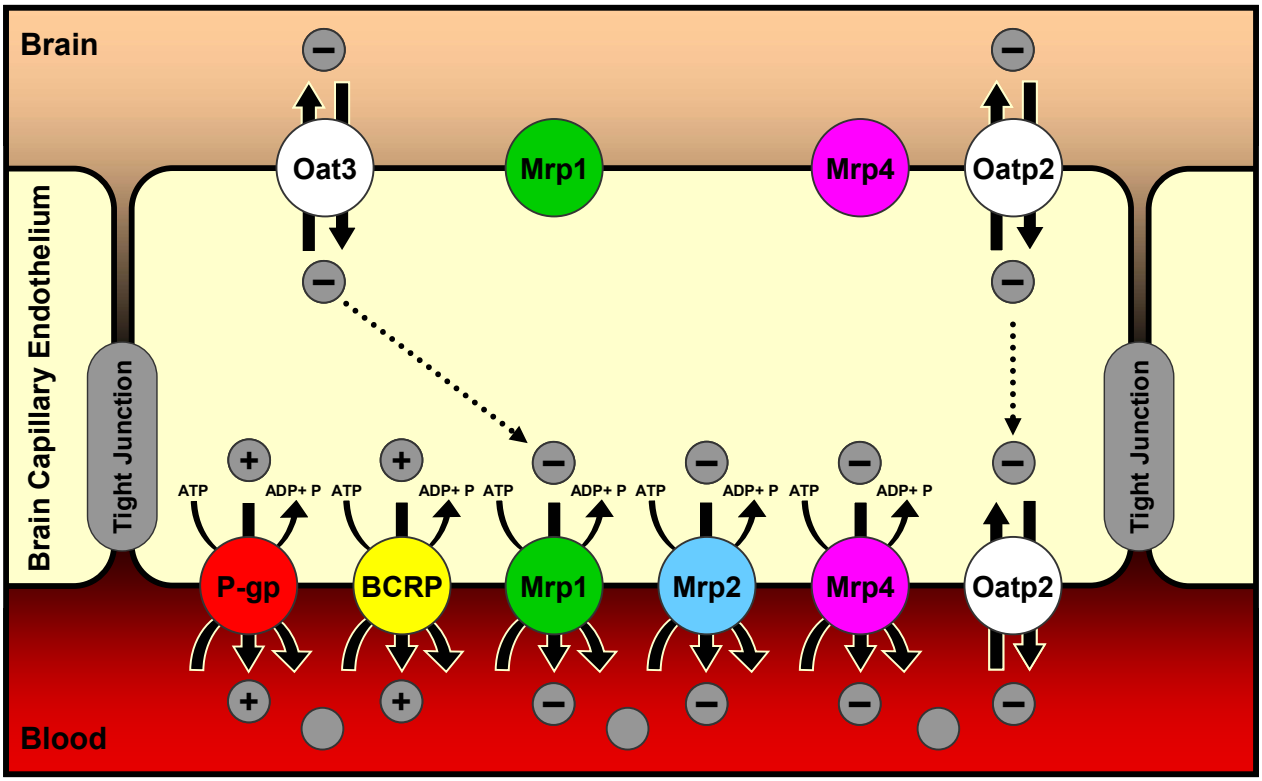

Figure 1.5
Drug transporters at the blood-brain barrier

Luminal membrane (blood side): P-gp, BCRP, Mrp 1, 2, 4 and Oatp2
Abluminal membrane (brain side): Oat3, Mrp1, Mrp4 and Oatp2
modified from (Bauer et al., 2005)

1.2 P-glycoprotein

1.2.1 P-glycoprotein – Historical Background

In 1960, Goldstein et al. reported acquired resistance to actinomycin D in HeLa cell lines (Goldstein et al., 1960). This was also observed by Biedler and Riehm in a chinese hamster ovary cell line (Biedler and Riehm, 1970). In addition, they found that the cells were resistant to multiple drugs. Shortly afterwards, Dano et al. showed active outward transport of daunomycin by resistant cells and proposed an active efflux pump to cause resistance by transporting drugs out of the cell (Dano, 1973). In 1976, Juliano and Ling identified this efflux pump (Juliano and Ling, 1976). The glycoprotein they found appeared to be unique to mutant cells that displayed altered drug permeability. Thus, they named it *permeability-glycoprotein* (P-glycoprotein or P-gp). However, it quickly became clear that P-glycoprotein is a primary, active efflux pump that uses the energy of ATP to transport its substrates out of cells, even against a concentration gradient (Sharom, 1997). The discovery of P-gp was groundbreaking, because it explained multidrug resistance (mdr, resistance to multiple chemotherapeutics), a frequently observed phenomenon in tumors. In the mid to late 1980s, P-glycoprotein was also found to be physiologically expressed in normal excretory and barrier tissues such as liver, kidney and intestine (Thiebaut et al., 1987).
In 1989, two independent research groups found expression of P-gp at the human blood-brain barrier (Cordon-Cardo et al., 1989; Thiebaut et al., 1989) and several years later it was also found to be present in isolated brain capillaries from mouse, rat, pig and cow (Jette and Beliveau, 1993; Jette et al., 1993; Nobmann et al., 2001; Tsai et al., 2002). At the blood-brain barrier, P-gp is highly expressed in the luminal membrane of endothelial cells, a perfect location to protect the brain from xenobiotics (Beaulieu et al., 1997; Biegel et al., 1995; Shirai et al., 1994; Sugawara, 1990; Tanaka et al., 1994; Tsuji et al., 1992). Therefore, P-glycoprotein is generally recognized to be the most important element of the selective, active blood-brain barrier for xenobiotics and thus, has been a main focus of blood-brain barrier research over the last decade.

1.2.2 P-glycoprotein – Expression, Structure & Function

In humans, P-glycoprotein is encoded by the *ABCB1* gene (**A**TP-**b**inding **c**assette, subfamily **B**, member **1**), better known as *MDR1* (**m**ulti**d**rug **r**esistance gene **1**; Table 1.1) (Bodor et al., 2004; Ueda et al., 1986). Another isoform in humans is *MDR2* (Chin et al., 1989). Three isoforms have been identified in rodents: *mdr1a*, *mdr1b*, and *mdr2* (Hsu et al., 1990). The *Mdr1* gene products confer multidrug resistance, whereas the *Mdr2* gene products secrete phosphatidylcholine into bile at the canalicular membrane of hepatocytes (Smit et al., 1993). The isoforms exhibit a large structural overlap and human and rat gene products show homology of about 80% (van der Bliek et al., 1988).

MDR/TAP (ABC subfamily B)				
Species	**Gene symbol & name**	**Gene name**	**Expression**	**Function**
Human	***ABCB1*** (*MDR1*, *PGY1*, *CLCS*) Chromosome 7 (7q21, 28 exons) Protein: 1280 AA Aliases : **P-gp**, CD243, GP170, ABC20	**A**TP-**b**inding **c**assette, subfamily **B**, member **1**	Excretory and barrier tissues such as liver, kidney, intestine, placenta as well as blood-testis & blood-brain barriers	Protection of the body by ATP-dependent efflux transport of xenobiotics, including a large number of commonly used drugs in the clinic
Rodent	***Abcb1a*** (*mdr1a*, *mdr3*) ***Abcb1b*** (*mdr1b*, *mdr1*)			
Human	***ABCB4*** (*MDR2*, *MDR3*) Chromosome 7 (7q21, 28 exons) Protein: 1279 AA Aliases: MDR2/3, MDR3, PFIC-3, ABC21	**A**TP-**b**inding **c**assette, subfamily **B**, member **4**	Hepatocytes	Biliary phosphatidyl-choline secretion from hepatocytes
Rodent	***Abcb4*** (*mdr2*)			

Table 1.1
***MDR* isoforms**

TAP: **T**ransporter **A**ssociated with Antigen **P**rocessing
http://www.nutrigene.4t.com/humanabc.htm & http://www.gene.ucl.ac.uk/nomenclature/genefamily/abc.html

The *MDR1* gene product, P-glycoprotein, is a 170 kDa transmembrane protein that consists of 1280 amino acids. It is organized as a single polypeptide with two homologous halves (Figure 1.6, (Jones and George, 2000)). Each half contains a transmembrane domain (TMD) with 6 transmembrane α-helical segments and one ATP-binding domain (ABD). Intracellular and extracellular loops connect the transmembrane spanning segments and a highly charged, phosphorylated linker region connects the two halves with each other. This region also contains signature motifs characteristic for ABC transporters (ABC family signature, Walker A and B motifs). N-glycosylation takes place at the first extracellular loop.

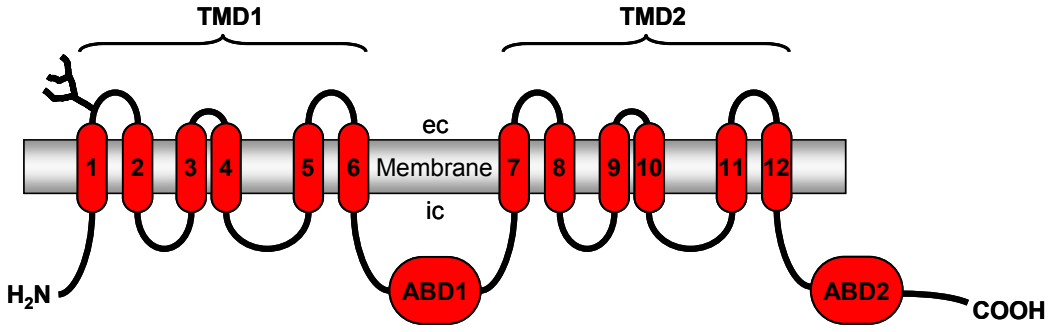

Figure 1.6
P-gp protein organization

P-glycoprotein consists of 2 transmembrane domains (TMD1 and TMD2), each of which has 6 transmembrane spanning α-helices and an ATP-binding domain (ABD). P-gp is N-glycosylated at the first extracellular loop (ec = extracellular, ic = intracellular). Modified from (Jones and George, 2000; Webb, 1997).

The shape of membranous P-glycoprotein has been determined by electron microscopy to be 6-fold symmetrical-toroidal (doughnut-shaped) with a diameter of 10 nm, and a large central pore of about 5 nm in diameter (Rosenberg et al., 1997). The transmembrane spanning segments form the central pore and mediate drug binding. They also direct trafficking of the protein to the cell membrane (Loo and Clarke, 1999). Loo et al. showed that the drug binding pocket is large enough to bind two different drugs simultaneously (Loo et al., 2003). Furthermore, they suggested a substrate-induced fit for binding since substrates cause size- and shape-dependent conformational changes of the transmembrane segments. This mechanism would also explain the broad substrate spectrum of P-glycoprotein. In general, P-gp substrates are mainly organic cations and uncharged compounds with a molecular weight between 300-2000 Da, they are amphiphilic or lipophilic in nature, and vary greatly in their chemical structure. P-gp substrates include a large number of clinically relevant drugs such as opioids, steroids, antibiotics, calcium-channel blockers, chemotherapeutics, immunosuppressants, anti-HIV drugs, and miscellaneous others (Chen and Simon, 2000). At present, physiological substrates have not been identified yet.

P-glycoprotein is expressed in barrier and excretory tissues, including kidney, liver, intestine, pancreatic duct, placenta, salivary ducts, cornea, testis, adrenal cortex, nasal mucosa, choroid plexus and the blood-brain barrier (Cordon-Cardo et al., 1990; Dey et al., 2003; Henriksson et al., 1997; Rao et al., 1999; Sugawara et al., 1988; Thiebaut et al., 1987; Thiebaut et al., 1989; Uematsu et al., 2001). P-glycoprotein protects the body from xenobiotics, by active, ATP-dependent efflux transport. Additional functions have been proposed such as regulatory functions in apoptosis and cell differentiation (Johnstone et al., 2000), indirect modulation of chloride channel activity (Valverde et al., 1992), and putative involvement in cholesterol esterification (Luker et al., 1999). In addition, P-glycoprotein is responsive to inflammatory mediators (McRae et al., 2003) and immunomodulation (Richaud-Patin et al., 2004). It is not clear whether these additional functions are limited to certain tissues and cells or whether they are a property of all cells expressing P-gp.

The species P-glycoprotein and its isoforms have been found in so far include mammals (human, mouse, rat, hamster, guinea pig, rabbit, dog, monkey, pig and cow) as well as insects, fish, amphibians and birds (Baas and Borst, 1988; Bard et al., 2002; Barnes, 2001; Bombardi et al., 2004; Bonfanti et al., 1998; Bosch et al., 1996; Dey et al., 2003; Fricker et al., 2002; Melaine et al., 2002; Pardridge et al., 1997).

1.2.3 P-glycoprotein - A Key Drug Export Pump at the Blood-Brain Barrier

Over the last decade, it has become clear that the multi-specific, xenobiotic drug efflux transporter, P-glycoprotein, plays an important role in blood-brain barrier function. Four factors – expression, localization, potency and multi-specificity - combine to make P-glycoprotein the key determinant of drug entry into the CNS (Begley, 2004a).
First, P-glycoprotein is highly expressed in capillary membranes of the blood-brain barrier (Figure1.7). Second, localization at the luminal membrane of capillary endothelial cells is consistent with P-gp being both a barrier to entry and a drug excretory pump. Third, potent ATP-driven pumping essentially prevents entry and accumulation of substrates into the cytoplasm of barrier cells. Fourth, the remarkably broad substrate spectrum of P-glycoprotein ensures that it will handle a large number of commonly prescribed drugs.
No experiments better highlight the importance of P-gp to blood-brain barrier function than those involving genetic modifications in which the transporter has been knocked out. *In vivo* dosing studies using genetic *mdr1*-knockout mice show 5-50-fold increased brain-to-plasma ratios of a large number of drugs that are P-gp substrates and therefore normally don't get into the brain (Schinkel et al., 1996).
Moreover, in a combined *in vitro/in vivo* approach, Fellner et al. used this principle to treat brain tumors in mice by chemically knocking out P-glycoprotein (Fellner et al., 2002). They identified P-gp as the major factor in limiting access of the anti-cancer therapeutic paclitaxel into the CNS. Pretreatment of mice with the P-gp-specific inhibitor, PSC833, not only increased brain levels of the anti-cancer drug paclitaxel (i.v. dosing), but also had a dramatic therapeutic effect on a paclitaxel-sensitive, intracerebrally implanted human glioblastoma. This tumor is generally refractory to treatment, because P-gp greatly restricts CNS penetration of most anti-cancer drugs. Importantly, combined PSC833-paclitaxel therapy decreased tumor volumes by 90%. In contrast, paclitaxel itself did not affect tumor size.

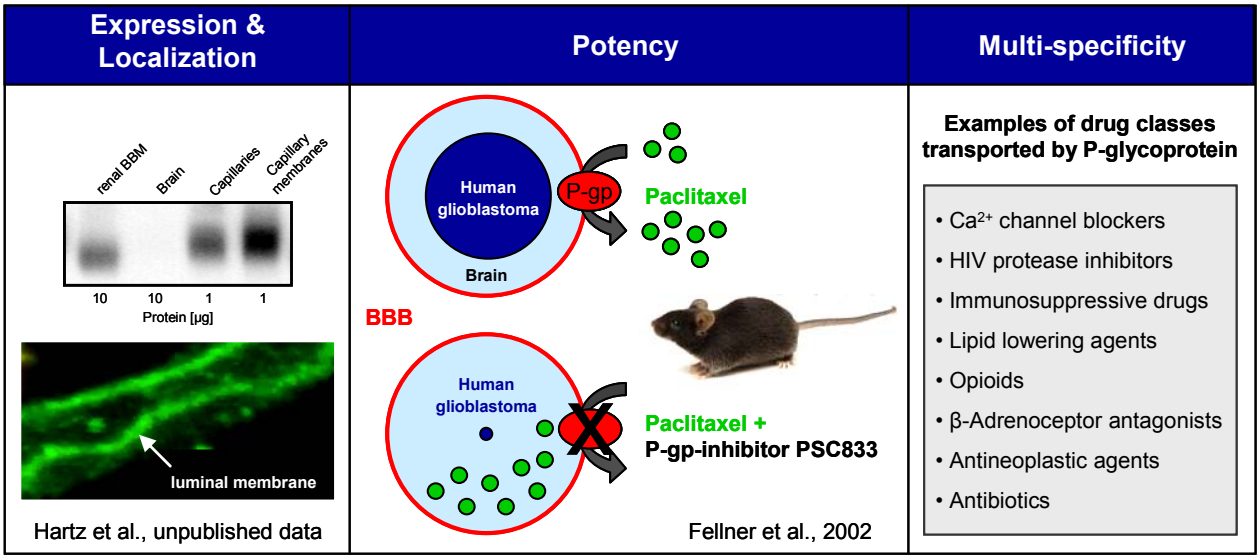

Figure 1.7
P-glycoprotein, a key determinant of drug entry into the CNS
P-glycoprotein is a key export pump at the blood-brain barrier because of its high expression, luminal localization at the capillary endothelium, its potent transport activity and its multi-specificity (Bauer et al., 2005).

1.3 Regulation of P-glycoprotein Function and Expression

P-glycoprotein is the key drug efflux transporter at the blood-brain barrier that prevents successful delivery of therapeutics into the brain. Therefore, a better understanding of physiological and pathological mechanisms that regulate P-gp at the blood-brain barrier holds the promise of improving drug therapy of CNS disorders. One approach to improve drug delivery to the brain and increase drug levels in the CNS in a controlled manner would be to manipulate expression and function of P-glycoprotein. In this regard, it would clearly be advantageous to be able to modulate P-gp function over the short-term while still having its protection over the long-term. However, although P-gp is the most widely studied ABC transporter, little is known about its regulation at the blood-brain barrier. Three general strategies have been used to manipulate P-glycoprotein:

1) **direct inhibition** of P-glycoprotein transport function by using specific inhibitors,
2) **short-term regulation** (minutes) of P-glycoprotein transport function through intracellular signaling, and
3) **long-term regulation** (within hours to days) of P-glycoprotein expression through specific manipulation of transcription.

The following section gives an overview of mechanisms currently known to regulate P-glycoprotein transport function and expression.

1.3.1 Direct Inhibition of P-glycoprotein Transport Function

One strategy to modulate P-glycoprotein at the blood-brain barrier is by direct inhibition. For this purpose, several P-gp inhibitors were developed and a large number of compounds have been screened for their P-gp-inhibitory potential (Avendano and Menendez, 2002; Pleban and Ecker, 2005). First generation P-glycoprotein inhibitors include, verapamil, quinidine, quinine, cyclosporin A, amiodarone and nifedipine (Ford et al., 1996; Leonard et al., 2002; Tsuruo et al., 1981; Twentyman, 1992). However, these compounds often caused toxic side effects *in vivo* due to their low potency, weak effectiveness and poor selectivity. This led to new P-gp inhibitors that were developed solely for the purpose of reversing drug resistance. Second generation inhibitors include valspodar (PSC833) and biricodar (VX-710), and third generation inhibitors include elacridar (GF120918), tariquidar (XR-9576), zosuquidar (LY-335979), and laniquidar (R-101933) (Kemper et al., 2004a; Kemper et al., 2003; Leonard et al., 2002; van Zuylen et al., 2000; Walker et al., 2004). Animal studies show that of the few relatively specific P-gp inhibitors available, PSC833 (valspodar) is the most effective in increasing brain drug levels in *in vivo* models (Kemper et al., 2003; Kemper et al., 2004b; Mayer et al., 1997). Phase I and phase II clinical studies looked promising and indicate that PSC833 can be administered safely to patients with corrected doses of chemotherapeutics (Advani et al., 2001). Unfortunately, phase III trials proved to be disappointing. No difference in survival rate between cancer patients that received chemotherapeutic plus PSC833 and patients that did not receive PSC833 could be observed. In addition, PSC833 caused severe hematological toxicity, even early deaths were reported (Advani et al., 2001). However, it should be mentioned that in these phase III studies PSC833 was administered chronically. Also, PSC833 was never tested in a study with brain cancer patients. The use of PSC833 to chemically knock out P-gp was not followed any further. It remains to be seen, how well other P-gp-specific inhibitors of the third and fourth generation will do in clinical studies.

1.3.2 Short-Term Regulation of P-glycoprotein Transport Function

Modulation of P-glycoprotein transport function through intracellular signaling is another way to manipulate the transporter at the blood-brain barrier. Intracellular signaling can be a rapid process that takes place within minutes and triggers numerous biological events. These changes are referred to as “short-term” effects in this thesis. Today, we know little about the regulation of P-glycoprotein at the blood-brain barrier over the short-term. However, in other tissues, regulatory mechanisms have been described that signal rapid changes in P-gp transport function. These include:

1) Phosphorylation of P-glycoprotein by protein kinase C
2) Membrane trafficking of P-glycoprotein
3) Ubiquitination triggering P-glycoprotein degradation
4) Interaction of P-glycoprotein with caveolin-1
5) Regulation of P-glycoprotein by endothelin-1

1.3.2.1 Phosphorylation of P-glycoprotein by Protein Kinase C

The protein kinase C (PKC) family is a group of homologous, phospholipase C-dependent serine/threonine kinases similar in size, structure and mode of action (Azzi et al., 1992). They modulate the biological function of their target proteins in a rapid and reversible manner by transferring phosphate from ATP to certain amino acid residues of the protein. By doing so, PKC participates in the signal transduction triggered by external stimulation of cells by various ligands including hormones, neurotransmitters and growth factors. Today, twelve members of the PKC family have been identified in mammals (Idris et al., 2001). They are classified as conventional (cPKC: α, β1, β2, γ), novel (nPKC: δ, ε, η, θ, μ), and atypical (aPKC: ι, ζ, λ) PKC isozymes. While activation of the conventional PKC members is Ca^{2+}-dependent, the novel and atypical isozymes do not require Ca^{2+} to be activated.
Numerous studies have examined the effects of PKC on P-glycoprotein transport function (Hofmann, 2001). Chambers et al. showed that activation of PKC rapidly increased P-gp transport function in a cell line within 15-30 min and proposed that phosphorylation might be an important mechanism of modulating P-gp transport activity (Chambers et al., 1990a; Chambers et al., 1990b). In contrast, studies by Miller et al. demonstrated PKC-mediated reduction of P-gp transport in teleost renal proximal tubule (Miller et al., 1998). Another study by Castro et al. confirmed PKC modulation of P-gp transport function. However, the findings also suggest that P-glycoprotein phosphorylation by PKC does not play a major role in regulating P-gp (Castro et al., 1999; Germann et al., 1995). The authors rather speculate on whether PKC indirectly modulates P-glycoprotein transport activity. Recent studies indicate that PKC isozymes differentially phosphorylate specific serine residues in the linker region of P-glycoprotein resulting in a change of P-gp ATPase activity and a modulation of P-gp-drug-binding. From the studies published so far, it can be speculated that regulation of P-glycoprotein transport function, thus activation or reduction of P-gp activity, through PKC depends on the PKC isozyme tissue expression pattern and therefore varies amongst tissues (Sachs et al., 1999).

1.3.2.2 Membrane Trafficking of P-glycoprotein

A second mechanism that could account for rapid changes in P-glycoprotein-mediated transport is trafficking between vesicular compartments and the plasma membrane.
Kipp and Arias reported membrane trafficking of several ABC transporters, including P-gp, **b**ile **s**alt **e**xport **p**ump (BSEP), and Mrp2 at the bile canalicular membrane of hepatocytes (Kipp and Arias, 2002). They showed cycling of P-glycoprotein between intracellular pools and the plasma membrane by demonstrating insertion of P-gp into the canalicular membrane in response to cyclic AMP (cAMP) and taurocholate (Figure 1.8). This effect was independent from protein biosynthesis. In addition, the microtubule disruptor, colchicine, and the PI3 kinase inhibitor, wortmannin, inhibited membrane insertion of P-glycoprotein. On the other hand, it was also demonstrated that cholestasis caused retrieval of P-glycoprotein from the canalicular membrane into intracellular vesicles (Gatmaitan et al., 1997; Kipp and Arias, 2002; Kipp et al., 2001). In another study Sai et al. used a hepatic cell line expressing GFP-tagged P-glycoprotein to visualize P-gp trafficking between the pericanalicular region and the bile canalicular membrane (Sai et al., 1999). This study also demonstrated an involvement of microtubules and PI3 kinase in P-glycoprotein membrane trafficking.
These results show that in hepatocytes, vesicular trafficking of P-glycoprotein modulates transport at the canalicular membrane. Whether similar mechanisms also regulate P-gp-mediated transport at the blood-brain barrier remains to be determined.

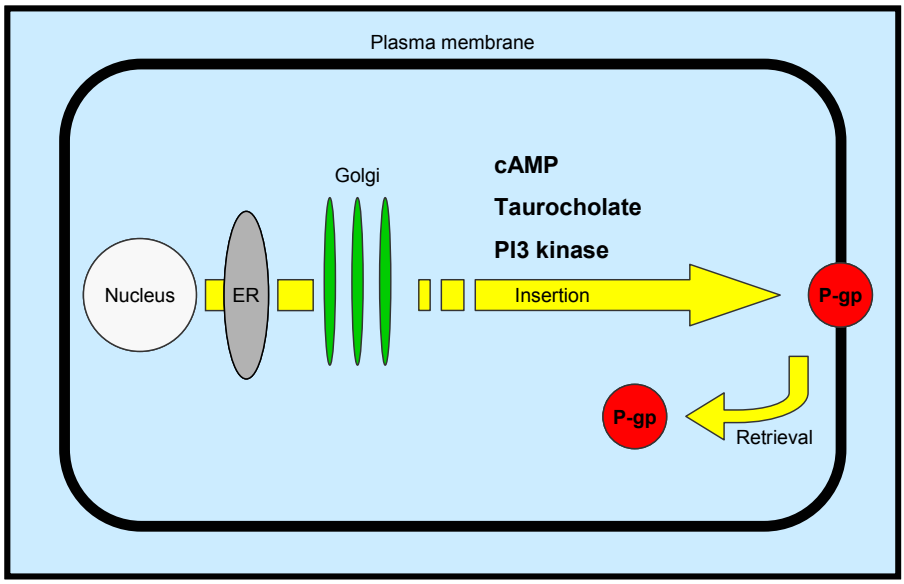

Figure 1.8
Membrane trafficking of P-glycoprotein in hepatocytes

Trafficking of P-glycoprotein between vesicular compartments and the plasma membrane: cAMP, taurocholate and PI3 kinase cause insertion of P-gp into the bile canalicular membrane of hepatocytes. Retrieval of P-gp from the membrane into intracellular vesicles was observed during cholestasis (Kipp and Arias, 2002).

1.3.2.3 Ubiquitination triggering P-glycoprotein Degradation

Another regulatory mechanism by which P-glycoprotein transport function could be modulated is through ubiquitination (Figure 1.9). Since ubiquitination triggers degradation of proteins, it is also referred to as the “kiss of death” for a protein (Ciechanover et al., 1980). Ubiquitin is an ubiquitiously expressed, small, 76 amino acid protein, the sequence of which is highly conserved amongst all creatures from insects to humans. During ubiquitination, target proteins are first labeled with ubiquitin molecules. The ubiquitin tag then signals the protein-transport machinery to shuttle the ubiquitin-labeled protein to the proteasome for degradation (Ciechanover, 1998). The proteasome removes the ubiquitin tag and digests the protein into small peptides. The balance between rates of ubiquitination (degradation) and translation (protein biosynthesis) therefore determines the concentration of a protein inside the cell.
Recently, Zhang et al. reported that P-glycoprotein stability and transport function is regulated by the ubiquitin-proteasome pathway (Zhang et al., 2004c). They compared a P-gp overexpressing breast cancer cell line with sensitive parental cells to demonstrate that enhanced ubiquitination resulted in reduced P-glycoprotein-mediated transport. Furthermore, the study also showed that P-gp is ubiquitinated independent of phosphorylation and that the process can be enhanced by inhibiting P-gp N-glycosylation. However, it is not yet clear how ubiquitination affects P-glycoprotein at the blood-brain barrier.

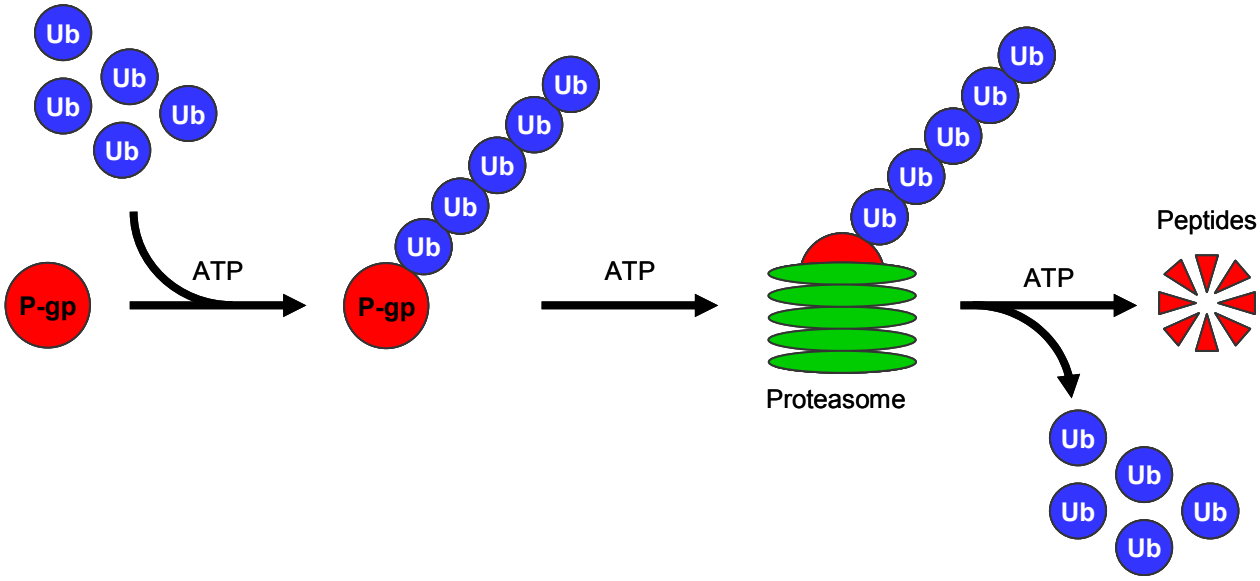

Figure 1.9
Ubiquitination triggering P-glycoprotein degradation

After conjugation with ubiquitin, tagged P-glycoprotein is transported to the proteasome and degraded into small peptides (Ciechanover, 1998; Zhang et al., 2004c).

1.3.2.4 Interaction of P-glycoprotein with Caveolin-1

Caveolae (“little caves”) are small, 50-100 nm plasma membrane invaginations that were discovered by Palade in 1953 (Palade, 1953). These invaginations are specialized lipid rafts enriched in glycosyl-phosphatidylinositol (GPI) anchored receptors such as the folate receptor, signaling receptors such as insulin, bradykinin and endothelin receptors, Src-like kinases and other signal transduction molecules (PKC, MAP kinase, PI3 kinase; Figure 1.10) (Anderson, 1998). The main components of caveolae, however, are small, 22 kDa transmembrane proteins, the caveolins; three isoforms (caveolin 1-3) are known today (Okamoto et al., 1998). Caveolins are directly involved in signaling. For example, caveolin-1α interacts with G-proteins, PKC and NO synthase.
Interestingly, P-glycoprotein and caveolin-1α were found to be co-localized at the blood-brain barrier of humans and rhesus monkeys (Schlachetzki and Pardridge, 2003). This was confirmed by Jodoin et al., who isolated caveolar microdomains from bovine brain capillary endothelial cells (Jodoin et al., 2003). Furthermore, they also demonstrated that P-glycoprotein transport function was downregulated by caveolins 1 and 2 through a caveolin-binding motif in the N-terminus of P-gp. It remains to be seen, whether this mechanism can be used to modulate P-glycoprotein transport function.

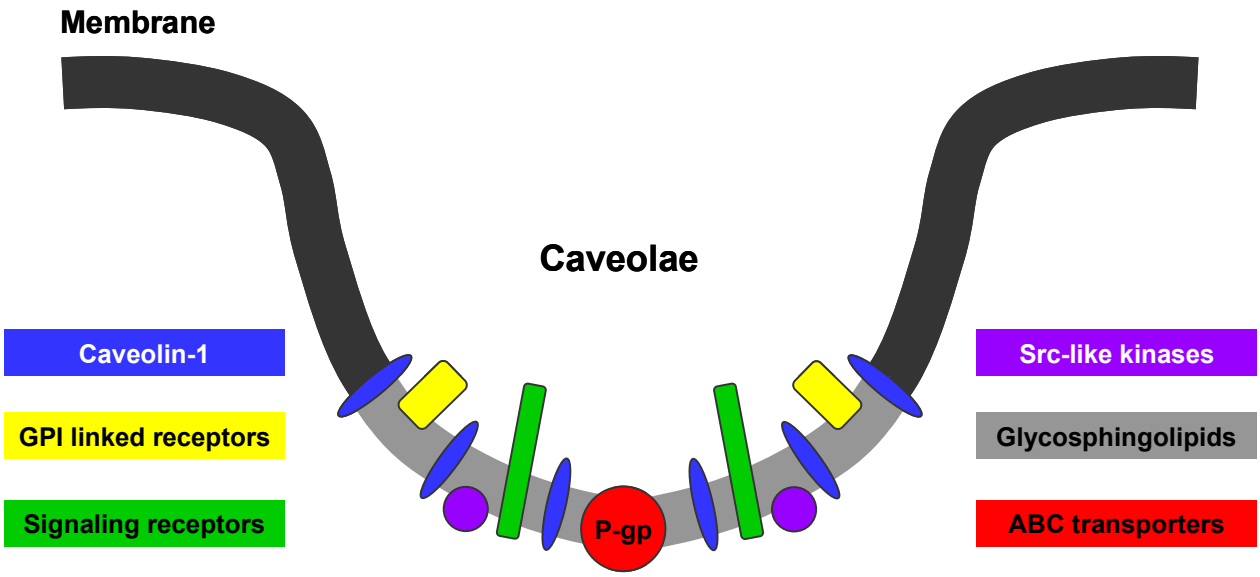

Figure 1.10
Co-localization of caveolin-1 and P-glycoprotein in caveolae of the brain capillary endothelium
Caveolae are “centers for signal transduction” enriched with signal transduction molecules such as glycosyl-phosphatidylinositol (GPI) linked receptors, signaling receptors, Src-like kinases and other signal transduction molecules (PKC, MAP kinase, PI3 kinase).

1.3.2.5 Regulation of P-glycoprotein by Endothelin-1

ET-1 is a 21 amino acid vasoconstrictor polypeptide hormone that was first described by Hickey et al. in 1985 (Figure 1.11, (Hickey et al., 1985)). However, it was Yanagisawa et al., who shortly afterwards revealed the primary structure, synthesis and biological activity of ET-1 and who analyzed and cloned the gene as well (Yanagisawa et al., 1988a; Yanagisawa et al., 1988b). Three endothelin isoforms are known today: ET-1, ET-2 and ET-3; these are three separate gene products. Due to 2 disulfide bonds in the molecule, endothelins have the appearance of a shepherd's crook (Figure 1.11) (Highsmith, 1998; Webb, 1997).

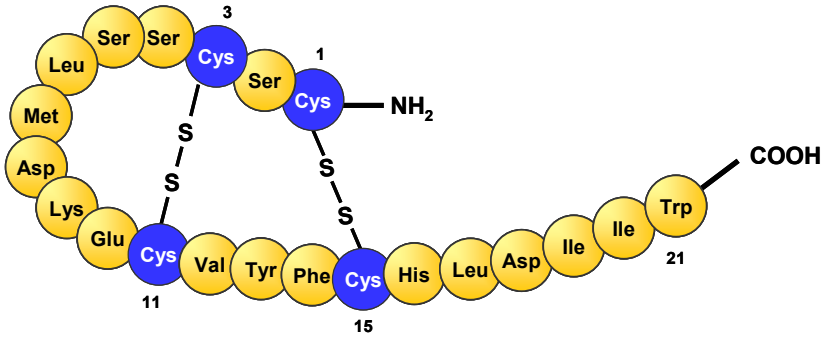

Figure 1.11
Endothelin-1 protein structure

Each endothelin isoform consists of 21 amino acids and 2 intra-chain disulfide bonds. The C-terminal sequence is necessary for biological activity and is conserved among the isoforms. The figure depicts the structure for ET-1 (Highsmith, 1998).

All endothelins are synthesized as precursors, the so-called prepro-endothelins (212 amino acids) that are processed to "big-ETs" (38-41 amino acids). The endothelin-converting enzyme (ECE) then cleaves big-ET to the biologically active endothelin isoforms (21 amino acids) (Highsmith, 1998; Offermanns, 2004; Rang, 1999) (Figure 1.12).
Endothelins signal through two G-protein coupled receptors, the endothelin A (ET_A) and endothelin B (ET_B) receptors. The ET_A receptor affinity of ET-1 and ET-2 is in the subnanomolar range (K_i ~ 20-60 pM), whereas the affinity of ET-3 to the A-type receptor is more than 2 orders of magnitude lower (K_i ~ 6500 pM). However, all three isoforms have equal affinities (K_i ~ 15 pM) for the ET_B receptor (Highsmith, 1998). ET receptors are different in their tissue distribution, ligand binding and signal transduction (Offermanns, 2004).
The ET_A receptor is present in many tissues, but is most highly expressed in aorta, heart and kidney (Webb, 1997). The ET_B receptor is predominantly expressed in brain, lung, kidney and aorta (Ogawa et al., 1991; Webb, 1997). In addition, the B-type receptor is highly expressed in endothelial cells, whereas highest expression of the A-type receptor is in smooth muscle cells. In the vascular system, ET_A and ET_B have opposite effects: the A-type receptor causes long-lasting vasoconstriction, whereas the B-type receptor mediates transient vasodilation (Kedzierski and Yanagisawa, 2001; Levin, 1995).

In the kidney, endothelins regulate renal blood flow, glomerular hemodynamics and sodium and water homeostasis (Offermanns, 2004). Endothelins are also involved in the pathology of acute ischemic renal failure, vascular rejection of transplanted kidneys as well as cyclosporin, cisplatin and radiocontrast agent nephrotoxicity (Bruzzi et al., 1997; Clavell and Burnett, 1994; Hocher et al., 1997).
Recently, Miller et al. described a new role for ET-1 in the kidney: regulation of ATP-driven drug excretion by efflux transporters in the renal proximal tubule (Masereeuw et al., 2000; Miller, 2002). Studies with isolated tubules from killifish (*fundulus heteroclitus*) showed that short-term exposure to ET-1 activates a signaling pathway that affects transport function of P-glycoprotein and Mrp2 (Masereeuw et al., 2000; Miller et al., 2002a). Endothelin-1 rapidly reduced transport mediated by these efflux transporters and signaling was found to be linear, going through ET_B, nitric oxide synthase (NOS), guanylyl cyclase (GC), protein kinase G (PKG), and protein kinase C (PKC).

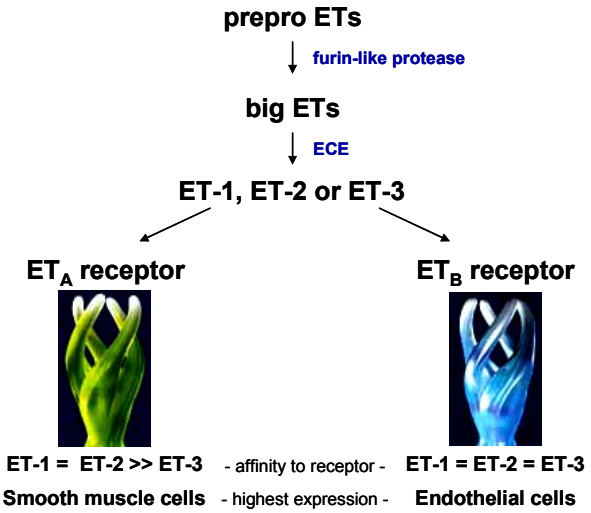

Figure 1.12
Biosynthetic pathway of endothelins (ETs)
Endothelin precursors (prepro-ETs) are cleaved to "big ETs", an intermediate form. The endothelin converting enzyme (ECE) cleaves the big ETs into the biologically active endothelins, ET-1, ET-2, and ET-3 that act through the ET_A and ET_B receptors.

In the brain the endothelin system affects multiple functions: neuromodulation, neurosecretion, neurotransmission, control of neuropeptide release from pituitary and hypothalamus, modulation of behaviour and brain metabolism (Kedzierski and Yanagisawa, 2001; Nie and Olsson, 1996; Willette, 1995). In addition, the ET system is activated in several CNS disorders such as Alzheimer's disease, multiple sclerosis, brain tumors, migraine, acute ischemic cerebral infarction, vasospasm, stroke, HIV-encephalitis and trauma (Cardell et al., 1994; Didier et al., 2002; Egidy et al., 2000; Highsmith, 1998; Minami et al., 1995; Nie and Olsson, 1996; Speciale et al., 2000). During inflammation that often accompanies CNS disorders, ET-1 is greatly elevated.
With regard to the blood-brain barrier, little is known about ET-1 signaling. However, ET-1 was reported to be produced and released by cerebral capillary endothelial cells (Bacic et al., 1992; Durieu-Trautmann et al., 1993; Lee et al., 1990; Yakubu and Leffler, 1999; Yoshimoto et al., 1990). In addition, both the ET_A and ET_B receptors are expressed in the capillary endothelium (Hartz et al., 2004; Rubanyi and Polokoff, 1994; Stanimirovic et al., 1994; Willette, 1995). These findings and the data for renal proximal tubule (above) suggest a possible role of ET-1 at the blood-brain barrier. Therefore, one part of this thesis was to examine ET-1 regulation of P-glycoprotein at the blood-brain barrier.

1.3.3 Long-Term Regulation of P-glycoprotein

In addition to direct inhibition and functional modulation, transcriptional regulation is a third possibility to modulate P-gp protein expression and transport function. This mechanism works over the long-term, i.e. hours to days rather than minutes. Transcriptional regulation of *MDR1* gene expression is complex and not yet completely understood. Transcription of the *MDR1* gene is regulated through the binding of several *trans*-acting proteins to consensus *cis*-elements in the promoter region. Figure 1.13 shows the promoter region of human *MDR1* (Labialle et al., 2002). Unlike its murine homologue, the *hMDR1* promoter lacks a TATA-box and contains an initiator element (INR). For the *hMDR1* gene, several promoter elements have been found so far, including a GC-box, a Y-box, a p53 element, an inverse MED1 element, an AP-1 element, and a heat shock element (HSF1), to name a few. A more detailed description can be found in (Labialle et al., 2004; Labialle et al., 2002).

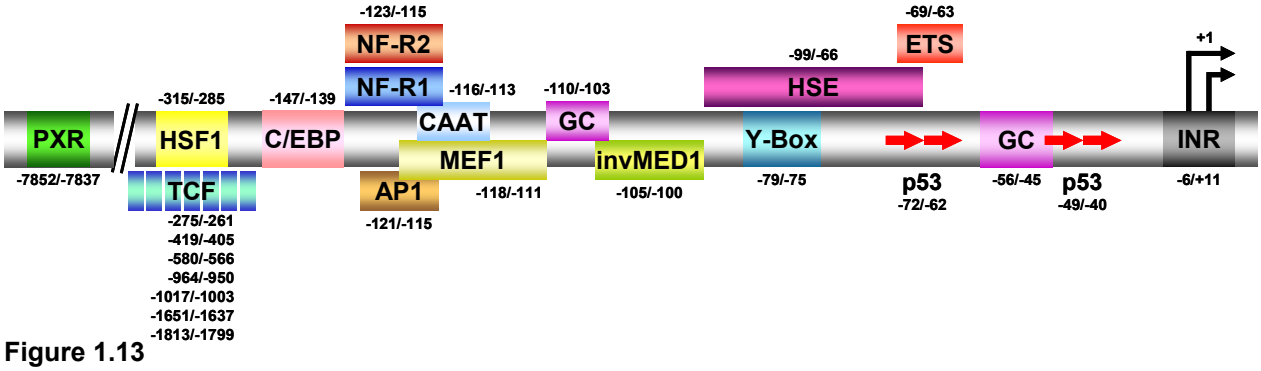

Figure 1.13
Promoter region of human *MDR1* modified from (Labialle et al., 2002)

INR:	initiator element –sequences between -6 and +11 are sufficient for proper initiation of transcription
GC-Box:	GC-rich region – binding site for nuclear transcription factor SP1 (specificity protein 1)
Y-Box:	inverted CCAAT element – binding site for nuclear factor Y (NF-Y) and Y-box binding protein (YB-1)
p53:	proposed binding sites for p53 tumor suppressor protein
AP-1:	activator protein 1 binding site for c-*jun* and c-*fos* transcription factors
CAAT:	CAAT element binds a complex of nuclear factor κB, p65 and c-*fos* proteins
C/EBP:	binding site for CCAAT-box/enhancer binding proteins (C/EBP)
HSE:	heat shock elements – binding sites for heat-shock transcription factors (HSF)
TCF:	T cell factor elements – involved in over-expression of P-gp in tumor cells
invMed1:	inverted mediator-1 element *cis*-activates hMDR1
MEF1:	MDR1 promotor-enhancing factor 1 upregulates hMDR1
NF-R1/2:	binding site for recently discovered transcription regulatory proteins, NF-R1/2
ETS:	binding site for *ets* ('E twenty-six') proteins
PXR:	binding site for nuclear receptor PXR (pregnane X receptor)

Geick et al. found that the ligand-activated orphan nuclear receptor, pregnane X receptor, PXR, regulates transcription of the human *MDR1* (*hMDR1*) gene. They discovered a complex regulatory cluster of several binding sites for PXR in the 5'-upstream region of *hMDR1* (Geick et al., 2001). Three DR4 motifs (direct repeats of a AG(G/T)TCA motif with a spacer of four nucleotides in between the binding motif), one DR3 motif, and one ER6 motif (everted repeat) were identified at about -8 kb. Electrophoretic mobility shift assays further revealed that PXR binds as a heterodimer with the retinoid X receptor α (RXRα) to all DR4 motifs (Geick et al., 2001). In addition, reporter gene assays confirmed that this cluster of response elements is responsible for PXR-mediated *hMDR1* induction. Importantly, PXR is the only ligand-activated nuclear receptor known to control transcriptional regulation of *MDR1*, and thus expression of P-gp. The second part of this thesis describes PXR regulation of P-glycoprotein at the blood-brain barrier.

1.3.3.1 The Pregnane X Receptor – A Ligand-Activated Nuclear Receptor

Recently, Kliewer et al., Bertilsson et al. and Blumberg et al. identified independently from each other a new member of the orphan nuclear receptor family, the pregnane X receptor, PXR (*NR1I2)* (Bertilsson et al., 1998; Blumberg et al., 1998; Kliewer et al., 1998). Nuclear receptors (NRs) are receptors in the nucleus and the cytoplasm that belong to the largest superfamily of ligand-activated transcription factors. They are involved in a wide variety of biological functions, including cell growth and differentiation, embryonic development as well as metabolism and efflux transport (Zhang et al., 2004b).

The history of NRs is closely linked to the history of hormone research. In the mid to late 1960s, studies showed that steroid hormones regulate gene expression through interaction with cognate receptors (Aranda and Pascual, 2001; Mangelsdorf et al., 1995). Consequently, the first nuclear receptors were discovered in the 1970s and named “endocrine nuclear hormone receptors” (Figure 1.14) (Fannon et al., 2001). With the introduction of DNA libraries, a huge resource of unidentified sequences was available for screening of highly conserved motifs. Thus, several nuclear receptors were found. However, their physiological roles and ligands remained unclear and therefore, were designated as “orphan nuclear receptors”. Further studies identified ligands for some of the orphan receptors and they were adopted (“adopted orphan receptors”) (Chawla et al., 2001; Schmuth, 2003). Today, 49 nuclear receptors have been identified in the human genome.

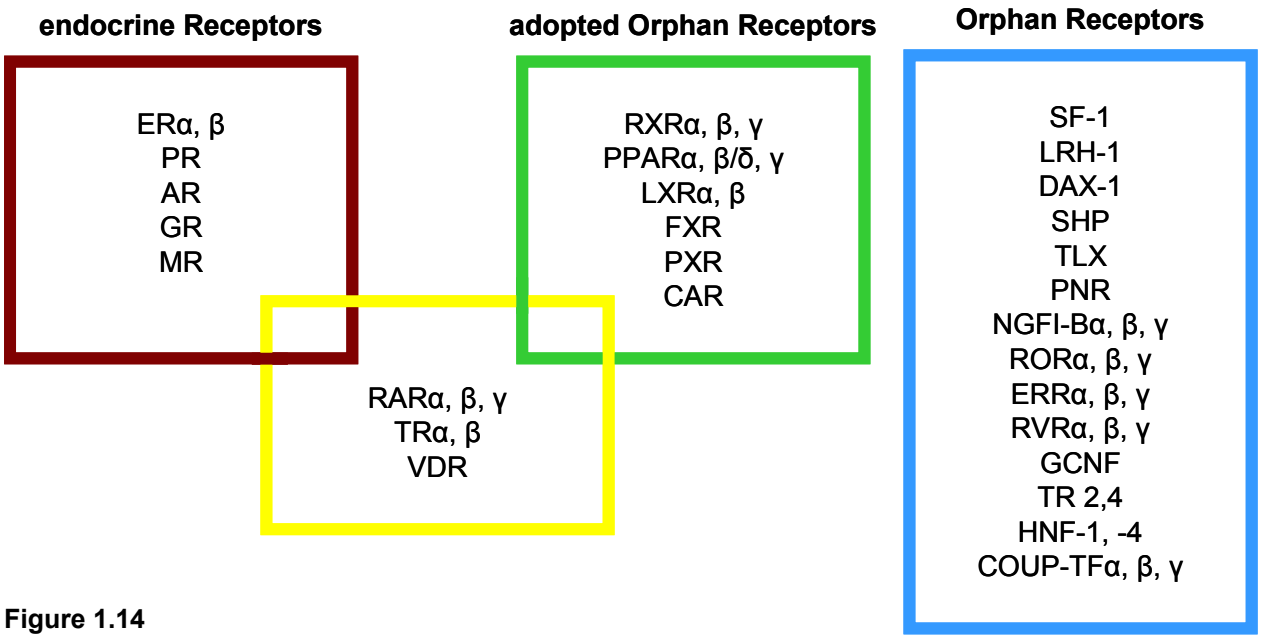

Figure 1.14

Endocrine receptors:
Estrogen receptor (ER), progesterone receptor (PR), androgen receptor (AR), glucocorticoid receptor (GR) and mineralocorticoid receptor (MR).

Adopted orphan receptors:
Retinoid X receptor (RXR), peroxisome proliferator-activated receptor (PPAR), liver X receptor (LXR), farnesoid X receptor (FXR), pregnane X receptor (PXR), constitutive androstane receptor (CAR).
The retinoic acid receptor (RAR), thyroid hormone receptor (TR) and vitamin D receptor (yellow box) display characteristics of both endocrine and adopted orphan receptors (Chawla et al., 2001).

Orphan receptors:
Nuclear receptors without known ligands. For more detailed information see (Maglich et al., 2001).

Nuclear receptors (NRs) regulate gene expression in response to extracellular and intracellular signals. These signals are mediated through non-peptide, small, lipophilic NR ligands such as steroid and thyroid hormones that are cell-permeable and absorbable. Upon activation by a ligand, the NR binds to specific DNA sequences (response elements) in the regulatory promoter region of their target genes. Classic endocrine receptors and most orphan receptors bind as homodimers, whereas the adopted orphan nuclear receptors found so far heterodimerize with the retinoid X receptor α (RXRα, Figure 1.15) (Schmuth, 2003). The response elements (also referred to as “hormone response elements, HRE” or “xenobiotic response elements, XRE”) are hexameric sequence motifs, e.g. AGTTCA (Figure 1.15). They are organized either as direct, inverted or everted repeats (DR, IR, ER) with spacer base pairs in between the motifs (e.g. 4 bases in between a direct repeat motif: DR4) (Aranda and Pascual, 2001).

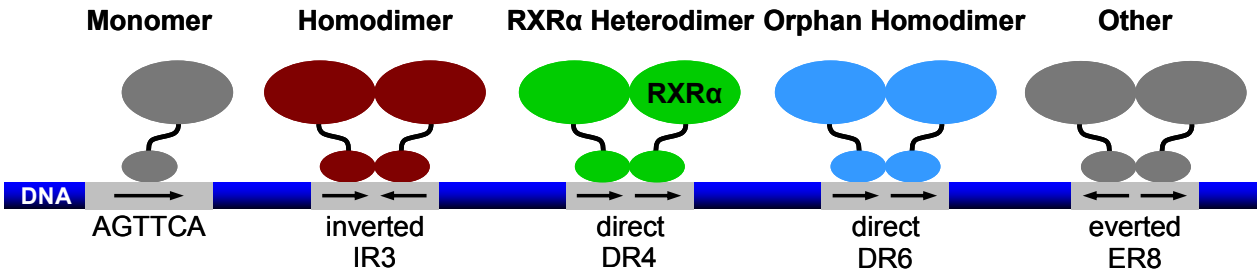

Figure 1.15
DNA binding of nuclear receptors

Most nuclear receptors bind as homo- or heterodimers to specific DNA binding sequences (direct (DR), inverted (IR) and everted (ER) repeats; (Schmuth, 2003)).

1.3.3.2 The Pregnane X Receptor – Structure & Ligand Specificity

Like the protein structure of other NRs, PXR has 4 domains. (1) A modulator region harboring an activation function (AF-1), (2) a DNA binding domain (DBD) with two zinc-finger motifs, and (3) a flexible hinge region connecting the DBD with (4) the ligand binding domain (LBD) that is also associated with an activation function (AF-2) (Figure 1.16) (Handschin and Meyer, 2003; Lazar, 2002).

Figure 1.16
Protein domain structure of PXR

PXR protein is structured in 4 domains: (1) a modulator domain with activation function (AF-1), (2) a DNA binding domain (DBD) with two zinc-finger motifs, (3) a hinge domain connecting the DBD and LBD, and (4) the ligand binding domain (LBD) with an activation function (AF-2).

The DBD is a highly conserved domain that is nearly identical across species. For example, the DBDs of rat and human PXR share 96% of their amino acid sequence (Tirona et al., 2004; Watkins et al., 2001). The LBD consists of 12 hydrophobic α-helices that form a spherical, 1500 $Å^3$ large ligand binding cavity, which is the reason for the broad ligand spectrum of PXR (Watkins et al., 2003b; Watkins et al., 2002; Watkins et al., 2001). In contrast to the DBD, the LBDs of rat and human PXR share only 76% amino acid identity (Zhang et al., 1999) (Table 1.2). This explains the species difference with regard to PXR ligand specificity. For example, hyperforin, rifampicin and paclitaxel activate human PXR but not rodent PXR. On the other hand, the prototypical rodent PXR activator, pregnenolone-carbonitrile (PCN) does not activate human PXR (Honkakoski et al., 2003; Jones et al., 2000; Kliewer et al., 1999; Moore et al., 2000a; Wentworth et al., 2000).

	DBD	LBD	Ligands
human PXR	100	100	Hyperforin, Rifampicin, Paclitaxel, Dexamethasone
rat PXR	96	76	PCN, Dexamethasone

Table 1.2
Comparison of human PXR and rat PXR

The DNA binding domain (DBD) of rat and human PXR share 96% amino acid identity, whereas the ligand binding domain (LBD) is only 76% identical. Therefore, PXR has species-dependent ligand specificity: hyperforin, rifampicin and paclitaxel only activate human PXR but not rodent PXR. PCN on the other hand only activates rodent PXR but not human PXR.

1.3.3.3 PXR Signaling

PXR activation occurs through binding of endogenous and exogenous ligands. Endogenous ligands include metabolic precursors, intermediates and end products of steroid and thyroid hormone synthesis as well as bile acid synthesis; exogenous ligands include environmental toxins, dietary compounds and drugs (Lazar, 2002). PXR ligands are small, lipophilic and therefore cell-permeable molecules. Inside the cell, they bind to corepressor inactivated PXR, which upon ligand binding undergoes a conformational change causing dissociation of the corepressor. Ligand-bound, activated PXR translocates into the nucleus where it forms a heterodimer with another nuclear receptor, the retinoid X receptor α (RXRα). The complex of PXR, RXRα and coactivators then binds to the xenobiotic response element (XRE) in the regulatory promoter region of PXR's target genes (Watkins et al., 2003a). As a consequence, transcription of target genes increases, and mRNA is translated into protein, which then is responsible for the physiological effects (Jacobs et al., 2003).

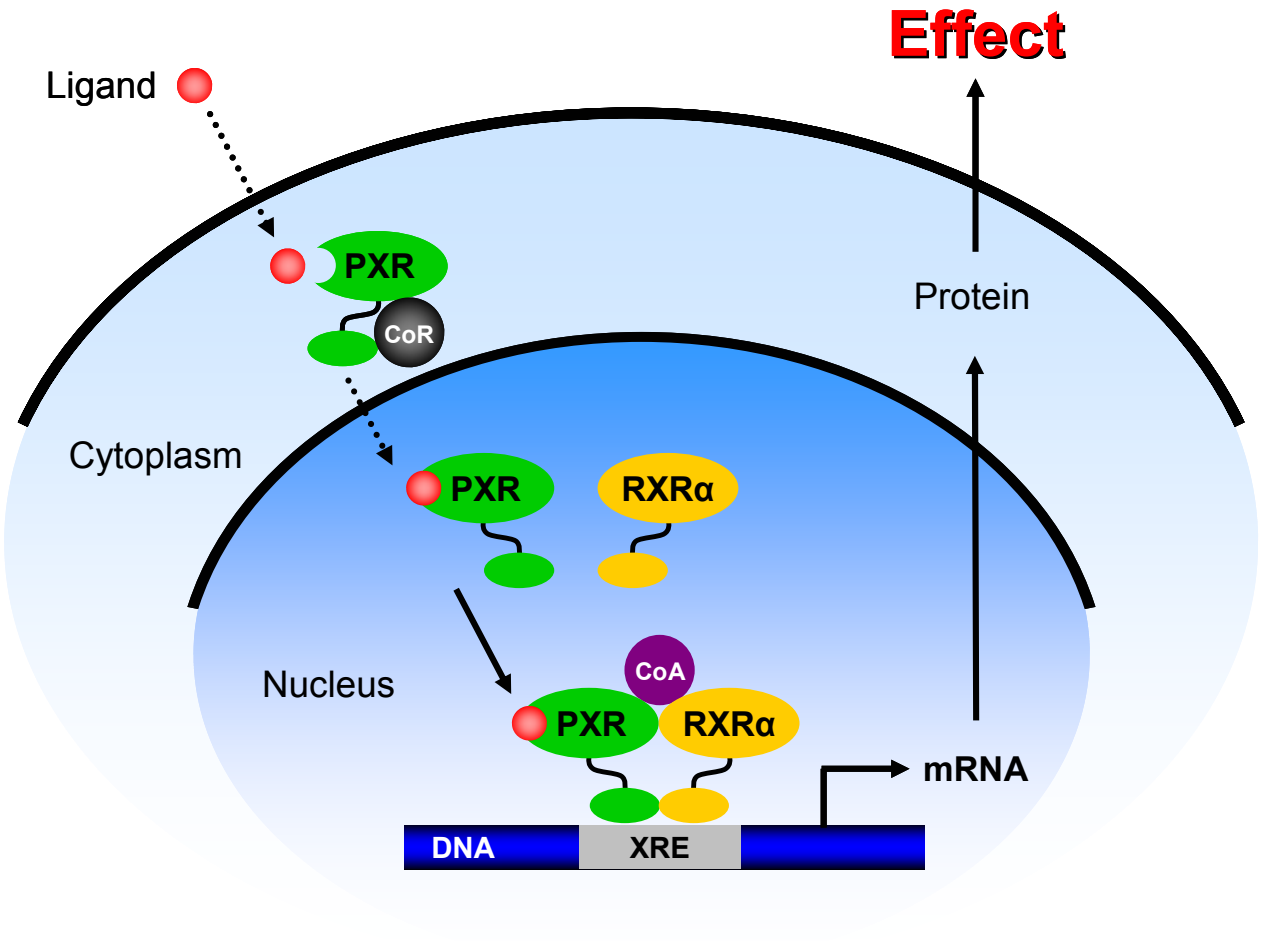

Figure 1.17
PXR signal transduction

A ligand binds to inactivated PXR in the cytoplasm. PXR undergoes a conformational change, the corepressor (CoR) dissociates. Activated PXR translocates into the nucleus and heterodimerizes with RXRα (retinoid X receptor α). The complex of PXR, RXR α and coactivators (CoA) binds to the xenobiotic response element (XRE) in the promoter region of a target gene. This results in increased transcription of the gene, and eventually increased protein expression and a physiological effect.

1.3.3.4 The Pregnane X Receptor – Regulation of Xenobiotic Defense

PXR defines a novel steroid-signaling pathway, because it is activated by naturally occurring steroids such as pregnenolone and progesterone, as well as synthetic glucocorticoids and antiglucocorticoids. Importantly, PXR is also activated by a wide range of xenobiotics, including dietary compounds, toxicants, and a large number of commonly prescribed drugs (Schuetz and Strom, 2001; Watkins et al., 2002). Upon activation, PXR coordinately regulates a number of target genes that are involved in xenobiotic phase I and phase II metabolism as well as phase III efflux transport (Figure 1.18). Therefore, PXR is considered to be a ‘‘master regulator’’ of xenobiotic removal (Dussault and Forman, 2002). Moreover, it is anticipated that PXR, xenobiotic metabolizing enzymes, and efflux transporters are regulated as a core network of defense mechanisms (Kliewer et al., 2002; Kliewer et al., 1998; Rosenfeld et al., 2003; Sonoda et al., 2003). Efflux transporters regulated by PXR include organic anion transporting polypeptide isoform 2, Oatp2 (*SLCO1A4*); bile salt export pump, BSEP (*ABCB11*); multidrug resistance-associated proteins isoforms 2 and 3, Mrp2 and Mrp3 (*ABCC2, ABCC3*); and P-glycoprotein, P-gp (*ABCB1, MDR1*) (Eloranta and Kullak-Ublick, 2005; Geick et al., 2001; Handschin and Meyer, 2003; Kliewer et al., 1998; Sonoda et al., 2003; Synold et al., 2001; Teng et al., 2003).

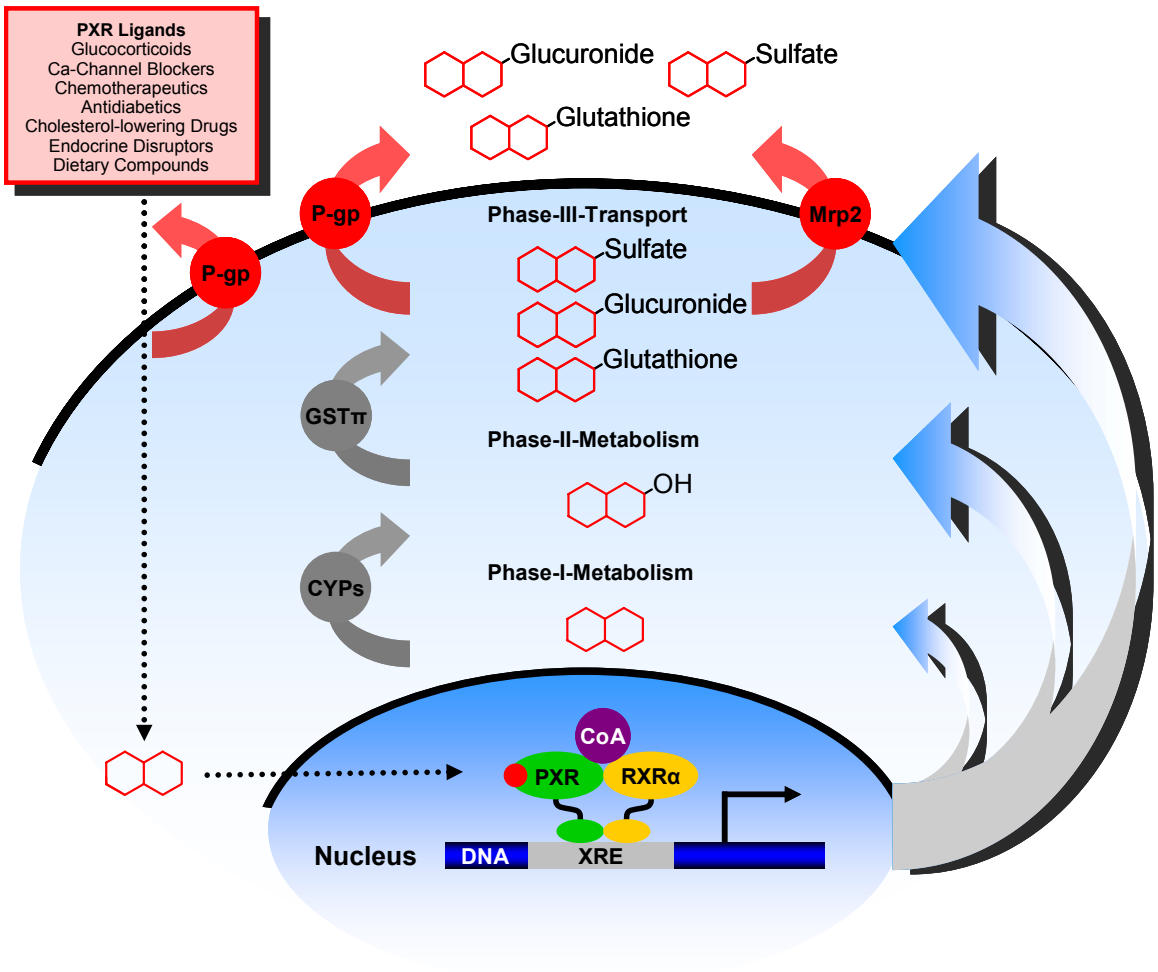

Figure 1.18
PXR – “Master Regulator” of metabolism and efflux transport
PXR coordinately regulates phase I and phase II metabolism as well as phase III efflux transport.

2 Objectives

Treatment of central nervous system (CNS) disorders is greatly impaired by poor CNS drug delivery. The structure responsible for low brain penetration is the non-fenestrated brain capillary endothelium that constitutes the blood-brain barrier. An important element of active, selective barrier function is the ATP-driven xenobiotic efflux transporter, P-glycoprotein (P-gp). Recently, P-gp has been shown to be highly expressed in the luminal membrane of the brain capillary endothelium, where it effectively restricts entry to the brain of a myriad of CNS drugs. Thus, understanding mechanisms that regulate P-glycoprotein is a key to improve therapy of CNS disorders. At present however, nothing is known about regulation of P-glycoprotein expression and transport function at the blood-brain barrier.
The objective of this thesis was to uncover mechanisms of P-glycoprotein regulation using isolated rat brain capillaries as an *ex vivo* model of the blood-brain barrier. First, the model had to be characterized and validated by looking at structure, morphology and viability of isolated rat brain capillaries and by identifying efflux transporters and tight junctional proteins. The model was then used to address the following hypotheses:

1) Endothelin-1 regulates P-gp transport function at the blood-brain barrier.

Recent studies from Miller et al. using renal proximal tubules showed that the peptide hormone endothelin-1 (ET-1) rapidly reduced transport mediated by P-glycoprotein (Miller, 2002; Terlouw et al., 2001). This was the first finding that linked ET-1 to the control of xenobiotic efflux transport and that demonstrated ET-1 regulation of P-glycoprotein.

The *first objective* was to test the hypothesis that ET-1 regulates P-glycoprotein transport function in isolated rat brain capillaries over the short-term.

2) PXR regulates P-gp expression and transport function at the blood-brain barrier.

Recent reports focusing primarily on liver demonstrated transcriptional regulation of P-glycoprotein by the ligand-activated nuclear receptor, pregnane X receptor (PXR). PXR is considered to be a “master regulator” of xenobiotic removal and as such to regulate a core network of defense mechanisms including efflux transporters. Importantly, PXR is the only nuclear receptor known so far to regulate transcription of P-glycoprotein. Since PXR is expressed in excretory and barrier tissues and since P-gp is the major xenobiotic efflux transporter at the blood-brain barrier protecting the CNS, PXR might be involved in the regulation of P-glycoprotein in brain capillaries.

The *second objective* was to test the hypothesis that PXR is expressed in isolated rat brain capillaries where it regulates P-glycoprotein expression and transport function.

3 Results and Discussion

This section is divided into three parts:

3.1. The *Ex Vivo* Blood-Brain Barrier Model
This part describes isolated rat brain capillaries used to examine P-glycoprotein regulation at the blood-brain barrier.

3.2. Rapid Regulation of P-glycoprotein at the Blood-Brain Barrier by Endothelin-1
This part summarizes the results for rapid regulation of P-glycoprotein by endothelin-1 (Hartz et al., 2004).

3.3. Pregnane X Receptor Upregulation of P-glycoprotein Expression and Transport Function at the Blood-Brain Barrier
In this part the results are presented for long-term regulation of P-glycoprotein *in vitro* and *in vivo* by the nuclear receptor PXR (Bauer et al., 2004).

3.1 The *Ex Vivo* Blood-Brain Barrier Model

3.1.1 Isolation of Intact Rat Brain Capillaries

Isolated rat brain capillaries were used as an *ex vivo* model of the blood-brain barrier to study functional and transcriptional regulation of P-glycoprotein. Capillaries were isolated based on a method previously published by Goldstein et al., Dallaire et al. and Miller et al. (Dallaire et al., 1991; Goldstein et al., 1975; Miller et al., 2000) with modifications according to Hartz et al. (Hartz et al., 2004).
Brains were removed from euthanized rats and brain tissue was homogenized. Capillaries were separated from myelin by density centrifugation. Using a glass bead column, capillaries were purified from red blood cells, other contaminating cells and cell debris. The isolation yielded about 25-30 mg of enriched capillaries per gram brain tissue (wet weight). Figure 3.1 shows a representative image of isolated rat brain capillaries. In addition to capillaries, the capillary enriched fraction also contained some red blood cells, larger vessels and some cell debris.

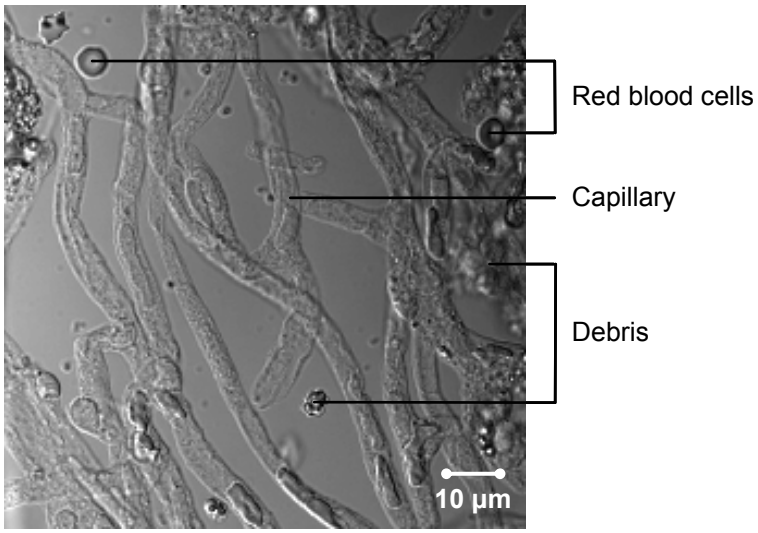

Figure 3.1
Transmitted light image of isolated rat brain capillaries
Capillaries were predominant in the isolated fraction. Besides capillaries, the fraction also contained some red blood cells and a small amount of debris.

After isolation, capillaries retained their tubular structure and showed active transport for at least 8 hours (Bauer et al., 2004). Thus, duration of experiments was limited to about 8 hours after isolation. Experiments were conducted by incubating isolated capillaries with modulators and fluorescent substrates. Transport was followed using a confocal microscope and images were analyzed with an imaging software program. The combination of isolated rat brain capillaries as an *ex vivo* model with laser scanning confocal microscopy proved to be a powerful tool to visualize and measure P-gp-mediated transport at the blood-brain barrier. (Bauer et al., 2004; Hartz et al., 2004; Miller et al., 2000; Nobmann et al., 2001).

3.1.2 Structure and Morphology of Isolated Rat Brain Capillaries

Isolated rat brain capillaries had a tubular structure; some capillaries were branched, and in some, red blood cells were entrapped in the lumens. Capillaries were 5-8 µm in diameter and approximately 100-200 µm in length with open lumens; capillary ends were collapsed. Figure 3.2 shows a representative transmitted light image of a branched rat brain capillary with an attached pericyte and a red blood cell in the lumen. All of the findings are in accordance with previous reports on the structure of isolated brain capillaries by Dallaire et al. and Miller et al. (Dallaire et al., 1991; Miller et al., 2000).

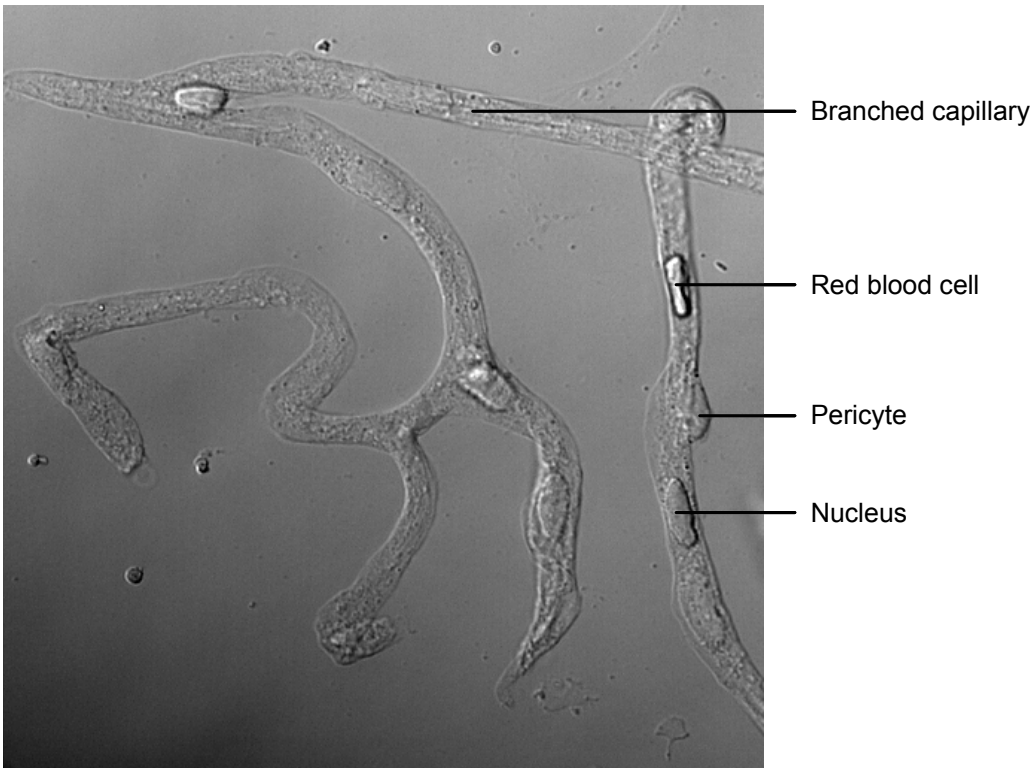

Figure 3.2
Transmitted light image of a branched rat brain capillary

The image shows a branched rat brain capillary. A pericyte is attached to the surface of the capillary and a red blood cell is entrapped in the capillary lumen.

Transmission electron microscopy (TEM) was used to further examine the integrity of isolated capillaries at the ultra-structural level. Intact mitochondria were detected in most capillaries, indicating structural and functional integrity. Figure 3.3 shows a TEM image of a capillary in cross-section: nucleus, mitochondria, vesicles, endothelial plasma membrane (luminal and abluminal) and the cytoplasm of the endothelial cell can be identified. A pericyte is attached to the endothelial cell and a red blood cell is entrapped in the capillary lumen.

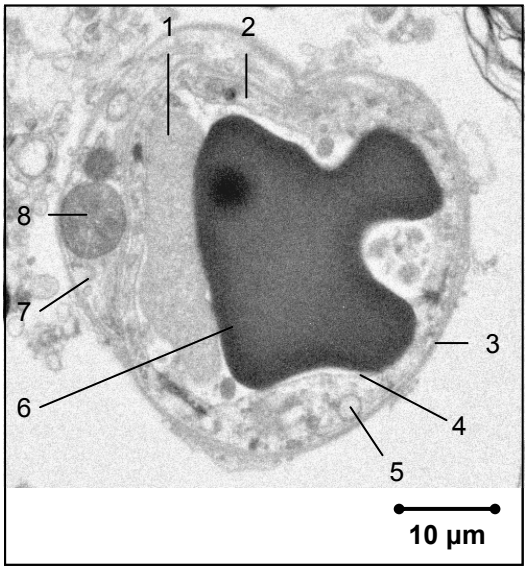

Figure 3.3
TEM image of a capillary in cross-section
(x 6,000)

1 Endothelial cell nucleus
2 Cytoplasm
3 Abluminal membrane
4 Luminal membrane
5 Vesicle
6 Red blood cell in capillary lumen
7 Pericyte
8 Mitochondrion of pericyte

Tight junctions were seen at higher magnification. Figure 3.4A shows a tight junction between two capillary endothelial cells; an arrow points to the focal connection. An enlargement of the tight junction with the focal connection between the two interacting plasma membranes is shown in Figure 3.4B.

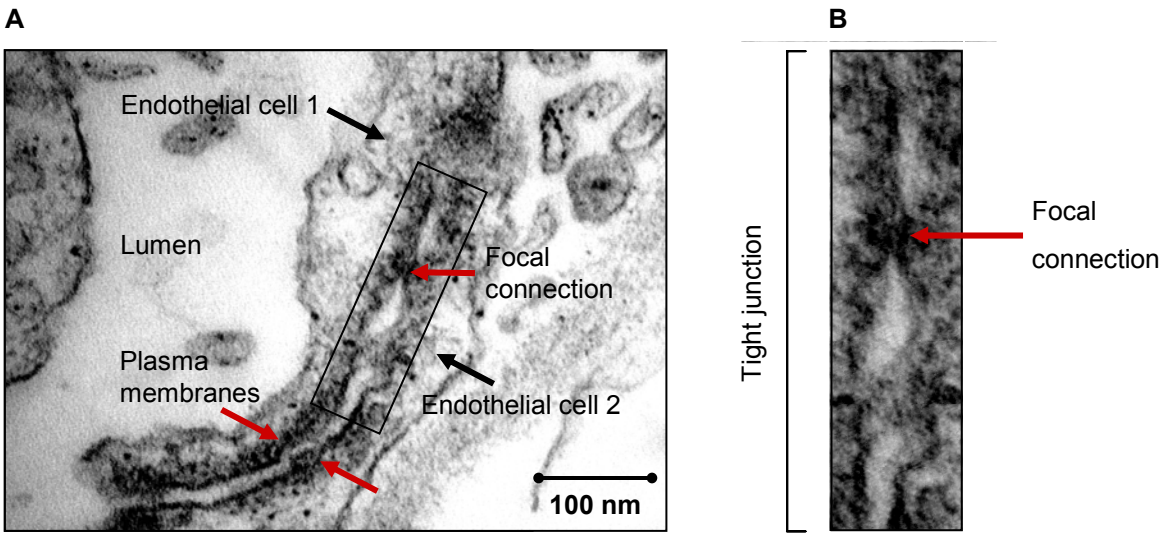

Figure 3.4
Tight junction between two brain endothelial cells

A: Structure of a tight junction between endothelial cells of brain capillaries (x 87,000)
B: Enlargement of the tight junction with focal connection

3.1.3 Viability of Isolated Rat Brain Capillaries

Isolated capillaries are metabolically active and readily oxidize glucose, fatty acids and pyruvate (Betz and Goldstein, 1986; Goldstein et al., 1975). Transport of glucose, amino acids and ions takes place as well (Betz and Goldstein, 1986). However, unlike endothelial cells in culture, isolated capillaries maintain their metabolic activity for only a short period of time. Limited viability of isolated capillaries is likely due to a decrease of ATP. Despite a period of up to 42 hours between death and isolation of the capillaries, Choi and Pardridge demonstrated that many biochemical functions remained in isolated capillaries from human (Choi and Pardridge, 1986). Capillaries from killifish were viable for up to 24 hours, whereas viability of capillaries from pig and rat was reported to last only for about 4-8 hours (Miller et al., 2002a; Miller et al., 2000).

To test the viability of isolated rat brain capillaries, energy-dependent P-gp-mediated NBD-CSA transport was monitored over a period of 24 hours. 1 mM sodium cyanide (NaCN) was used as a metabolic inhibitor to block ATP synthesis; 5 µM PSC833 was used to directly inhibit P-gp. Figure 3.5 shows P-gp-mediated transport of NBD-CSA into capillary lumens 0, 6 and 24 hours after isolation. NaCN and PSC833 decreased luminal NBD-CSA fluorescence to about 50% of untreated capillaries at 0 and 6 hours. The effects of both inhibitors were the same for freshly isolated capillaries and capillaries maintained in buffer for 6 and 24 hours indicating complete inhibition by NaCN and PSC833. The uninhibited component (insensitive to NaCN and PSC833) is approximately 50% of control values and likely reflects non-specific NBD-CSA binding. Accumulation of NBD-CSA remained unchanged over a period of 6 hours. In contrast, luminal NBD-CSA fluorescence decreased after 24 hours to the same levels seen for capillaries treated with NaCN and PSC833 indicating loss of energy-dependent transport after 24 hours. Obviously, capillaries maintained in buffer retain transport function for at least 6 hours, but not 24 hours.

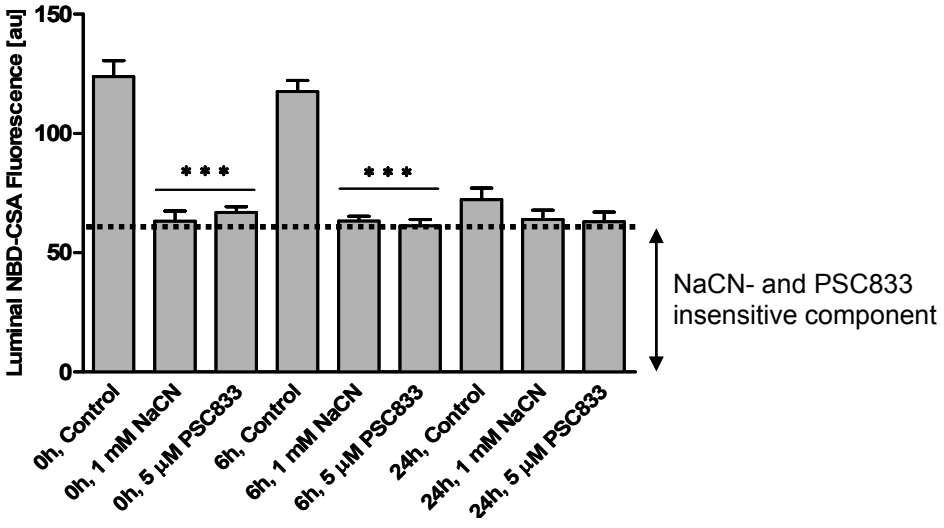

Figure 3.5
P-gp-mediated transport of NBD-CSA into capillary lumens 0, 6 and 24 hours after isolation

NBD-CSA fluorescence in capillary lumens was unchanged after 6 hours and about twice the luminal fluorescence of capillaries treated with NaCN and PSC833. After 24 hours, luminal fluorescence in untreated capillaries and capillaries treated with NaCN and PSC833 was the same, indicating absence of energy-dependent transport of NBD-CSA. The component insensitive to NaCN and PSC833 reflects non-specific binding (mean ± SEM, n=10, $^{***}p < 0.001$ compared to controls).

3.1.4 Detection of Proteins Expressed in Isolated Rat Brain Capillaries

3.1.4.1 Tight Junction Proteins

3.1.4.1.1 ZO-1 (*TJP1*)

The **z**onula **o**ccludens proteins (ZO-1, ZO-2, ZO-3) are named after their localization at the *zonula occludens* (Latin: *zonula occludens* = tight junctions), the structure forming tight junctions (Vorbrodt and Dobrogowska, 2003). ZO-1 was the first tight junction-associated protein to be identified (Stevenson et al., 1986). It is always part of tight junctions but was also found in cells without the tight junction protein complex such as astrocytes (Howarth et al., 1992). In the brain, all ZO proteins are ubiquitously expressed (Dermietzel and Krause, 1991).

The ZO proteins belong to the MAGUK protein family (**m**embrane-**a**ssociated **gu**anylate **k**inase-like proteins). Members of this family possess 3 defined core regions: a SH3 (src-homology 3) domain, a PDZ (**p**ostsynaptic density protein, **d**isc-large, **Z**O-1) domain and a domain for guanylate kinase. These domains are important for the interaction of ZO proteins with other junction proteins like occludin and claudin (Kniesel and Wolburg, 2000; Wolburg and Lippoldt, 2002). The ZO proteins are located submembranously below the plasma membrane. They are considered to form a link between tight junctions and the cytoskeleton to stabilize transmembrane proteins. In addition, they are thought to play a role in signal transduction (Bazzoni and Dejana, 2004).

Using Western blot analysis, ZO-1 was detected in brain homogenate, capillary lysate and capillary membrane fraction at 220 kDa (Figure 3.6). This molecular weight is in accordance with the molecular weight reported in the literature (Stevenson et al., 1986). The strong signal for ZO-1 from brain lysate correlates with previous findings showing that ZO-1 is abundantly expressed in the brain (Dermietzel and Krause, 1991; Howarth et al., 1992). Due to the association of ZO-1 with the membrane, capillary crude membranes also show a strong signal (Bazzoni and Dejana, 2004; Stevenson et al., 1986).

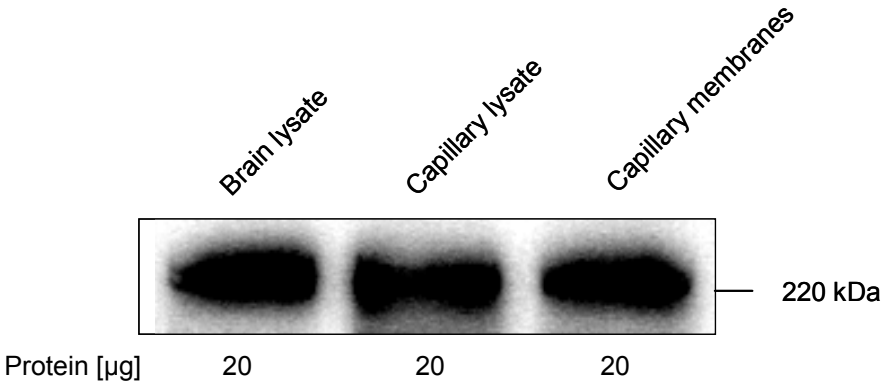

Figure 3.6
Western blot for ZO-1

ZO-1 is expressed in capillary membranes, capillary lysate as well as brain lysate, indicating expression also in other brain cells.

Figures 3.7A and B show isolated brain capillaries immunostained for ZO-1 (ZO-1 is green; nuclei are red). The staining displays bright and well-defined lines along cell-cell contacts. The negative control (incubation with secondary antibody only) shows no signal (Figure 3.7C).

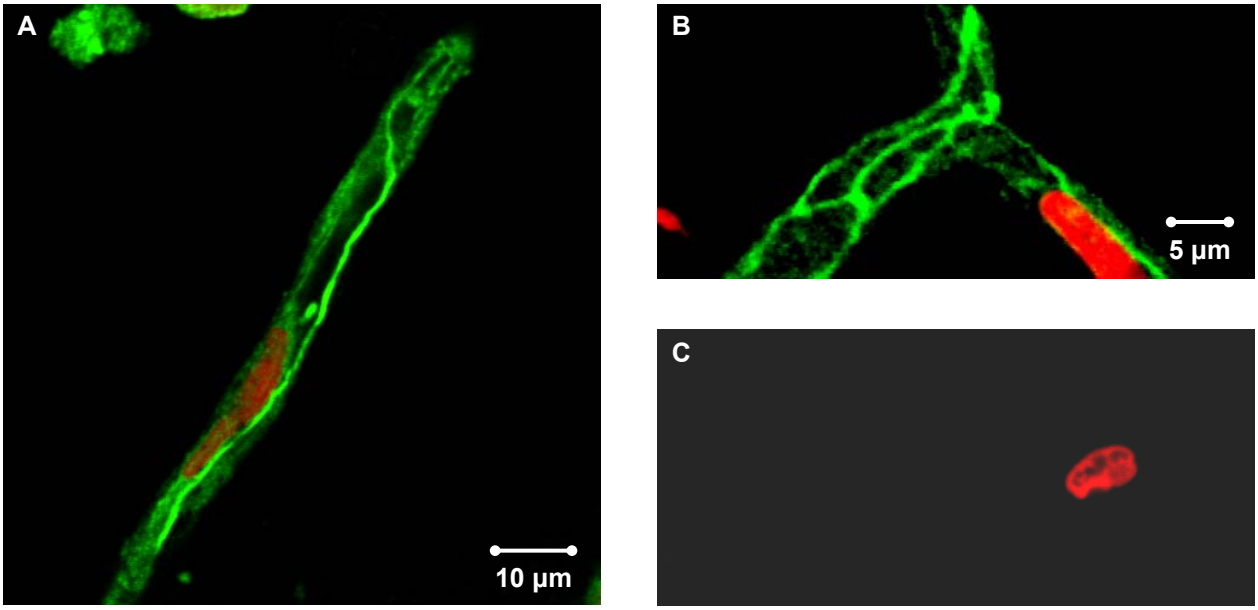

Figure 3.7
Immunostaining of capillaries for ZO-1

A and B: ZO-1 staining (green) along cell-cell contacts of brain capillaries, nuclei (red) are counterstained with propidium iodide

C: Negative control (green and red channel)

3.1.4.1.2 Occludin (*OCLN*)

Occludin (Latin: *occludere* = occlude) is a tight junctional transmembrane protein that consists of 4 membrane-spanning regions and 2 extracellular loops. Both amino and carboxy termini are localized in the cytoplasm; the carboxy terminal has a ZO-1 binding domain (Balda and Matter, 2000; Furuse et al., 1993; Kniesel and Wolburg, 2000). In the brain, occludin is expressed in neurons and astrocytes and at high levels in brain capillary endothelial cells. In other tissues occludin is expressed at much lower levels (Vorbrodt and Dobrogowska, 2003). Although it is not required for the formation of tight junctions, occludin is considered to regulate barrier properties by sealing the junctions and contributing to intercellular adhesion (Wolburg and Lippoldt, 2002). In addition, there is evidence that occludin regulates size-selective paracellular diffusion of hydrophilic molecules and facilitates transepithelial migration of leukocytes at the blood-brain barrier (Balda and Matter, 2000; Huber et al., 2000).
Figure 3.8 shows a Western blot for occludin. The protein was detected at 65 kDa, which is consistent with the molecular weight reported in the literature (Furuse et al., 1993). Due to low levels of occludin in the brain, no signal was found in total brain lysate (Vorbrodt and Dobrogowska, 2003). There is a weak signal for occludin in the capillary fraction and a strong signal in the membrane fraction. This enrichment confirms previously published data on the localization of occludin in brain capillaries (Furuse et al., 1993; Kniesel and Wolburg, 2000).

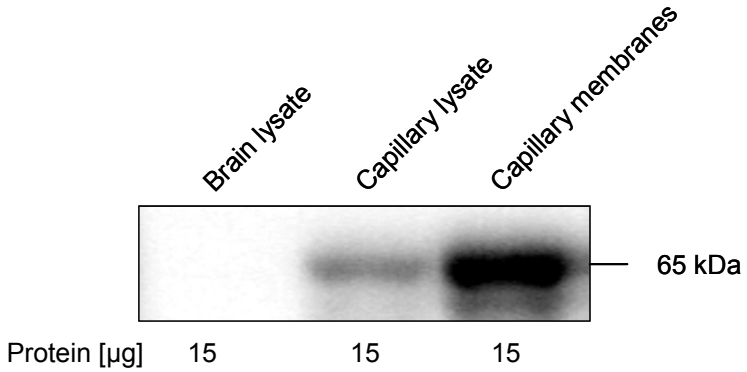

Figure 3.8
Western blot for occludin
Occludin is highly enriched in capillary membranes compared to capillary lysate. Brain lysate does not express occludin.

Figure 3.9 shows occludin immunostaining (green) in isolated rat brain capillaries (Figures 3.9A and B). Nuclei are counterstained with propidium iodide (red). The staining suggests localization of occludin along cell-cell contacts. This has previously been reported by Furuse et al. (Furuse et al., 1993). There is no signal in the negative control (Figure 3.9C).

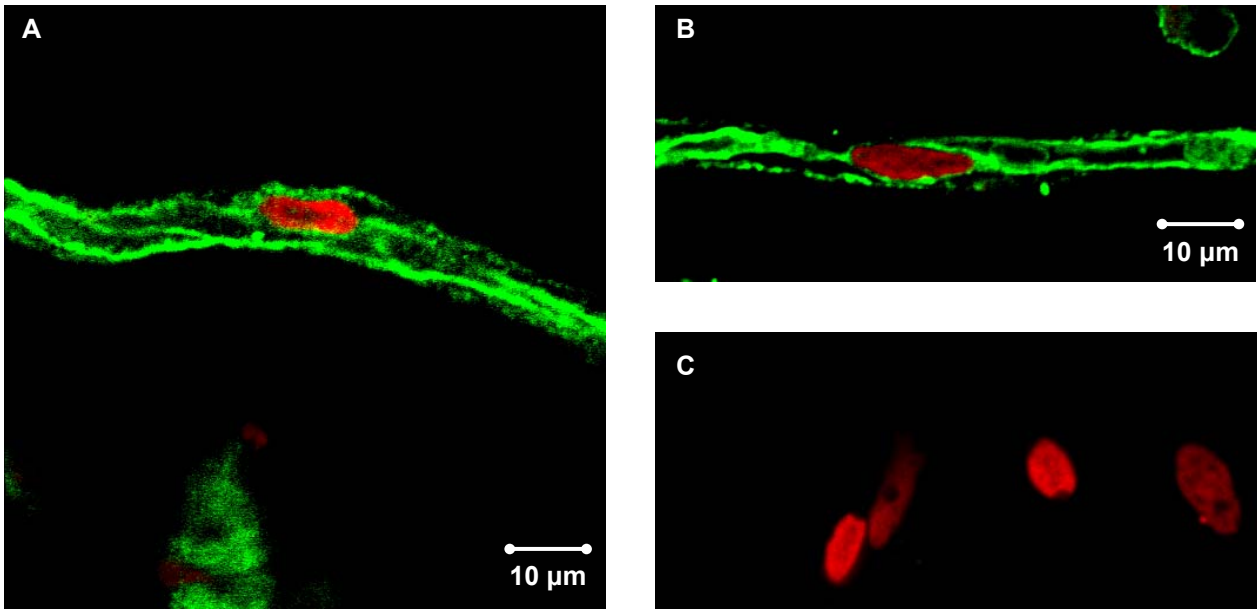

Figure 3.9
Immunostaining of capillaries for occludin

A and B: Occludin staining (green) along cell-cell contacts of brain capillaries, nuclei (red) are counterstained with propidium iodide

C: Negative control (green and red channel)

3.1.4.1.3 Claudin-1 and Claudin-5 (*CLDN1* and *CLDN5*)

Claudins (Latin: *claudere* = to close) are transmembrane proteins that are essential for the formation of tight junctions. They consist of 4 transmembrane domains, 2 extracellular loops and 2 cytoplasmic terminals (Furuse et al., 1998; Turksen and Troy, 2004). Claudins form dimers and bind to claudins on adjacent cells to produce the primary seal of tight junctions. They constitute the backbone of the tight junctional strands and are the major structural element of the actin-myosin fibrils. Thus, claudins create a tight junctional barrier and determine barrier properties (Anderson, 2001).
Currently, 24 claudin isoforms are known in humans. However, at the blood-brain barrier only claudin-1 and claudin-5 have been detected, where they regulate and maintain blood-brain barrier function (Morita et al., 1999). Nitta et al. showed that claudin-5 selectively increased permeability of molecules smaller than 800 Da (Nitta et al., 2003). Therefore, claudin-5 is believed to be a critical regulator of blood-brain barrier permeability (Matter and Balda, 2003a).
The Western blot for Claudin-1 (Figure 3.10) shows weak bands for brain and capillary lysate and a strong band for capillary membranes. This indicates enrichment of claudin-1 in the membrane fraction. In accordance with the literature, the claudin-1 bands appear at 22 kDa (Furuse et al., 1998).

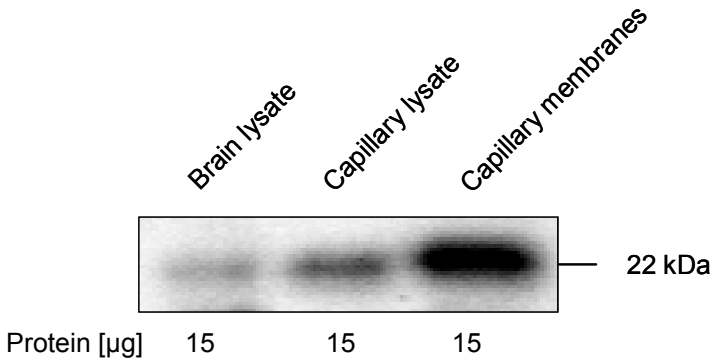

Figure 3.10
Western blot for claudin-1

Claudin-1 is highly enriched in capillary membranes.
Brain and capillary lysate show only weak bands.

Images of capillaries immunostained for claudin-1 (green) display staining along cell-cell contacts of capillary endothelial cells (Figures 3.11A and B). The negative control shows no signal (Figure 3.11C).

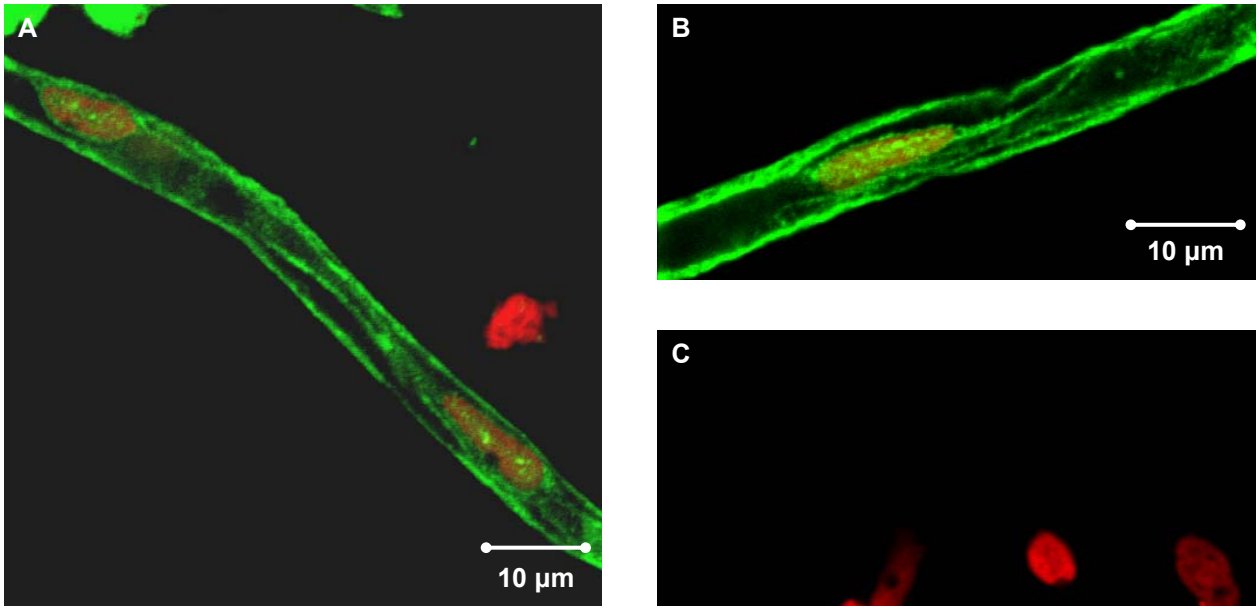

Figure 3.11
Immunostaining of capillaries for claudin-1

A and B: Claudin-1 staining (green) along cell-cell contracts; nuclei (red) are counterstained with propidium iodide

C: Negative control (green and red channel)

The Western blot for claudin-5 shows bands with capillary lysate and capillary membranes at 22 kDa (Figure 3.12). The signal for capillary lysate is slightly higher than the signal for the capillary membranes. Brain lysate shows no signal for claudin-5.

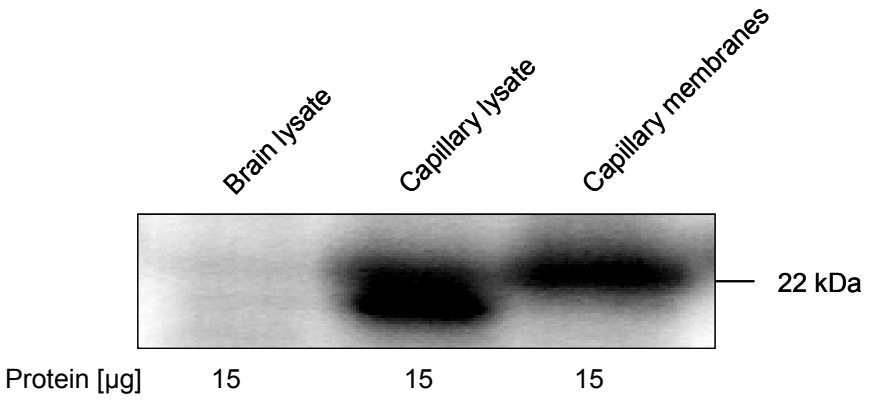

Figure 3.12
Western blot for claudin-5

Capillary lysate and capillary membranes show intense bands for claudin-5; brain lysate shows no signal.

3.1.4.1.4 JAM-A (*F11R*)

The 3 homologous **j**unctional **a**dhesion **m**olecule proteins (JAM-A, -B, -C) are members of the immunoglobulin superfamily. They are single-span proteins with 2 immunoglobulin-like domains and a short cytoplasmic tail with a PDZ-binding motif (Bazzoni and Dejana, 2004; Martin-Padura et al., 1998). JAM proteins associate laterally with tight junctional strands and mediate homophilic and heterophilic interactions in the tight junctional region (Nitta et al., 2003). Besides facilitating the assembly of tight junctions, they are also involved in the transmigration of leukocytes (Anderson, 2001; Bazzoni and Dejana, 2004). JAM-A contributes to the organization of tight junctions by interfering with other junctional proteins like ZO-1 via the PDZ binding motif (Wolburg and Lippoldt, 2002).
The Western blot in Figure 3.13 shows no JAM-A signal for brain lysate, a moderate band for capillary lysate and a strong band for capillary membranes. This indicates that JAM-A is associated with the membrane. The bands for JAM-A come at 32 kDa, which is consistent with previous reports (Bazzoni and Dejana, 2004; Martin-Padura et al., 1998).

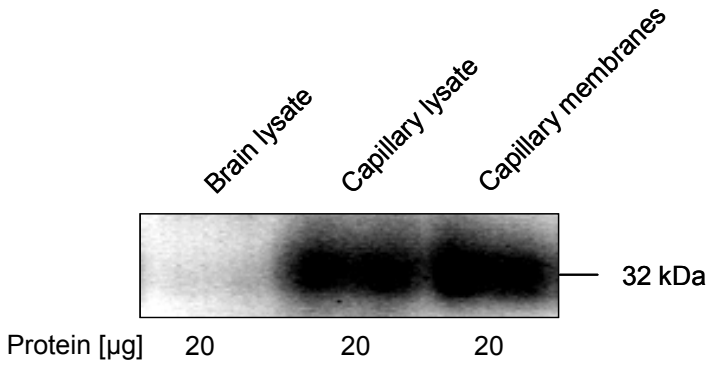

Figure 3.13
Western blot for JAM-A

JAM-A was detected in capillary lysate and capillary membranes, but not in brain lysate.

3.1.4.2 Transport Proteins

3.1.4.2.1 GLUT-1 (*SLC2A1*)

GLUT-1 (**Glu**cose **T**ransport Facilitator 1) is a uniporter facilitating glucose transport into the brain along a concentration gradient. Within the brain, GLUT-1 is predominantly expressed in brain capillaries (Boado and Pardridge, 1990; Pardridge et al., 1990a). Therefore, GLUT-1 is considered to be a blood-brain-barrier-specific protein (Nag, 2003; Orte et al., 1999). Although the brain corresponds to only 2% of the body weight, it metabolizes 20% of the total energy of the body (75 mg glucose/minute). This demand for energy of the brain is served by GLUT-1, which is expressed at the abluminal and luminal membranes of the capillaries in a ratio of 4:1 (Farrell and Pardridge, 1991). The capacity of the brain to store energy is very limited. Therefore, it is almost exclusively dependent on GLUT-1-mediated glucose transport, demonstrating the importance of GLUT-1 for proper brain function (Peters et al., 2004).
Figure 3.14 shows a Western blot for GLUT-1. The transporter was detected at 42 kDa in rat brain capillary lysate and capillary membrane fraction. 10 µg of total protein from capillary lysate gave a weak signal, while 0.1 µg of total membrane protein was sufficient for the detection of GLUT-1 in the membrane fraction. A stronger band was obtained for 1 µg of capillary membranes than for 10 µg of total capillary lysate, indicating that GLUT-1 is highly enriched in the capillary membrane. In brain homogenate, GLUT-1 was not detectable. Similar observations have been made before by several other groups (Bolz et al., 1996; Farrell and Pardridge, 1991; Pardridge et al., 1990a; Stewart et al., 1994).

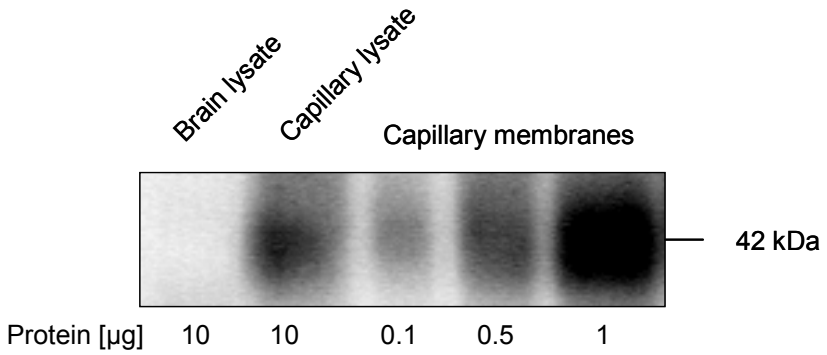

Figure 3.14
Western blot for GLUT-1

Capillary lysate and capillary membranes show bands for GLUT-1. 0.1-1 µg of total membrane protein display strong signals for GLUT-1. In brain lysate, GLUT-1 was undetectable.

3.1.4.2.2 Na^+/K^+-ATPase (*ATP1A1-4*, *ATP1B1-4*)

The Na^+/K^+ transporting ATPase (Na^+/K^+-ATPase) is a membrane transporter that maintains a high sodium and potassium gradient across the cell membrane. This electrochemical gradient is important for vital functions of every cell in the body. The Na^+/K^+-ATPase builds up this gradient by actively transporting 3 Na^+ ions out of the cell and 2 K^+ ions into the cell using the energy of ATP hydrolysis. In polarized cells such as brain capillary endothelial cells, Na^+/K^+-ATPase is located at the abluminal membrane transporting Na^+ ions from the cytoplasm of the endothelial cell into the brain interstitial fluid in exchange for K^+ ions (Betz et al., 1980). All its isoforms (α1-4 and β1-4) are expressed at the blood-brain barrier, where they are involved in K^+ regulation, fluid secretion and in maintaining a Na^+ gradient for facilitated nutrient transport (Betz, 1986; Betz and Goldstein, 1986; Zlokovic et al., 1993).
Figure 3.15 shows a Western blot for Na^+/K^+-ATPase α-1 (*ATP1A1*). At 110 kDa, intense bands were detected for brain lysate as well as for capillary membranes. Na^+/K^+-ATPase is slightly enriched in the capillary membrane when compared to brain lysate.

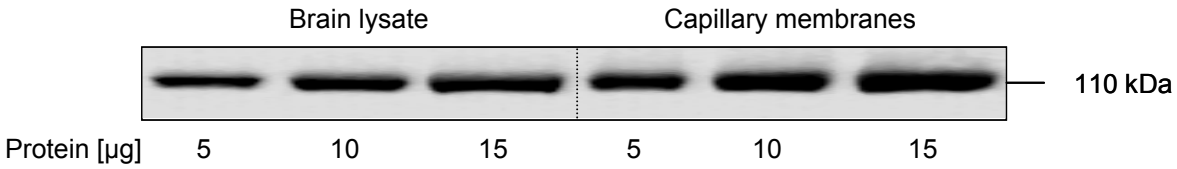

Figure 3.15
Western blot for Na^+/K^+-ATPase α-1

Brain lysate and capillary membranes show bands for Na^+/K^+-ATPase α-1 at 110 kDa. The signal for capillary membranes is slightly stronger, indicating an enrichment of Na^+/K^+-ATPase α-1 in capillary membranes.

Figure 3.16A shows a rat brain capillary immunostained for Na^+/K^+-ATPase α-1 (green). Nuclei were counterstained with propidium iodide (red). The negative control (incubation with secondary antibody only) shows no staining (Figures 16.B-E).

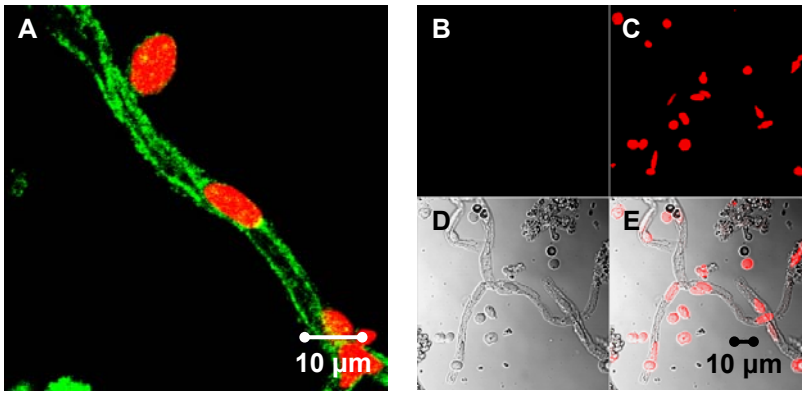

Figure 3.16
Immunostaining of capillaries for Na^+/K^+-ATPase α-1

A: Capillary immunostained for Na^+/K^+-ATPase α-1 (green) and counterstained for nuclei (red)
B: Negative control (green channel)
C: Negative control (red channel)
D: Transmitted light image
E: Overlay of images B, C and D

3.1.4.3 ABC Transporter Proteins

3.1.4.3.1 BCRP (*ABCG2*)

The **b**reast **c**ancer **r**esistance **p**rotein (BCRP, MXR (mitoxantrone resistance protein) or ABCP1) is an ABC half transporter that functions as a homodimer or possibly heterodimerizes with other ABCG isoforms (Hori et al., 2004). In addition to the endogenous substrate estrone-3-sulfate, exogenous compounds like daunorubicin, etoposide, methotrexate, rhodamine-123 and mitoxantrone as well as sulfated conjugates of sterols and drugs are transported by BCRP. Since there is an overlap in substrate specificity with P-gp, BCRP is considered to play a similar role in drug absorption and disposition. Like P-gp, BCRP can cause multidrug resistance (Sarkadi et al., 2004). BCRP is expressed at high levels in the placenta and lower levels in breast, ovary, small intestine, colon, liver and brain (Allikmets et al., 1998; Maliepaard et al., 2001; Sarkadi et al., 2004). Immunohistocemical studies demonstrated luminal localization of BCRP in rat and human brain capillaries (Cooray et al., 2002; Hori et al., 2004). At the blood-brain barrier, BCRP might be involved in brain-to-blood efflux transport of xenobiotics thereby restricting their penetration into the brain. However, so far there is no evidence for active BCRP-mediated drug efflux at the blood-brain barrier yet (Lee et al., 2005).
The Western blot for BCRP in Figure 3.17 shows a weak band for capillary lysate and a more intense band for capillary membranes (50 µg protein). Whole brain lysate shows no signal, whereas renal brush border membranes (positive control) showed a very strong signal with 5 µg of total protein. No signal was detected for brain lysate, but enrichment of BCRP in capillary membranes suggests that in the CNS BCRP is predominantly expressed in capillary membranes.

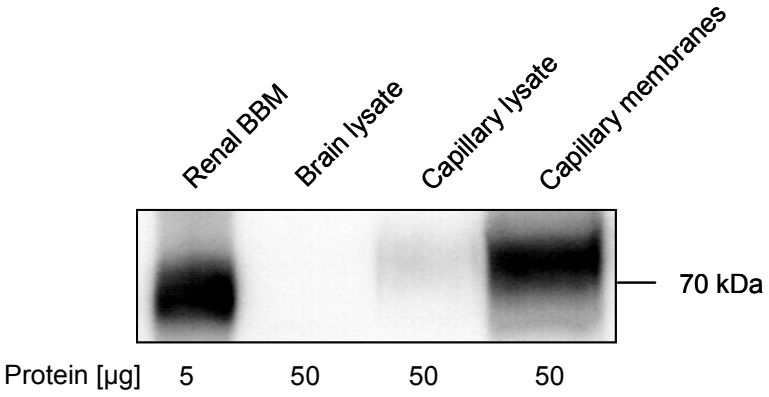

Figure 3.17
Western blot for BCRP

BCRP is highly enriched in capillary membranes compared to capillary lysate. Brain lysate does not show a BCRP signal, indicating expression restricted to brain capillaries. Renal brush border membranes (BBM) were used as positive control and showed strong BCRP expression with 5 µg of protein.

Capillaries immunostained for BCRP show distinct staining along the capillary membrane (Figure 3.18A). The images in Figure 3.18B and C indicate luminal localization of BCRP, which confirms the findings of Hori et al. and Zhang et al. (Hori et al., 2004; Zhang et al., 2003a). The negative control displays no staining (Figure 3.18D-G).

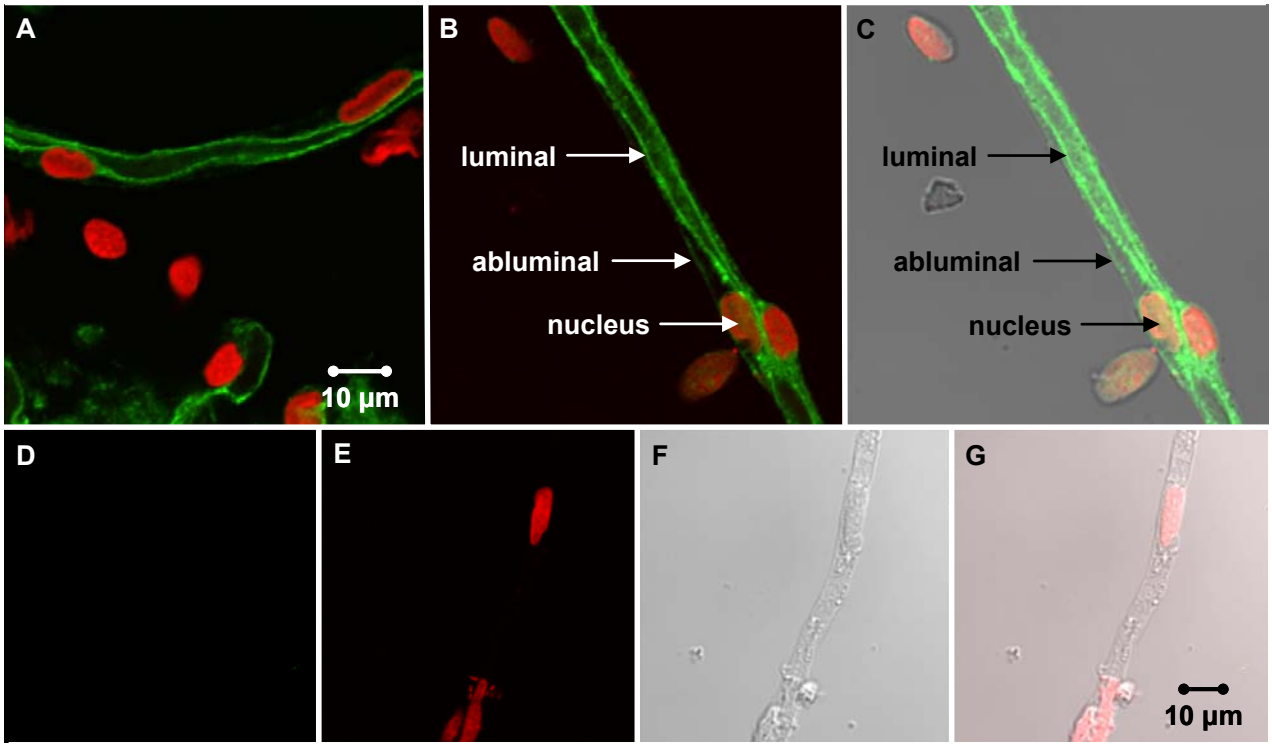

Figure 3.18
Immunostaining of brain capillaries for BCRP

A: Capillary immunostained for BCRP (green) and counterstained for nuclei (red)
B: Capillary immunostained for BCRP indicating luminal localization of BCRP
C: Overlay of transmitted light image and image B
D: Negative control (green channel)
E: Negative control (red channel)
F: Transmitted light image
G: Overlay of images D, E and F

3.1.4.3.2 Mrp1 (*ABCC1*)

Multidrug **r**esistance-associated **p**roteins (MRPs) are efflux transporters that are also members of the ABC superfamily. They mainly transport organic anions, glutathione, glucuronide or sulfate conjugated compounds and various nucleoside analogues. To date, 9 MRPs are known (http://www.gene.ucl.ac.uk/nomenclature/genefamily/abc.html). All MRPs contain 2 transmembrane domains connected by a cytoplasmic linker region that is necessary for proper transport function. As with P-glycoprotein, the MRPs can confer multidrug resistance (Lee et al., 2001a; Renes et al., 2000). Mrp1 is both glycosylated and phosphorylated. It is ubiquitously expressed in the body, with high levels in lung and kidney. Physiologically, Mrp1 seems to play a role in the regulation of intracellular redox potential, flux of organic anions, inflammatory mediation, and elimination of potentially toxic endo- and xenobiotics. Although it has been implicated in resistance to a number of anticancer agents (e.g. etoposide, doxorubicin, vincristine), its role in drug resistance is not yet fully understood (Cole et al., 1992; Lee et al., 2001a; Wijnholds, 2002). Within the brain, Mrp1 is expressed in astrocytes, microglia, capillary endothelial cells and choroid plexus (Dallas et al., 2003; Lee et al., 2001a; Schinkel, 2001). Recent studies localize Mrp1 to the luminal membrane in brain microvessel endothelial cells (Sugiyama et al., 2003a; Zhang et al., 2004a). However, localization and contribution of Mrp1 at the blood-brain barrier is controversial. Other groups have found Mrp1 in the abluminal membrane (Cisternino et al., 2003).
The Western blot for Mrp1 shows weak bands for brain and capillary lysate and a strong band for capillary membranes (Figure 3.19). This indicates enrichment of Mrp1 in capillary membranes, which is in accordance with previous findings (Schinkel, 2001).

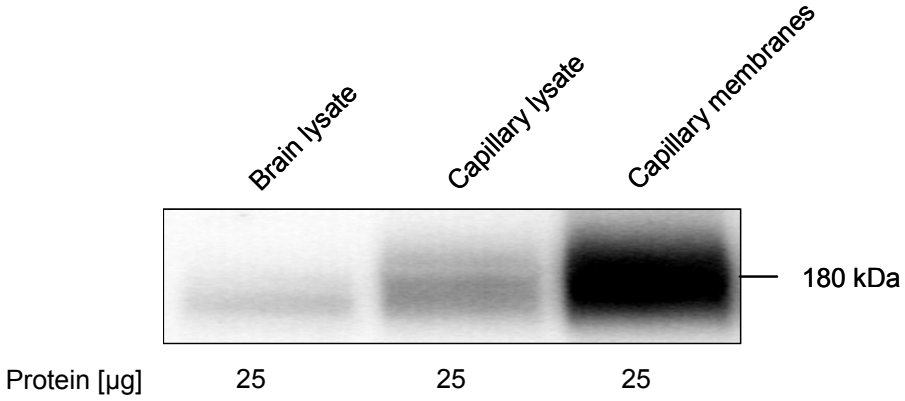

Figure 3.19
Western blot for Mrp1
Brain and capillary lysate show weak Mrp1 expression, whereas capillary membranes show strong Mrp1 expression.

Figure 3.20 shows Mrp1 immunostaining in rat brain capillaries. Mrp1 staining is located on the luminal rather than on the abluminal membrane (Figures 3.20A and B). The negative control shows no staining (Figures 3.20D-E).

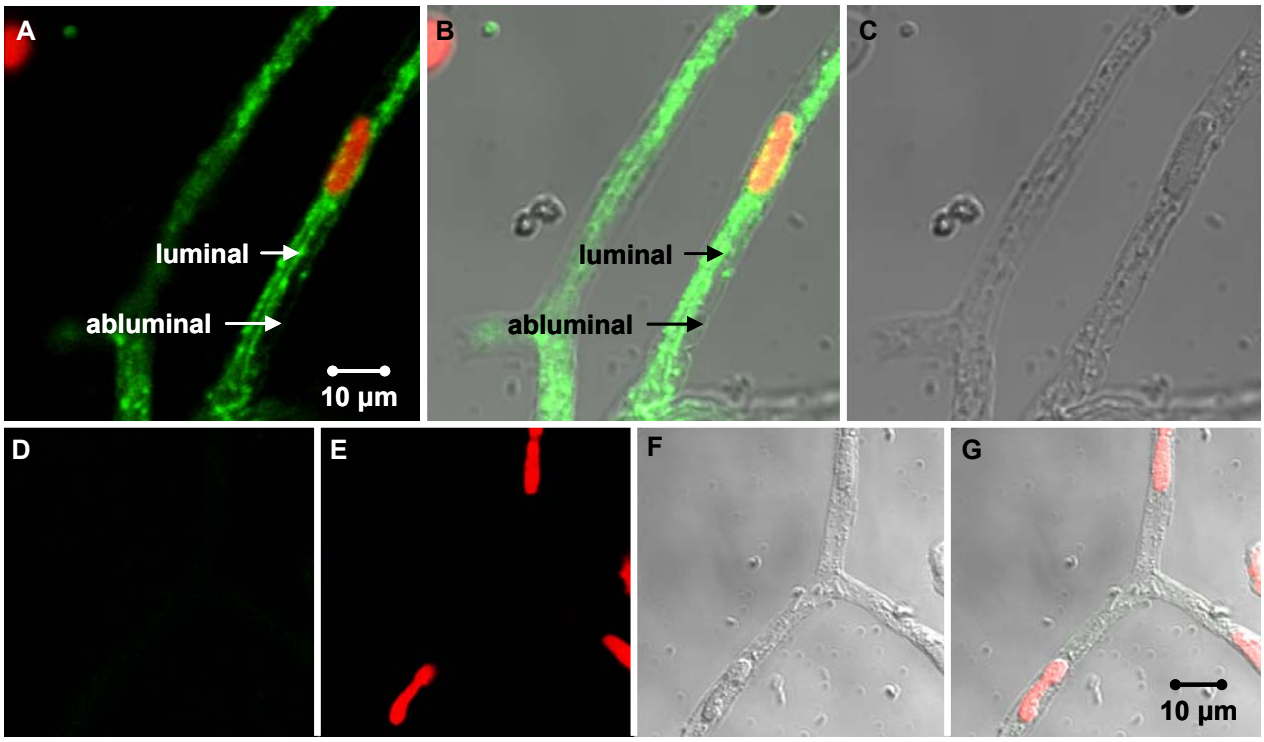

Figure 3.20
Immunostaining of capillaries for Mrp1

A: Image of a capillary immunostained for Mrp1 (green) and counterstained for nuclei (red)
B: Overlay of transmitted light image and image A
C: Transmitted light image
D: Negative control (green channel)
E: Negative control (red channel)
F: Transmitted light image
G: Overlay of images D, E and F

3.1.4.3.3 Mrp2 (*ABCC2*)

The **m**ultidrug **r**esistance-associated **p**rotein isoform 2 (Mrp2), also known as canalicular multispecific organic anion transporter (cMOAT), is mainly expressed in liver, intestine, and kidney tubules (Chan et al., 2004). Most of its substrates are glutathione, glucuronide or sulfate conjugates. Mrp2 plays an important role in the biliary excretion of glucuronated bilirubin: A mutation in the Mrp2 gene leads to a defect in Mrp2 protein causing accumulation of bilirubin and hepatic inflammation, a disease known as Dubin-Johnson Syndrome (Lee et al., 2001a). There are conflicting reports about the expression of Mrp2 at the blood-brain barrier. Using RT-PCR and Western blot analysis, Zhang et al. showed mRNA expression of Mrp1, 4, 5 and 6, but Mrp2 mRNA expression was undetectable in bovine brain microvessel endothelial cells as well as in capillary-enriched fractions (Zhang et al., 2000; Zhang et al., 2004a). However, Miller et al. detected Mrp2 protein expression and function in isolated rat and porcine brain capillaries (Fricker et al., 2002; Miller et al., 2002a; Miller et al., 2000). Furthermore, Potschka et al. demonstrated that Mrp2 contributes to barrier function by preventing entry of analeptic drugs into the CNS of rats (Potschka et al., 2003).
Using RT-PCR, no signal for Mrp2 was detected in brain (Figure 3.21, lane 1) and brain capillaries (lane 2), whereas kidney (lane 3) and liver (lane 4) displayed strong bands for Mrp2. This is in accordance with previous reports (Zhang et al., 2000; Zhang et al., 2004a).

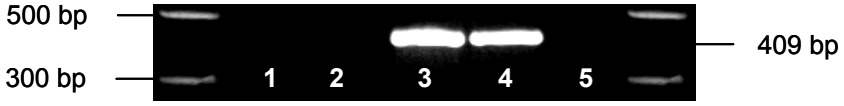

Figure 3.21
RT-PCR for Mrp2

No signal was detected for brain (lane 1) and brain capillaries (lane 2), but strong signals were found for kidney (lane 3) and liver (lane 4).

Although no Mrp2 mRNA could be detected in brain and brain capillaries, Mrp2 protein was found to be expressed in these tissues. The Western blot in Figure 3.22 shows Mrp2 expression in renal brush border membranes (BBM, positive control), brain lysate, capillary lysate and capillary membranes. In comparison to brain and capillary lysate, Mrp2 is slightly enriched in capillary membranes.

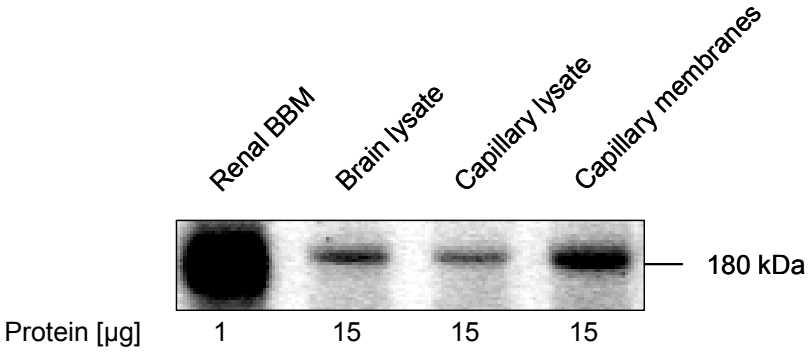

Figure 3.22
Western blot for Mrp2

Mrp2 expression was detected in renal brush border membranes (BBM), brain lysate, capillary lysate and capillary membranes.

Rat brain capillaries immunostained for Mrp2 (Figure 3.23) display distinct staining and suggest localization in the luminal membrane. The findings from Western blot and immunostaining confirm reports from Miller et al. (Miller et al., 2000). Based on these data, there is strong evidence for luminal expression of Mrp2 at the blood-brain barrier in the rat.

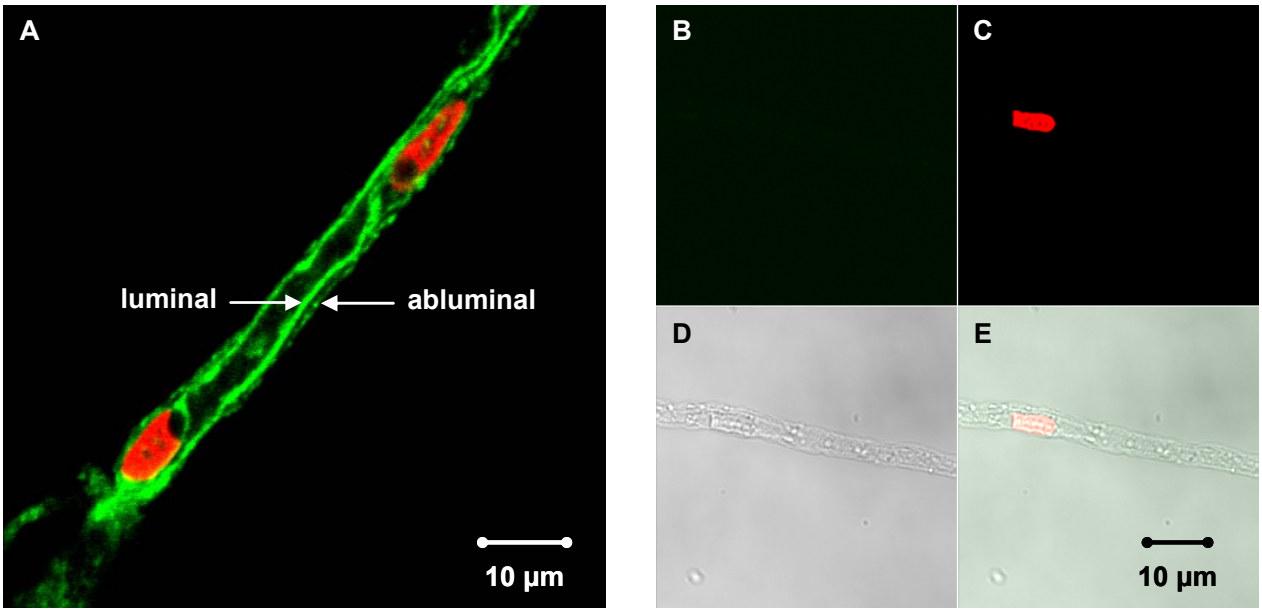

Figure 3.23
Immunostaining of capillaries for Mrp2

A: The image shows a capillary immunostained for Mrp2 (green) and counterstained for nuclei (red). The staining suggests luminal localization of Mrp2.
B: Negative control (green channel)
C: Negative control (red channel)
D: Transmitted light image
E: Overlay of images B, C and D

3.1.4.3.4 Mrp4 (*ABCC4*)

Another member of the multidrug resistance-associated protein family is Mrp4 (also MOAT-B), which is structurally closer to P-glycoprotein than any other Mrp transporter (Belinsky et al., 1998). Mrp4 is expressed in jejunum, kidney, lung, gallbladder and brain (Kool et al., 1997; Taipalensuu et al., 2001; van Aubel et al., 2002; Zhang et al., 2000). Leggas et al. were the first ones to show Mrp4 protein expression in brain capillaries and they localized it to the luminal membrane (Leggas et al., 2004). This was confirmed by Nies et al. in human brain capillaries (Nies et al., 2004). However, Zhang et al. reported Mrp4 protein in both luminal and abluminal membrane from bovine brain capillary endothelial cells (Zhang et al., 2003a; Zhang et al., 2000; Zhang et al., 2004a).
Originally, Mrp4 was considered to be a nucleotide analogue pump, transporting cyclic nucleotides such as cAMP and cGMP (Chen et al., 2001; Jedlitschky et al., 2004). However, Mrp4 also transports substrates like methotrexate, folic acid, estradiol-17-β-glucuronide, bile acids, and prostaglandins as well as antiviral and antiretroviral compounds (Adachi et al., 2002; Chan et al., 2004; Chen and Klaassen, 2004; Leggas et al., 2004). Recent studies have demonstrated that Mrp4 mediates resistance to purine analogues like nucleoside-based antiviral drugs and anticancer drugs like topotecan and thiopurines that are used for the treatment of acute lymphoblastic leukemia (Adachi et al., 2002; Leggas et al., 2004). These findings suggest that Mrp4 may contribute to blood-brain barrier function by protecting the brain from cytotoxic agents and that it may cause resistance to certain therapeutic drugs. However, the importance of Mrp4 in drug transport at the blood-brain barrier is not clear yet.
Mrp4 expression in rat brain capillaries was examined by Western blot and immunohistochemistry. The Western blot in Figure 3.24 shows bands for Mrp4 from renal brush border membranes, brain lysate, and capillary membranes. Capillary lysate shows no Mrp4 signal, indicating that Mrp4 is exclusively expressed in the membrane of brain capillaries. The band for Mrp4 from whole brain lysate suggests Mrp4 expression in other brain cells like astrocytes, neurons or microglia (Dallas et al., 2004; Nies et al., 2004).

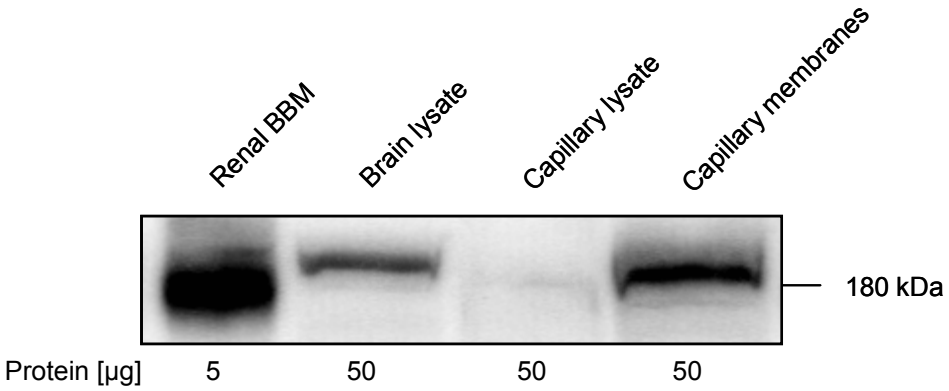

Figure 3.24
Western blot for Mrp4

Mrp4 expression in capillary membranes, but not capillary lysate. The Mrp4 signal for brain lysate is to be caused by Mrp4 expressed in other brain cells. Renal brush border membranes (BBM) served as positive control.

Images of capillaries immunostained for Mrp4 exhibit strong luminal staining (Figure 3.25A-B). Moreover, high magnification images show luminal and abluminal Mrp4 staining, suggesting expression in both membranes (Figure 3.25C). In addition to capillaries, blood cells in capillary lumens and other brain cells present in the preparation (indicated with white triangles in image A) display staining for Mrp4 as well. No staining was observed in the negative control (Figure 3.25D-G).

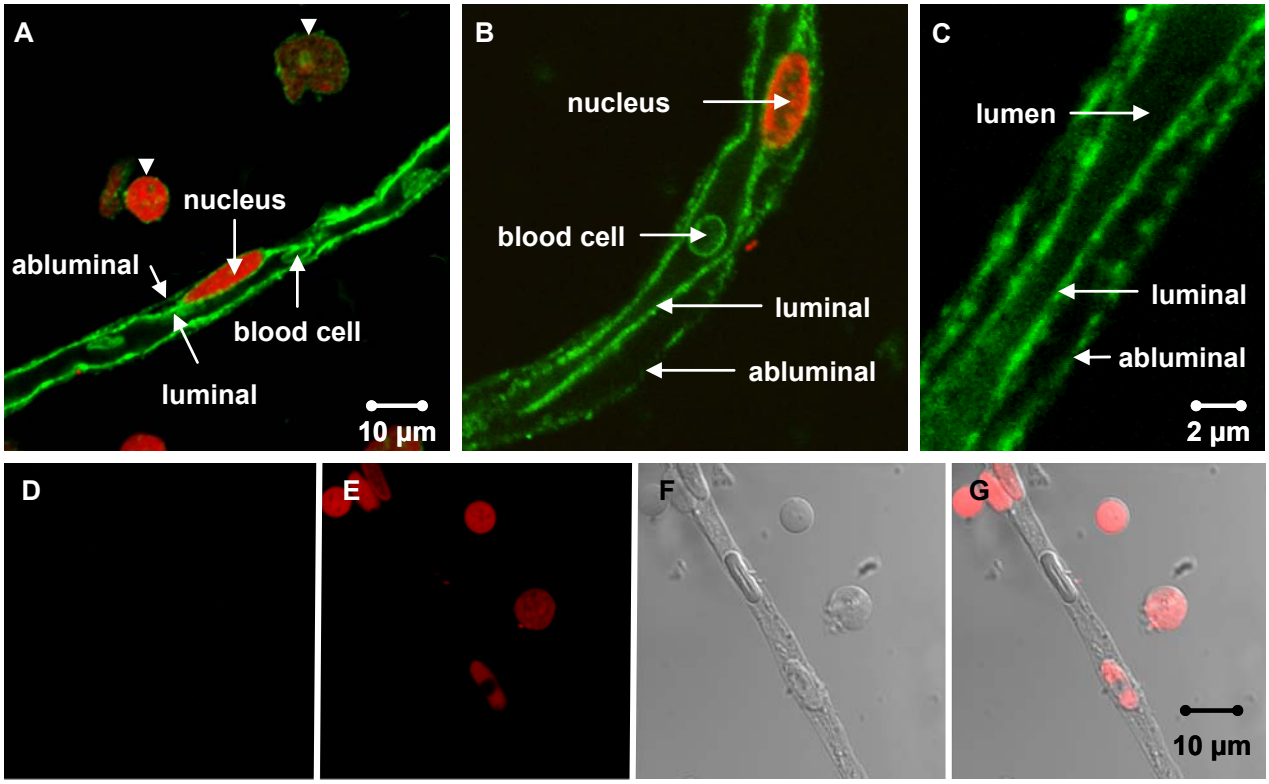

Figure 3.25
Immunostaining of capillaries for Mrp4

A-B: Capillaries immunostained for Mrp4 (green) and counterstained for nuclei (red). Strong luminal and weak abluminal staining for Mrp4. Blood cells as well as brain cells present in the preparation also express Mrp4 (white triangles in A).
C: Magnification of an immunostained brain capillary showing luminal and abluminal staining for Mrp4
D: Negative control (green channel)
E: Negative control (red channel)
F: Transmitted light image
G: Overlay of D, E and F

3.1.4.3.5 P-glycoprotein (*ABCB1*)

P-glycoprotein (P-gp) is a phosphorylated and glycosylated transmembrane protein that belongs to the ATP-binding cassette (ABC) superfamily (Lin and Yamazaki, 2003; Schinkel, 1999). P-gp functions as an efflux transporter that protects the body from toxic endogenous and exogenous compounds by pumping them out of cells. Since P-gp is expressed in barrier and excretory tissues, it is a key determinant for the absorption, distribution and elimination of a large number of xenobiotics including therapeutic drugs. Overexpression of P-gp, e.g. in tumor cells, leads to the phenomenon of multi-drug resistance. Therefore, the gene encoding P-gp protein is known as '***m****ulti****d****rug* ***r****esistance gene*' (*MDR1*). In rodents, P-gp is encoded by two genes, *mdr1a* and *mdr1b*, which have the same function as *MDR1* in humans (Fromm, 2004; Schinkel, 1999; Schinkel, 2001).
In the brain, multiple cell types such as astrocytes, microglia and choroid plexus epithelial cells express P-gp. However, the highest expression is found in capillary endothelial cells. In the luminal membrane of the capillary endothelium, P-gp contributes to the blood-brain barrier by protecting the CNS from potential toxins. The downside of this defense mechanism is restricted brain penetration of therapeutics, which complicates the therapy of many CNS disorders (Begley, 2004a; Jette et al., 1993; Lee et al., 2001b; Schinkel, 2001).
To detect P-gp expression in isolated capillaries, RT-PCR, Western blot and immunohistochemistry were performed. For RT-PCR, total RNA was isolated from capillaries, brain, choroid plexus, kidney and liver. After RT-PCR, amplification products were electrophoresed on an agarose gel. Signals for *mdr1a* (668 bp) and *mdr1b* (420 bp) were detected in all samples (Figure 3.26A and B). Negative controls (no RT product) showed no signal (lanes 6). Since the isolated capillary fraction contains other brain cells (see also 3.1.1 The *Ex Vivo* Blood-Brain Barrier Model), it cannot be ruled out that the signal for P-gp in the capillary fraction comes in part from contaminating cells. However, the signal for *mdr1a* is higher for capillaries (Figure 3.26A, lane 1) than for brain (Figure 3.17A, lane 2); therefore, it is likely that the *mdr1a* signal derives from the capillaries rather than other brain cells.

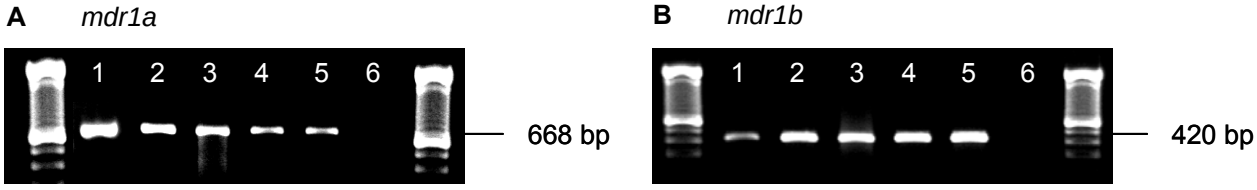

Figure 3.26
RT-PCR for *mdr1a* and *mdr1b*

A: ***mdr1a***
capillaries (lane 1), brain (lane 2), choroid plexus (lane 3), kidney (lane 4), liver (lane 5), negative control (lane 6)

B: ***mdr1b***
capillaries (lane 1), brain (lane 2), choroid plexus (lane 3), kidney (lane 4), liver (lane 5), negative control (lane 6)

In order to detect P-gp protein expression, two different antibodies were used, C219 and mdr Ab-1. C219 is a monoclonal antibody that recognizes a highly conserved cytoplasmic amino acid sequence; mdr Ab-1 is a polyclonal antibody that recognizes a cytoplasmic C-terminal epitope of P-gp. Rat brain lysate was used for comparison and rat kidney brush border membranes were used as positive control (Jette and Beliveau, 1993; Thiebaut et al., 1987).
Figure 3.27A shows a Western blot for P-gp detected with C219. In Figure 3.27B, mdr Ab-1 was used to detect P-gp. All bands for P-gp come at about 180 kDa. Both blots exhibit very low background signal. The blot developed with C219 (Figure 3.27A) shows no signal for brain lysate and a weak band for P-gp with brush border membranes (15 µg of total protein each). For capillary membranes, P-gp was detected with total protein as low as 0.1 µg. 15 µg total membrane protein showed a very strong signal. Using mdr Ab-1 antibody (Figure 3.27B), P-gp was detected in brain lysate (10 µg protein) and brush border membranes (5 µg protein). 0.01 µg protein were sufficient to detect P-gp in capillary membranes; 1 µg protein shows an intense band.

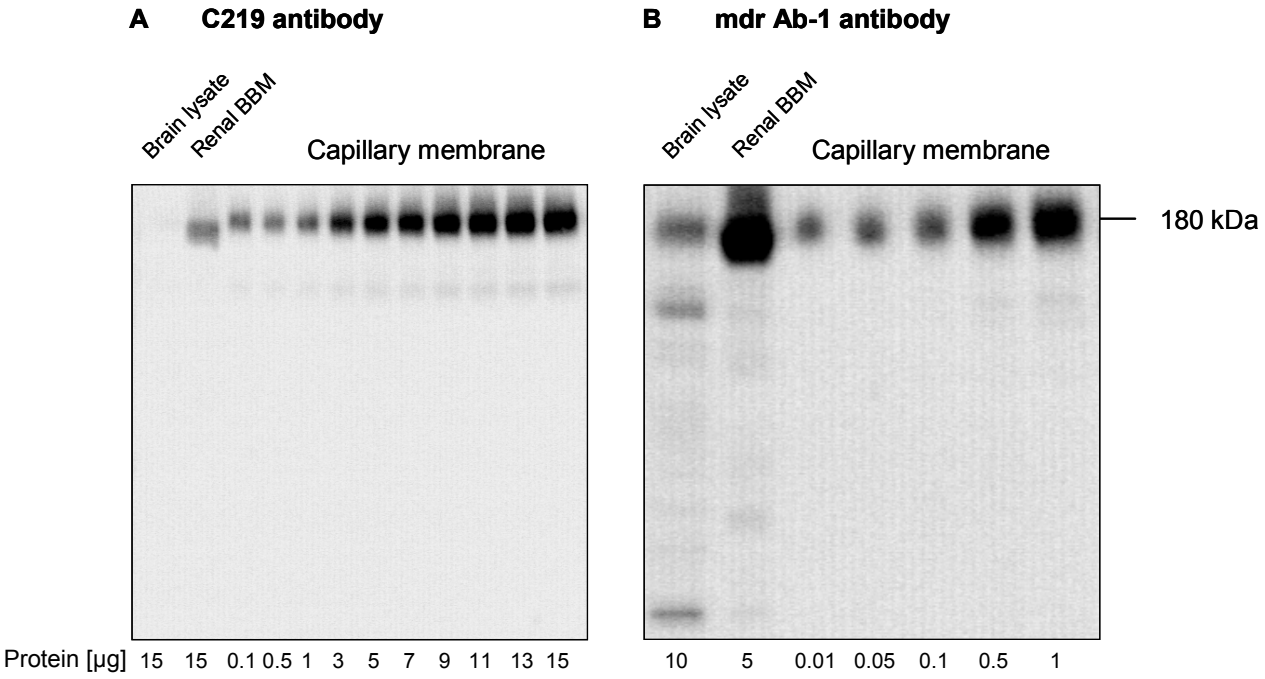

Figure 3.27
Western blot for P-glycoprotein using C219 and mdr Ab-1 antibody

A: **P-gp detected with C219 antibody**
The blot developed with C219 shows no signal for brain lysate, a weak signal for renal brush border membranes (BBM) and strong bands for capillary membranes. Band intensities increase with increasing protein amount.

B: **P-gp detected with mdr Ab-1 antibody**
Using the polyclonal mdr Ab-1 antibody, P-gp was detected in brain lysate, renal brush border membranes (BBM) and capillary membranes. 0.01 µg protein were sufficient for the detection of P-gp in capillary membranes.

Using the slot blot technique, 0.01 µg of total capillary membrane protein were sufficient to detect P-gp with C219 antibody (Figure 3.28). The signal for P-gp increased with increasing protein amounts of capillary membranes.

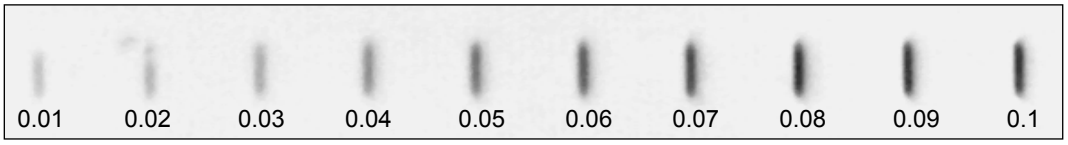

Figure 3.28
Slot blot for P-glycoprotein using C219
Detection of P-gp in capillary membranes on a slot blot using C219 antibody. 0.01 µg protein were sufficient to obtain a signal for P-gp with C219.

Figure 3.29 shows isolated capillaries immunostained for P-gp using C219 (Figure 3.29A) or mdr Ab-1 (Figure 3.29B), respectively. Nuclei were counterstained with propidium iodide. Luminal staining for P-gp was obtained with both antibodies. The negative controls for both antibodies showed no signal (Figures 3.29A1-4 and B1-4).

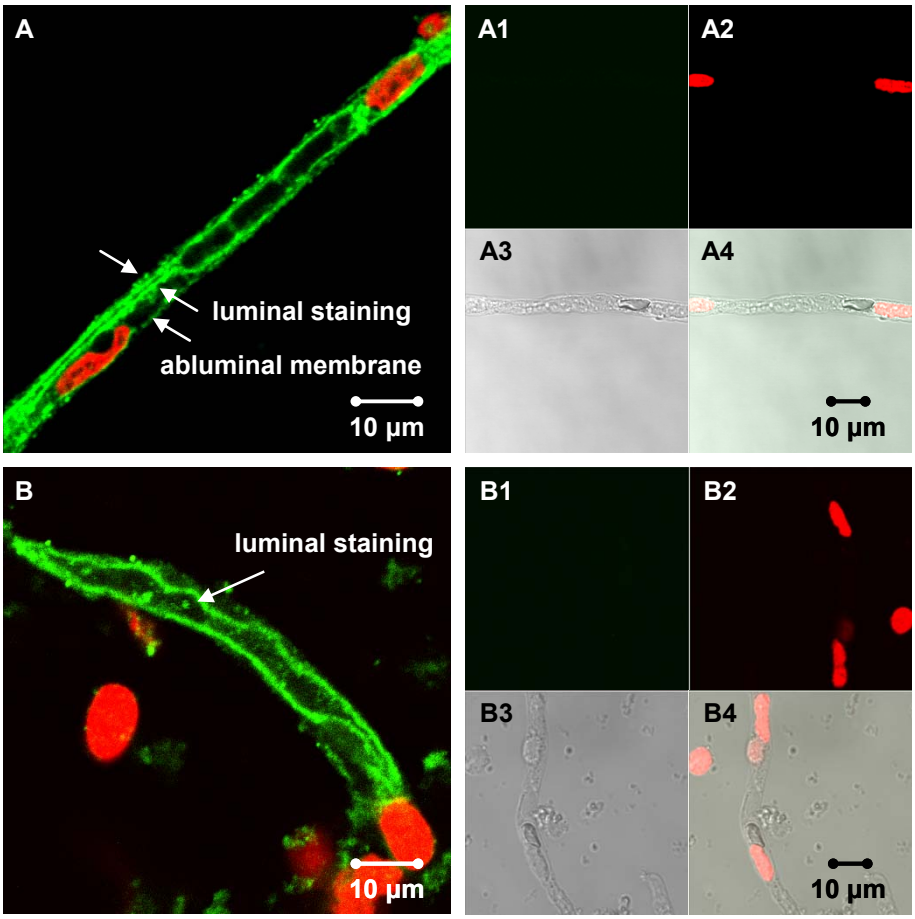

Figure 3.29
Immunostaining of capillaries for P-glycoprotein

A: **C219 antibody**
Rat brain capillaries show luminal staining for P-gp (green). Images A1-4 show the negative control (A1 green channel, A2 red channel, A3 transmitted light image, A4 overlay of images A1-3).

B: **mdr Ab-1 antibody**
Capillaries exhibit luminal staining for P-gp (green). Images B1-4 show the negative control (B1 green channel, B2 red channel, B3 transmitted light image, B4 overlay of images B1-3).

The capillary in Figure 3.30A was immunostained for P-gp (green) using C219 as primary antibody; nuclei were counterstained with propidium iodide (red). Figures 3.30B and C show a cross-section of the capillary. Both cross-sections demonstrate retained tubular structure of this capillary.

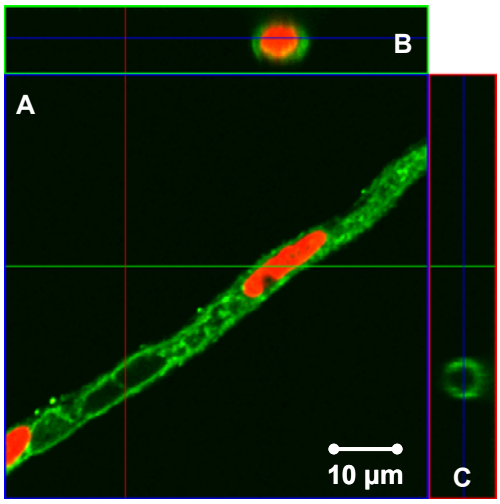

Figure 3.30
Cross-section of a capillary immunostained for P-gp

A: Immunostaining for P-gp with C219 (green); nuclei are counterstained with propidium iodide (red) X-Y Projection
B: X-Z Projection
C: Y-Z Projection

3.1.5 Discussion of Part 3.1:

The *Ex Vivo* Blood-Brain Barrier Model

For the work presented in this thesis, isolated rat brain capillaries were used as an *ex vivo* blood-brain barrier model. Brain capillaries have been isolated since 1969, when Siakatos et al. reported for the first time the isolation of capillaries from human and bovine brain (Saikotos, 1969). Today, several techniques are used for isolating brain capillaries, each of which yields intact and metabolically active microvessels (Dallaire et al., 1991; Goldstein et al., 1975; Miller et al., 2000). In this thesis, a protocol based on mechanical homogenization and density gradient centrifugation was followed to isolate brain capillaries from rat (Bauer et al., 2004; Hartz et al., 2004). Using this method, a fraction highly enriched in capillaries was obtained (Figure 3.1).

Brain capillaries can be isolated from a variety of species such as killifish, shark, mouse, rat, pig, cow and human (Choi and Pardridge, 1986; Dallaire et al., 1991; Goldstein et al., 1975; Lee et al., 2005; Miller et al., 2002a; Miller et al., 2000; Nobmann et al., 2001; Pardridge et al., 1985). Although brain capillaries have now been isolated for more than 35 years, they have so far mainly been used for the culture of endothelial cells and have only been characterized on a functional level, e.g. by enzyme assays (Bauer et al., 2003; Choi and Pardridge, 1986; Goldstein et al., 1984; Goldstein et al., 1975; Pardridge et al., 1985). Recently, Miller et al. used freshly isolated brain capillaries from pig, rat and fish to study transport function of efflux transport proteins (Miller, 2003; Miller et al., 2002a; Miller et al., 2000). However, there is no comprehensive study showing thorough characterization (morphology, mRNA, protein expression, localization and function) of brain capillaries for any single species. Therefore, the first part of the Results and Discussion part describes the characterization of isolated rat brain capillaries with regard to structure, morphology, viability, expression of marker proteins and their localization.

Diameter, size and morphology of isolated rat brain capillaries were similar to those previously reported (Figures 3.1-2) (Dallaire et al., 1991; Goldstein et al., 1975; Miller et al., 2000). At the ultra-structural level, intact mitochondria and intact tight junctions were identified, indicating structural integrity, as shown before by Goldstein et al. (Goldstein et al., 1975; Shivers et al., 1984). Importantly, capillaries were viable for at least 6 hours after isolation (Figure 3.5). However, viability seems to vary between species. Capillaries from killifish were shown to be viable for up to 24 hours, whereas a viability of 4-8 hours was reported for capillaries from pig and rat (Fricker et al., 2002; Miller et al., 2002a; Miller et al., 2000). Interestingly, Choi and Pardridge found that some biochemical functions of human capillaries remained intact for up to 42 hours after isolation (Choi and Pardridge, 1986).

Since tight junctions are an important element of blood-brain barrier function, several junctional proteins were additionally studied on a molecular level. Expression of the tight junction proteins ZO-1, occludin, claudin-1, claudin-5 and JAM-A was detected by Western blotting (Figures 3.6, 3.8, 3.10, 3.12 and 3.13) (Kniesel and Wolburg, 2000; Nitta et al., 2003; Wolburg and Lippoldt, 2002). In accordance with previously published findings, immunostaining showed localization of ZO-1, occludin and claudin-1 along cell-cell contacts (Figures 3.7, 3.9, 3.11) (Gao and Shivers, 2004; Lippoldt et al., 2000; Virgintino et al., 2004).

More than 90% of glucose transport to the brain is mediated by GLUT-1, a transporter protein highly expressed in the brain capillary endothelium (Farrell and Pardridge, 1991; Pardridge et al., 1990a). Consistent with reports from Pardridge and Boado, GLUT-1

was found in capillary lysate; expression was highly enriched in capillary membranes (Figure 3.14) (Boado and Pardridge, 1990). Expression of Na^+/K^+-ATPase was also detected (Figure 3.15). Betz et al. localized Na^+/K^+-ATPase to the abluminal membrane of rat brain capillaries (Betz et al., 1980; Goldstein et al., 1984). However, from the immunostaining shown in Figure 3.16, a clear statement with regard to the localization of Na^+/K^+-ATPase cannot be made.

In addition, isolated rat brain capillaries also express ABC-transporters such as BCRP, Mrp1, 2, 4 and P-glycoprotein. The breast cancer resistance protein, BCRP, was found to be enriched in isolated capillary membranes (Figure 3.17) and was localized to the luminal membrane (Figure 3.18). This is in accordance with recently found evidence for BCRP expression at the blood-brain barrier of humans, pigs, rats and mice (Cisternino et al., 2004; Cooray et al., 2002; Eisenblatter and Galla, 2002; Hori et al., 2004; Zhang et al., 2003a). Lee et al. studied BCRP-mediated brain efflux of dehydroepiandrosterone sulfate and mitoxantrone in mice and demonstrated a minor role for BCRP in active efflux (Lee et al., 2005). In contrast, Cisternino et al. showed that BCRP limits brain uptake of mitoxantrone and prazosin in mice (Cisternino et al., 2004). In conclusion, the exact role of BCRP at the blood-brain barrier remains to be elucidated.

Mrp1 expression in isolated rat brain capillaries was demonstrated by Western blot experiments confirming the findings of Regina et al. and Kusuhara et al. (Kusuhara et al., 1998; Regina et al., 1998). Immunostaining suggested luminal localization of Mrp1, which supports the findings of Zhang et al. and Sugiyama et al. (Sugiyama et al., 2003a; Zhang et al., 2004a). However, it is controversial, to which membrane Mrp1 is localized. Other groups found Mrp1 in the abluminal membrane of polarized cells (Flens et al., 1996; Schinkel, 2001). Cisternino et al. demonstrated lack of Mrp1-mediated efflux at the luminal side of mouse brain endothelial cells and concluded that Mrp1 is not present in the luminal membrane, but instead expressed in the abluminal membrane (Cisternino et al., 2003).

Conflicting reports also exist on the expression of Mrp2 at the blood-brain barrier (Miller et al., 2000; Nies et al., 2004; Zhang et al., 2000). RT-PCR data showed no signal for Mrp2 in brain and capillaries (Figure 3.21), which is in accordance with reports from Zhang et al. (Zhang et al., 2000; Zhang et al., 2004a). However, Western blot analysis and immunostaining clearly demonstrated Mrp2 expression in isolated rat brain capillaries (Figures 3.22-23). This supports studies from Miller et al., who detected Mrp2 protein expression and function in isolated capillaries from pig and rat (Fricker et al., 2002; Miller et al., 2002a; Miller et al., 2000). Furthermore, studies by Miller et al. and Potschka et al. demonstrated Mrp2 function at the blood-brain barrier of rats (Miller et al., 2002a; Potschka et al., 2003).

Recently, Mrp4 was reported to be expressed in brain capillaries from human, bovine, and mouse (Leggas et al., 2004; Nies et al., 2004; Zhang et al., 2000). In the rat, Mrp4 was shown to be localized in the membranes of capillaries (Figure 3.25), which is consistent with findings by others (Leggas et al., 2004; Nies et al., 2004). Furthermore, high magnification images showed both abluminal and luminal Mrp4 expression, as previously demonstrated by Zhang et al. (Zhang et al., 2004a). Western blot analysis revealed expression of Mrp4 in capillary membranes (Figure 3.24). Both Western blot and immunostaining indicate that Mrp4 is also expressed in other brain cells as well as blood cells. This is in accordance with reports of Mrp4 expression in astrocytes, neurons, microglia as well as platelets and macrophages (Jedlitschky et al., 2004; Jorajuria et al., 2004). Additionally, Leggas et al. provided first evidence that Mrp4 confers drug

resistance at the blood-brain barrier (Leggas et al., 2004), which is consistent with luminal localization.

Using RT-PCR, *mdr1a* and *mdr1b* mRNA expression was detected in isolated rat brain capillaries. Western blot of capillary membranes showed P-gp protein expression (Figures 3.27-28) and immunostaining localized P-gp to the luminal membrane of capillaries (Figures 3.29-30). Previous studies employing immunohistochemistry and luminal membrane isolation also demonstrated luminal localization of P-gp at the capillary endothelium (Cordon-Cardo et al., 1989; Matsuoka et al., 1999; Pardridge, 1998; Schinkel, 1999; Stewart et al., 1996; Thiebaut et al., 1987; Thiebaut et al., 1989). In addition, P-gp was localized in the luminal membrane of capillary endothelial cells by immunoelectronmicroscopy (Biegel et al., 1995; Sugawara, 1990; Tanaka et al., 1994).

3.1.6 Summary of Part 3.1:

The *Ex Vivo* Blood-Brain Barrier Model

Rat brain capillaries were isolated following a standard protocol based on mechanical homogenization and density gradient centrifugation (Bauer et al., 2004; Hartz et al., 2004). Isolations yielded a fraction enriched in brain capillaries (Figure 3.1) with very small amounts of larger vessels, red blood cells, other brain cells and cell debris. Using confocal microscopy, isolated brain capillaries revealed intact structure and morphology (Figure 3.2). On an ultra-structural level, endothelial cell nuclei, cytoplasm, abluminal and luminal membranes, intracellular vesicles, intact mitochondria and tight junctions were identified by transmission electron microscopy (Figures 3.3-4). Capillaries were viable for at least 6 hours after isolation, as determined by transport experiments (Figure 3.5). Figure 3.31 summarizes proteins detected in isolated rat brain capillaries.
Tight junction proteins (ZO-1, occludin, claudin-1, claudin-5 and JAM-A) were localized to endothelial cell-cell contacts (Figures 3.6-13). In addition, GLUT-1 and Na^+/K^+-ATPase were found to be expressed in capillaries and isolated capillary membranes (Figures 3.14-16).
Moreover, several drug efflux transporters were also found to be expressed in isolated rat brain capillaries. Western blots showed expression of Mrp1, 2 and 4 as well as BCRP in capillary membranes (Figures 3.17, 3.19, 3.22 and 3.24), which was confirmed by immunostaining (Figures 3.18, 3.20, 3.23 and 3.25). Importantly, P-gp protein expression was detected in capillary membranes using two different antibodies (C219 and mdr Ab-1) (Figures 3.27-28). Immunostaining localized P-gp to the luminal membrane of rat brain capillaries (Figures 3.29). Using RT-PCR, expression of *mdr1a* and *mdr1b* mRNA was also detected in capillaries as well as in brain, choroid plexus, kidney and liver (Figure 3.26).

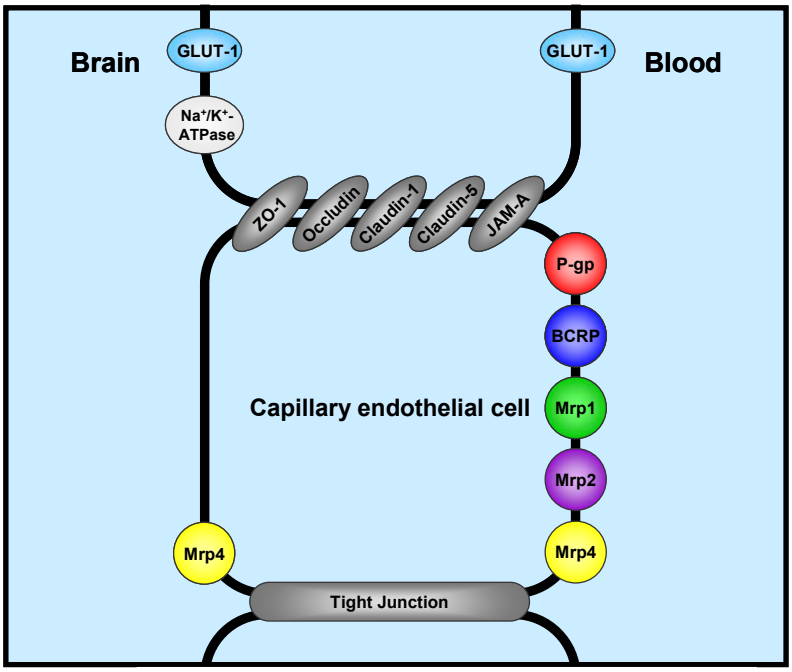

Figure 3.31
Proteins expressed in isolated rat brain capillaries

Isolated rat brain capillaries express tight junction proteins (ZO-1, occludin, claudin-1, claudin-5 and JAM-A) and transport proteins (GLUT-1, Na^+/K^+-ATPase, P-gp, BCRP, Mrp1, 2 and 4).

3.2 Rapid Regulation of P-glycoprotein at the Blood-Brain Barrier by Endothelin-1

3.2.1 P-gp-mediated NBD-CSA Transport in Isolated Rat Brain Capillaries

3.2.1.1 Auto-Fluorescence of Isolated Rat Brain Capillaries

The combination of confocal microscopy and image analysis is a powerful tool to assess P-glycoprotein function in isolated brain capillaries. Capillaries are incubated with the fluorescent P-gp-specific substrate NBD-cyclosporin A (NBD-CSA: [N-ε(4-nitrobenzofurazan-7-yl)-D-Lys^{8}]-cyclosporine A) and then imaged with a confocal microscope. Using image analysis software, images are quantitated by measuring luminal accumulation of NBD-CSA (Hartz et al., 2004; Miller, 2003; Miller et al., 2000).
Isolated rat brain capillaries were examined for auto-fluorescence with the settings used for experiments and exhibited no auto-fluorescence (Figure 3.32).

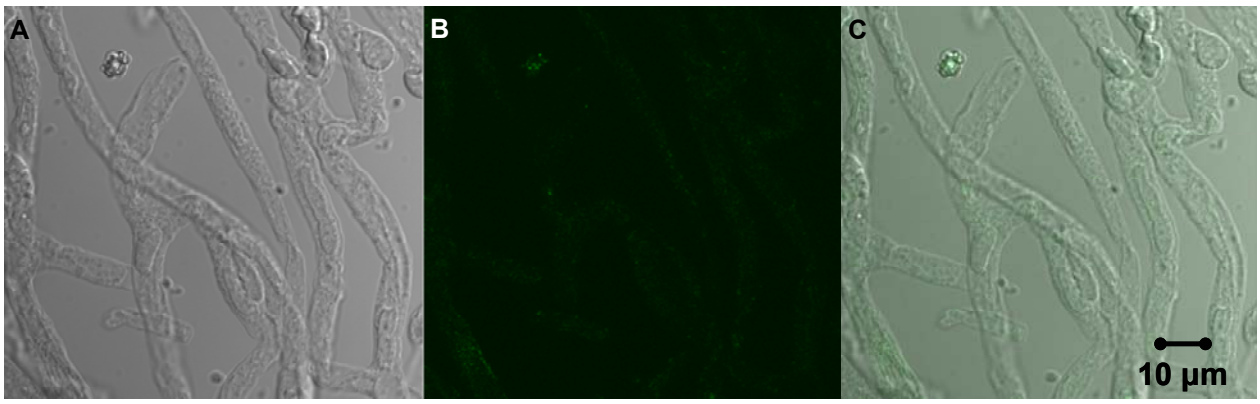

Figure 3.32
Isolated rat brain capillaries exhibit no auto-fluorescence

A: Transmitted light image of isolated rat brain capillaries

B: Confocal fluorescent image of capillaries
The image displays no fluorescence indicating that capillaries exhibit no auto-fluorescence under these experimental conditions.

C: Overlay of A and B

3.2.1.2 Effect of Temperature on P-gp-mediated NBD-CSA Transport

To optimize experimental conditions, P-gp-mediated transport of NBD-CSA into the lumen of isolated rat brain capillaries was measured at different temperatures (4°C, 22°C and 37°C). Figure 3.33 shows how temperature affects accumulation of NBD-CSA in capillary lumens. At 4°C, luminal NBD-CSA fluorescence was 47% lower than at room temperature (22°C). This might be caused by a slow down of metabolic activity resulting in lower ATP synthesis, which is required for energy-dependent transport by P-gp. Surprisingly, NBD-CSA accumulation was about 23% higher at room temperature than at 37°C. At 37°C, a higher enzymatic degradation leading to a loss of viability could be responsible for decreased luminal fluorescence. A higher metabolic activity than at 4˚C and a higher viability than at 37˚C could add up to a higher P-gp-mediated NBD-CSA transport at 22˚C. Therefore, all further experiments were conducted at room temperature.

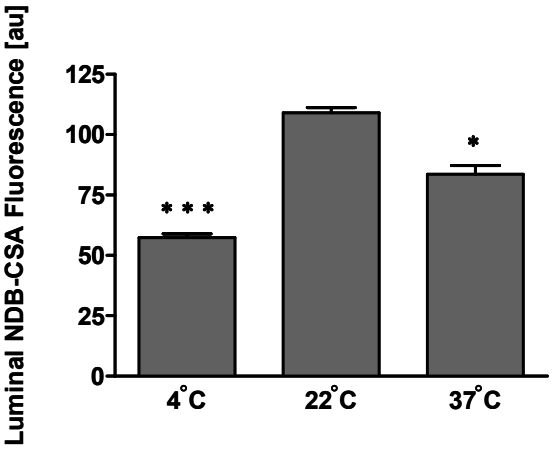

Figure 3.33
Effect of temperature on luminal NBD-CSA fluorescence

Accumulation of NBD-CSA was highest at 22°C, lower at 37°C and lowest at 4°C (mean ± SEM, n=10, * $p < 0.05$ and *** $p < 0.001$ compared to 22˚C).

3.2.1.3 Effect of DMSO on P-gp-mediated NBD-CSA Transport

Some chemicals and compounds used in the experiments first had to be solubilized in dimethyl sulfoxide (DMSO). To exclude an effect of DMSO on P-gp-mediated NBD-CSA transport, capillaries were exposed to 0.1% of the solvent (highest concentration of DMSO capillaries were exposed to in experiments) and NBD-CSA transport was followed using a confocal microscope. 0.1% DMSO did not have an effect on P-gp-mediated luminal NBD-CSA fluorescence (Figure 3.34).

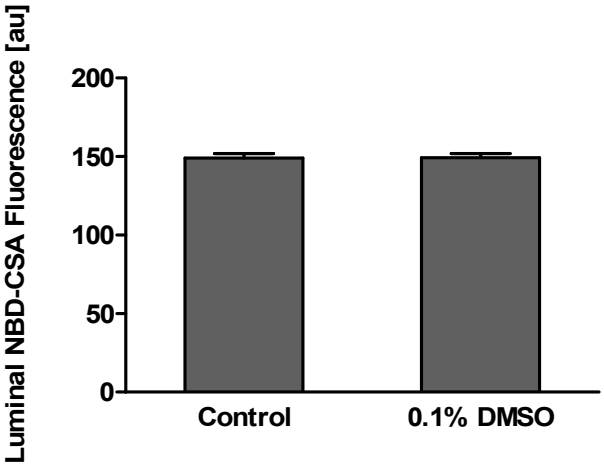

Figure 3.34
No effect of 0.1% DMSO on luminal NBD-CSA fluorescence

0.1% DMSO did not alter P-gp-mediated NBD-CSA transport (mean ± SEM, n=10).

3.2.1.4 Time-course of P-gp-mediated NBD-CSA Transport

NBD-CSA rapidly accumulated in the lumens of isolated rat brain capillaries. Figure 3.35A shows a representative image of a capillary after 60 min of incubation with 2 µM NBD-CSA at room temperature. Fluorescence intensity is low in the bath, moderate in the endothelium, and highest in the capillary lumen. To inhibit P-gp-mediated NBD-CSA transport, the specific P-glycoprotein inhibitor, PSC833 ((3'-keto-Bmt')-[Val (2)]-cyclosporin A, valspodar), was used (Fellner et al., 2002; Kemper et al., 2003). 5 µM PSC833 blocked luminal NBD-CSA accumulation completely (Figure 3.35B).

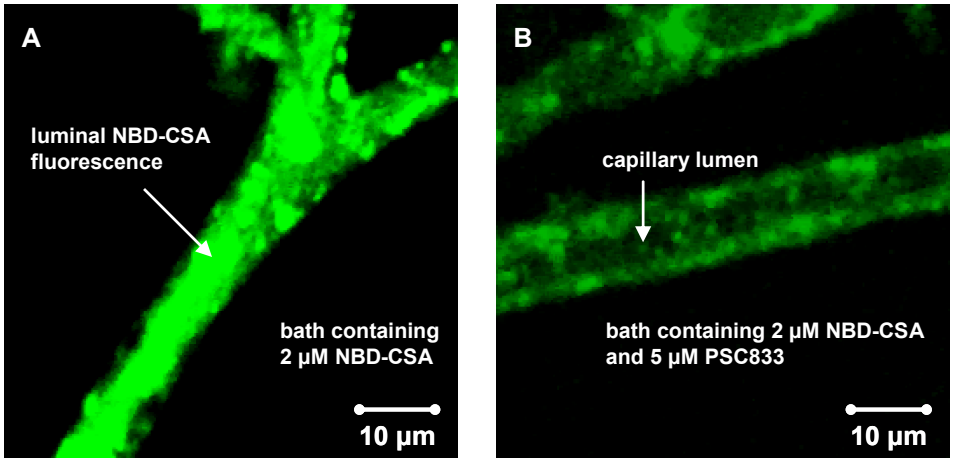

Figure 3.35
NBD-CSA accumulation in brain capillaries with and without PSC833

A: Accumulation of NBD-CSA in capillary lumen after 60 min of incubation with 2 µM NBD-CSA.

B: 5 µM PSC833 significantly reduced luminal NBD-CSA fluorescence.

Over a period of 60 min, capillaries for each time point were randomly chosen to follow NBD-CSA accumulation. In control capillaries, luminal NBD-CSA fluorescence increased rapidly and reached steady-state levels after approximately 30 min (Figure 3.36). Exposing capillaries to 5 µM PSC833 decreased luminal NBD-CSA fluorescence significantly for each time point to about 45% of the corresponding control value.

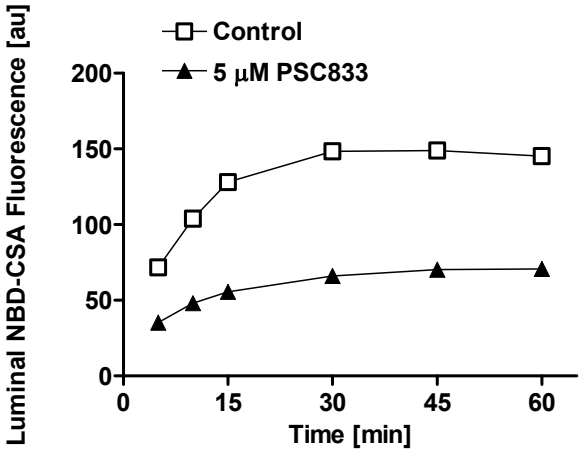

Figure 3.36
Time course of luminal NBD-CSA fluorescence with and without the P-gp inhibitor, PSC833

NBD-CSA rapidly accumulated in the lumens of control capillaries. Luminal NBD-CSA fluorescence reached steady state levels after 30 min. 5 µM PSC833 prevented luminal NBD-CSA accumulation (mean ± SEM, n=7).

At steady state about 45-50% of fluorescence remained in the lumen when capillaries were treated with PSC833. This component of fluorescence was insensitive to the P-gp inhibitor, PSC833 (Figures 3.33 and 3.34), and to the metabolic inhibitor, NaCN (Figure 3.29). It likely reflects non-specific NBD-CSA binding to the tissue (Bauer et al., 2004; Hartz et al., 2004).

3.2.1.5 P-gp-Specific Transport of NBD-CSA into Capillary Lumens

P-glycoprotein-mediated NBD-CSA transport was further examined by exposing capillaries to PSC833. Figure 3.37 shows the PSC833 effect on P-gp-mediated NBD-CSA transport into the lumens of isolated rat brain capillaries. PSC833 decreased luminal NBD-CSA fluorescence in a concentration-dependent manner. 5 µM PSC833 gave maximal inhibition of P-glycoprotein and decreased NBD-CSA fluorescence to 30-40% of the control. The PSC833-sensitive component reflects active P-gp-mediated NBD-CSA transport. Again, the component insensitive to PSC833 likely represents non-specific binding of NBD-CSA. Since 5 µM PSC833 gave maximal inhibition, this concentration was used for all further experiments.

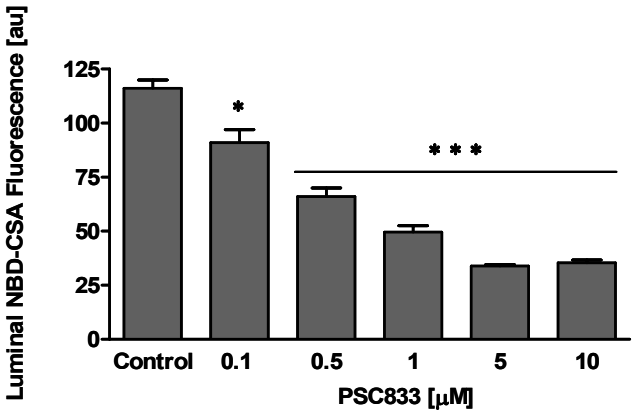

Figure 3.37
Concentration-dependence of PSC833 on P-gp-mediated NBD-CSA transport into capillary lumens

Concentration-dependent decrease of luminal NBD-CSA fluorescence with 0.1-10 µM PSC833. 5 µM PSC833 had a maximal inhibitory effect on P-gp transport function (mean ± SEM, n=10, * $p < 0.05$, *** $p < 0.001$).

Inhibition studies were also done using well-known P-gp substrates (verapamil, ivermectin and cyclosporin A), as well as compounds mainly transported by Mrp1 and Mrp2 (MK571, leukotriene C_4 (LTC_4), probenecid) (Ford and Hait, 1990; Nobmann et al., 2001; Saeki et al., 1993).

Verapamil and ivermectin reduced luminal NBD-CSA fluorescence to about 60% of controls, which is comparable to the effect of PSC833 (Figure 3.38A). Non-fluorescent cyclosporin A (CSA) decreased luminal NBD-CSA fluorescence in a concentration-dependent manner (Figure 3.38B): with 1 µM CSA luminal fluorescence was reduced by 20.7 ± 9.4%, with 5 µM CSA by 29.5 ± 8.1% and with 10 µM CSA by 39.1 ± 8.1%. The Mrp-inhibiting compounds, LTC_4, MK571 and probenecid did not alter luminal NBD-CSA accumulation (Figure 3.38C), indicating as expected that Mrps (likely Mrp1 and Mrp2) are not involved in NBD-CSA transport into capillary lumens.

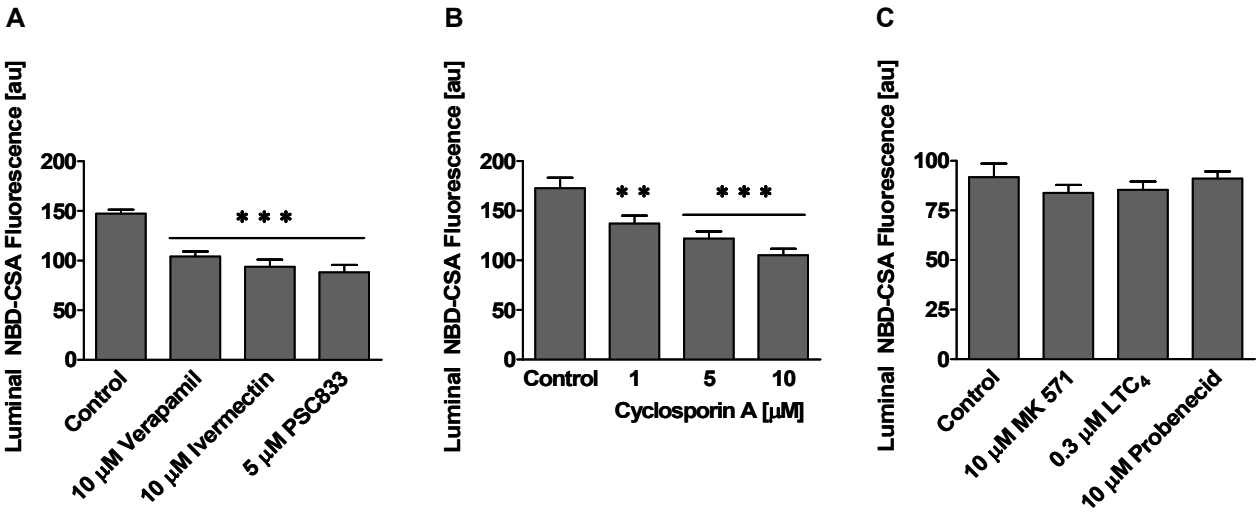

Figure 3.38
Effects of verapamil, ivermectin, PSC833 and Mrp substrates/inhibitors on luminal NBD-CSA fluorescence in isolated rat brain capillaries

A: Verapamil and ivermectin reduced luminal NBD-CSA fluorescence to the same extent as PSC833 (mean ± SEM, n=10, *** $p < 0.001$).

B: Concentration-dependent response of non-fluorescent cyclosporin A on P-gp-mediated NBD-CSA transport into capillary lumens (mean ± SEM, n=10, ** $p < 0.01$, *** $p < 0.001$).

C: Mrp substrates and inhibitors (MK 571, LTC_4, and probenecid) did not change luminal accumulation of NBD-CSA (mean ± SEM, n=10).

3.2.1.6 Summary of Part 3.2.1:

P-gp-mediated NBD-CSA Transport in Isolated Rat Brain Capillaries

Bath-to-lumen transport of the fluorescent cyclosporin A derivative, NBD-CSA, into the lumens of freshly isolated rat brain capillaries was followed using a confocal microscope. Luminal accumulation of NBD-CSA was imaged and fluorescence intensity was analyzed with imaging software.

Brain capillaries did not exhibit any auto-fluorescence under experimental conditions (Figure 3.32). Transport of NBD-CSA was maximal at room temperature (Figure 3.33); concentrations of up to 0.1% DMSO did not affect luminal NBD-CSA accumulation (Figure 3.34). Over a period of 60 min, capillaries rapidly accumulated NBD-CSA; luminal fluorescence reached steady state levels after 30 min (Figures 3.35A and 3.36). The P-gp inhibitor, PSC833, reduced luminal accumulation in a concentration-dependent manner to about 40-50% of control values (Figure 3.37). The P-gp substrates verapamil, ivermectin and cyclosporin A reduced NBD-CSA transport (Figures 3.38A and B); Mrp substrates and inhibitors were without effect (Figure 3.38C). These findings indicate that concentrative, specific and energy-dependent transport of NBD-CSA in isolated rat brain capillaries is mediated by P-glycoprotein.

3.2.2 Effects of Endothelin-1 on P-gp Transport

3.2.2.1 Effects of Endothelin-1 on Luminal NBD-CSA Accumulation

Previous work with renal proximal tubules from killifish demonstrated rapid reduction of P-glycoprotein and Mrp2 function by endothelin-1 (ET-1) (Masereeuw et al., 2000; Miller, 2002; Terlouw et al., 2001). Considering that endothelin receptors are also expressed in brain capillaries and that the cerebral capillary endothelium produces and releases ET-1, this hormone could also play a role in regulating P-gp transport function at the blood-brain barrier (Durieu-Trautmann et al., 1993; Yoshimoto et al., 1990).
In the following experiments, isolated rat brain capillaries were exposed to subnanomolar to nanomolar concentrations of ET-1, and then, P-gp-mediated NBD-CSA transport was measured after 60 min incubation with 2 µM NBD-CSA. ET-1 decreased steady state luminal NBD-CSA fluorescence in a concentration-dependent manner (Figure 3.39A). ET-1 at 0.1 nM reduced luminal fluorescence by 32.5 ± 3.8%. The maximal effect was found with 1 nM ET-1 (decrease to 49.4 ± 3.8% of the control value).
When capillaries were first loaded to steady state with NBD-CSA and ET-1 was then added (at zero time-point), luminal fluorescence declined rapidly to less than 50% of control levels (time point 60 min) (Figure 3.39B). Removing ET-1 from the medium restored luminal NBD-CSA fluorescence (time point 150 min). Luminal fluorescence in control capillaries remained constant over the entire time course of the experiment.

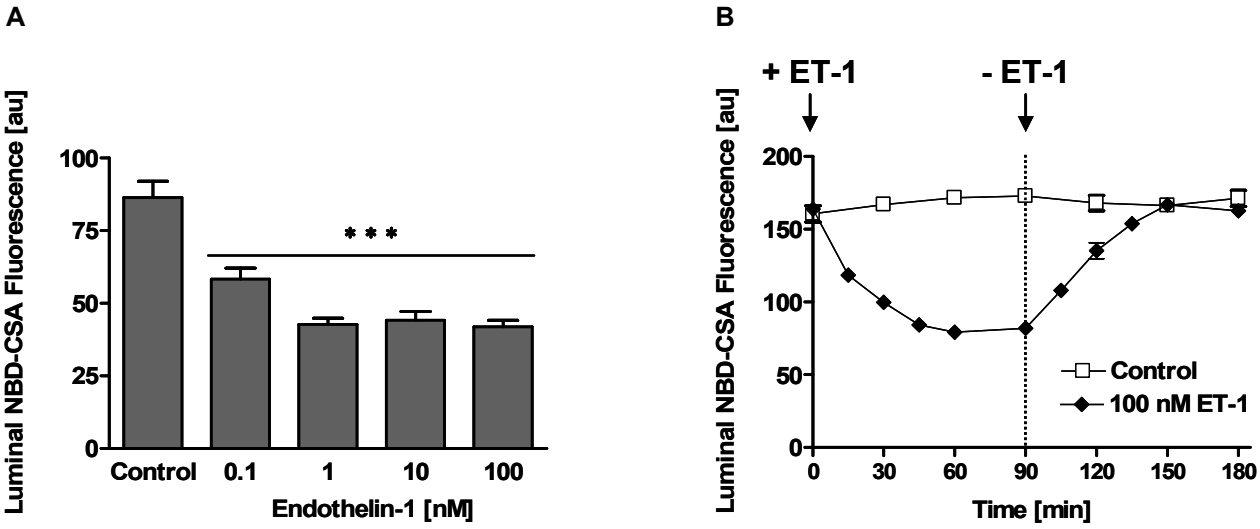

Figure 3.39
Effect of endothelin-1 on luminal NBD-CSA fluorescence

A: Concentration-dependent effect of ET-1 on P-gp-mediated transport of NBD-CSA in capillary lumens
ET-1 decreased luminal NBD-CSA fluorescence in a concentration-dependent manner. 1 nM ET-1 had a maximal effect on luminal NBD-CSA fluorescence (mean ± SEM, n=10, *** $p < 0.001$).

B: Time course of the ET-1 effect on luminal NBD-CSA fluorescence
When ET-1 was added to capillaries preloaded with NBD-CSA (time point 0 min), luminal fluorescence rapidly decreased (maximal effect after 60 min). Upon removal of ET-1 (time point 90 min), fluorescence increased and steady state levels were reached after 60 min (time point 150 min) (mean ± SEM, n=7).

3.2.2.2 Effects of PSC833 and Mannitol on Luminal NBD-CSA Accumulation

The decrease in luminal NBD-CSA accumulation caused by ET-1 could have resulted from 1) reduced P-gp transport function or from 2) an opening of tight junctions and leakage of pumped dye out of the lumen. The effects of PSC833 and mannitol on luminal NBD-CSA accumulation were examined and compared to the time-dependent effect of ET-1 shown in Figure 3.39B.

PSC833 inhibits P-gp transport function by direct interaction; mannitol osmotically opens tight junctions at the blood-brain barrier (Kroll and Neuwelt, 1998; Tan et al., 2000). PSC833 reduced luminal fluorescence within 45 min (Figure 3.40A) to 52.7 ± 2.8% of the control value. 30 min after PSC833 removal (time point 75 min), luminal fluorescence was back to control levels. Mannitol showed the same pattern as ET-1 and PSC833: a rapid decrease in luminal fluorescence after adding to capillaries and an increase to control levels after removal from the medium (Figure 3.40B).

These results demonstrate rapid and reversible effects for ET-1, PSC833 and mannitol on luminal NBD-CSA fluorescence. However, the data do not allow any conclusions on whether the decrease of luminal NBD-CSA fluorescence caused by ET-1 results from reduced P-gp function, from open tight junctions or an overlapping effect of both.

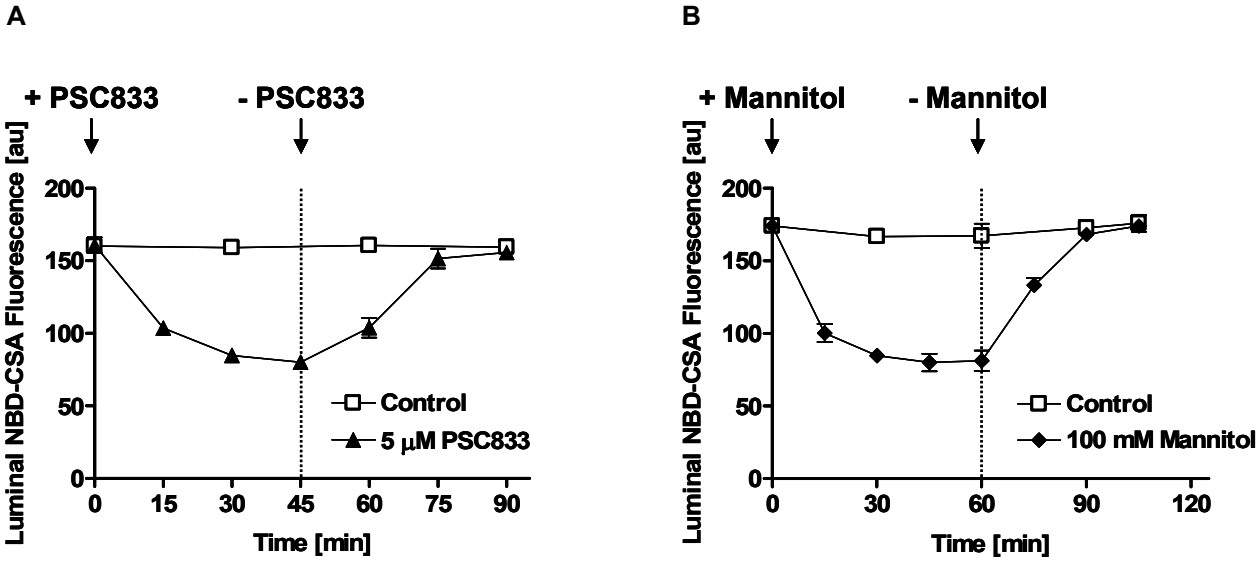

Figure 3.40
Effects of PSC833 and mannitol on luminal NBD-CSA fluorescence

A: Time course of the PSC833 effect on luminal NBD-CSA fluorescence
After adding PSC833 to preloaded capillaries, luminal fluorescence decreased. Upon removal of PSC833, fluorescence returned to control levels (mean ± SEM, n=7).

B: Time course of the mannitol effect on luminal NBD-CSA fluorescence
Mannitol rapidly decreased luminal NBD-CSA fluorescence. When mannitol was removed, the effect was completely restored within 30 min (mean ± SEM, n=7).

3.2.2.3 Kinetic Efflux Assay to Examine the Effect of ET-1

In order to experimentally distinguish between P-gp inhibition and opening of tight junctions, a kinetic assay based on the efflux of a preloaded fluorescent test compound from the lumens of capillaries was developed. This assay had to be independent from P-gp transport function, therefore, the compound used was Texas Red (sulforhodamine 101, free acid, MW 625 Da). Texas Red is a rhodamine-based, fluorescent organic anion that is a substrate for the multidrug resistance-associated protein isoform 2 (Mrp2), another ABC-transporter located at the luminal membrane of brain capillaries (part 3.1.3.3, Figures 3.21-23). In the same manner as P-gp transports NBD-CSA, Mrp2 pumps Texas Red into the capillary lumen (Hartz et al., 2004; Miller et al., 2002a; Miller et al., 2002b; Miller et al., 2000). Luminal Texas Red fluorescence can then be quantitated accordingly as described above.
First, Texas Red was tested for its Mrp2 specificity in rat brain capillaries (Figure 3.41). The P-gp inhibitor PSC833 did not affect steady-state luminal accumulation of Texas Red. The Mrp2 inhibitor LTC_4, however, significantly reduced luminal Texas Red accumulation to 52.4 ± 2.9% of the control. Importantly, Texas Red accumulation was not affected by 100 nM ET-1, a concentration 100 times higher than that causing maximal reduction in NBD-CSA accumulation in capillary lumens (Figure 3.39).

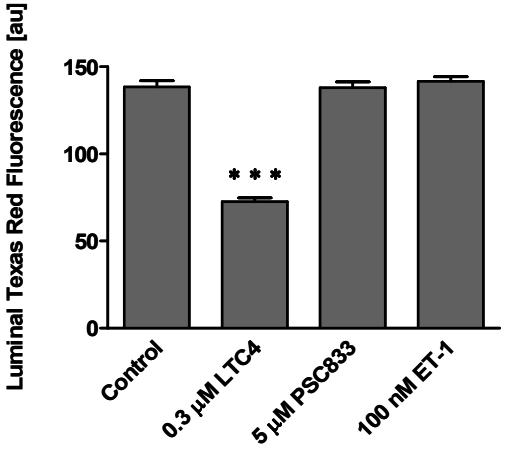

Figure 3.41
Effects of LTC_4, PSC833 and ET-1 on Texas Red transport
The Mrp2 inhibitor LTC_4 significantly decreased Texas Red transport; PSC833 and ET-1 had no effect (mean ± SEM, n=10, *** $p < 0.001$).

Figure 3.41 shows that ET-1 does not affect Texas Red transport: If ET-1 had opened tight junctions; Texas Red would have leaked out of the lumens, which would have resulted in a decreased luminal Texas Red fluorescence compared to the control. Since ET-1 did not cause such a decrease in luminal Texas Red fluorescence, it is likely that ET-1 has no effect on tight junctions. To prove this point, a kinetic assay based on Texas Red efflux from brain capillary lumens was developed.

For the kinetic efflux assay, capillaries were preloaded with Texas Red, washed with buffer, and then dye efflux was followed over a period of 60 min using confocal microscopy. Mannitol, sucrose and 1-*O*-pentylglycerol, compounds known to open tight junctions, were used as positive controls. At high concentrations, mannitol and sucrose both increase permeability by osmotically opening tight junctions, whereas 1-*O*-pentylglycerol opens tight junctions by a so far unknown, non-osmotic mechanism (Erdlenbruch et al., 2003; Kroll and Neuwelt, 1998).
Figure 3.42 shows representative images for rapid efflux of Texas Red after adding 30 mM 1-*O*-pentlylglycerol. After 10-15 min, luminal fluorescence was substantially reduced (Figures 3.42C and D); after 60 min, fluorescence was essentially undetectable (Figure 3.42F).

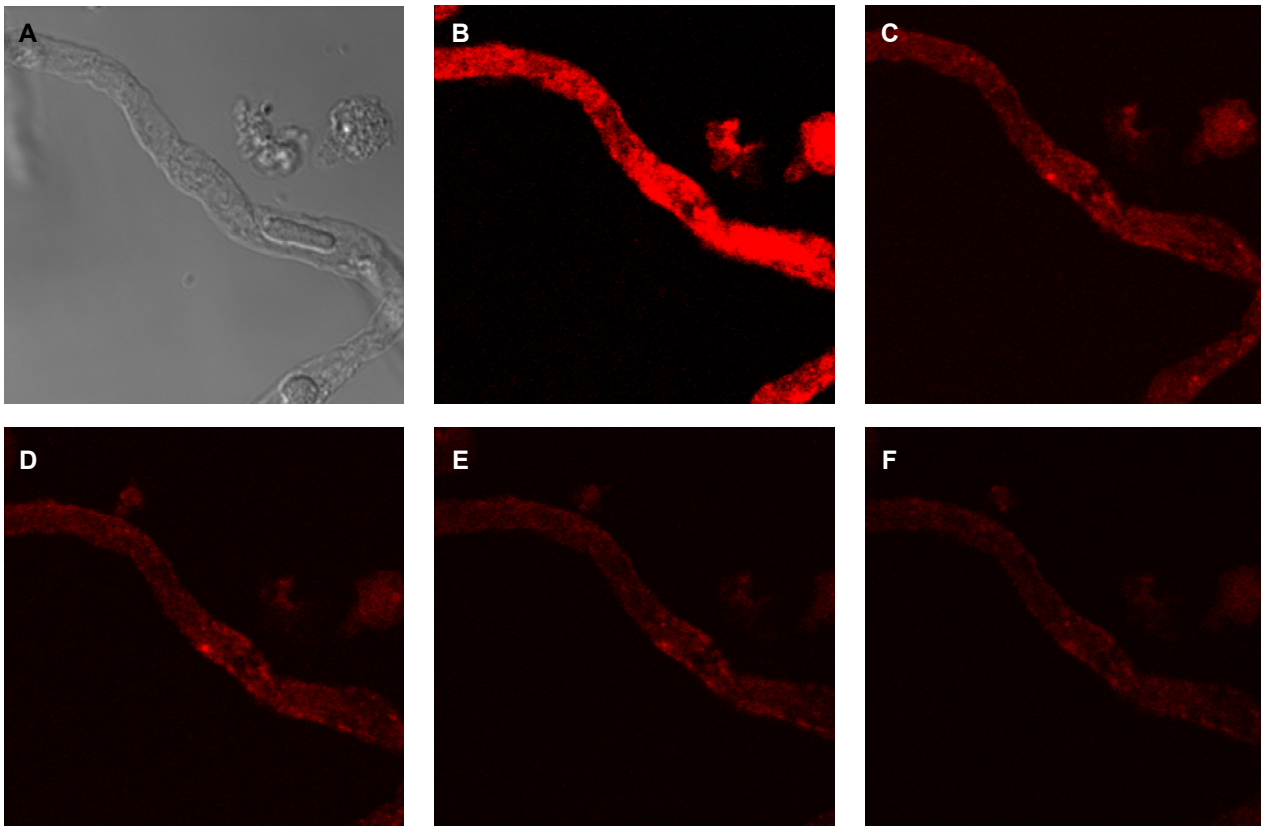

Figure 3.42
Efflux of Texas Red with 30 mM 1-*O*-pentylglycerol over time

A: Transmitted light image of an isolated rat brain capillary
B: Capillary loaded with 2 µM Texas Red after washing with buffer (start)
C: Capillary after 10 min
D: Capillary after 15 min
E: Capillary after 30 min
F: Capillary after 60 min

Figure 3.43 shows the time course of Texas Red efflux from preloaded capillaries treated with mannitol, sucrose, 1-*O*-pentylglycerol and ET-1. In control capillaries (Figure 3.43A), loss of dye from the lumen was slow, but significant (14.8 ± 4.5% lost after 15 min, 50.1 ± 3.2% lost after 30 min; 64.7 ± 3.2% lost after 60 min). Mannitol, sucrose and 1-*O*-pentylglycerol, however, showed significantly increased Texas Red efflux compared to control capillaries: after 5 min, luminal fluorescence was reduced to about 50% (50% efflux) and to about 30% (70% efflux) after 30 min. In contrast, 100 nM ET-1 did not alter Texas Red efflux (Figure 3.43B).

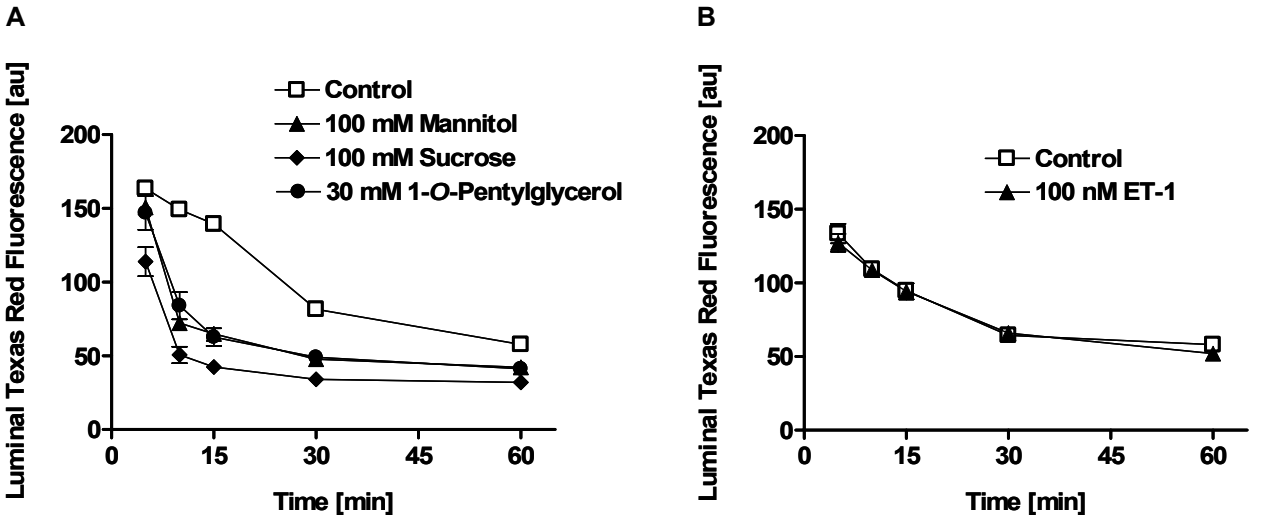

Figure 3.43
Texas Red efflux from capillaries

A: Effects of mannitol, sucrose and 1-*0*-pentylglycerol on Texas Red efflux
Osmotic agents (mannitol, sucrose) as well as 1-*0*-pentylglycerol enhanced efflux of Texas Red substantially (mean ± SEM, n=7).

B: Effect of ET-1 on Texas Red efflux
ET-1 did not alter efflux of Texas Red (mean ± SEM, n=7).

By modeling Texas Red efflux as a first-order process and calculating rate constants using nonlinear regression, *k*-values were obtained for control capillaries, ET-1-, mannitol-, sucrose- and 1-*O*-pentylglycerol-treated capillaries. The mean efflux rate constant for capillaries exposed to 100 nM ET-1 was 0.53 ± 0.003 min^{-1} (Table 3.1). This value is not different from that of control capillaries (0.53 ± 0.004 min^{-1}). Mannitol and 1-*O*-pentylglycerol increased efflux rate about 4-fold and sucrose increased Texas Red efflux about 6-fold.

Treatment	k [min^{-1}] ± SEM
Control	0.053 ± 0.004
100 nM ET-1	0.053 ± 0.003
100 mM Mannitol	0.192 ± 0.009
100 mM Sucrose	0.293 ± 0.011
30 mM 1-*O*-Pentylglycerol	0.183 ± 0.005

Table 3.1
Texas Red mean efflux rate constants

k-values for Texas Red efflux from capillaries exposed to ET-1, mannitol, sucrose and 1-*O*-pentylglycerol (mean ± SEM min^{-1}, control n=42, ET-1 n=21, mannitol n=42, sucrose n=7, 1-*O*-pentylglycerol n=7).

3.2.2.4 Summary of Part 3.2.2:

Effects of Endothelin-1 on P-gp Transport

Exposing capillaries to nanomolar concentrations of ET-1 rapidly diminished luminal NBD-CSA fluorescence (Figure 3.39). This effect was concentration-dependent and reversible: removing ET-1 restored luminal NBD-CSA fluorescence to control levels. PSC833, a P-gp inhibitor and mannitol, which osmotically opens tight junctions, had comparable effects on luminal NBD-CSA fluorescence (Figure 3.40). Mrp2-mediated Texas Red transport was unchanged with PSC833 and ET-1 (Figure 3.41). Compounds that open tight junctions highly increased Texas Red efflux from preloaded capillaries (Figure 3.43A). However, ET-1 had no effect on Texas Red efflux (Figure 3.43B and Table 3.1). Thus, ET-1 decreased luminal NBD-CSA fluorescence by decreasing P-gp function and not by opening tight junctions.

3.2.3 Regulation of P-glycoprotein by Endothelin-1

3.2.3.1 ET-1 Signals through the ET_B Receptor

3.2.3.1.1 Expression of ET_A and ET_B Receptors in Rat Brain Capillaries

In mammals, endothelins (ET-1, ET-2 and ET-3) act through two receptors: the endothelin A (ET_A) and the endothelin B (ET_B) receptor. Both receptors are classical G-protein-coupled membrane proteins with seven transmembrane domains. ET-1 and ET-2 have subnanomolar affinity for the ET_A receptor, whereas ET-3 has a 100-fold lower affinity (Kedzierski and Yanagisawa, 2001). The A-type receptor is mainly expressed on smooth muscle cells where its stimulation leads to an increase in intracellular calcium. All three endothelin isoforms have subnanomolar affinities for the ET_B receptor. The B-type receptor is predominantly expressed on endothelial cells, where it stimulates the release of NO and prostacyclin (Highsmith, 1998; Offermanns, 2004). In the CNS, ET_A and ET_B receptors are expressed by endothelial cells, glial cells and neurons (Kedzierski and Yanagisawa, 2001; Levin, 1995; Willette, 1995). At the blood-brain barrier, ET-1 seems to stimulate Na^+/K^+-ATPase, Na^+/H^+ exchanger and $Na^+/K^+/Cl^-$ co-transporter through ET_A receptors (Kawai et al., 1995a; Kawai et al., 1995b). Kobari et al. demonstrated ET_B receptor-mediated dilatation in cerebral microvessels in cats (Kobari et al., 1994).

Expression of ET_A and ET_B receptors in isolated rat brain capillaries was examined by Western blot analysis and immunohistochemistry. The Western blot for the ET_A receptor in Figure 3.44 shows bands at 40 kDa for capillary lysate but not for capillary membranes.

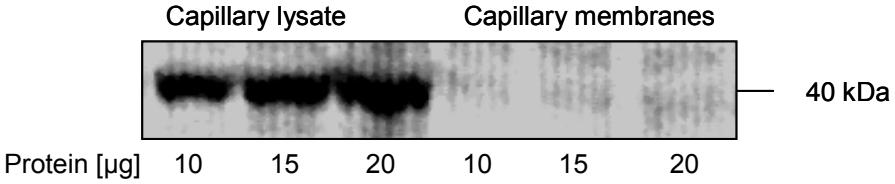

Figure 3.44
Western blot for the ET_A receptor

The ET_A receptor was detected at 40 kDa in capillary lysate, but not in capillary membranes.

The immunostaining of the ET_A receptor in brain capillaries shows weak and diffuse fluorescence extending over the cytoplasm (Figure 3.45A). This suggests intracellular rather than membranous localization of the A-type receptor and supports the Western blot data (Figure 3.44). To obtain a weak signal for the ET_A receptor in image A, a very high laser power had to be used. This strong laser intensity also caused a faint signal for the negative control (Figure 3.45B).

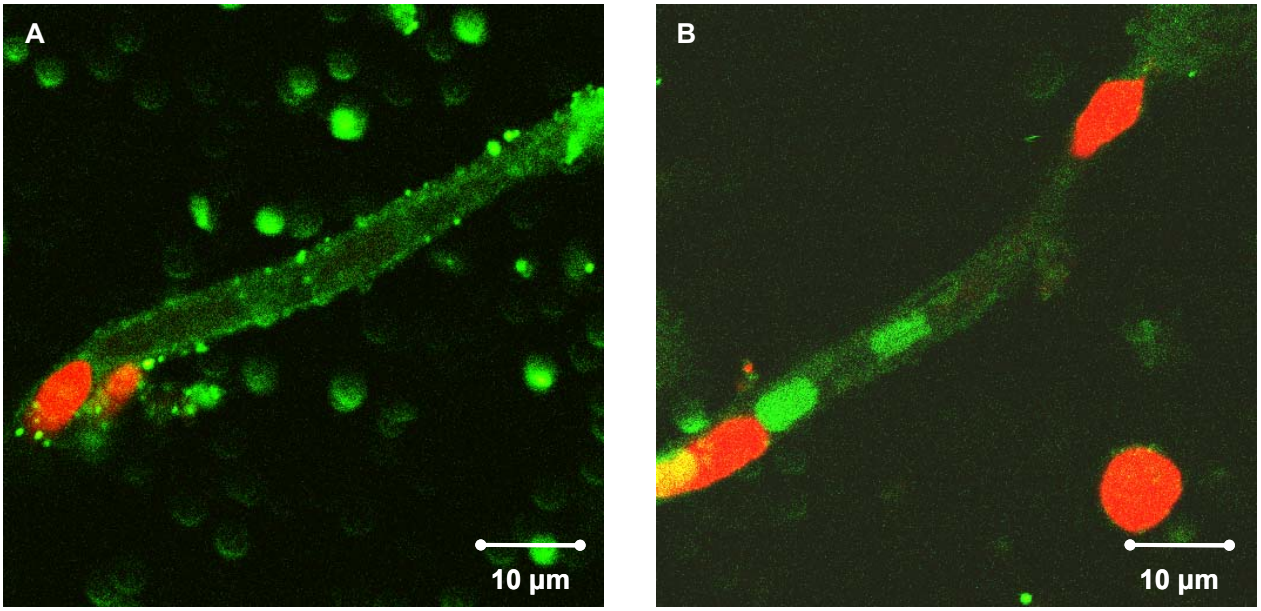

Figure 3.45
Immunostaining of capillaries for the ET_A receptor

A: Weak and diffuse immunostaining of the ET_A receptor

B: Negative control (green and red channel)

The Western blot in Figure 3.46 shows strong bands at 40 kDa for the ET_B receptor in capillary lysate and capillary membranes. The amount of expressed receptor in capillary lysate is significantly higher than in capillary membranes. This suggests intracellular ET_B receptor pools.

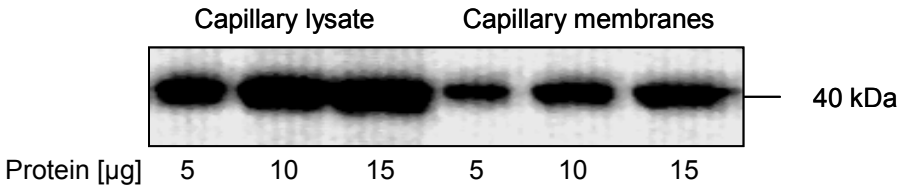

Figure 3.46
Western blot for the ET_B receptor

Capillary lysate and capillary membranes show intense bands for the ET_B receptor at 40 kDa.

Images of capillaries immunostained for the ET_B receptor show a distinct staining along both, the luminal and abluminal capillary membranes (Figure 3.47A). The negative control shows no staining (Figure 3.47B-E).

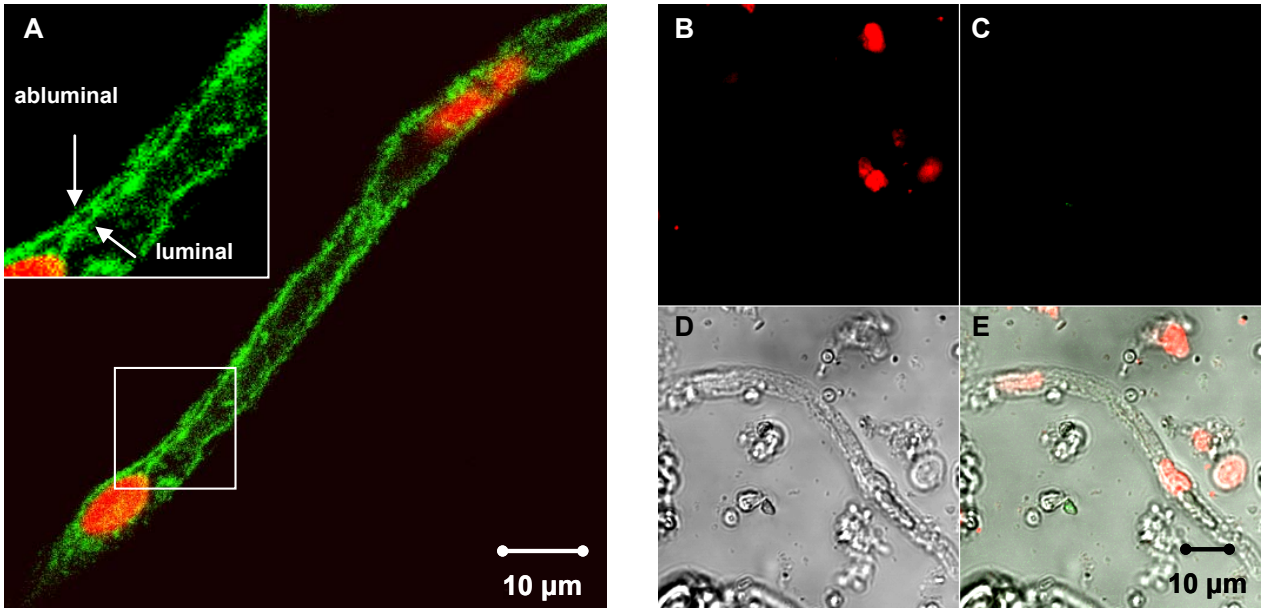

Figure 3.47
Immunostaining of capillaries for the ET_B receptor

A: Luminal and abluminal staining for the ET_B receptor
B: Negative control (red channel)
C: Negative control (green channel)
D: Transmitted light image
E: Overlay of images B, C and D

3.2.3.1.2 ET_B Receptor Mediates ET-1 Signaling

To determine through which receptor ET-1 signals the decrease in P-gp function (Figure 3.39), experiments were done with specific antagonists for both receptors. To block the A-type receptor, JKC-301 was used (Figure 3.48A). This ET_A receptor antagonist had no effect on P-gp-mediated NBD-CSA transport itself. Importantly, JKC-301 did not affect ET-1 signaling. In contrast, the ET_B receptor antagonist RES-701-1, which also had no effect on P-gp transport function by itself, completely abolished the ET-1-mediated decrease in luminal NBD-CSA fluorescence (Figure 3.48B).

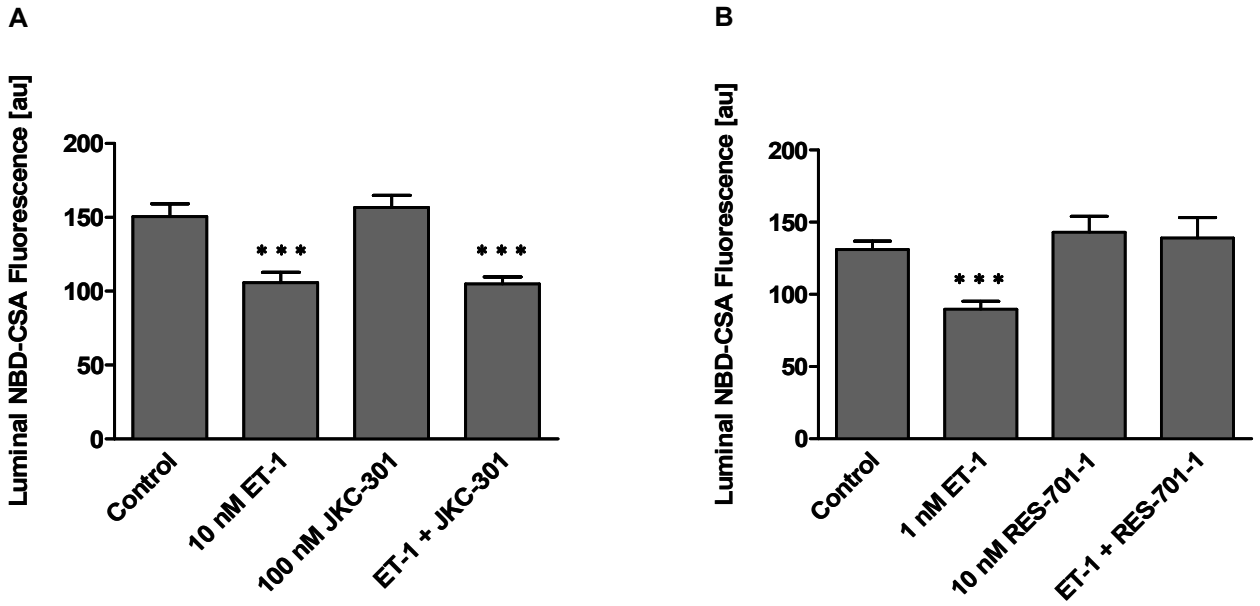

Figure 3.48
Effects of ET_A and ET_B receptor antagonists on ET-1 signaling

A: JKC-301, an ET_A receptor antagonist, did not reverse the ET-1 effect (mean ± SEM, n=10, *** $p < 0.001$).

B: The ET_B receptor antagonist RES-701-1 completely abolished the ET-1 effect (mean ± SEM, n=10, *** $p < 0.001$).

Sarafotoxin S6c, the venom of the snake *Atractapsis Engaddensis*, is a potent and selective agonist for the ET_B receptor. Like ET-1, subnanomolar to nanomolar concentrations of sarafotoxin S6c significantly reduced P-gp-mediated transport. Figure 3.49 shows the concentration-dependent effect of sarafotoxin S6c on NBD-CSA fluorescence in capillary lumens.

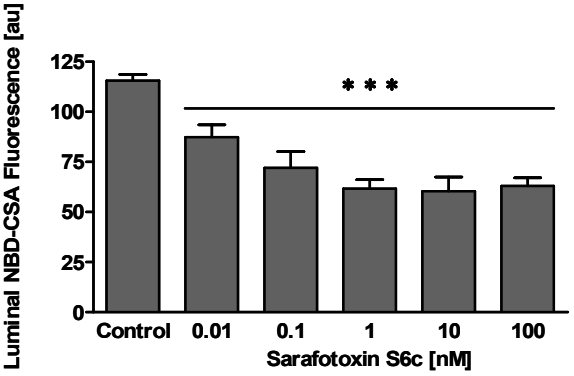

Figure 3.49
Concentration-dependent effect of sarafotoxin S6c on NBD-CSA fluorescence in capillary lumens

The ET_B receptor agonist sarafotoxin S6c reduces luminal NBD-CSA accumulation in a concentration-dependent manner (mean ± SEM, n=10, *** $p < 0.001$).

The ET_A antagonist JKC-301 did not reverse the effect of sarafotoxin S6c (Figure 3.50A). In contrast, RES-701-1 completely blocked the sarafotoxin-caused decrease in luminal NBD-CSA fluorescence (Figure 3.50B).

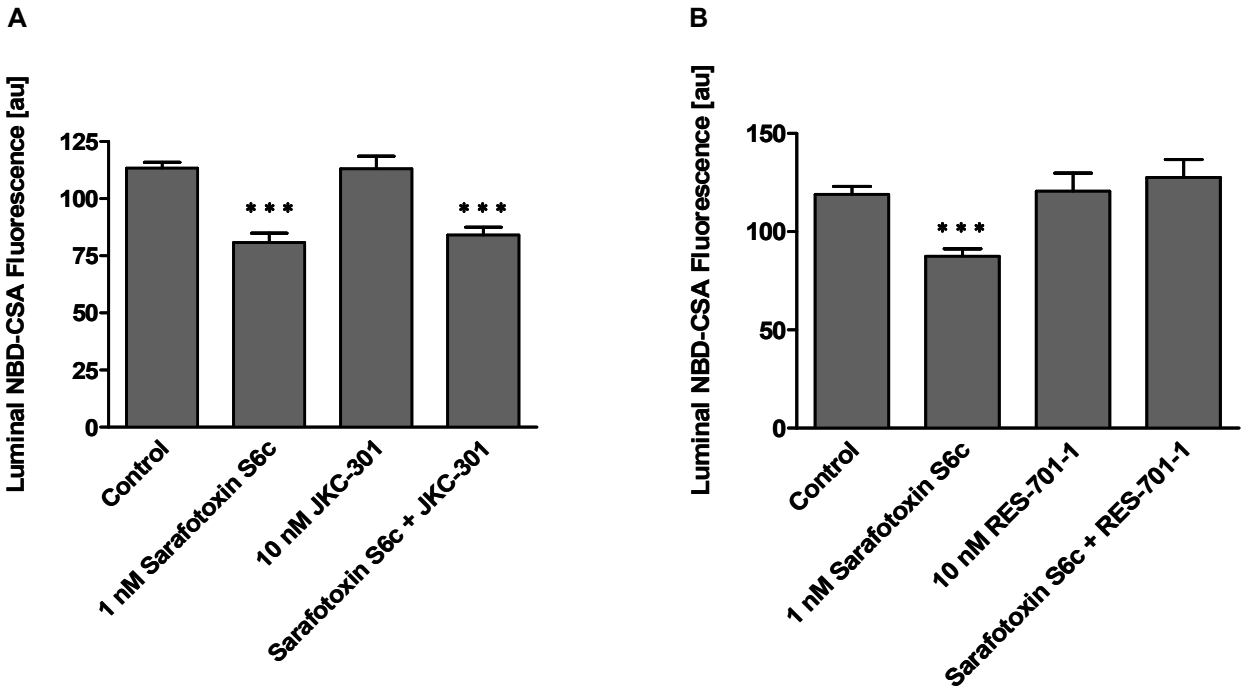

Figure 3.50
Effects of ET_A and ET_B receptor antagonists on sarafotoxin S6c response

A: The ET_A receptor antagonist JKC-301 did not reverse the sarafotoxin S6c effect (mean ± SEM, n=10, *** $p < 0.001$).

B: The ET_B receptor antagonist RES-701-1 completely abolished the sarafotoxin S6c effect (mean ± SEM, n=10, *** $p < 0.001$).

ET-1 and sarafotoxin S6c, both significantly reduced P-gp-mediated NBD-CSA transport in isolated rat brain capillaries in a concentration-dependent manner (Figures 3.39A and 3.49). This decrease was fully abolished by the ET_B receptor antagonist RES-701-1 (Figures 3.48B and 3.50B), whereas blocking of the A-type receptor with JKC-301 did not reverse the ET-1-mediated decrease in luminal NBD-CSA fluorescence (Figures 3.48A and 3.50A). These results indicate that ET-1 decreased P-gp function by acting through an ET_B receptor.

3.2.3.2 NO Synthase is Involved in ET-1 Signaling

Previous studies demonstrated modulation of P-gp function by nitric oxide (Miller, 2002; Notenboom et al., 2002). In order to examine whether NO and NO synthase (NOS), respectively, are involved in the signaling pathway, sodium nitroprusside (SNP), a NO donor, was used to mimic NOS activation. The dose-response for SNP on P-gp-mediated NBD-CSA transport into capillary lumens is shown in Figure 3.51. Like ET-1, SNP caused a concentration-dependent reduction of luminal NBD-CSA fluorescence. A concentration as low as 10 nM SNP gave a maximal decrease to about 60% of the control.

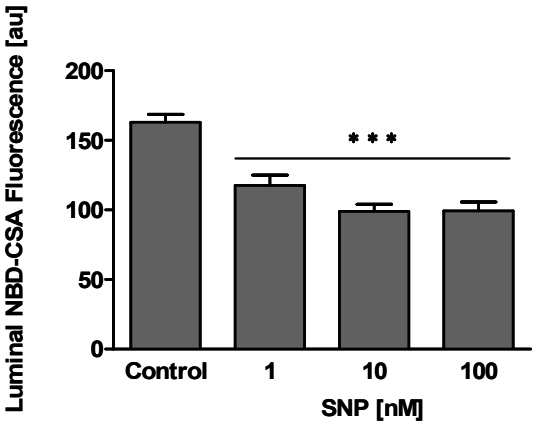

Figure 3.51
Concentration-dependent effect of SNP on NBD-CSA fluorescence in capillary lumens

Concentration-dependent reduction of luminal NBD-CSA fluorescence with SNP (mean ± SEM, n=10, *** $p < 0.001$).

L-NMMA (N^G-monomethyl-L-arginine) is a non-selective NOS inhibitor that inhibits all NOS isoforms: endothelial (eNOS), neuronal (nNOS) and inducible (iNOS) NO synthases. L-NMMA did not affect luminal NBD-CSA accumulation or the SNP-mediated decrease of luminal fluorescence (Figure 3.52A). Blocking NOS abolished the effect of ET-1 (Figure 3.52B) indicating that NOS activation is involved in the ET-1 signaling pathway.

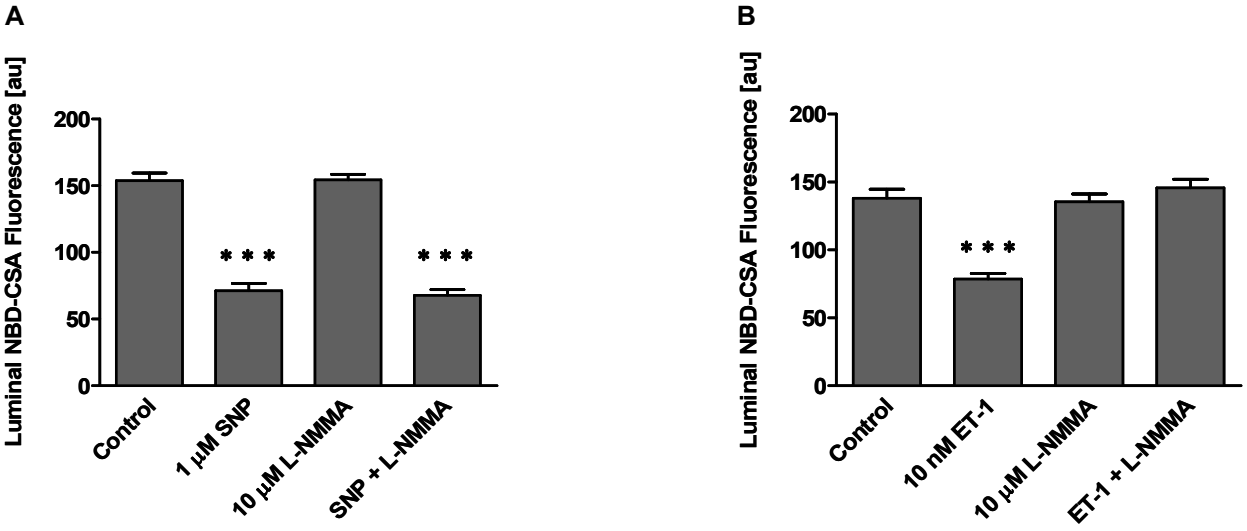

Figure 3.52
Inhibition of NO synthase with L-NMMA

A: L-NMMA did not reverse the SNP effect (mean ± SEM, n=10, *** $p < 0.001$).

B: L-NMMA abolished the ET-1 effect by NOS inhibition (mean ± SEM, n=10, *** $p < 0.001$).

3.2.3.3 Protein Kinase C is Involved in ET-1 Signaling

To examine whether protein kinase C (PKC) is part of the ET-1 signaling pathway, capillaries were exposed to PKC agonists and antagonists. The phorbol ester, phorbol-12-myristate-13-acetate (PMA), which activates PKC, decreased P-gp-mediated NBD-CSA transport (Figure 3.53A). This decrease was concentration-dependent; 10 nM PMA caused a maximal decrease. Bisindolylmaleimide I (BIM) is a potent inhibitor for all PKC isoforms. BIM had no effect on luminal NBD-CSA accumulation by itself, but it blocked completely the effect of PMA (Figure 3.53B).

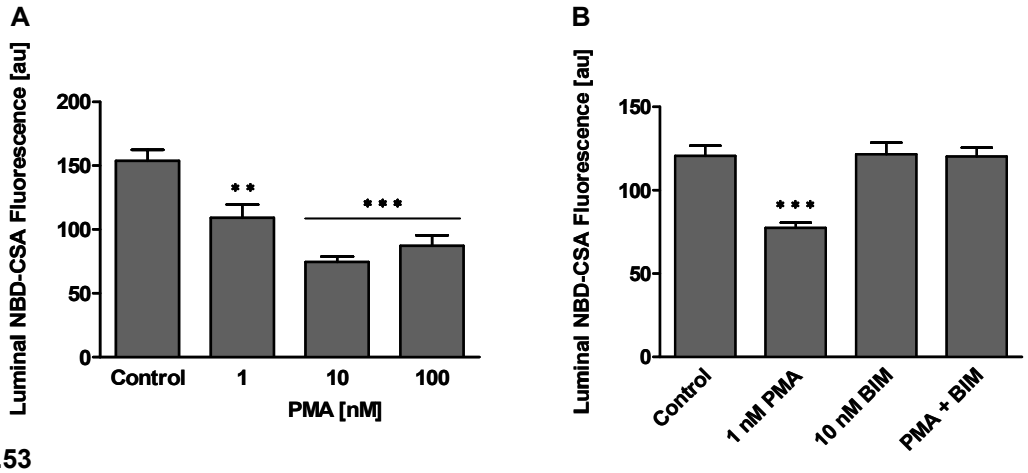

Figure 3.53
Effect of the PKC agonist PMA on luminal NBD-CSA fluorescence

A: Concentration-dependent effect of PMA. The PKC agonist PMA decreased luminal NBD-CSA fluorescence in a concentration-dependent manner (mean ± SEM, n=10, *** $p < 0.001$).

B: Reversal of the PMA effect by the PKC antagonist BIM (mean ± SEM, n=10, *** $p < 0.001$).

To determine whether PKC is involved in the ET-1 signaling pathway, BIM was used to block ET-1 signaling. Figures 3.54A and B show that BIM completely blocked the decrease in luminal NBD-CSA fluorescence caused by SNP and ET-1. These results indicate that PKC signaling followed both, ET-1 binding and NOS activation. Thus, ET-1, acting through an ET_B receptor, activated NOS and PKC, and this chain of events rapidly decreased P-glycoprotein transport function.

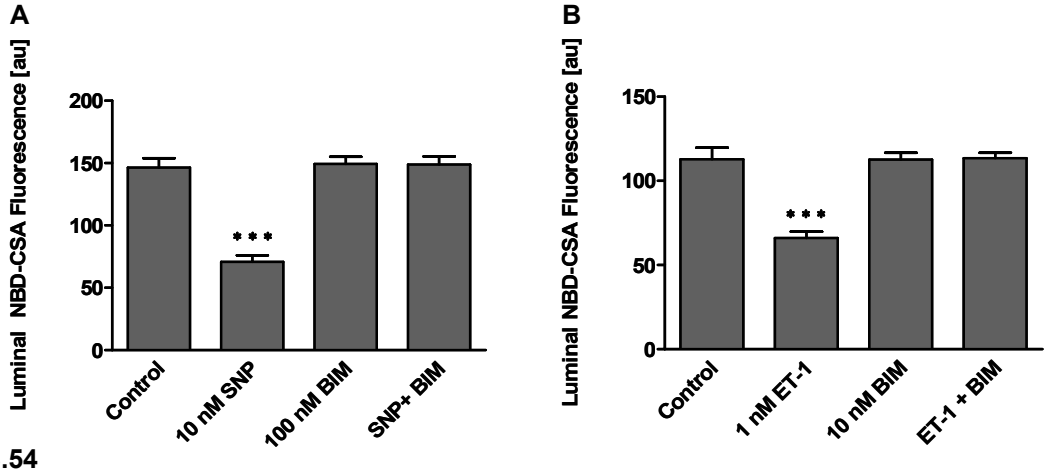

Figure 3.54
PKC inhibition reversed the effects of SNP and ET-1

A: Reversal of the SNP effect by PKC inhibition with BIM (mean ± SEM, n=10, *** $p < 0.001$).

B: Reversal of the ET-1 effect by BIM (mean ± SEM, n=10, *** $p < 0.001$).

3.2.3.4 Effects of ET-1, SNP, PMA and Mannitol on P-gp Expression

A decrease in P-gp-mediated transport could have resulted from either reduced transport function or decreased P-gp expression. Capillaries were incubated for 1h with ET-1, SNP, PMA or mannitol and immunostained for P-gp. In addition, membranes were isolated and Western blots for P-gp were performed.
Figure 3.55 shows the result from a quantitative immunostaining of P-gp from capillaries treated with ET-1, SNP, PMA or mannitol over 1 hour. P-gp protein expression remained unchanged, indicated by no change in P-gp immunofluorescence.

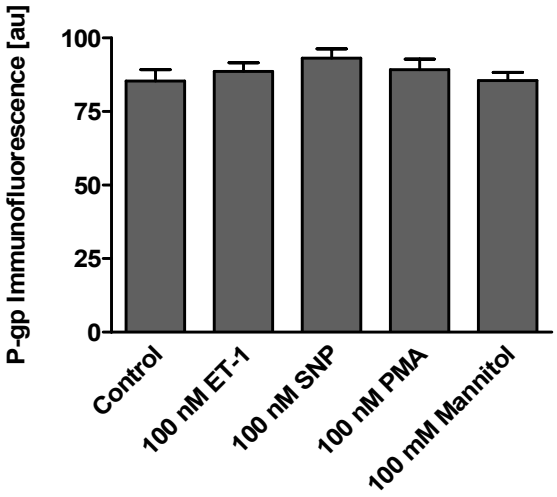

Figure 3.55
Effects of ET-1, SNP, PMA and mannitol on P-gp expression

Exposing capillaries for 1h to ET-1, SNP, PMA or mannitol did not alter luminal membrane P-gp immunofluorescence indicating no change in P-gp expression (mean ± SEM, n=15).

The Western blot for P-gp in Figure 3.56 shows that P-gp protein expression remained unchanged after 1-hour exposure to ET-1, SNP, PMA and mannitol, confirming the finding from the immunostaining. These findings strongly indicate that the decrease in luminal NBD-CSA accumulation caused by these compounds is due to reduced P-gp transport function without downregulation of P-gp protein expression.

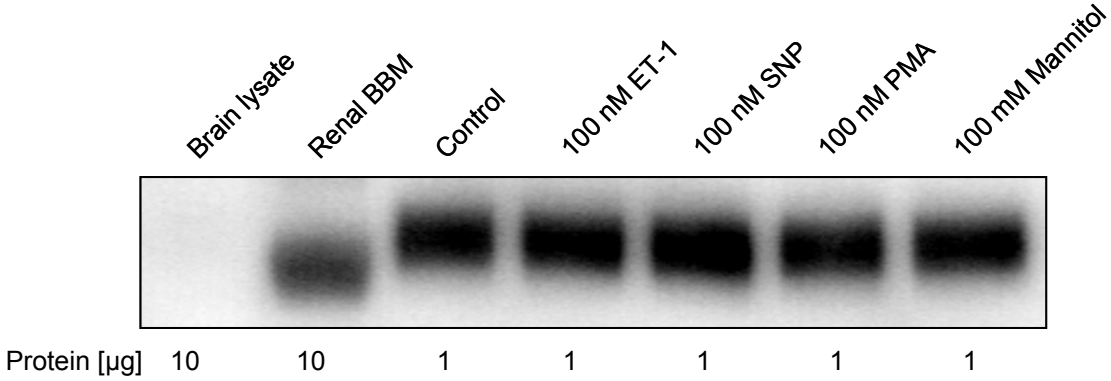

Figure 3.56
Western blot for P-glycoprotein

No change in capillary membrane P-glycoprotein expression after exposing capillaries for 1 hour to ET-1, SNP, PMA or mannitol.

3.2.3.5 Summary of Part 3.2.3:

Regulation of P-glycoprotein by Endothelin-1

Western blot and immunostaining demonstrated expression of both, ET_A and ET_B receptor in isolated rat brain capillaries (Figures 3.44-47). However, only the ET_B receptor was detected in capillary membranes.

Like ET-1, the ET_B receptor agonist sarafotoxin S6c reduced P-gp-mediated NBD-CSA transport in a concentration-dependent manner (Figure 3.49). Only the ET_B receptor antagonist reversed the effects of ET-1 and sarafotoxin S6c (Figures 3.48 and 3.50). This indicates that ET-1 decreased P-gp-mediated NBD-CSA transport by signaling through the ET_B receptor. The NO donor SNP also decreased luminal fluorescence in a concentration-dependent manner (Figure 3.51). A NO synthase inhibitor completely reversed the effect of ET-1 suggesting that NOS is involved in the signaling pathway (Figure 3.52B). Experiments with PKC activators and PKC inhibitors implicate that PKC is part of the ET-1 signaling pathway, with PKC activation following NOS activation (Figures 3.53-54). P-gp protein expression remained unchanged in capillaries exposed to ET-1, SNP, PMA or mannitol for 1 hour (Figures 3.55-56).

Together, the findings support the hypothesis that ET-1 decreased P-gp transport function by signaling through an ET_B receptor, NOS and PKC.

3.2.4 Discussion of Part 3.2:

Rapid Regulation of P-glycoprotein at the Blood-Brain Barrier by Endothelin-1

For the work in the second part of the Results and Discussion, isolated rat brain capillaries were used in combination with fluorescent dyes and confocal laser scanning microscopy to measure P-glycoprotein transport function at the blood-brain barrier. This model system has previously been shown by Miller et al. to be a powerful tool to study transport at the blood-brain barrier (Miller, 2003; Miller et al., 2002a; Miller et al., 2000). It enables one to visualize and follow bath to lumen transport of fluorescent dyes that are substrates for efflux pumps present in the brain capillary endothelium (Fricker et al., 2002; Miller et al., 2000; Nobmann et al., 2001).

First, the *ex vivo* model system was optimized with regard to microscopy settings, incubation temperature and incubation time (Figures 3.32, 3.33 and 3.36). In addition, 0.1% DMSO in the incubation buffer was found to have no effect on capillary function (Figure 3.34).

With the basic experimental settings optimized, rat brain capillary P-glycoprotein was studied for its specificity to transport NBD-CSA. For this purpose, inhibition experiments were conducted using well-known P-glycoprotein substrates such as verapamil, ivermectin and cyclosporin A as well as the specific P-glycoprotein inhibitor PSC833 (Achira et al., 1999; Kusunoki et al., 1998; Mayer et al., 1997; Watanabe et al., 1995). In addition, capillaries were incubated with compounds mainly transported by Mrp1 and Mrp2, in order to exclude any contribution to NBD-CSA transport by Mrps. All experiments clearly indicated that NBD-CSA is specifically transported by P-glycoprotein: PSC833 prevented luminal accumulation (Figures 3.35B and 3.36) and reduced fluorescence in a concentration-dependent manner to about 40-50% of control values (Figure 3.37). In previous studies with isolated brain capillaries from rat, pig and fish, concentrative, energy-dependent and PSC833-sensitive bath-to-lumen transport of NBD-CSA was also demonstrated (Fellner et al., 2002; Miller, 2003; Miller et al., 2002a; Schramm et al., 1995). A combined *in vitro/in vivo* study by Fellner et al. showed that co-administration of the anticancer drug paclitaxel and PSC833 enhanced paclitaxel levels in brains leading to significant reduction of brain tumor size in mice (Fellner et al., 2002). Preclinical and clinical studies also showed that PSC833 inhibits P-glycoprotein in humans resulting in higher paclitaxel plasma levels (Advani et al., 2001; Fracasso et al., 2000; Mayer et al., 1997). The P-gp substrates verapamil, ivermectin and cyclosporin A also reduced transport of NBD-CSA (Figures 3.38A and B), whereas Mrp substrates and inhibitors were without effect (Figure 3.38C). These results confirm the studies by Miller et al. and Nobmann et al., who clearly established that NBD-CSA is specifically transported by P-glycoprotein into lumens of isolated brain capillaries of rat and pig (Fellner et al., 2002; Miller et al., 2000; Nobmann et al., 2001). However, another multispecific efflux pump, BCRP, is also expressed at the luminal membrane of rat brain capillaries (Figures 3.17-18) (Cooray et al., 2002; Hori et al., 2004). Although BCRP and P-gp share substrates, PSC833 is at best a low-affinity inhibitor of BCRP, and does not affect BCRP-mediated transport (Sarkadi et al., 2004; Tan et al., 2000; Zhang et al., 2003a). Although the participation of yet-unidentified transporters cannot be excluded, these data strongly suggest that the concentrative, specific and energy-dependent transport of NBD-CSA in isolated rat brain capillaries is mediated by P-glycoprotein. To date, the brain capillary *ex vivo* blood-brain barrier model has been used to look at transport of fluorescent P-glycoprotein and Mrp2

substrates and to test compounds for their potential to inhibit transport (Fellner et al., 2002; Fricker et al., 2002; Miller, 2003; Miller et al., 2002a; Miller et al., 2000; Nobmann et al., 2001).

In this thesis, for the first time, this model system was used to unravel signaling at the blood-brain barrier. More specifically, the short-term regulation of P-glycoprotein at the blood-brain barrier by the peptide hormone endothelin-1 (ET-1) was studied. Subnanomolar to nanomolar concentrations of ET-1 rapidly and reversibly reduced P-glycoprotein-mediated transport of NBD-CSA into capillary lumens (Figure 3.39). It should be stressed that decreased luminal accumulation of NBD-CSA caused by ET-1 was not accompanied by increased capillary permeability (caused by opening of tight junctions). This was shown by using a kinetic assay based on efflux of preloaded Texas Red from the lumens of capillaries. ET-1 did not increase Texas Red efflux compared to efflux from control capillaries (Figure 3.43, Table 3.1), suggesting that tight junctions were not affected. It is also noteworthy that Mrp2-mediated Texas Red transport into capillary lumens was unaffected by 100 nM ET-1 (Figure 3.41), a concentration 100 times higher than that causing maximal reduction of P-glycoprotein mediated NBD-CSA transport. This is further proof that ET-1 did not open tight junctions. Moreover, this observation is interesting since it is different from renal proximal tubules, where ET-1 was shown to reduce Mrp2 transport function (Masereeuw et al., 2000; Miller, 2002; Notenboom et al., 2002; Terlouw et al., 2001).

The literature contains conflicting reports as to the effects of ET-1 on brain capillary permeability. For example, injection of ET-1 into the brain has been reported to increase permeability (Miller et al., 1996; Narushima et al., 2003; Narushima et al., 1999) or to have no significant effect (Hughes et al., 2003). In these *in vivo* studies, permeability measurements were made after many hours to days of ET-1 treatment. In the present experiments, capillaries were exposed to ET-1 for only 1 to 2 hours. Thus, it is possible that ET-1 does increase brain capillary permeability over longer time periods whereas decreased P-glycoprotein transport function with no change in capillary permeability is an early effect of ET-1 exposure (Hartz et al., 2004).

Taken together, from these data, it was concluded that ET-1-mediated reduction of P-gp transport function rather than an opening of tight junctions caused the decrease in luminal NBD-CSA fluorescence.

Further experiments were conducted to reveal the signaling pathway through which ET-1 changes P-glycoprotein function. NBD-CSA transport was reduced by ET-1 activation of ET_B receptor and subsequent activation of two intracellular enzymes, NO synthase (NOS) and protein kinase C (PKC). ET-1 actions were mimicked by the ET_B receptor agonist sarafotoxin S6c; both ET-1 and sarafotoxin S6c effects were blocked by an ET_B receptor antagonist but not by an ET_A receptor antagonist (Figures 3.48-3.50). Consistent with previous findings, both the ET_A and ET_B receptor were found to be expressed in isolated rat brain capillaries (Kedzierski and Yanagisawa, 2001; Levin, 1995; Willette, 1995). The A-type receptor was expressed in capillary lysate, but not in capillary membranes (Figures 3.44 and 3.45). The ET_B receptor was highly expressed in capillary lysate as well as in capillary membranes (Figures 3.46 and 3.47). The signal for ET_B in capillary membranes was lower than the one for capillary lysate, which might reflect intracellular pools as previously reported (Bremnes et al., 2000). In addition, the B-type receptor was immunolocalized to both, the luminal and abluminal membranes of the capillary endothelium (Figure 3.47, inlet). Thus, ET-1 released into the blood or produced in the brain *in vivo* could affect P-gp-mediated transport at the blood-brain barrier.

SNP, which generates NO, also reduced P-glycoprotein-mediated transport, presumably mimicking the effects of NOS activation (Figure 3.51). The NOS inhibitor, L-NMMA, did not reverse the SNP-mediated decrease of luminal NBD-CSA fluorescence but abolished the ET-1 effect (Figure 3.52). Since L-NMMA inhibits all NOS isoforms, further studies are needed to clarify which isoform is activated by ET-1.
However, at present, there are no NOS isoform-specific inhibitors commercially available.
Activation of PKC with nanomolar concentrations of phorbol-12-myristate-13-acetate (PMA) also reduced P-glycoprotein-mediated NBD-CSA transport into capillary lumens (Figure 3.53A). A PKC inhibitor, BIM, could block this effect (Figure 3.53B). Inhibition of PKC also blocked the effects of ET-1 and SNP (Figure 3.54). However, at present it is not clear how PKC modifies P-glycoprotein function. Given the rapid time course of action seen with isolated brain capillaries, three types of mechanism seem possible:

1) PKC directly phosphorylates the transporter changing turnover number or substrate affinity.
   However, this hypothesis is contradictory to Chambers et al., who found that P-gp phosphorylation by PKC stimulated P-gp transport in KB-V1 cells (Chambers et al., 1990a; Chambers et al., 1990b; Chambers et al., 1992). On the other hand, Germann et al. suggested that phosphorylation of P-glycoprotein has no effect on its transport function at all (Germann et al., 1995).
2) PKC phosphorylates an accessory protein that modifies P-glycoprotein activity.
3) PKC influences P-glycoprotein trafficking, stimulating retrieval from the plasma membrane into a vesicular compartment.
   This has been demonstrated for P-glycoprotein and other ABC transporters in hepatocytes (Kipp and Arias, 2002; Kipp et al., 2001).

At present, however, it cannot be distinguished between the three possibilities.

Taken together, the minimal signaling pathway of ET-1-mediated reduction in P-glycoprotein transport function in isolated rat brain capillaries that fits the data is linear, going from the ET_B receptor over NOS to PKC (Hartz et al., 2004).

3.2.5 Summary of Part 3.2:

Rapid Regulation of P-glycoprotein at the Blood-Brain Barrier by Endothelin-1
(Hartz et al., 2004)

Freshly isolated rat brain capillaries were used to study short-term regulation of P-glycoprotein transport function at the blood-brain barrier. Accumulation of P-glycoprotein-specific, fluorescent NBD-cyclosporin A (NBD-CSA) in capillary lumens was followed using confocal microscopy. Confocal images were analyzed and quantitated using imaging software.
Preliminary experiments revealed that brain capillaries did not exhibit auto-fluorescence (Figure 3.32), that NBD-CSA transport was maximal at room temperature (Figure 3.33) and that concentrations of up to 0.1% DMSO did not affect luminal NBD-CSA accumulation (Figure 3.34).
Over a period of 60 min, capillaries rapidly accumulated NBD-CSA; luminal fluorescence reached steady state levels after 30 min (Figures 3.35A and 3.36). The P-gp-specific inhibitor PSC833 reduced luminal fluorescence in a concentration-dependent manner (Figures 3.35B, 3.36 and 3.37). The P-gp substrates verapamil, ivermectin and cyclosporin A reduced NBD-CSA transport (Figures 3.38A and B); Mrp substrates and inhibitors were without effect (Figure 3.38C).
Exposing capillaries to nanomolar concentrations of ET-1 rapidly diminished luminal NBD-CSA fluorescent in a concentration-dependent manner (Figure 3.39A); this effect was reversible (Figure 3.39B). PSC833 and mannitol, which osmotically opens tight junctions, had comparable effects on luminal NBD-CSA fluorescence (Figure 3.40). Mrp2-mediated Texas Red transport was unchanged with PSC833 and ET-1 (Figure 3.41). Texas Red efflux from preloaded capillaries, however, was highly increased by compounds that open tight junctions (Figure 3.43A). Importantly, ET-1 had no effect on Texas Red efflux, suggesting that ET-1 does not affect tight junctional permeability (Figure 3.43B and Table 3.1).
Western blot and immunostaining demonstrated that both, ET_A and ET_B receptor are expressed in isolated rat brain capillaries. However, only the ET_B receptor was detected in capillary membranes (Figures 3.44-47). Like ET-1, the ET_B receptor agonist sarafotoxin S6c reduced P-gp-mediated NBD-CSA transport in a concentration-dependent manner (Figure 3.49). Only an ET_B receptor antagonist reversed the effects of ET-1 and sarafotoxin S6c, but not an ET_A receptor antagonist (Figures 3.48 and 3.50). The NO donor SNP also decreased luminal fluorescence in a concentration-dependent manner (Figure 3.51). A NO synthase inhibitor completely reversed the effect of ET-1 suggesting that NOS is involved in the signaling pathway (Figure 3.52B). Experiments with PKC activators and inhibitors implicate that PKC is part of the ET-1 signaling pathway (Figures 3.53-54). P-gp protein expression remained unchanged in capillaries exposed to ET-1, SNP, PMA or mannitol for 1 hour (Figures 3.55-56).
Altogether, these findings indicate that concentrative, specific and energy-dependent transport of NBD-CSA in isolated rat brain capillaries is mediated by P-glycoprotein. Furthermore, they show that ET-1 decreased P-gp transport function by acting through an ET_B receptor followed by activation of NOS and PKC. Figure 3.57 summarizes the findings on rapid regulation of P-glycoprotein at the blood-brain barrier by endothelin-1.

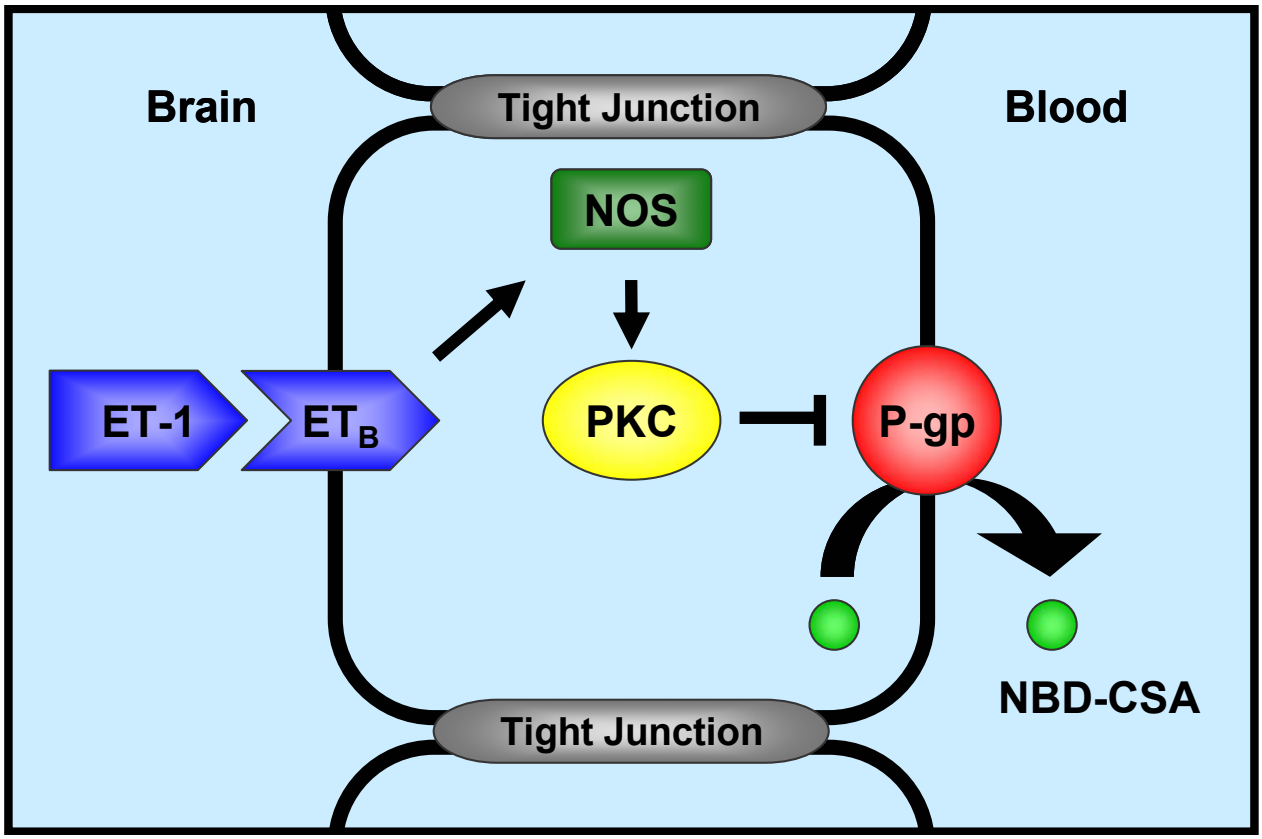

Figure 3.57
Rapid regulation of P-glycoprotein at the blood-brain barrier by endothelin-1

ET-1 rapidly decreased P-gp transport function in isolated rat brain capillaries by signaling through an ET_B receptor, NOS and PKC.

3.3 Pregnane X Receptor Upregulation of P-glycoprotein Expression and Transport Function at the Blood-Brain Barrier

3.3.1 Detection of Pregnane X Receptor in Isolated Rat Brain Capillaries

The pregnane X receptor (PXR, *NR1I2*) is a ligand-activated, nuclear transcription factor. In liver, PXR regulates a network of multiple target genes, mainly those encoding drug metabolizing enzymes and drug transporters (Kliewer et al., 1998). PXR activation occurs upon binding by its ligands, which include endogenous compounds (e.g. steroids, bile acids, metabolites) as well as xenobiotics (e.g. large number of drugs, dietary compounds, pollutants) (Jacobs et al., 2003). PXR is abundantly expressed in liver and intestine, and was also detected in other tissues. It is the only nuclear receptor known to regulate P-glycoprotein expression (Geick et al., 2001)

The objective of this part was to examine whether PXR is expressed at the blood-brain barrier and whether it regulates P-gp in brain capillaries. PXR expression in isolated rat brain capillaries was analyzed by RT-PCR, Western blot analysis and immunohistochemistry. Figure 3.58 shows RT-PCR for PXR mRNA. A 353 bp product was obtained for the control tissues liver and kidney, and more importantly for brain homogenate and brain capillaries. To confirm the identity of the band, the PCR product was sequenced and found to be 100 % identical only to a portion of the rat PXR gene (GenBank accession no. AF151377).

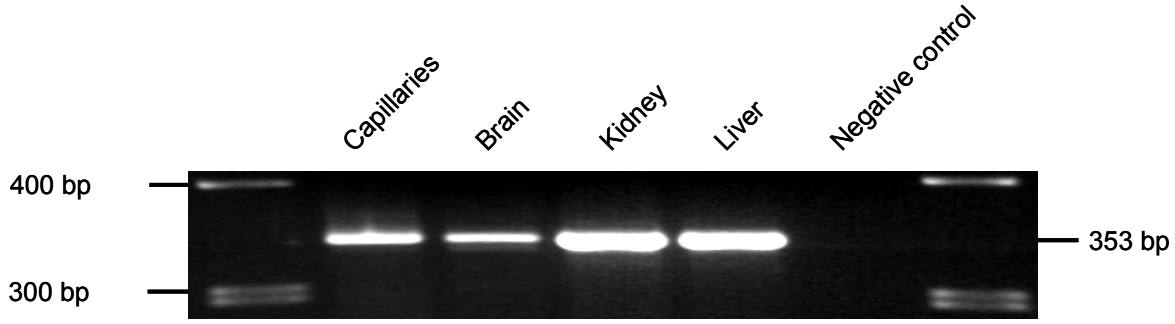

Figure 3.58
RT-PCR for rat PXR

Capillaries, brain, kidney and liver show bands of a 353 bp rat PXR-specific amplicon.

Figure 3.59 shows a Western blot for PXR from capillary nuclear protein. In the left lane, the membrane was incubated with PXR antibody only; in the right lane, the membrane was incubated with antigen-blocked antibody. Therefore, bands that appear in the left lane are specific for PXR. The weak band at about 50 kDa is likely to be PXR. The band at about 105 kDa might be a heterodimer of PXR and the nuclear receptor RXRα. Another band at about 100 kDa might be PXR homodimer, the formation of which has been reported in the literature before (Watkins et al., 2003a). The bands between 105 kDa and 160 kDa might be PXR-RXRα heterodimer in complex with coactivators or corepressors (Glass, 1994; Mangelsdorf et al., 1995; Watkins et al., 2003a). However, none of the bands has been sequenced and therefore, cannot clearly be identified.

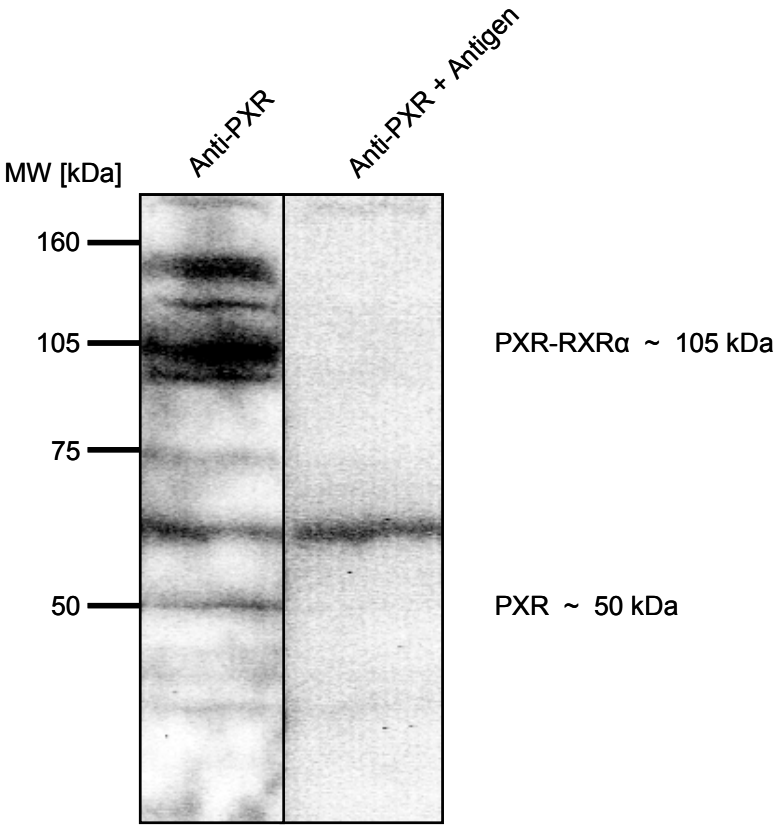

Figure 3.59
Western blot for PXR from capillary nuclear proteins

Left lane: Membrane incubated with PXR antibody. The capillary nuclear fraction shows a weak band at 50 kDa likely representing PXR and a strong band at 105 kDa likely representing PXR-RXRα.

Right lane: Membrane incubated with antigen-blocked PXR antibody. The band at 60 kDa is due to unspecific binding of either primary or secondary antibody.

Figure 3.60 shows capillaries immunostained for PXR. Immunofluorescence (Figure 3.60A) is extending over endothelial cell cytoplasm and nucleus. The strong staining supports the findings of the RT-PCR and the Western blot.

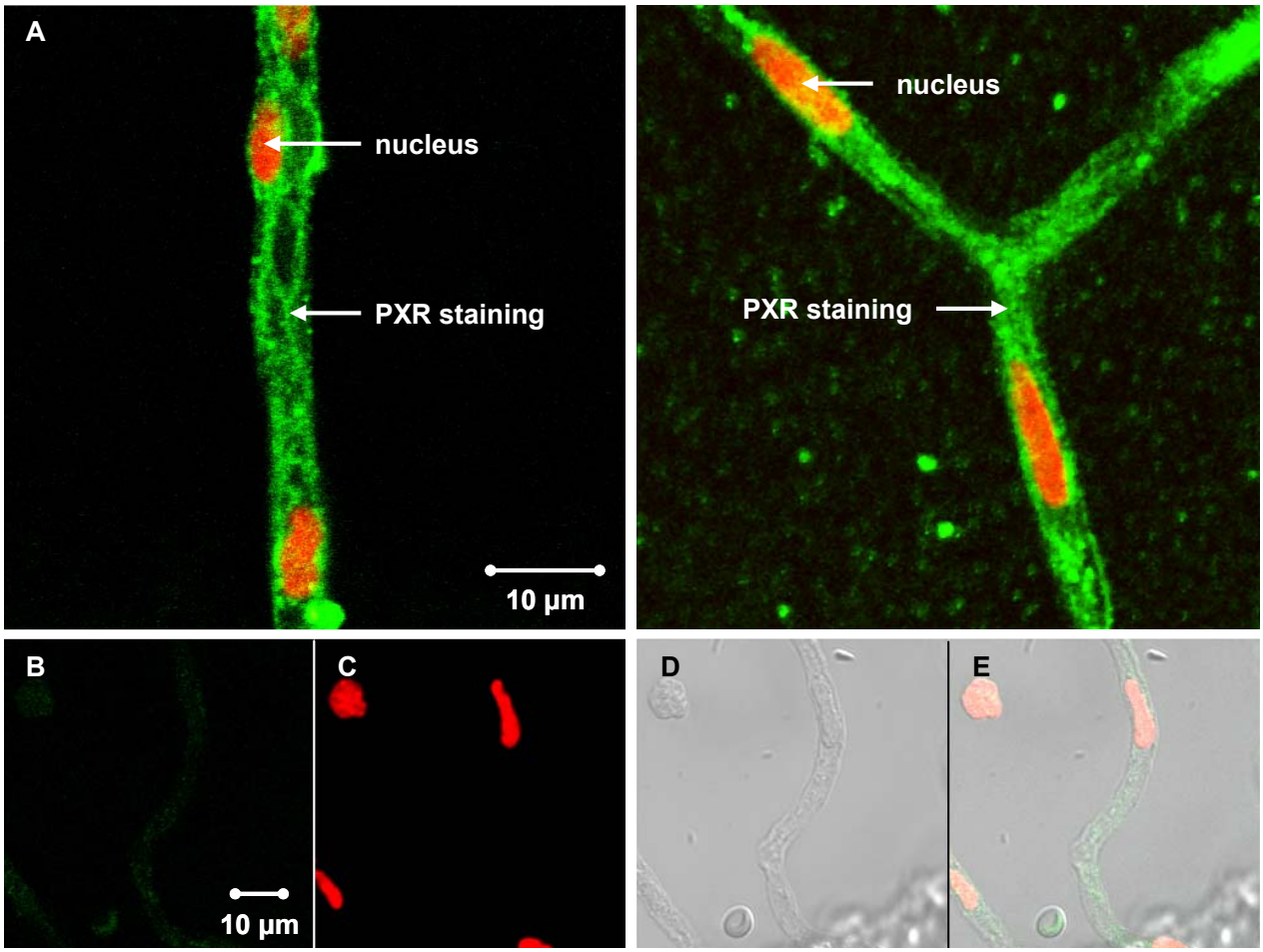

Figure 3.60
Immunostaining of capillaries for PXR

A: Rat brain capillaries immunostained for PXR (green) and counterstained for nuclei (red) PXR immunofluorescence extends over endothelial cell cytoplasm and nucleus.
B: Negative control (green channel)
C: Negative control (red channel)
D: Transmitted light image
E: Overlay of images B, C and D

3.3.2 Summary of Part 3.3.1: Detection of PXR in Isolated Rat Brain Capillaries

PXR mRNA expression in brain capillaries was detected by RT-PCR (Figure 3.58); the PCR product was confirmed by direct sequencing to be 100% identical only to the rat PXR gene. Western blot analysis showed PXR protein expression in the nuclear fraction of capillaries (Figure 3.59). Immunostaining PXR in isolated brain capillaries showed extending immunofluorescence over cytoplasm and nucleus (Figure 3.60). This is the first evidence of PXR expression in brain and rat brain capillaries (Bauer et al., 2004).

3.3.3 *In Vitro* Induction of P-gp Expression and Transport Function by PXR

3.3.3.1 *In Vitro* Experiments with PCN

3.3.3.1.1 Effects of PCN, Hyperforin and Paclitaxel on P-gp Expression

In order to examine PXR regulation of P-glycoprotein expression at the blood-brain barrier, isolated rat brain capillaries were exposed to the PXR ligands, pregnenolone-16α-carbonitrile (PCN), the St. John's wort constituent, hyperforin, and the anti-cancer therapeutic, paclitaxel. Since PXR shows remarkable species differences in ligand specificity, PCN activates rodent PXR but not human PXR (hPXR) (Kliewer et al., 1998; Xie et al., 2004). In contrast, hyperforin and paclitaxel are potent activators of hPXR but do not activate rodent PXR (Moore et al., 2000a; Synold et al., 2001; Wentworth et al., 2000).
Isolated rat brain capillaries were treated for 6 hours with 10 µM PCN, hyperforin or paclitaxel, respectively. Then, capillary membranes were isolated and analyzed for P-gp expression by Western blotting (Figure 3.61). Membranes from capillaries treated with 10 µM PCN showed a significant stronger signal for P-gp in comparison to membranes from control capillaries. Importantly, hyperforin and paclitaxel had no effect on P-gp expression levels in rat brain capillaries.

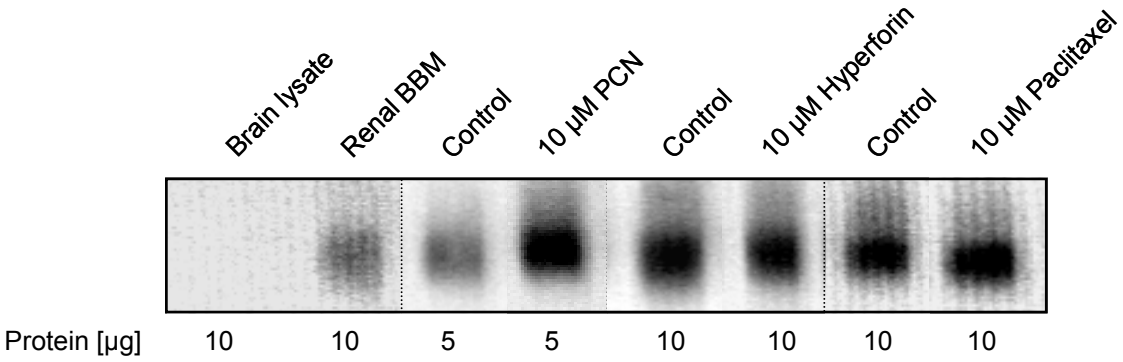

Figure 3.61
Western blot for P-gp with membranes from capillaries treated with 10 µM PCN, hyperforin or paclitaxel

Membranes of capillaries treated with 10 µM PCN show strong P-gp induction compared to membranes from control capillaries. There is no change in band intensity with membranes from capillaries treated with hyperforin or paclitaxel.

3.3.3.1.2 Time-Dependent Induction of P-gp Expression by PCN

To examine the time-dependent increase in P-gp expression by PXR activation, isolated capillaries were exposed to 5 µM PCN. After 0, 1, 3 and 6 hours, capillaries were fixed and immunostained for P-gp; images were taken using a confocal microscope.
Figure 3.62 shows representative images of capillaries immunostained for P-gp (green), nuclei were counterstained with propidium iodide (red). The top panel shows that in control capillaries P-gp immunofluorescence remained unchanged over the period of the 6-hour time course. In contrast, capillaries treated with PCN showed significantly increased P-gp immunofluorescence after 3 hours (Figure 3.62 bottom panel). After 6 hours, the fluorescent signal for immunostained P-gp had increased even more.

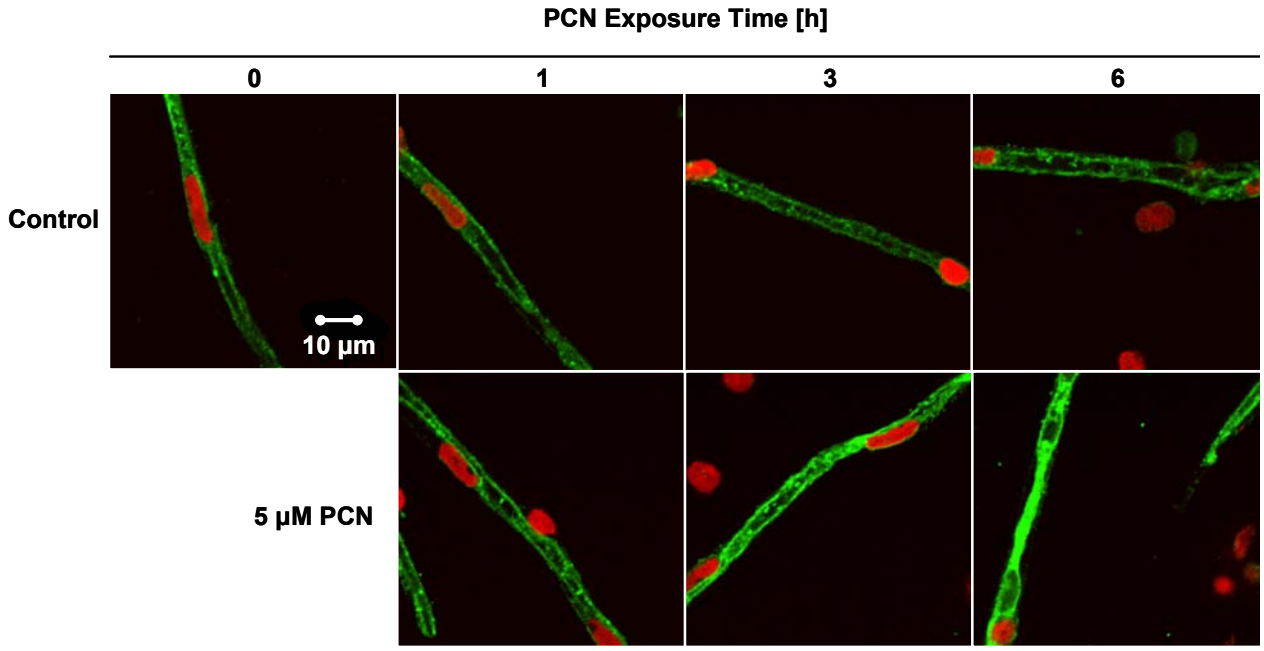

Figure 3.62
Capillaries immunostained for P-gp after 0, 1, 3 and 6 hours of exposure to 5 µM PCN

Exposing capillaries to 5 µM PCN significantly increased P-gp immunofluorescence in a time-dependent manner (bottom panel) compared to the corresponding control at the same time point (top panel).

Confocal images of untreated control capillaries and 5 µM PCN-treated capillaries were analyzed and P-gp immunofluorescence in the luminal membrane of capillaries was quantitated using imaging software. P-gp immunofluorescence data is presented in Figure 3.63 as a function of time. In accordance with the immunostainings in Figure 3.62, luminal membrane immunofluorescence in PCN-treated capillaries increased significantly after 3 hours and increased further after 6 hours. Over this period, luminal membrane immunofluorescence in control capillaries did not change.
These results demonstrate that PXR activation increases P-gp expression in the luminal membrane of isolated rat brain capillaries. P-glycoprotein induction in this model occurs over a period of 6 hours.

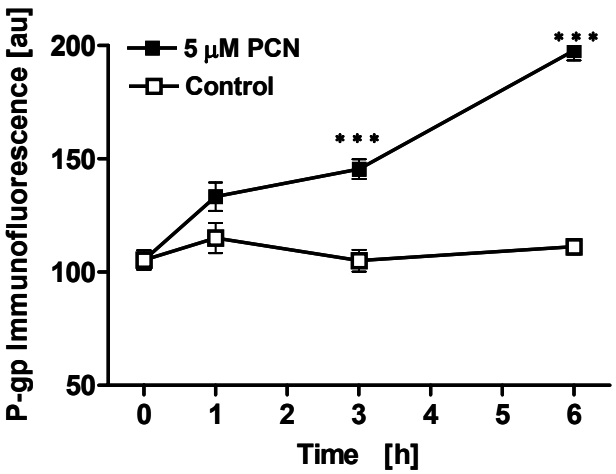

Figure 3.63
Time course of P-gp immunofluorescence from capillaries exposed to 5 µM PCN

P-gp immunofluorescence of control capillaries was unchanged over a period of 6 hours. Capillaries treated with 5 µM PCN showed a significant increase in P-gp immunofluorescence in the same period of time (pooled tissue from 10 rats, mean ± SEM, n=15, *** $p < 0.001$).

3.3.3.1.3 Concentration-Dependent Induction of P-gp Expression by PCN

Isolated capillaries were exposed to 1, 5 and 10 µM PCN for 6 hours. Then, capillaries were immunostained for P-gp. Figure 3.64 shows representative images for control and PCN-treated capillaries. Capillaries treated with 1 and 5 µM PCN displayed a significantly stronger staining than control capillaries. However, immunofluorescence of capillaries exposed to 10 µM PCN was only slightly higher than immunofluorescence of control capillaries. This is possibly due to toxic effects of PCN at higher concentrations.

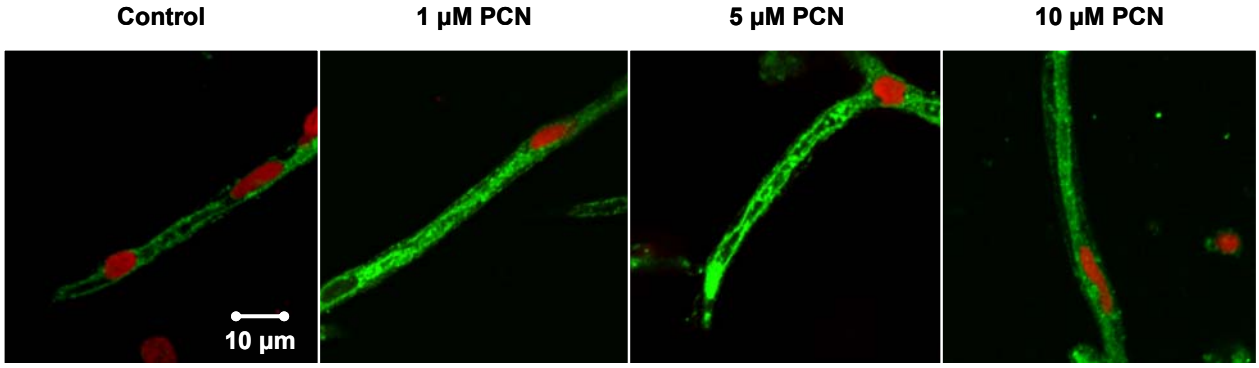

Figure 3.64
Immunostaining for P-gp of capillaries treated with 0, 1, 5 and 10 µM PCN

PCN caused an increase in P-gp immunofluorescence (green). Capillaries treated with 5 µM PCN showed the strongest P-gp immunofluorescence. Nuclei were counterstained with propidium iodide (red).

Figure 3.65 summarizes immunostaining data from 5 experiments. P-gp immunofluorescence is presented as a function of PCN concentration. P-gp induction was concentration-dependent: 1 µM PCN increased P-gp immunofluorescence on average to 135 ± 5.4% of the control value, 3 µM PCN to 149 ± 4.9% and a maximal increase to 186 ± 17% of the control was observed with 5 µM PCN. Capillaries treated with 10 µM PCN showed about 25% lower P-gp immunofluorescence than capillaries exposed to 5 µM PCN, again suggesting PCN toxicity at higher concentrations.

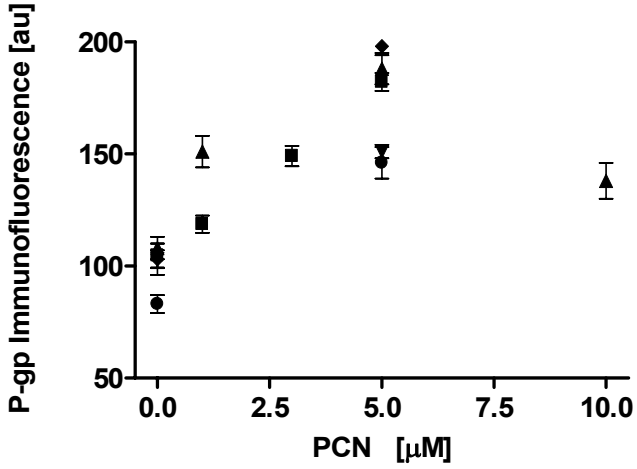

Figure 3.65
Concentration-dependent increase of P-gp immunofluorescence by PCN

PCN increased P-gp immunofluorescence in luminal membranes of capillaries in a concentration-dependent manner (mean ± SEM, summarized data from 5 experiments, each point represents the average luminal membrane P-gp immunofluorescence from 15-20 capillaries of pooled tissue from 3-10 rats per single preparation).

After 6-hour exposure of capillaries to 0, 1, 3 and 5 µM PCN, capillary membranes were isolated and Western blot analysis for P-gp was performed. Membranes from capillaries treated with 1, 3 and 5 µM PCN displayed increased band intensities when compared to the control (Figure 3.66). The increase caused by PCN was concentration-dependent: 1 µM PCN had the weakest effect, 3 µM PCN had a moderate effect and 5 µM PCN caused the highest increase in P-gp expression.

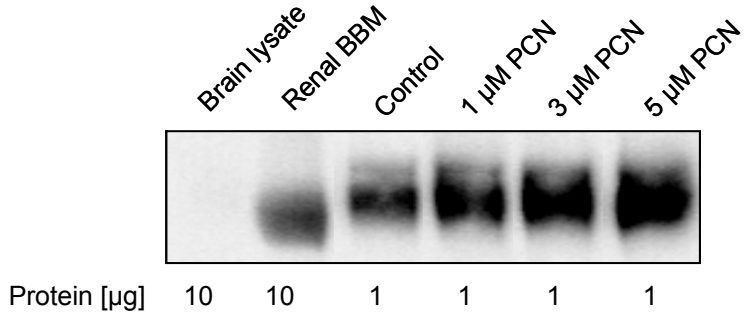

Figure 3.66
Western blot for P-gp with membranes from capillaries exposed to 0, 1, 3 and 5 µM PCN

PCN increased P-gp band intensity in a concentration-dependent manner. The increase was weak with 1 µM PCN, moderate with 3 µM PCN and strongest with 5 µM PCN.

In order to guarantee equal protein-loading of the gels, expression of Na^+/K^+-ATPase, used as housekeeping gene and plasma membrane marker, was examined. Samples were also probed for GAPDH (glycerylaldehyde-phosphate dehydrogenase), a cytoplasmic protein, to evaluate purity of crude membrane preparations.
Figure 3.67 shows a Western blot for Na^+/K^+-ATPase and GAPDH from the same brain capillary crude membrane preparation as shown in Figure 3.66. It shows membranous expression of Na^+/K^+-ATPase in capillaries. Importantly, Na^+/K^+-ATPase expression levels were not changed in PCN-treated rats. In addition, only faint GAPDH bands were observed for isolated membranes (renal as well as capillary crude membranes), whereas the signal for total brain homogenate was strong. Since this Western blot is representative for all *in vitro* experiments, Western blots for Na^+/K^+-ATPase and GAPDH are not shown for the following experiments.

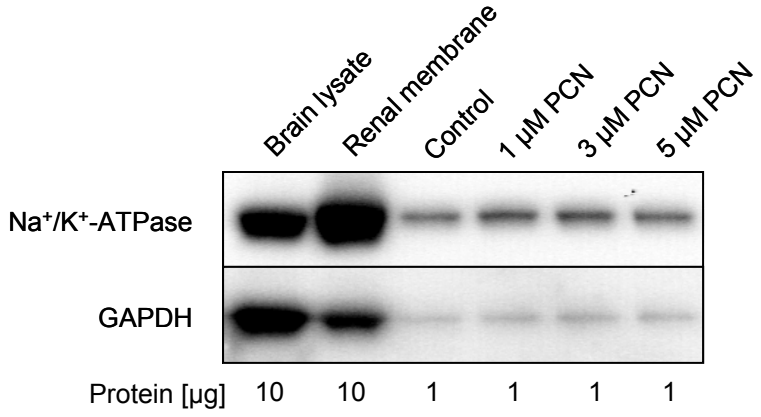

Figure 3.67
Western blot for Na^+/K^+-ATPase and GAPDH with capillary membranes from PCN-treated rats

PCN did not change expression of Na^+/K^+-ATPase, indicating equal gel-protein-loading. The capillary membrane fraction shows only faint GAPDH bands indicating a pure membrane preparation.

3.3.3.1.4 Concentration-Dependent Induction of P-glycoprotein Transport Function by PCN

To determine whether PCN also increased P-glycoprotein transport function at the blood-brain barrier, isolated rat brain capillaries were exposed to 0-5 µM PCN for 6 hours, and NBD-CSA transport was measured. In order to assess P-gp-specific transport, some capillaries were also incubated with the metabolic inhibitor NaCN and the P-gp inhibitor PSC833.

Figure 3.68 shows that PCN increased luminal NBD-CSA fluorescence in a concentration-dependent manner: 1 µM PCN increased P-gp-specific transport to 119 ± 5%, 3 µM PCN to 163.5 ± 4.8% and 5 µM PCN to 202 ± 4.7% of the control. With 5 µM PCN, specific NBD-CSA transport had more than doubled. Fluorescence intensity to NaCN or PSC833 was not changed by PCN.

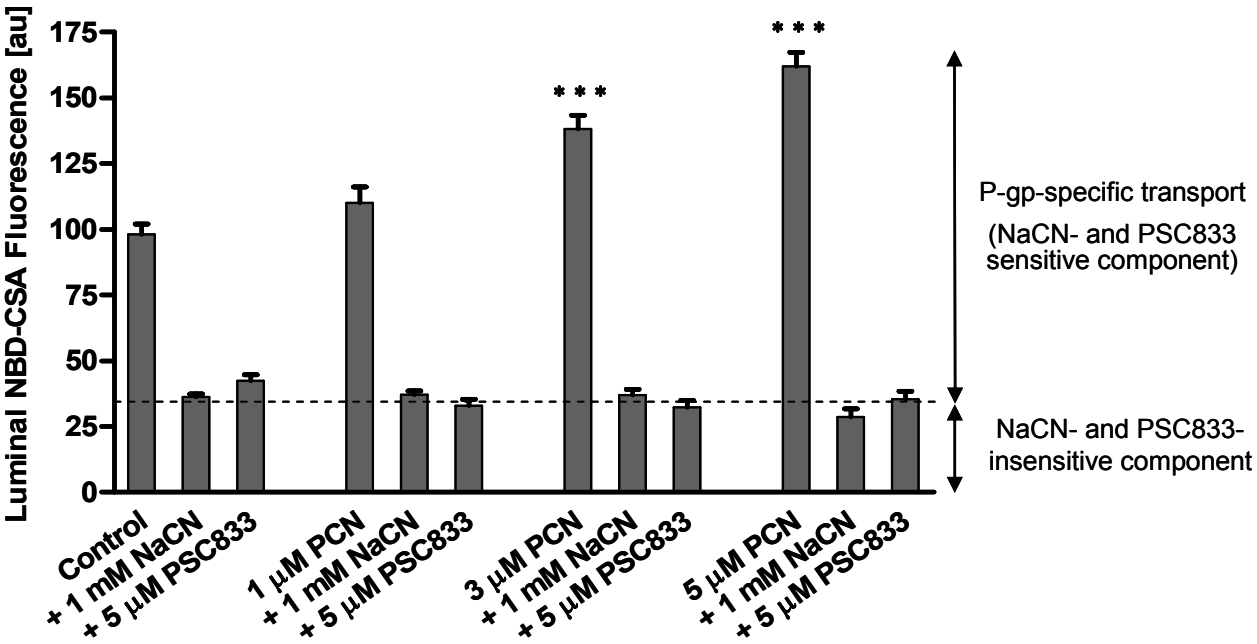

Figure 3.68
Concentration-dependent increase of P-glycoprotein transport function by PCN

P-gp-mediated NBD-CSA transport was significantly increased in capillaries treated with 3 and 5 µM PCN. 1 µM PCN had no significant effect. PCN did not alter fluorescence insensitive to 1 mM NaCN and 5 µM PSC833 (mean ± SEM, n=20, *** $p < 0.01$).

Figure 3.69 summarizes data from 5 transport experiments. It shows P-gp-mediated NBD-CSA transport as a function of PCN concentration. P-gp transport increased with 1 - 5 µM PCN to about 164-269 % of the control, respectively. NBD-CSA fluorescence in capillaries exposed to 10 µM PCN showed a decline in NBD-CSA transport, which is likely to be PCN toxicity.

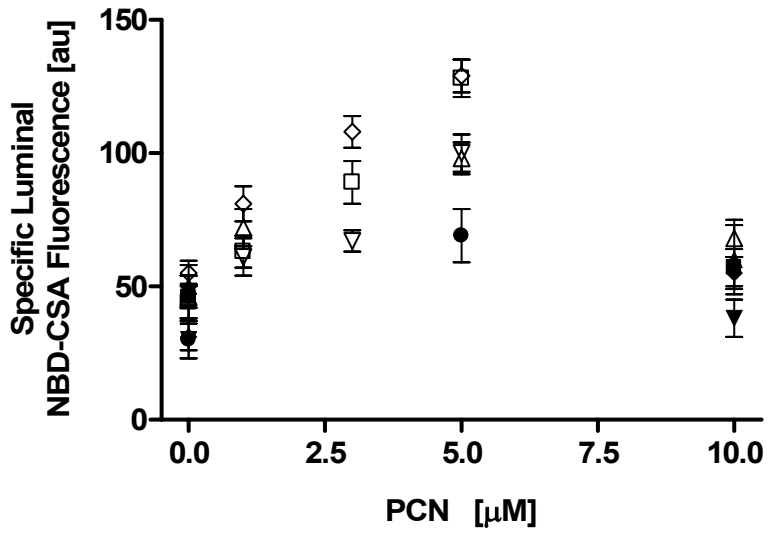

Figure 3.69
P-gp-mediated NBD-CSA transport as a function of PCN concentration

Concentration-dependent increase of P-gp-mediated NBD-CSA transport into capillary lumens after a 6-h exposure to PCN. Transport was maximal for 5 µM PCN-treated capillaries. 10 µM PCN had a toxic effect, shown as a decline in luminal NBD-CSA fluorescence (mean ± SEM, summarized data from 5 experiments, each point represents the average luminal membrane P-gp immunofluorescence from 15-20 capillaries of pooled tissue from 3-10 rats per single preparation).

3.3.3.2 *In Vitro* Experiments with Dexamethasone

3.3.3.2.1 Time-Dependent Induction of P-gp Expression by Dexamethasone

The glucocorticoid dexamethasone is a widely prescribed anti-inflammatory drug that is being used for the treatment of diseases with an inflammatory component, e.g. meningitis, arthritis or severe allergic reactions (Offermanns, 2004; Rang, 1999). Dexamethasone induces metabolizing enzymes and transporters in the liver (Hartley et al., 2004; Lehmann et al., 1998; Zhang et al., 2003b). However, the molecular mechanism of this phenomenon remained unclear for a long time. Recently, it has been reported that dexamethasone is a potent PXR activator. But unlike PCN, dexamethasone activates both rodent and human PXR (Kliewer et al., 2002; Lehmann et al., 1998).
Exposing capillaries to 0.5 µM dexamethasone increased P-gp immunofluorescence in a time-dependent manner (Figure 3.70). After 3-hour exposure, P-gp immunofluorescence was significantly increased. A further increase was measured after 6 hours. P-gp immunofluorescence of control capillaries remained the same over the entire time course.

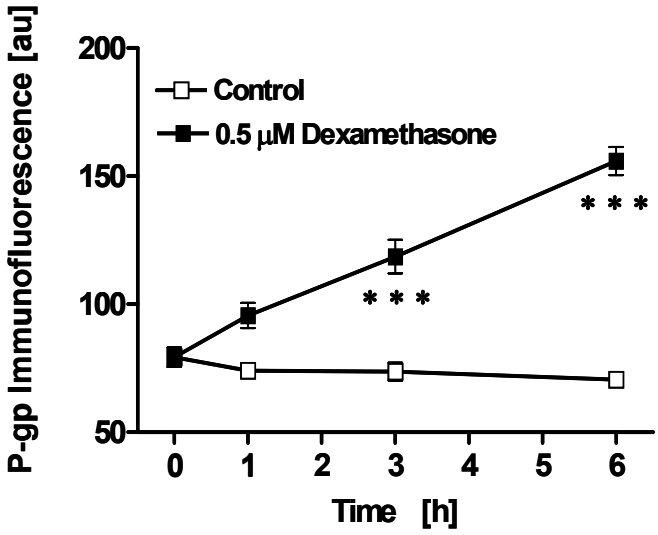

Figure 3.70
Time-dependent increase of P-gp immunofluorescence by dexamethasone

Induction of P-glycoprotein expression in brain capillaries measured as P-gp immunofluorescence. 0.5 µM dexamethasone caused a significant, time-dependent increase in luminal membrane P-gp immunofluorescence (mean ± SEM, n=15, *** $p < 0.001$).

3.3.3.2.2 Concentration-Dependent Induction of P-glycoprotein Expression by Dexamethasone

The effects of dexamethasone on P-gp expression were further examined by exposing isolated capillaries to different concentrations of dexamethasone for 6 hours. Capillaries incubated with 0.1 and 0.5 µM dexamethasone displayed higher P-gp immunofluorescence than control capillaries (Figure 3.71). 0.01 µM dexamethasone had no effect.

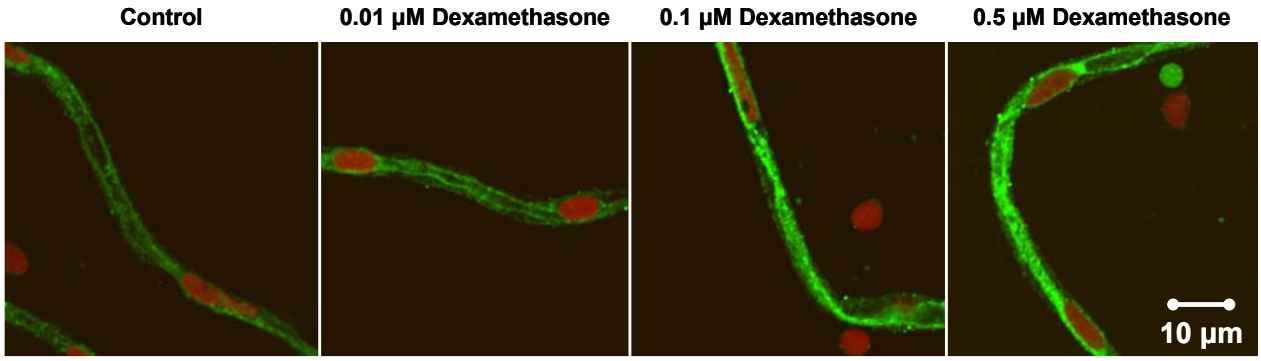

Figure 3.71
P-gp immunostaining with capillaries exposed to dexamethasone

Increased luminal membrane P-gp immunofluorescence in capillaries treated with 0.1 µM and 0.5 µM dexamethasone for 6 hours in comparison to the control capillaries (no dexamethasone). P-gp immunofluorescence was not increased in capillaries exposed to 0.01 µM dexamethasone.

Figure 3.72 summarizes data from 5 immunostaining experiments. Isolated capillaries were exposed to 0.01-0.5 µM dexamethasone for 6 hours. With 0.1 to 0.5 µM dexamethasone, P-gp immunofluorescence significantly increased on average to 176 ± 9% ($p < 0.01$) of the control. There was no change with 0.01 µM dexamethasone.

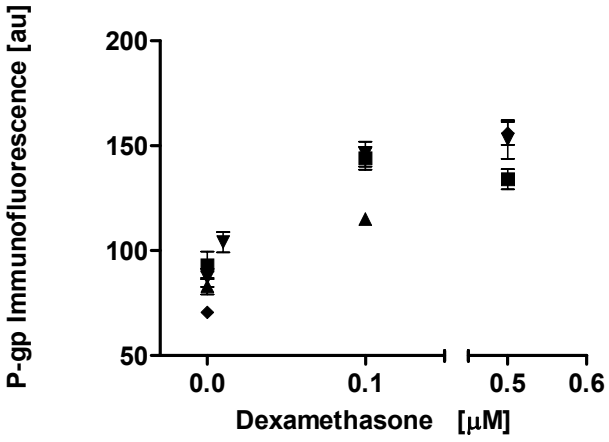

Figure 3.72
P-gp immunofluorescence as a function of dexamethasone concentration

Increase of P-gp immunofluorescence in capillaries exposed for 6 hours to 0.1-0.5 µM dexamethasone *in vitro*. P-gp immunofluorescence of control capillaries and capillaries exposed to 0.01 µM dexamethasone was unchanged (mean ± SEM, summarized data from 5 experiments, each point represents the average luminal membrane P-gp immunofluorescence from 15-20 capillaries of pooled tissue from 3-10 rats per single preparation).

Figure 3.73 shows a Western blot for P-gp with membranes from capillaries exposed to 0.1-5 µM dexamethasone for 6 hours. Capillaries treated with 0.1, 1 and 5 µM desamethasone display stronger bands for P-gp compared to the control, indicating increased P-gp expression. Highest induction levels were observed when capillaries were exposed to 1 µM dexamethasone.

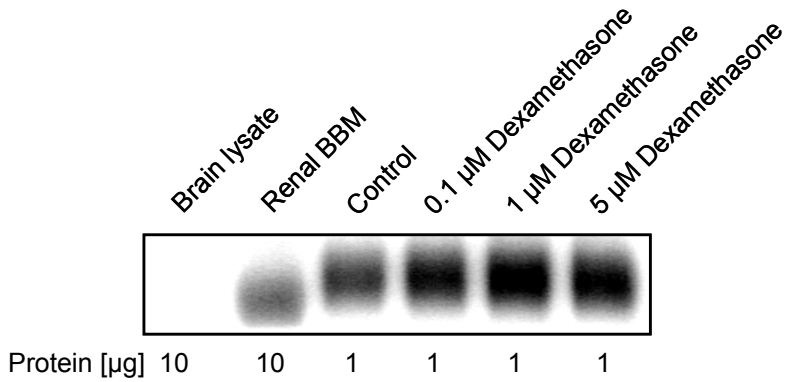

Figure 3.73
Western blot for P-gp with membranes from capillaries exposed to dexamethasone

Membranes from capillaries treated with 0.1-5 µM dexamethasone show stronger band intensities for P-gp than control capillaries. The highest induction of P-gp expression levels was observed with 1 µM dexamethasone.

3.3.3.2.3 Concentration-Dependent Induction of P-gp Transport Function by Dexamethasone

P-gp transport activity also increased when isolated rat brain capillaries were exposed to dexamethasone. Figure 3.74 shows P-gp-specific transport (NaCN- and PSC833 sensitive) from 5 experiments with dexamethasone-incubated capillaries. Treating capillaries with 0.01-0.5 µM dexamethasone for 6 hours markedly increased accumulated luminal NBD-CSA. 0.01 µM dexamethasone increased P-gp transport function to 173.5 ± 8.2% and 0.1 µM dexamethasone to 193.9 ± 6.3%, respectively, of the control. A more than 2-fold increase (214.3 ± 6.1%) of P-gp transport function was observed with 0.5 µM dexamethasone.

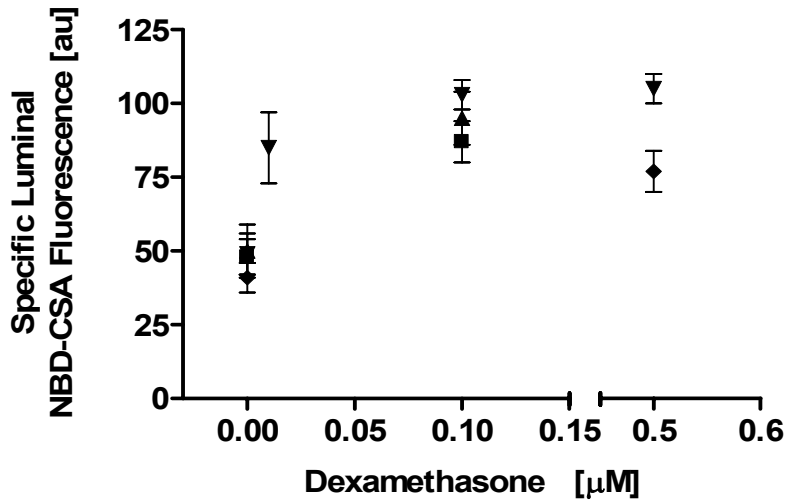

Figure 3.74
P-gp-mediated NBD-CSA transport as a function of dexamethasone concentration

Capillaries treated with 0.01-0.5 µM dexamethasone for 6 hours showed an increase in P-gp-mediated transport (mean ± SEM, summarized data from 5 experiments, each point represents the average luminal NBD-CSA fluorescence from 10-15 capillaries of pooled tissue from 3-10 rats per single preparation).

3.3.3.3 Summary of Part 3.3.3:

In Vitro Induction of P-gp Expression and Transport Function by PXR

The rodent-specific PXR activator PCN increased P-gp expression in isolated rat brain capillaries in a time- and concentration-dependent manner (Figures 3.62-66). After 3 hours, P-gp immunofluorescence was significantly increased and was even higher after 6 hours. Over this period of time, 5 µM PCN had the strongest effect on P-gp induction. The increase in P-gp expression was accompanied by a parallel increase in P-gp transport function (Figures 3.68-69). In accordance with the literature, hyperforin and paclitaxel, both of which only activate human PXR but not rodent PXR, had no effect on P-gp expression in rat brain capillaries (Figure 3.61) (Jones et al., 2000; Watkins et al., 2001). Dexamethasone, another PXR ligand, also increased P-gp expression and transport function. Like PCN, the increase of P-gp expression caused by dexamethasone was both time- and concentration-dependent (Figures 3.70-73). With 5 µM PCN or 0.1-0.5 µM dexamethasone, P-gp transport function had more than doubled (Figures 3.68-69 and 3.74).

3.3.4 PXR Induction of P-gp Expression and Transport Function *In Vivo*

3.3.4.1 *In Vivo* Dosing Experiments with PCN

3.3.4.1.1 Dose-Dependent Induction of P-gp Expression by PCN

For *in vivo* experiments, five rats per group were dosed daily for 3 days by i.p. injection with 10-50 mg/kg PCN in corn oil. Control animals received corn oil alone. 24 hours after the last injection, animals were euthanized, decapitated, and brains were taken immediately for capillary isolation. Capillaries were used for NBD-CSA transport experiments and P-gp immunostaining. Capillary membranes were isolated for further analysis by Western blotting. In addition, livers and kidneys were removed and snap-frozen in liquid nitrogen until use.
Figure 3.75 shows representative confocal images of isolated capillaries immunostained for P-gp from PCN-treated and untreated animals. Capillaries from animals treated with 10 or 25 mg/kg PCN show markedly stronger P-gp immunofluorescence in the luminal membrane than capillaries from control animals.

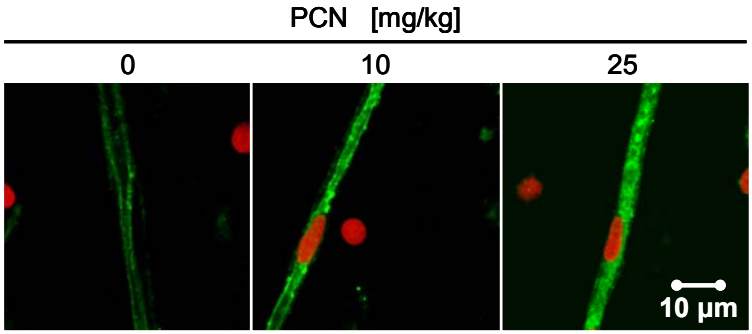

Figure 3.75
P-gp immunostaining of capillaries from rats dosed with 10 or 25 mg/kg PCN

Isolated capillaries from rats treated with 10 or 25 mg/kg PCN display stronger P-gp immunofluorescence in the luminal membrane than capillaries from control rats.

Confocal images of capillaries immunostained for P-gp were analyzed and P-gp immunofluorescence was quantitated. The data are presented in Figure 3.76. PCN increased P-gp immunofluorescence in a dose-dependent manner: 10 mg/kg PCN increased P-gp immunofluorescence to 130.7 ± 2.6 % (1.3-fold) of the control value; 25 mg/kg PCN increased P-gp immunofluorescence to 169.1 ± 5.4 % (1.7 fold).

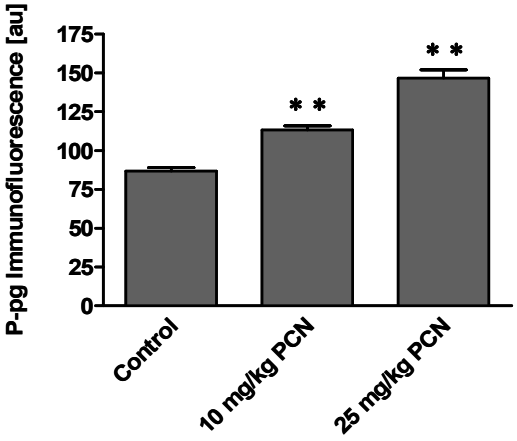

Figure 3.76
P-gp immunofluorescence of capillaries from PCN-treated rats

Luminal membranes of capillaries from rats treated with 10 or 25 mg/kg PCN show significantly higher immunofluorescence for P-gp than control capillaries: 10 mg/kg PCN increased P-gp immunofluorescence to about 130 %; 25 mg/kg PCN to about 170 % of control values (mean ± SEM, n=15, ** $p < 0.01$).

Brain capillaries, kidneys and livers from animals dosed for 3 days with 10 and 25 mg/kg PCN were also used to isolate crude membranes for further analysis by Western blotting. Figure 3.77 shows P-gp Western blots; total brain lysate and renal brush border membranes (BBM) were used as negative and positive controls for P-gp, respectively. Membranes isolated from brain capillaries, kidneys and livers from PCN-treated animals, showed markedly increased P-gp expression to controls. P-glycoprotein expression in liver and kidney membranes increased with increasing PCN dose, whereas P-gp expression levels in capillary membranes looked the same for both, 10 and 25 mg/kg PCN.

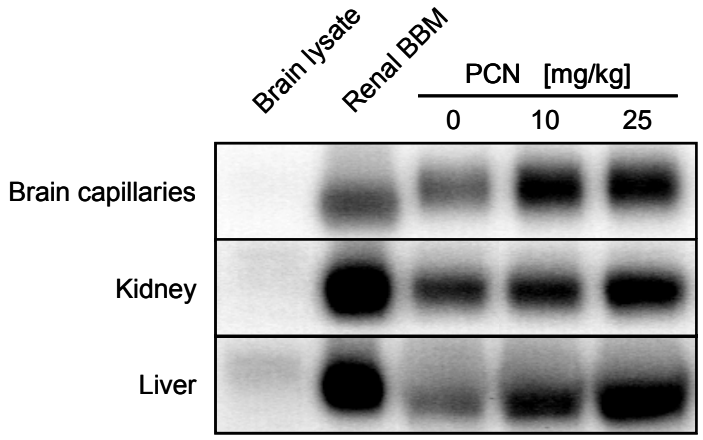

Figure 3.77
Western blot for P-gp with membranes from capillaries, kidney and liver from PCN-treated rats

Dosing animals for 3 days with 10 and 25 mg/kg PCN increased P-gp expression in crude membranes isolated from brain capillaries (1 µg protein/lane), kidney and liver (10 µg protein/lane). 10 µg protein/lane were loaded for brain lysate and renal BBM, respectively.

Figure 3.78 shows a Western blot for Na^+/K^+-ATPase and GAPDH from the same brain capillary crude membrane preparation to demonstrate equal protein loading (Na^+/K^+-ATPase) and purity of the membrane preparation (GAPDH).

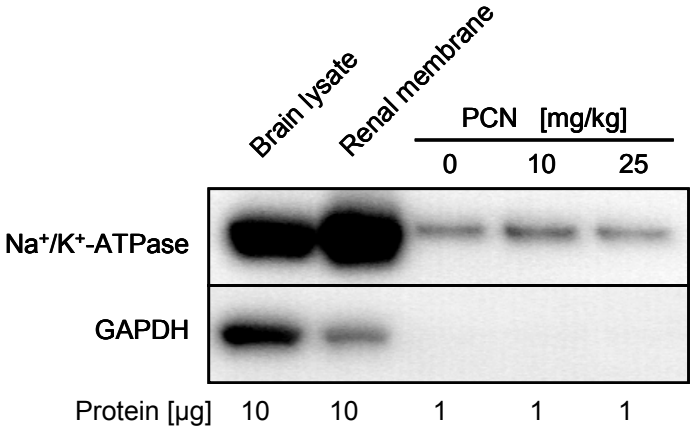

Figure 3.78
Western blot for Na^+/K^+-ATPase and GAPDH with capillary membranes from PCN-treated rats

PCN did not change expression of Na^+/K^+- ATPase, indicating equal gel-protein-loading. The capillary membrane fraction shows only faint GAPDH bands indicating a pure membrane preparation.

3.3.4.1.2 Dose-Dependent Induction of P-gp Transport Function by PCN

The *in vivo* effect of PCN on P-gp function at the blood-brain barrier was determined by NBD-CSA transport into the lumens of isolated brain capillaries from treated and untreated animals. Figure 3.79 presents P-glycoprotein-specific (PSC833-sensitive) transport of NBD-CSA into capillary lumens of 10 or 25 mg/kg PCN-dosed rats. In comparison to control capillaries, PCN-treated animals exhibited significantly higher luminal accumulation of NBD-CSA. This increase was dose-dependent: 10 mg/kg PCN increased luminal NBD-CSA fluorescence from 41 to 76 fluorescence units (increase to 185.4 ± 5 % of the control) and 25 mg/kg increased luminal NBD-CSA fluorescence to 90 fluorescence units (increase to 219.5 ± 5.5 % of the control).

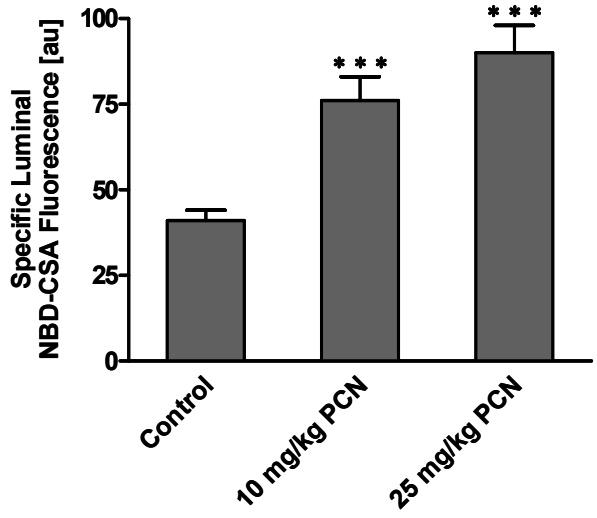

Figure 3.79
P-gp-mediated transport in capillaries from PCN-treated animals

PCN increased P-glycoprotein-mediated luminal NBD-CSA accumulation in a dose-dependent manner (mean ± SEM, n=15, *** $p < 0.001$).

3.3.4.2 *In Vivo* Dosing Experiments with Dexamethasone

3.3.4.2.1 Dose-Dependent Induction of P-gp Expression by Dexamethasone

The *in vitro* experiments presented above (Part 3.3.2.2) demonstrated induction of P-gp expression and transport function by the PXR ligand dexamethasone. Since dexamethasone is a widely prescribed drug, it was important to study its effects on P-gp expression and function at the blood-brain barrier *in vivo*. Thus, rats were dosed daily i.p. with dexamethasone for 3 days (1-50 mg/kg in corn oil). Control animals received vehicle only.

The images in Figure 3.80 show capillaries immunostained for P-glycoprotein. P-glycoprotein is shown in green, nuclei are in red. Luminal membrane P-gp immunofluorescence was markedly higher in capillaries from animals treated with dexamethasone when compared to control capillaries. The effect was higher with 5 mg/kg dexamethasone than with 1 mg/kg dexamethasone.

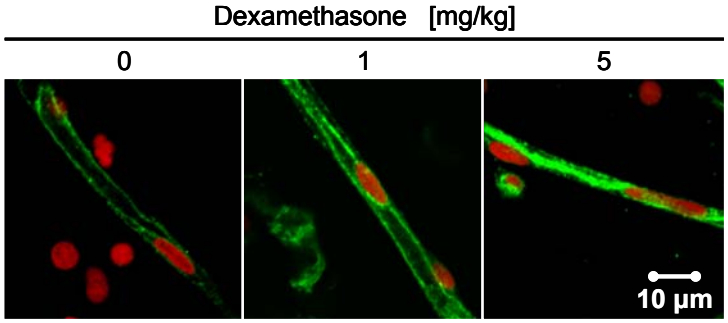

Figure 3.80
Capillaries from dexamethasone-treated rats immunostained for P-gp

P-gp immunofluorescence (green) in luminal membranes is markedly increased in capillaries from dexamethasone-treated animals in comparison to capillaries from untreated animals.

Figure 3.81 shows the corresponding, quantitated P-gp immunofluorescence data. Dexamethasone significantly increased P-gp immunofluorescence in a dose-dependent manner: 1 mg/kg dexamethasone increased P-gp to 147.7 ± 3.4 % (1.5-fold) and 5 mg/kg dexamethasone increased P-gp immunofluorescence to 199.2 ± 3.1 % (2-fold) of the control. Dosing animals with 50 mg/kg dexamethasone did not cause any further increase of P-gp immunofluorescence (increase to 196.4 ± 3.8 % of the control).

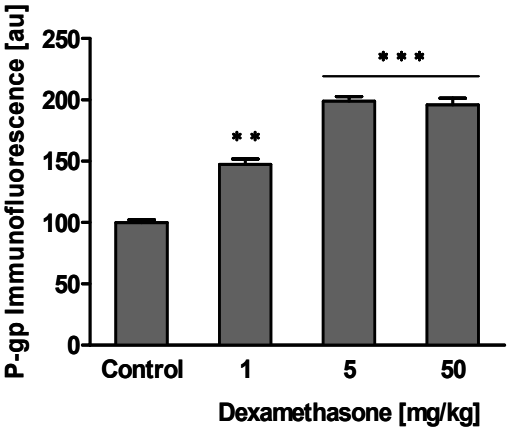

Figure 3.81
P-gp immunofluorescence of capillaries from dexamethasone-treated animals

Dosing rats with 1 and 5 mg/kg dexamethasone caused a dose-dependent increase of P-gp immunofluorescence in the luminal membrane of brain capillaries. 50 mg/kg dexamethasone caused no further increase (mean ± SEM, n=20, ** $p < 0.05$, *** $p < 0.01$).

In addition to immunostaining, the change of P-gp protein expression was confirmed by Western blotting of membranes from brain capillaries, kidney and liver (Figure 3.82). The increase of P-gp was dose-dependent. As PCN, dexamethasone also induced P-gp in kidney and liver.

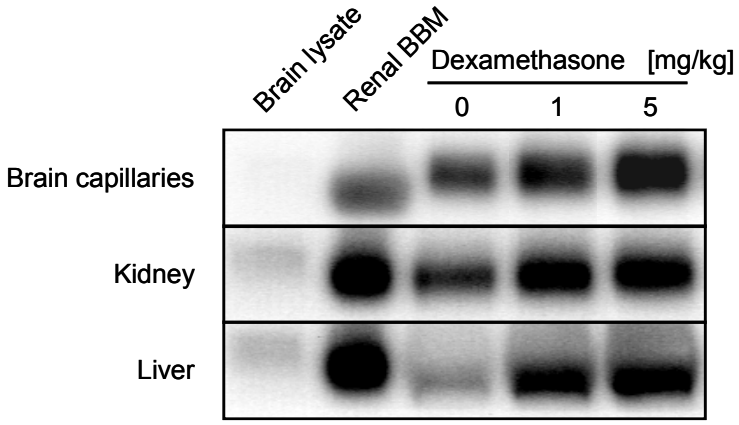

Figure 3.82
Western blot for P-glycoprotein with capillary, kidney and liver membranes from dexamethasone-treated animals

Dosing animals for 3 days with 1 and 5 mg/kg dexamethasone increased P-gp protein expression in crude membranes isolated from brain capillaries (1 µg protein/lane), kidney and liver (10 µg protein/lane). 10 µg protein/lane were loaded for brain lysate and renal BBM, respectively.

3.3.4.2.2 Dose-Dependent Induction of P-glycoprotein Transport Function by Dexamethasone

To examine whether dexamethasone also increased P-glycoprotein function, P-gp-mediated NBD-CSA transport was determined in capillaries isolated from control rats and dexamethasone-dosed rats. Figure 3.83 shows luminal NBD-CSA fluorescence as a measure of P-gp-specific function (PSC833-sensitive) in capillaries from untreated rats and rats dosed with 1 or 5 mg/kg dexamethasone.
Dexamethasone increased luminal NBD-CSA fluorescence in capillary lumens in a dose-dependent manner. A dose of 1 mg/kg dexamethasone increased luminal fluorescence to 176.3 ± 5.2 % ($p < 0.01$) and 5 mg/kg dexamethasone increased it to 252.3 ± 4.9 % ($p < 0.001$) of the control.

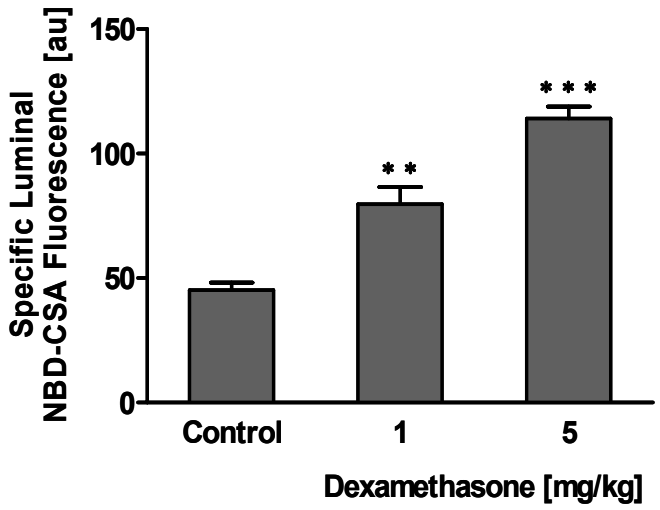

Figure 3.83
Increase of P-gp-mediated NBD-CSA transport by dexamethasone

Dexamethasone increased P-glycoprotein transport function in a dose-dependent manner. (mean ± SEM, ** $p < 0.01$, *** $p < 0.001$)

3.3.4.3 Correlation of P-gp Transport Function and P-gp Protein Expression in Isolated Brain Capillaries from PCN- and Dexamethasone-Dosed Rats

Brain capillaries from PCN- and dexamethasone-dosed rats (10-25 mg/kg PCN or 1-5 mg/kg dexamethasone daily i.p. for 3 days) were isolated for NBD-CSA transport experiments and quantitative P-gp immunostaining. Figure 3.84 shows P-gp transport and protein expression as a function of PCN and dexamethasone dose. Quantitative P-gp immunostaining of capillaries showed that P-glycoprotein expression in the luminal membrane increased as dose levels of PCN and dexamethasone were raised (Figure 3.84A). With 25 mg/kg PCN, P-glycoprotein immunofluorescence increased by about 1.7-fold compared to the control (increase to 169 ± 5%). With 5 mg/kg dexamethasone, P-gp immunofluorescence more than doubled (increase to 234 ± 6%).
In addition, NBD-CSA transport experiments revealed a dose-dependent increase of P-gp function in brain capillaries from dosed animals (Figure 3.84B). Luminal NBD-CSA accumulation increased to 220 % and 260 % of control values in capillaries from 25 mg/kg PCN- or 5 mg/kg dexamethasone-treated rats, respectively. As was observed for the *in vitro* experiments (part 3.3.2), dexamethasone was a 5-10-fold more potent inducer of P-gp immunofluorescence and luminal NBD-CSA fluorescence than PCN.

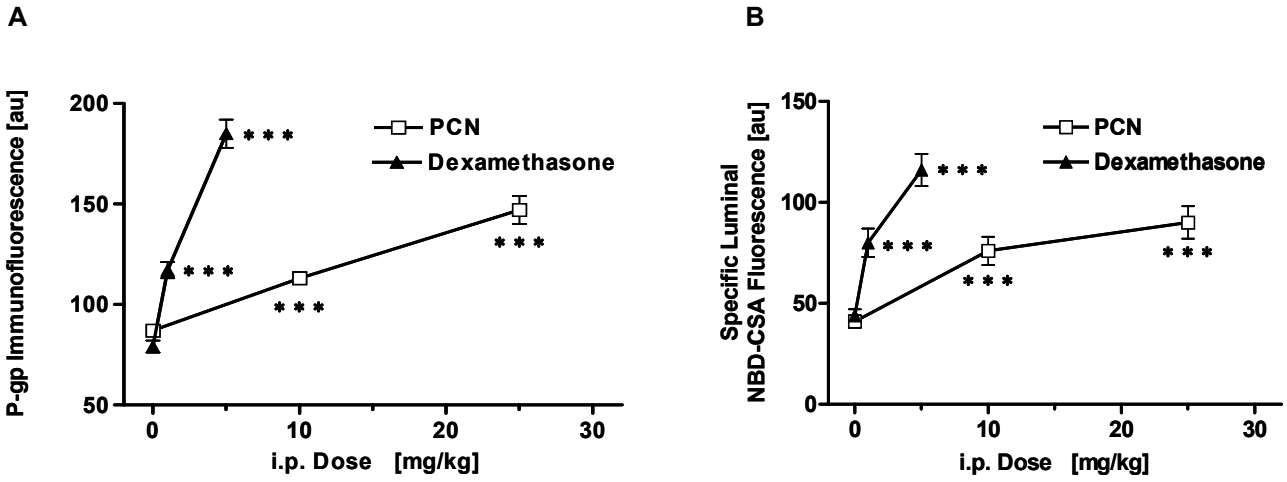

Figure 3.84
PCN and dexamethasone induce P-glycoprotein immunofluorescence and luminal NBD-CSA fluorescence *in vivo*

A: Dose-dependent increase of P-gp immunofluorescence in the luminal capillary membrane of PCN- or dexamethasone-dosed rats (mean ± SEM, n=20, *** $p < 0.001$).

B: Dose-dependent increase of luminal NBD-CSA fluorescence in capillaries isolated from PCN- or dexamethasone-treated rats (mean ± SEM, n=10, *** $p < 0.001$).

Quantitative P-gp immunostaining and NBD-CSA transport data from 5 independent *in vivo* experiments with PCN- and dexamethasone-dosed rats were correlated. Each data point represents the mean value of 15-20 capillaries from pooled tissue of 3-10 rats per single preparation. Figure 3.85 shows specific luminal NBD-CSA fluorescence (P-gp transport function) plotted against P-gp immunofluorescence (P-gp protein expression in luminal capillary membrane). Control values cluster at the bottom left (A), values for animals given low doses of PXR ligand cluster in the middle (B), and values for animals given high doses of PXR ligand cluster in the upper right (C). Importantly, both P-gp immunofluorescence and luminal NBD-CSA fluorescence increased in parallel as PXR was activated by increasing doses of ligand. This indicates that newly synthesized P-gp protein was also functional.

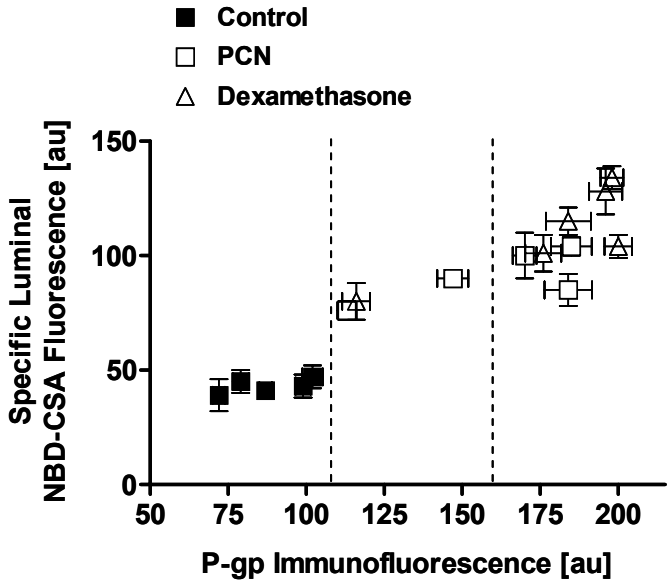

Figure 3.85
***In vivo* correlation of P-gp transport function and P-gp protein expression**

Summary of data from 5 *in vivo* experiments of PCN- or dexamethasone-dosed rats: (A) control values, (B) values for animals given low doses of PCN or dexamethasone, (C) values for animals given high doses of PCN or dexamethasone. Luminal NBD-CSA fluorescence and P-gp immunofluorescence in luminal capillary membranes increased in parallel with increasing doses of PXR ligand, indicating that newly synthesized P-gp protein is also functional (mean ± SEM, summarized data from 5 experiments, each point represents the average luminal NBD-CSA fluorescence from 10-15 capillaries of pooled tissue from 3-10 rats per single preparation).

3.3.4.4 Summary for Part 3.3.4:

***In Vivo* Induction of P-glycoprotein Expression and Transport Function by PXR**

Dosing rats with PCN and dexamethasone increased P-gp protein expression and transport function in brain capillaries. This increase ranged between 1.3-fold for low PCN concentrations (10mg/kg) and about 2-fold for 25 mg/kg PCN (Figures 75-79). Dexamethasone doses of 1-5 mg/kg caused doubling of P-gp expression and transport function (Figures 3.80-83). Both PXR ligands also induced P-gp expression in liver and kidney (Figures 3.77 and 3.82).

These *in vivo* data demonstrated for the first time that P-glycoprotein expression and transport function at the blood-brain barrier both increased in parallel when rats were treated with PXR ligands (Bauer et al., 2004).

3.3.5 Discussion of Part 3.3:

Pregnane X Receptor Upregulation of P-glycoprotein Expression and Transport Function at the Blood-Brain Barrier
(Bauer et al., 2004)

The third part of this thesis describes the long-term regulation of P-glycoprotein by the pregnane X receptor (PXR) in isolated rat brain capillaries. PXR is a ligand-activated transcription factor that controls P-gp mRNA expression in liver and intestine (Geick et al., 2001; Kullak-Ublick and Becker, 2003; Synold et al., 2001). Although PXR is highly expressed in liver, kidney and certain regions of the gut, previous experiments did not detect any evidence of PXR mRNA expression in whole brain homogenates (Jones et al., 2000; Kliewer et al., 1998; Zhang et al., 1999). However, capillaries comprise less than 0.1% of brain volume. If PXR expression were restricted primarily to brain capillaries, mRNA levels in whole brain might be below the detection limits of the technique used in those studies (Northern blotting). Using RT-PCR, PXR mRNA was detected in whole brain homogenates and in isolated brain capillaries (Figure 3.58). The PCR product was confirmed by direct sequencing to be identical only to the rat PXR gene. Consistent with this, Western blot analysis from capillary nuclear protein showed a weak band at the right molecular weight for PXR (~ 50 kDa) and a much stronger band at about 105 kDa, which might represent PXR-RXRα heterodimer (Figure 3.59). These bands should be specific, since in parallel Western blot experiments, PXR-antibody was blocked with antigen so that specific and unspecific bands, respectively, could be distinguished from each other. The bands between 105 and 160 kDa might be PXR-RXRα heterodimer with coactivator and/or corepressor (Glass, 1994; Mangelsdorf et al., 1995; Watkins et al., 2003a). However, none of the bands has been sequenced yet and therefore, cannot clearly be identified. Additionally, immunostaining of isolated brain capillaries showed PXR immunofluorescence extending over endothelial cell cytoplasm and nucleus (Figure 3.60), which confirms the previous findings.
PCN is the prototypical ligand for rodent PXR but a poor ligand for the human ortholog. In contrast, paclitaxel and hyperforin are high-affinity ligands for human PXR but not for rodent PXR (Jones et al., 2000; Moore et al., 2000b; Watkins et al., 2001). In accordance with this, PXR activation with PCN increased P-gp protein expression in isolated rat brain capillaries, whereas hyperforin and paclitaxel had no effect (Figure 3.61). These data validate the model as a useful tool to study long-term effects on P-glycoprotein expression at the blood-brain barrier.
In initial time course experiments, P-glycoprotein immunofluorescence in the luminal membrane of capillaries increased significantly after 3-hour exposure to PCN and increased further after 6 hours (Figures 3.62-63). Exposing capillaries to increasing concentrations of PCN caused concentration-dependent increases in immunoreactive P-glycoprotein in the luminal membrane of capillaries as shown by quantitative immunostaining and Western blotting (Figures 3.64-66). Importantly, PCN also increased P-glycoprotein transport function in isolated capillaries (Figures 3.68-69).
The widely prescribed anti-inflammatory glucocorticoid dexamethasone is also a ligand for rodent PXR (Kliewer et al., 2002). Exposing capillaries to this drug also increased P-gp protein expression in capillary membranes (quantitative immunostaining, Western blot) and increased P-gp transport function in a time- and concentration-dependent manner (Figures 3.70-74). Interestingly, dexamethasone induction occurred at concentrations (0.01-0.5 µM) that were at least an order of magnitude lower than those for

PCN, suggesting that dexamethasone is a more potent P-gp inducer. However, it cannot be excluded that dexamethasone also activated the glucocorticoid receptor, which synergistically might have affected P-gp induction, as reported previously (Pascussi et al., 2001).

To determine whether in vivo exposure to PXR ligands altered P-glycoprotein expression at the blood-brain barrier, rats were injected i.p. with PCN or dexamethasone daily for 3 days. Capillaries were isolated 24 hours after the last dosing and P-glycoprotein expression and transport function were measured. Livers and kidneys were also removed; crude membrane fractions were isolated and analyzed by Western blotting. P-gp protein expression was increased by both PCN and dexamethasone in Western blots of brain capillary plasma membranes (Figures 3.77 and 3.82). In agreement with previously published studies (Demeule et al., 1999; Salphati and Benet, 1998), immunoreactive P-glycoprotein in liver and kidney crude membranes was also increased (Figures 3.77 and 3.82). Quantitative immunostaining of capillaries showed that luminal P-glycoprotein immunofluorescence increased as dose levels were raised; at the highest doses used, immunofluorescence about doubled (Figures 3.75-76 and Figures 3.80-81). When P-glycoprotein-specific transport was measured, significant dose-dependent increases were found (Figures 3.79 and 3.83). Importantly, P-glycoprotein-mediated NBD-CSA transport and immunofluorescence correlated (Figure 3. 85), suggesting that both immunofluorescence and specific transport increased in parallel as PXR was activated by increasing dose of ligand.

The present results identify one underlying mechanism by which drug export pump activity at the blood-brain barrier is modulated. They show that PXR is expressed in brain capillaries and that P-glycoprotein expression and transport function at the blood-brain barrier increase after in vitro or in vivo exposure to the PXR ligands, PCN and dexamethasone. Thus, one consequence of exposure to PXR ligands is selective tightening of the blood-brain barrier to those chemicals that are P-glycoprotein substrates.

The results, which show the consequences of receptor activation in rats dosed with PXR ligands, provide a “proof of principle” with regard to PXR expression and action in the blood-brain barrier. The extent, to which other PXR ligands will alter blood-brain barrier function in vivo in rats or in other species, will depend on several interrelated factors. For example, the nature of the ligand, its pharmacokinetics and the exposure (dosing protocol) will determine whether ligand accumulates in brain capillary endothelial cells at sufficient levels to affect gene expression. Certainly, for PXR ligands that are also P-glycoprotein substrates, accumulation may be limited at the barrier itself or more distally at the intestine or liver. So far, PXR is the only nuclear receptor known to regulate P-glycoprotein and to be expressed at the blood-brain barrier. However, the blood-brain barrier does express other multi-specific drug metabolizing enzymes and transporters that are regulated by PXR in other tissues, e.g., cytochrome P450s, glutathione transferases, Mrps, and organic anion transport polypeptides (Chen et al., 2003; Guo et al., 2002; Kast et al., 2002). In liver and gut, ligand-activated nuclear receptors regulate a network of genes that encode enzymes responsible for xenobiotic oxidation and conjugation as well as excretory transport of xenobiotics and products of xenobiotic metabolism (Rosenfeld et al., 2003). To what extent such a regulatory network is also present at the blood-brain barrier is unclear.

Taken together, upregulation of P-glycoprotein has important clinical implications. On the one hand, P-glycoprotein is responsible for the efflux of neurotoxic chemicals and metabolites from the CNS and increased pump expression should provide increased

neuroprotection. On the other hand, many P-glycoprotein substrates are used therapeutically, e.g., to treat brain tumors, viral and bacterial infections and epileptic seizures, and increased pump expression also implies reduced access of those drugs to sites of action within the CNS. Thus, a better understanding of the mechanisms that regulate the selective barrier to drug entry also holds the promise of treatments, e.g., drugs or dietary modifications that could downregulate pump expression. For example, transient P-glycoprotein downregulation could provide a window in time during which normally impermeant drugs would be able to access sites within the CNS. Whether this can be done effectively through manipulation of PXR or through other faster acting regulatory mechanisms remains to be demonstrated.

3.3.6 Summary of Part 3.3:

Pregnane X Receptor Upregulation of P-glycoprotein Expression and Transport Function at the Blood-Brain Barrier
(Bauer et al., 2004)

PXR mRNA expression in brain capillaries was detected by RT-PCR (Figure 3.58); the PCR product was confirmed by direct sequencing to be 100% identical only to the rat PXR gene. Western blot analysis showed PXR protein expression in the nuclear fraction of capillaries (Figure 3.59). Immunostaining PXR in isolated brain capillaries showed immunofluorescence extending over cytoplasm and nucleus (Figure 3.60). The rodent-specific PXR activator, PCN, induced P-gp expression in isolated rat brain capillaries in a time- and concentration-dependent manner (Figures 3.62-66). After 3 hours, P-gp immunofluorescence was significantly increased and was even higher after 6 hours. Dose-response experiments showed that 5 µM PCN had the strongest effect on P-gp induction. The increase in P-gp expression was accompanied by a parallel increase in P-gp transport function (Figures 3.68-69). Activators of human PXR (hyperforin and paclitaxel) had no effect on P-gp expression in rat brain capillaries (Figure 3.61). Dexamethasone, another PXR ligand, also increased P-gp expression and transport function. The increase of P-gp expression was both time- and dose-dependent as seen before with PCN (Figures 3.70-73). With 5 µM PCN or 0.1-0.5 µM dexamethasone, P-gp transport activity had more than doubled (Figures 3.68-69 and 3.74). Dosing rats with PCN or dexamethasone increased P-gp protein expression and transport function in brain capillaries (Figures 3.75-83). Protein expression and transport more than doubled with the highest doses used. P-gp expression in liver and kidney was also induced (Figures 3.77 and 3.82). Importantly, both P-gp protein expression and transport function in brain capillaries increased in parallel when rats were given increasing doses of PXR ligand (Figure 3.85).
The present *in vitro* and *in vivo* data provide a “proof of principle” with regard to PXR expression and action in brain capillaries. For the first time, these results demonstrate a molecular basis for regulation of the xenobiotic transporter P-glycoprotein at the blood-brain barrier (Figure 3.86) (Bauer et al., 2004).

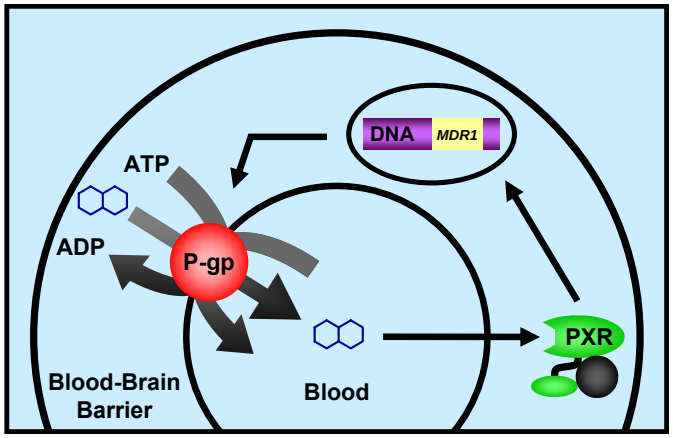

Figure 3.86
Pregnane X Receptor upregulation of P-gp expression and activity at the blood-brain barrier

The scheme illustrates upregulation of P-gp expression by PXR. Binding of PXR ligands (blue) like PCN or dexamethasone activates the pregnane X receptor (PXR). PXR translocates into the nucleus, binds to the xenobiotic response element (XRE) and induces transcription of its target gene, *Mdr1*. This leads to an increase of P-gp protein expression in the luminal membrane of brain capillaries and causes higher P-gp-mediated drug efflux.

4 Summary and Outlook

4.1 Summary

The objective of this thesis was to study regulation of P-glycoprotein using isolated rat brain capillaries as an *ex vivo* model of the blood-brain barrier. The studies addressed the following hypotheses:

1. Endothelin-1 regulates P-gp transport function at the blood-brain barrier

2. PXR regulates P-gp expression and transport function at the blood-brain barrier

Characterization of isolated rat brain capillaries showed that this *ex vivo* model is a suitable and powerful tool to study blood-brain barrier function. Confocal microscopy and transmission electron microscopy revealed intact morphology and ultra-structure of freshly isolated capillaries. P-glycoprotein transport function was assessed by measuring accumulation of the fluorescent, P-gp-specific substrate, NBD-cyclosporine A (NBD-CSA) in the lumens of isolated rat brain capillaries using confocal microscopy and quantitated by image analysis. Importantly, transport experiments showed that capillaries were viable for at least 6 hours. P-glycoprotein expression was detected in capillary membranes and immunostaining localized P-gp to the luminal membrane. In addition to P-gp, expression of other drug efflux transporters and tight junction proteins was also found. In essence, these findings demonstrate that freshly isolated rat brain capillaries can be used as an *ex vivo* blood-brain barrier model to study P-glycoprotein expression and transport function.

1. Rapid Regulation of P-glycoprotein at the Blood-Brain Barrier by Endothelin-1

Exposing capillaries to 0.1-100 nM ET-1 rapidly (within 1 hour) and reversibly reduced luminal NBD-CSA accumulation. Importantly, a kinetic dye efflux assay showed that tight junctions were not affected by ET-1. Sarafotoxin S6c, an ET_B receptor agonist, also reduced P-gp-mediated transport; the effects of ET-1 and sarafotoxin S6c were blocked by an ET_B receptor antagonist, but not by an ET_A receptor antagonist. Immunostaining localized the ET_B receptor to the luminal and abluminal membranes of brain capillaries. NBD-CSA transport was also reduced by the NO donor, sodium nitroprusside (SNP), and by the protein kinase C (PKC) activator, PMA. Inhibition of NO synthase (NOS) or PKC blocked the effects of ET-1; PKC inhibition blocked the effects of SNP and PMA. Thus, P-glycoprotein at the blood-brain barrier is regulated in the short-term by ET-1 acting through an ET_B receptor, NOS, NO and PKC (Hartz et al., 2004).
Taken together, this is the first evidence for hormonal signaling causing rapid and reversible changes of P-gp-mediated transport at the blood-brain barrier (Figure 4.1: 1. Functional Modulation by Endothelin-1). ET-1 regulation of P-glycoprotein may be of clinical importance, since this hormone has been implicated in many CNS disorders.

2. Pregnane X Receptor Upregulation of P-glycoprotein Expression and Transport Function at the Blood-Brain Barrier

Expression of the nuclear receptor, PXR, was detected in isolated rat brain capillaries by RT-PCR, Western blot analysis and immunostaining. Six hour exposure of isolated capillaries to the PXR ligands, PCN (1-10 µM) or dexamethasone (0.1-0.5 µM), significantly increased expression of P-gp in the plasma membrane; maximal stimulation was about 2-fold. Consistent with this, P-gp immunostaining demonstrated significantly increased immunoreactivity at the luminal membrane of capillaries. Increased (2-fold) P-gp-mediated NBD-CSA transport into capillary lumens was also detected. No such increases in P-gp expression were found when capillaries were exposed to ligands that activate human PXR (hyperforin, paclitaxel), but do not activate rodent PXR. Importantly, 2-3-fold increases in P-glycoprotein expression and transport function were also found in capillaries isolated from rats dosed with PCN and dexamethasone (Bauer et al., 2004).

In this thesis for the first time it is shown that the nuclear receptor PXR is expressed at the blood-brain barrier, where it regulates expression and function of P-glycoprotein (Figure 4.1: 2. Transcriptional Regulation by PXR). Since P-gp is a major determinant for CNS entry of drugs and since a large number of drugs activate PXR, these findings might have important clinical implications for patients receiving multiple drugs over longer periods of time.

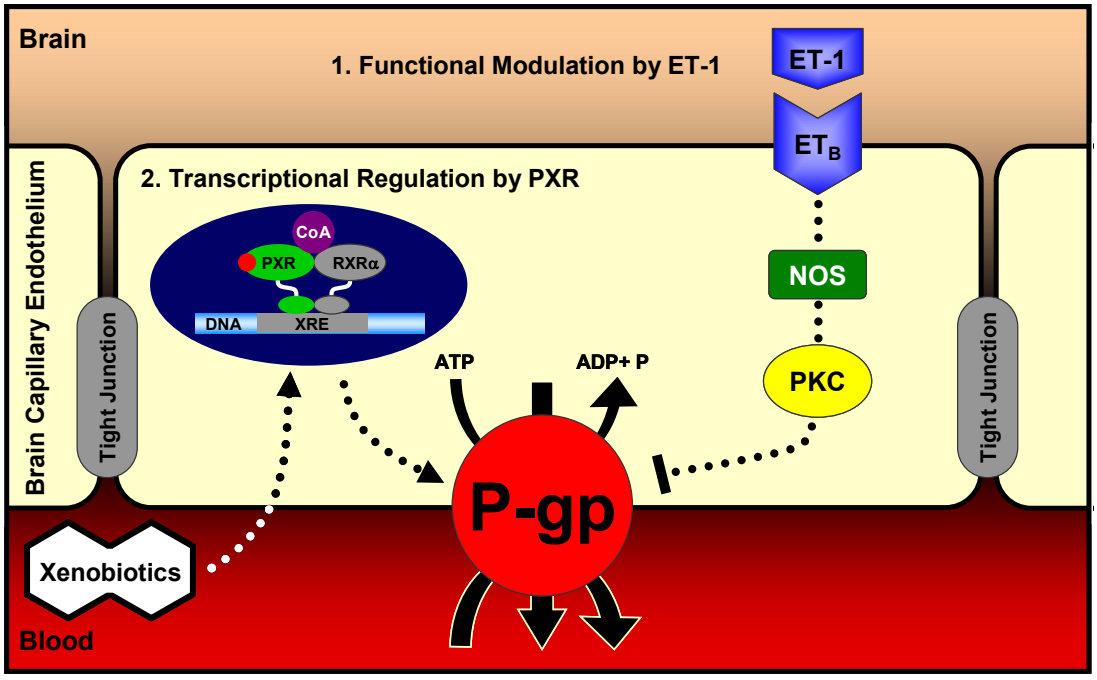

Figure 4.1
Modulation of P-gp transport function and expression

1. Functional modulation of P-glycoprotein by endothelin-1:
ET-1 modulates P-glycoprotein transport function at the blood-brain barrier over the short-term by acting through the ET_B receptor, NO synthase (NOS) and protein kinase C (PKC) (Hartz et al., 2004).

2. Transcriptional regulation of P-glycoprotein by PXR:
Activation of PXR by ligands regulates transcription of Mdr1 resulting in increased P-glycoprotein expression and transport function (Bauer et al., 2004).

4.2 Outlook

Effect of inflammatory mediators on P-glycoprotein at the blood-brain barrier

At present, little is known about the physiological role of endothelin-1 at the blood-brain barrier. However, it is clear that many CNS disorders are accompanied by inflammation, that endothelin-1 is involved in many inflammatory CNS diseases and that endothelin-1 is released in the brain's innate immune response (Nie and Olsson, 1996; Willette, 1995). Therefore, inflammatory mediators present in the brain during CNS disorders could act through ET-1 to affect P-glycoprotein at the blood-brain barrier. In addition, inflammation in the periphery could also affect the brain and modulate P-glycoprotein at the blood-brain barrier.

Nuclear receptor regulation of efflux transporters at the blood-brain barrier

In liver and gut, nuclear receptors regulate a network of genes encoding xenobiotic efflux pumps that are involved in excretory transport (Rosenfeld et al., 2003). Although PXR is the only nuclear receptor that is known to regulate P-glycoprotein, brain capillaries express other efflux transporters (Geick et al., 2001; Labialle et al., 2002). Thus, it is likely that PXR controls transcription of multiple transporters at the blood-brain barrier. For example, preliminary data indicate PXR regulation of Mrp2 in rat brain capillaries (Bauer et al., 2004). Moreover, recent molecular findings show also expression of other nuclear receptors in brain capillaries. However, it is not known if these receptors are involved in efflux transporter regulation. Therefore, it remains to be determined, (1) which nuclear receptors are actually expressed at the blood-brain barrier, (2) if they are involved in transporter regulation and (3) if nuclear receptors and efflux transporters are part of a regulatory network at the blood-brain barrier.

5 Materials and Methods

5.1 Materials

5.1.1 Chemicals

Albumin bovine serum, Fraction V	Sigma-Aldrich, St. Louis, MO, USA
Ampicillin	Sigma-Aldrich, St. Louis, MO, USA
Bacto™ Agar	BD Diagnostic Systems, Sparks, MD, USA
Bacto™ Tryptone	BD Diagnostic Systems, Sparks, MD, USA
Bacto™ Yeast Extract	BD Diagnostic Systems, Sparks, MD, USA
BD Advantage™ UltraPure, PCR Deoxynucleotide Mix	BD Biosciences Clontech, Palo Alto, CA, USA
BenchTop PCR Markers	Promega Corporation, Madison, WI, USA
Bio-Rad Protein Assay, Dye Reagent Concentrate	Bio-Rad Laboratories, Hercules, CA, USA
Bisindolylmaleimide I	EMD Biosciences/Calbiochem®, San Diego, CA, USA
Boric Acid	Sigma-Aldrich, St. Louis, MO, USA
BupH™ Tris Buffered Saline Packs	Pierce Biotechnology, Rockford, IL, USA
Cacodylic Acid, Sodium Salt, Trihydrate	Electron Microscopy Sciences, Fort Washington, USA
Calcium Chloride (anhydrous, $CaCl_2$)	Sigma-Aldrich, St. Louis, MO, USA
CelLytic™-MT Mammalian Tissue Lysis / Extraction Reagent	Sigma-Aldrich, St. Louis, MO, USA
Chloroform	Mallinckrodt Baker, Phillipsburg, NJ, USA
Complete®, EDTA-free, Protease Inhibitor Cocktail Tablets	Roche Diagnostics Corporation, Roche Applied Science, Hague Road, IN, USA
Corn Oil	Sigma-Aldrich, St. Louis, MO, USA
Cyclosporin A	Sigma-Aldrich, St. Louis, MO, USA
DEPC-treated Water	Research Genetics (Invitrogen), Huntsville, AL, USA
Dexamethasone (9α-Fluoro-16 α-methylprednisolone)	Sigma-Aldrich, St. Louis, MO, USA
Dimethyl Sulfoxide (DMSO)	Sigma-Aldrich, St. Louis, MO, USA
Dithiothreitol (DTT)	Sigma-Aldrich, St. Louis, MO, USA
DMP-30 [2,4,6-Tri(dimethylaminomethyl) phenol]	Electron Microscopy Sciences, Fort Washington, USA
DyeEx™ 2.0 Spin Kit	Qiagen, Valencia, CA, USA
EDTA (ethylenediamine tetra-acetic acid)	Sigma-Aldrich, St. Louis, MO, USA
Endothelin 1, Human and Porcine	EMD Biosciences/Calbiochem®, San Diego, CA, USA
Ethidium Bromide	Sigma-Aldrich, St. Louis, MO, USA
Ethyl Alcohol 200 Proof ACS/USP Grade	Pharmaco™ Products, Brookfield, CT, USA
Ficoll® 400	Sigma-Aldrich, St. Louis, MO, USA
Full-Range Rainbow™ Molecular Weight Markers	Amersham Biosciences, Piscataway, NJ, USA
Gel Loading Buffer II	Ambion, Austin, TX, USA
GeneAmp® 10x PCR Buffer II & $MgCl_2$	Applied Biosystems, Foster City, CA, USA
α-D (+) Glucose	Sigma-Aldrich, St. Louis, MO, USA
Glutaraldehyde, 25%	Sigma-Aldrich, St. Louis, MO, USA
Glutaraldehyde, 50%	Electron Microscopy Sciences, Fort Washington, USA
Hydrochloric Acid (HCl)	Sigma-Aldrich, St. Louis, MO, USA
Hyperforin	Sigma-Aldrich, St. Louis, MO, USA

Ivermectin	Sigma-Aldrich, St. Louis, MO, USA
JKC-301	EMD Biosciences/Calbiochem®, San Diego, CA, USA
Lead Nitrate, Reagent, A.C.S.	Electron Microscopy Sciences, Fort Washington, USA
Leukotriene C_4 (LTC_4)	Sigma-Aldrich, St. Louis, MO, USA
Methanol	Caledon Laboratories LTD., Georgetown, Canada
Magnesium Chloride ($MgCl_2 \cdot 6H_2O$)	Sigma-Aldrich, St. Louis, MO, USA
Magnesium Sulfate ($MgSO_4 \cdot 7H_2O$)	Sigma-Aldrich, St. Louis, MO, USA
D-Mannitol	Sigma-Aldrich, St. Louis, MO, USA
2-Mercaptoethanol	Bio-Rad Laboratories, Hercules, CA, USA
MK 571 (sodium salt)	Cayman Chemical, Ann Arbor, MI, USA
MuLV Reverse Transcriptase	Applied Biosystems, Foster City, CA, USA
NBD-CSA: [N-ε(4-nitrobenzofurazan-7-yl)-D-Lys^8]-cyclosporine A	Custom-synthesized by Novartis, Basel, CH
L-NMMA: N^G-Monomethyl-L-arginine acetate salt	EMD Biosciences/Calbiochem®, San Diego, CA, USA
NuPAGE® Antioxidant	Invitrogen Corporation, Carlsbad, CA, USA
NuPAGE® LDS Sample Buffer (4x)	Invitrogen Corporation, Carlsbad, CA, USA
NuPAGE® MOPS SDS Running Buffer (20x)	Invitrogen Corporation, Carlsbad, CA, USA
NuPAGE® Reducing Agent (10x)	Invitrogen Corporation, Carlsbad, CA, USA
NuPAGE® Transfer Buffer (20x)	Invitrogen Corporation, Carlsbad, CA, USA
Osmium Tetroxide	Electron Microscopy Sciences, Fort Washington, USA
Paclitaxel	Sigma-Aldrich, St. Louis, MO, USA
Paraformaldehyde	Sigma-Aldrich, St. Louis, MO, USA
Paraformaldehyde, 16%	Electron Microscopy Sciences, Fort Washington, USA
PCR-grade Water	BD Biosciences Clontech, Palo Alto, CA, USA
1-*O*-Pentylglycerol	Dr. Erdlenbruch, Children's Clinic, University of Göttingen, Germany
Phosphatase Inhibitor Cocktail 2	Sigma-Aldrich, St. Louis, MO, USA
Potassium Chloride (KCl)	Sigma-Aldrich, St. Louis, MO, USA
Potassium Phosphate, Monobasic (KH_2PO_4)	Sigma-Aldrich, St. Louis, MO, USA
5-Pregnen-3β-ol-20-one-16α-carbonitrile (PCN)	Sigma-Aldrich, St. Louis, MO, USA
Phorbol-12-Myristate-13-Acetate (PMA)	EMD Biosciences/Calbiochem®, San Diego, CA, USA
2-Propanol	Mallinckrodt Baker, Phillipsburg, NJ, USA
Probenecid	Sigma-Aldrich, St. Louis, MO, USA
Propidium Iodide	Sigma-Aldrich, St. Louis, MO, USA
Propylene Oxide, EM Grade	Electron Microscopy Sciences, Fort Washington, USA
PSC833	Novartis AG, Basle, Switzerland
Random Hexamers	Applied Biosystems, Foster City, CA, USA
RES-701-1	EMD Biosciences/Calbiochem®, San Diego, CA, USA
RNase Inhibitor	Applied Biosystems, Foster City, CA, USA
RNaseZap™	Ambion, Austin, TX, USA
Sarafotoxin S6c	Sigma-Aldrich, St. Louis, MO, USA
Seakem® GTG® Agarose	Cambrex Bio Science Rockland, Rockland, ME, USA
Sodium Citrate, Dehydrate, Reagent	Electron Microscopy Sciences, Fort Washington, USA
Sodium Nitroprusside Dihydrate	Sigma-Aldrich, St. Louis, MO, USA
Sodium Phosphate, Dibasic (Na_2HPO_4)	Sigma-Aldrich, St. Louis, MO, USA
Sodium Chloride (anhydrous, NaCl)	Sigma-Aldrich, St. Louis, MO, USA
Sodium Cyanide (NaCN)	Sigma-Aldrich, St. Louis, MO, USA

Sodium Hydroxide (NaOH 1N)	Sigma-Aldrich, St. Louis, MO, USA
Sodium Pyruvate	Sigma-Aldrich, St. Louis, MO, USA
Sucrose	Sigma-Aldrich, St. Louis, MO, USA
SuperBlock® Blocking Buffer (TBS)	Pierce Biotechnology, Rockford, IL, USA
SuperSignal® West Pico Chemiluminescent Substrate	Pierce Biotechnology, Rockford, IL, USA
Surfact-Amps® 20	Pierce Biotechnology, Rockford, IL, USA
Surfact-Amps® X-100	Pierce Biotechnology, Rockford, IL, USA
Texas Red (sulforhodamine 101, free acid)	Sigma-Aldrich, St. Louis, MO, USA
Tris Base	Sigma-Aldrich, St. Louis, MO, USA
Trizol® Reagent	Invitrogen Corporation, Carlsbad, CA, USA
Uranyl Acetate, Reagent, A.C.S.	Electron Microscopy Sciences, Fort Washington, USA
(±)-Verapamil Hydrochloride	Sigma-Aldrich, St. Louis, MO, USA

5.1.2 Equipment and Materials

ABI Prism 377 DNA Sequencer	Applied Biosystems, Foster City, CA, USA
Beckman Allegra™ 21R Centrifuge, S 4180 Swinging Bucket Rotor	Beckman Coulter, Fullerton, CA, USA
Beckman L8-55M Ultracentrifuge, SW 41 Ti Swinging Bucket Rotor	Beckman Coulter, Fullerton, CA, USA
Beckman TL-100 Tabletop Ultracentrifuge, TLS-55 Swinging Bucket Rotor	Beckman Coulter, Fullerton, CA, USA
Beem™ Capsule Press	Electron Microscopy Sciences, Fort Washington, USA
Beem™ Embedding Capsules	Electron Microscopy Sciences, Fort Washington, USA
Black & Decker, 3/8” Drill	The Black & Decker Corporation, Towson, MD, USA
ChemiDoc™ Gel Documentation Systems	Bio-Rad Laboratories, Hercules, CA, USA
Costar® 96 Well Cell Culture Cluster, Polystyrene	Corning Incorporated, Corning, NY, USA
DNA Speed Vac® DNA 110, RD24 Rotor	Savant Instruments, Holbrook, NY, USA
Dounce Homogenisator, Clearance 130-180 µm	Kimble / Kontes, Vineland, NJ, USA
Dumont Forceps No. 5, Carbon Steel, 0.08 x 0.04 mm	Biomedical Research Instruments, Malden, MA, USA
Eppendorf Centrifuge 5415D, Eppendorf F45-24-11 Rotor	Brinkmann Instruments, Westbury, NY, USA
Eppendorf Centrifuge 5417 R, Aerosol-Tight Rotor FA45-30-11	Brinkmann Instruments, Westbury, NY, USA
Falcon® Cell Strainer, 100 µm Nylon	BD Biosciences, Bedford, MA, USA
Falcon® Ten-twenty-nine™ Petri Dish, 100x15 mm Style	BD Biosciences, Bedford, MA, USA
Formvar®/Carbon Coated Copper Grids	Electron Microscopy Sciences, Fort Washington, USA
FEI Tecnai™ G^2 12 Electron Microscope	FEI Company, Hillsboro, OR, USA
GeneQuant RNA/DNA Calculator	Biochrom Ltd, Cambridge, UK
Glass Beads, 0.45-0.5 mm	B. Braun Biotech International GmbH, Melsungen, D
Hoefer™ HE 33, Mini Horizontal Submarine Unit	Amersham Biosciences, Piscataway, NJ, USA
Innova™ 2000 Platform Shaker	New Brunswick Scientific, Edison, NJ, USA
Invitrolon™ PVDF Membrane, Pore Size 0.45 µm	Invitrogen Corporation, Carlsbad, CA, USA
IR AutoFlow™ Incubator	NuAire, Plymouth, MN, USA
Leica Ultracut Ultramicrotome	Leica, Deerfield, IL, USA
Market Forge Sterilmatic STME Autoclave	Global Medical Instrumentation, Albertville, MN, USA

Mettler PM 1200 Balance	Mettler-Toledo, Columbus, OH, USA
Microscope Cover Glass, 40x40, No.1 Thickness	A. Daigger & Company, Vernon Hills, IL, USA
Monoject® 6cc Syringes with Luer Lock Tip	Sherwood Medical, St. Louis, MO, USA
Monoject® Aluminum Hub Hypodermic Needles 19 x 1.5”	Sherwood Medical, St. Louis, MO, USA
Monoject® Sterile Single-Use Syringe, Luer Tip, 50 ml	Sherwood Medical, St. Louis, MO, USA
Nalgene® Small Filter Unit Sterilization, 0.2 µm Cellulose Nitrate Membrane	Nalgene Nunc International, Rochester, NY, USA
NuPAGE™ Bis-Tris Gel 4-12%, 1.0 mm x 15 wells	Invitrogen Corporation, Carlsbad, CA, USA
Ohaus® Analytical Plus Balance	Ohaus Corporation, Pine Brook, NJ, USA
PCR Sprint Thermal Cycler	Therma Electron Corporation, Waltham, MA, USA
Pestle Tissue Grinder, Clearance 150-230 µm	Thomas Scientific, Swedesboro, NJ, USA
Pharmaseal K75 3-way Stopcock, Sterile	Scientific Products / Baxter Healthcare, Bedford, MA, USA
PP graduated Micro Tube, RNase/DNase free, 1.7 ml	PGC Scientifics, Frederick, MD, USA
PP Macro Filters, Polypropylene, 300 µm	Spectrum Laboratories, Rancho Dominguez, CA, USA
SafeSeal Microcentrifuge Tubes 1.7ml	PGC Scientifics, Frederick, MD, USA
Sorvall® RC-5B PLUS Superspeed Refrigerated Centrifuge, Sorvall® SM-24 Rotor and SS-34 Rotor	Kendro Laboratory Products, Newtown, CT, USA
Spectra/Mesh® Nylon Filters, 30 µm	Spectrum Laboratories, Rancho Dominguez, CA, USA
Spectrum® Micro Tissue Grinder	Spectrum Laboratories, Rancho Dominguez, CA, USA
Sponge Pad for XCell II™ Blotting	Invitrogen Corporation, Carlsbad, CA, USA
VersaMax™, Tunable Microplate Reader	Molecular Devices, Sunnyvale, CA, USA
Wild M7 S Microscope	Leica Microsystems AG, Heerbrugg, CH
Xcell II™ Blot Module (Version G)	Invitrogen Corporation, Carlsbad, CA, USA
Xcell SureLock™ Mini-Cell	Invitrogen Corporation, Carlsbad, CA, USA
Zeiss 510 NLO, (Zeiss Inverted Axiovert 100M Microscope)	Carl Zeiss MicroImaging, Thornwood, NY, USA
Zeiss LSM 410, (Axiovert 135 Microscope)	Carl Zeiss MicroImaging, Thornwood, NY, USA

5.1.3 Kits

BigDye® Terminator Cycle Sequencing Kit	Invitrogen Corporation, Carlsbad, CA, USA
GeneAmp® RNA PCR Kit	Applied Biosystems, Foster City, CA, USA
pcDNA3.1/V5-His© TOPO® TA Expression Kit, Version G	Invitrogen Corporation, Carlsbad, CA, USA
NE-PER® Nuclear and Cytoplasmic Extraction Reagents	Pierce Biotechnology, Rockford, IL, USA
Nuclei PURE Prep Nuclei Isolation Kit	Sigma-Aldrich, St. Louis, MO, USA
One Shot® TOP10	Invitrogen Corporation, Carlsbad, CA, USA
QIAEX II Agarose Gel Extraction Kit	Quiagen, Valencia, CA, USA
RNeasy® Mini Kit	Qiagen, Valencia, CA, USA
Titanium™ Taq PCR Kit	BD Biosciences Clontech, Palo Alto, CA, USA
UltraClean™ 6 Minute Mini Plasmid Prep Kit™	Mo Bio Laboratories, Solana Beach, CA, USA
Poly/Bed 812 Kit	Polysciences, Warrington, PA, USA

5.1.4 Antibodies

Alexa Fluor® 488 Chicken Anti-Rat IgG (H + L)	Molecular Probes, Eugene, OR, USA
Alexa Fluor® 488 Goat Anti-Mouse IgG (H + L)	Molecular Probes, Eugene, OR, USA
Alexa Fluor® 488 Goat Anti-Rabbit IgG (H + L)	Molecular Probes, Eugene, OR, USA
Alexa Fluor® 633 Donkey Anti-Goat IgG (H+L)	Molecular Probes, Eugene, OR, USA
Anti-Endothelin Receptor Type B	Alomone Labs, Jerusalem, Israel
Anti-ET_A-Receptor PAb (Polyclonal Antibody to Endothelin A Receptor)	Alexis Axxora, LCC, San Diego, CA, USA
Anti-GAPDH	Abcam Limited, Cambridgeshire, UK
Anti-Glucose Transporter 1 (Rabbit)	EMD Biosciences/Calbiochem®, San Diego, CA, USA
Anti-Mouse JAM-1 Antibody	R&D Systems, Minneapolis, MN, USA
Anti-Na^+/K^+ ATPase a-1	Upstate Biotechnology, Lake Placid, NY, USA
Fluorescein-Labeled Affinity Purified Antibody To Sheep IgG, (H+L)	Kirkegaard & Perry Laboratories, Gaithersburg, MD, USA
ImmunoPure® Goat Anti-Mouse IgG, (H+L), Peroxidase Conjugated	Pierce Biotechnology, Rockford, IL, USA
ImmunoPure® Goat Anti-Rabbit IgG, (H+L), Peroxidase Conjugated	Pierce Biotechnology, Rockford, IL, USA
ImmunoPure® Goat Anti-Rat IgG, (H+L), Peroxidase Conjugated	Pierce Biotechnology, Rockford, IL, USA
ImmunoPure® Rabbit Anti-Goat IgG, (H+L), Peroxidase Conjugated	Pierce Biotechnology, Rockford, IL, USA
ImmunoPure® Rabbit Anti-Sheep IgG, (H+L), Peroxidase Conjugated	Pierce Biotechnology, Rockford, IL, USA
mdr Ab-1	Oncogene Research Products, Cambridge, MA, USA
Monoclonal Antibody to Breast Cancer Resistance Protein (BXP-53)	Alexis Axxora, LCC, San Diego, CA, USA
Monoclonal Antibody to MRP2/cMOAT (M_2 III-6)	Alexis Axxora, LCC, San Diego, CA, USA
Monoclonal Mouse anti-Claudin-5	Zymed® Laboratories, South San Francisco, CA, USA
Mouse Monoclonal C219	Signet Laboratories, Dedham, MA, USA
Polyclonal Antibody to MRP1 (A23)	Alexis Axxora, LCC, San Diego, CA, USA
Polyclonal Antibody to MRP4 (human)	Alexis Axxora, LCC, San Diego, CA, USA
PXR (R-14)	Santa Cruz Biotechnology, Santa Cruz, CA, USA
Rabbit Anti-Claudin-1	Zymed® Laboratories, South San Francisco, CA, USA
Rabbit Anti-Occludin	Zymed® Laboratories, South San Francisco, CA, USA
Rabbit Anti-ZO-1	Zymed® Laboratories, South San Francisco, CA, USA

5.1.5 Enzymes

Hind III	New England Biolabs, Beverly, MA, USA
RNase-Free DNase	Qiagen, Valencia, CA, USA
Taq DNA Polymerase in Storage Buffer A (5 U/µl)	Promega Corporation, Madison, WI, USA
Xho I	New England Biolabs, Beverly, MA, USA

5.1.6 Primers

Mdr1a Forward primer (bases 1253-1278): 5'-CACTTCAGTTACCCGTCTCGAAAAGA-3' Reverse primer (bases 1895-1920): 5'-CCTTTCTCTCTCATGAGCTCATCATG-3'	Qiagen Inc., Valencia, CA, USA
Mdr1b Forward primer (bases 2264-2289): 5'-GCATACAACCAGTGTTTGCCATAGTG-3' Reverse primer (bases 2658-2683): 5'-GTAAAAGTGTAAGCTGCCAGCCATAG-3'	Qiagen Inc., Valencia, CA, USA
Mrp2 Forward primer (bases 2123-2147): 5'-GTATCAGCCATGCTGGGAGAAATGG-3' Reverse primer (bases 2507-2531): 5'-AGATTCTCGTCTTGCCAGCCAACAG-3'	Qiagen Inc., Valencia, CA, USA
PXR Forward primer (bases 538-560): 5'-GATGATCATGTCTGATGCCGCTG-3') Reverse primer (bases 890-868): 5'-AGGTTGGTAGTTCCAGATGCTG-3'	Qiagen Inc., Valencia, CA, USA
T7 Sequencing Primer 5'-TAATACGACTCACTATAGGG-3'	Invitrogen Corporation, Carlsbad, CA, USA
BGH Reverse Sequencing Primer 5'-TAGAAGGCACAGTCGAGG-3'	Invitrogen Corporation, Carlsbad, CA, USA

5.1.7 Software

EndNote, Version 7.0.0 (Bld 98)	ISI ResearchSoft, Carlsbad, CA, USA
GraphPad Prism®, Version 4.00	GraphPad Software Inc., San Diego, CA, USA
MegaView III Soft Imaging System (SIS)	Soft Imaging System Corp., Lakewood, CO, USA
Microsoft® Excel 2002, SP3	Microsoft Corporation, Redmond, WA, USA
Microsoft® Office XP	Microsoft Corporation, Redmond, WA, USA
Microsoft® PowerPoint® 2002, SP3	Microsoft Corporation, Redmond, WA, USA
Microsoft® Word 2002, SP3	Microsoft Corporation, Redmond, WA, USA
NIH ImageJ, Version 1.31	NIST Laboratories, Gaithersburg, MD, USA
Primer Express®, Version 8.0	Applied Biosystems, Foster City, CA, USA
Quantity One, Version 4.3.0	Bio-Rad Laboratories, Hercules, CA, USA
Scion Image Beta 4.02	Scion Corporation, Frederich, MD, USA
SoftMax® Pro, Version 3.1.2	Molecular Devices Corp., Sunnyvale, CA, USA
Zeiss LSM 510 NLO, Version 3.2 SP2	Carl Zeiss MicroImaging, Inc., Thornwood, NY, USA
Zeiss LSM Version 3.99	Carl Zeiss MicroImaging, Inc., Thornwood, NY, USA
Zeiss LSM 5 Image Examiner, Version 3.2	Carl Zeiss MicroImaging, Inc., Thornwood, NY, USA

5.1.8 Buffers

Phosphate Buffered Saline (PBS), pH 7.4

		Final concentration:
NaCl	8.00 g	136.90 mM
KCl	0.20 g	2.70 mM
Na_2HPO_4	1.15 g	8.10 mM
KH_2PO_4	0.20 g	1.46 mM
CaCl2 (anhyd.)	0.10 g	0.90 mM
$MgCl_2 \cdot 6H_2O$	0.10 g	0.50 mM
Na-pyruvate	0.11 g	1.00 mM
Glucose	0.90 g	5.00 mM
Distilled water ad	1000ml	

NaOH and HCl were used to adjust pH; buffer was filter sterilized (0.2 µm). Na-pyruvate and glucose were added prior to experiments.

Ca^{2+} and Mg^{2+}-free PBS, pH 7.4

		Final concentration:
NaCl	8.00 g	136.90 mM
KCl	0.20 g	2.70 mM
Na_2HPO_4	1.15 g	8.10 mM
KH_2PO_4	0.20 g	1.46 mM
Na-pyruvate	0.11 g	1.00 mM
Glucose	0.90 g	5.00 mM
Distilled water ad	1000ml	

NaOH and HCl were used to adjust pH; buffer was filter sterilized (0.2 µm). Na-pyruvate and glucose were added prior to experiments.

Tris-Borate-EDTA Buffer (TBE Buffer)

		Final concentration:
Tris base	108 g	0.89 M
Boric Acid	55 g	0.89 M
EDTA (pH 8.0), 0.5 M	40ml	20 mM
Distilled water ad	1000ml	

TBE buffer was filtered through a 0.2 µm filter-sterilizing unit.

5.1.9 Solutions for Capillary Isolation

1% BSA

		Final concentration:
Albumin bovine serum	1 g	1%
PBS ad	100ml	

30% Ficoll®

		Final concentration:
Ficoll®	30 g	30%
PBS ad	100ml	

5.1.10 Fixative for Immunohistochemistry

3% Paraformaldehyde/0.25% Glutaraldehyde Fixative

		Final concentration:
Paraformaldehyde	3 g	3%
Glutaraldehyde	0.25 g	0.25%
Ca^{2+} and Mg^{2+}-free PBS* ad	100ml	

* without glucose and Na-pyruvate

5.1.11 Culture Media

Luria Agar Plates, pH 7.2

		Final concentration:
Bacto™ Tryptone	10 g	1%
Bacto-Yeast Extract	5 g	0.5%
NaCl	10 g	171.1 mM
Bacto™ Agar	20 g	2%
Ampicillin	0.1 g	100 µg/ml
Distilled water ad	1000ml	

1N NaOH was used to adjust pH; mixture was autoclaved at 121˚C for 20 minutes, cooled down and dispensed into sterile petri dishes (30 ml per plate).

Luria-Bertani Medium, pH 7.5

		Final concentration:
Bacto™ Tryptone	10 g	1%
Bacto-Yeast Extract	5 g	0.5%
NaCl	10 g	171.1 mM
Ampicillin	0.1 g	100 µg/ml
Distilled water ad	1000ml	

1N NaOH was used to adjust pH; medium was autoclaved at 121˚C for 25 minutes.

SOC Medium, pH 7.0

		Final concentration:
Bacto™ Tryptone	20 g	2%
Bacto-Yeast Extract	5 g	0.5%
NaCl, 1 M	10ml	10 mM
KCl, 1 M	2.5ml	2.5 mM
$MgCl_2$, 2 M	5ml	10 mM
$MgSO_4$, 2 M	5ml	10 mM
Glucose, 2 M	10ml	20 mM
Distilled H_2O ad	1000ml	

SOC medium was filtered through a 0.2 µm filter-sterilizing unit.

5.1.12 RT and PCR Reagent Mixtures

RT Reagent Mix

		Final concentration:
Sample (RNA in H_2O)	9 µl	5 µg
Random hexamer, 50 µM	1 µl	2.5 µM
RNase inhibitor, 20 U/µl	1 µl	1 U/µl
PCR buffer II, 10x	2 µl	1x
dNTP mix, 10 mM each	2 µl	1 mM each
$MgCl_2$, 25 mM	4 µl	5 mM
MuLV RT, 50 U/µl	1 µl	2.5 U/µl
Total volume:	**20 µl**	

Touch Down-PCR Reagent Mix

		Final concentration:
Sample (RT product)	1-5 µl	
Forward primer, 10 µM	1 µl	0.2 µM
Reverse primer, 10 µM	1 µl	0.2 µM
PCR buffer II, 10x	5 µl	1x
dNTP mix, 10 mM each	1 µl	0.2 mM each
$MgCl_2$, 25 mM	4 µl	2 mM
Taq DNA Polymerase, 5 U/µl	0.5 µl	0.05 U/µl
PCR-graded H_2O	32.5-36.5 µl	
Total volume:	**50 µl**	

5.1.13 Reagents for Cloning and Sequencing

TOPO® Cloning Reaction Mixture

		Final concentration:
Sample (PCR product)	4 µl	
Salt solution	1 µl	200 mM NaCl, 10 mM $MgCl_2$
TOPO® vector, 10 ng/µl	1 µl	1.66 ng/µl
Total volume:	**6 µl**	

Double Restriction Mixture

		Final concentration:
Sample (plasmid DNA)	10 µl	
NEBuffer 2, 10x	1.5 µl	1x
BSA, 10x	1.5 µl	0.1%
Hind III	1 µl	1.3 U/µl
Xho I	1 µl	1.3 U/µl
Total volume:	**15.0 µl**	

BigDye® Terminator Sequencing Reaction

		Final concentration:
Sample (DNA)	11 µl	
T7 / BGH primer	1 µl	0.82 / 0.895 µM
BigDye® Terminator Master Mix	8 µl	
Total volume:	**20 µl**	

5.1.14 Reagents for Transmission Electron Microscopy

0.1 M Sodium Cacodylate Buffer

		Final concentration:
Sodium cacodylate buffer, 0.2 M	50ml	0.1 M
Distilled H_2O ad	100ml	

Filtered using 0.22 µm Nalgene® disposable filtration unit.

1% OsO_4

		Final concentration:
OsO_4, 2% in H2O	10ml	1%
Sodium cacodylate buffer, 0.2 M	10ml	0.1M

Fixative for TEM (Modified Karnovsky's Fixative: 2% Paraformaldehyde/2.5% Glutaraldehyde in 0.1M Sodium Cacodylate Buffer, pH 7.4)

		Final concentration:
Paraformaldehyde, 16%	12.5ml	2%
Glutaraldehyde, 70%	3.57ml	2.5%
Sodium cacodylate buffer, 0.2 M ad	50ml	0.1M
Distilled H_2O ad	100ml	

Fitered using 0.22 µm Nalgene® disposable filtration unit.

5% Uranyl Acetate

		Final concentration:
Uranyl acetate	5 g	5%
Distilled H_2O ad	100ml	

Reynold's Stain

		Final concentration:
Lead nitrate	1.33 g	80.4 mM
Sodium citrate	1.76 g	119.6 mM
Distilled H_2O* ad	50ml	

*Distilled water was degassed by boiling and cooling to room temperature in an airtight container. Carbonate-free 1 N NaOH was used to adjust pH to 12. Filtered using 0.22 µm Nalgene® disposable filtration unit.

Epoxy Resin/Propylene Oxide for Infiltration

		Final concentration:
Polybed 812	100ml	
Propylene oxide	100ml	
DMP-30	2ml	2%

Epoxy Resin for Embedment

		Final concentration:
Polybed 812	100ml	
DMP-30	2ml	2%

5.2 Methods

5.2.1 Animal Housing and Handling

Sprague Dawley outbred rats (male retired breeders, 500-750 g) were purchased from Taconic (Germantown, NY, USA) and used for all *in vitro* and *in vivo* experiments. Animals were acclimated to the housing facilities for at least 5 days after delivery and had free access to NIH #31M rodent diet (Zeigler Brothers, Gardners, PA, USA) and tap water. Rats were kept under controlled external conditions (1 animal/cage, 22 ± 1˚C, 40-60 % relative humidity, 12-hour light/dark cycle) and were watched at least once a day. Animal housing, dosing protocols and *in vivo* treatments were in accordance with NIEHS guidelines and the NIH Guide for the Use and Care of Laboratory Animals (U.S. Department of Health, 1985). Rats were euthanized by CO_2 inhalation and decapitated; tissue was harvested immediately. Tissue was kept at 4˚C in PBS for immediate use or snap-frozen in liquid nitrogen for later use.

5.2.2 Isolation of Rat Brain Capillaries

(Dallaire et al., 1991; Hartz et al., 2004; Miller et al., 2000)

Capillaries were isolated from fresh rat cerebral cortex using mechanical homogenization, density-gradient centrifugation and purification on a glass bead column.
Ice-cold PBS was used; all materials and tools were kept on ice over the whole procedure. The protocol described is for isolating capillaries from 10 rat brains. Rat brains (cerebrum) were purified from meninges and white matter using forceps and a stereomicroscope. Brain tissue was minced with a scalpel, then suspended 1:1 in PBS and homogenized with a pestle tissue grinder (clearance: 150-230 µm) by 10 up-and-down strokes using a drill. The suspension was further homogenized by 10 up-and-down strokes in a dounce homogenizer (clearance: 130-180 µm). An equal volume of 30% Ficoll® was added to a final concentration of 15%. The homogenate was centrifuged at 5,800 g for 20 min at 4°C in a Sorvall® RC-5B PLUS Superspeed refrigerated centrifuge. Floating fat and white matter were discarded; the pellet was resuspended in 1% BSA and filtered through a 300 µm mesh. The capillary suspension was passed over a glass bead column (30 ml of 0.45 mm glass beads in a 50 ml column, Ø 2.5 cm) and the column was washed with 400 ml 1% BSA. Capillaries adhering to the glass beads were washed off and collected by gentle agitation in 1% BSA followed by filtration through a 100 µm cell strainer. After centrifugation (300 g, 5 min, 4˚C, Allegra™ 21R centrifuge), the capillary pellet was washed twice with PBS and immediately used for transport experiments, immunohistochemistry or capillary membrane isolation. Purity of the preparation was confirmed under a light microscope. The yield of enriched capillary fraction was 25-30 mg per 1 g of brain tissue (wet weight).

5.2.3 Transport Experiments

(Bauer et al., 2004; Hartz et al., 2004; Schramm et al., 1995)

Freshly isolated capillaries were transferred to confocal imaging chambers, pre-incubated for 30 min with the corresponding modulator diluted in PBS, and then incubated in the dark for 1 hour at room temperature in PBS containing a fluorescent dye (NBD-CSA or Texas Red). For some experiments, capillaries were first loaded with the fluorescent marker to steady state and modulators were added then. Per group of treatment, images were acquired from 10-15 capillaries by confocal microscopy; luminal fluorescence intensity was quantitated using Scion Image Beta 4.02 or Zeiss LSM 5 Image Examiner 3.2. Specific luminal NBD-CSA fluorescence (P-gp-specific transport) was calculated by subtracting the PSC833/NaCN-insensitive component of fluorescence from the quantitated fluorescence values.

5.2.4 Kinetic Efflux Assay

(Hartz et al., 2004)

Capillary lumens were loaded with 2 µM Texas Red in PBS for 1 hour at room temperature to steady state. After washing the capillaries 3 times with PBS, luminal efflux of Texas Red was followed using a confocal microscope. Images of capillaries were taken for each time point and luminal Texas Red fluorescence was analyzed using Zeiss LSM 5 Image Examiner 3.2. Data were plotted as one phase exponential decay using GraphPad Prism® software 4.00.

5.2.5 Immunostaining

(Bauer et al., 2004; Hartz et al., 2004)

Ca^{2+} and Mg^{2+}-free PBS without glucose and Na-pyruvate was used for preparing all solutions (fixative, 0.1-0.5% Triton X-100, 1% BSA and propidium iodide nuclei staining solution). Rat brain capillaries were transferred to confocal imaging chambers and let attach to the bottom for 15-20 min. Fixation was done with 3% para-formaldehyde/0.25% glutaraldehyde for 10-15 min at room temperature. After washing 5 times with buffer, capillaries were permeabilized for 15-30 min with 0.1-0.5% Triton X-100, washed twice with buffer and blocked for 15-30 min with 1% BSA. Capillaries were then incubated for either 1-2 hours at 37°C or overnight in the refrigerator with primary antibody diluted in 1% BSA. After washing 5 times with 1% BSA, capillaries were incubated for 1-2 hours at 37°C with the corresponding fluorescence-labeled secondary antibody (1:1,000 dilution in 1% BSA). Capillaries were washed, nuclei were stained with 1 µg/ml propidium iodide for 5-15 min and afterwards, capillaries were washed again. Capillary immunostaining was watched using confocal microscopy. For quantitative immunostaining, images of 20 capillaries per group were acquired. Immunofluorescence was quantitated using NIH ImageJ 1.31.

5.2.6 Laserscanning Confocal Microscopy

(Bauer et al., 2004; Hartz et al., 2004; Miller, 2003; Schramm et al., 1995)

For transport studies, efflux experiments and immunostaining, laser scanning confocal microscopy was used (Zeiss LSM 410 invert or LSM 510 NLO Laser Scanning Microscope).
For transport studies with NBD-CSA, the 488 nm line of an argon ion laser provided the excitation. Images from experiments using Texas Red (transport and efflux studies) were obtained using a HeNe laser (excitation: 543 nm). Low laser intensity was used to avoid photobleaching of the dyes. Tissue auto-fluorescence was undetectable with the applied settings. To obtain an image, dye-loaded capillaries were viewed under transmitted light illumination. A single capillary, at least 50 µm in length with well-defined lumen and undamaged endothelium, was selected. The plane of focus was adjusted to cut through the center of the capillary lumen and a confocal image (512 x 512 x 8 bits) was acquired by averaging four scans. Fluorescence intensities were measured from stored images using Scion Image Beta 4.02 or Zeiss LSM 5 Image Examiner 3.2. For fluorescence quantitation, three luminal areas (> 20 μm^2 each) were selected from each capillary. Because luminal fluorescence intensity cannot be related to the actual concentration of accumulated compound in the lumen, data are reported as average measured pixel intensity. Arbitrary fluorescence units [au] range from 0-255.
Immunofluorescence was visualized by confocal microscopy using an argon ion laser (488 nm). To quantitate immunofluorescence, luminal membrane fluorescence was measured using NIH ImageJ 1.31. A 10 x 10 grid was superimposed on each image, and measurements were taken at every intersection of a grid line with a capillary luminal plasma membrane. The fluorescence intensity for each capillary was the mean of all measurements.

Confocal microscope	**Zeiss 510 NLO** **mounted on Zeiss Inverted Axiovert 100M**	**Zeiss LSM 410 invert** **mounted on Axiovert 135**
Fluorescent marker	1. NBD-CSA 2. Texas Red 3. Alexa Fluor® 488 4. Propidium iodide	NBD-CSA
Objective lens	Zeiss C-Apochromat 40x water immersion objective (numerical aperture = 1.2)	Zeiss C-Apochromat 40x water immersion objective (numerical aperture = 1.2)
Laser type	1. HeNe laser 2. Argon ion laser	Argon ion laser
Laser excitation	1. 543 nm 2. 488 nm	488 nm
Emission filter	1. Long Pass 560 nm 2. Band Pass 500-530 nm	Long Pass 500 nm
Beam splitters	1. HFT 488/543, NFT 490 2. HFT 488/543	FT 488/647 nm
Pinhole setting	≤ 1 Airy unit	≤ 1.7 Airy unit
Zoom	4	4

5.2.7 Plasma Membrane Isolation

(Bauer et al., 2004; Wakayama et al., 2002)

Crude plasma membrane fractions from liver, kidney or brain capillaries were obtained by differential centrifugation. Tissue was homogenized in mammalian tissue lysis buffer (CelLytic™MT) containing Complete™ protease inhibitor cocktail using a micro-homogenizer. After 1 hour on ice with occasional vortexing, samples were centrifuged at 10,000 g for 30 min. Denucleated supernatants were centrifuged at 100,000 g for 90 min (TL-100 tabletop ultracentrifuge). Pellets (crude plasma membranes) were resuspended in PBS containing protease inhibitor cocktail and phosphatase inhibitor and kept at -80˚C until use.

5.2.8 Isolation of Nuclear Proteins

Nuclear proteins from capillaries were isolated according to a protocol combining the Nuclei PURE Prep Nuclei Isolation Kit and the NE-PER® Nuclear und Cytoplasmic Extraction Reagents Kit. All steps were carried out on ice; all equipment used was pre-cooled; buffers contained inhibitors for phosphatases and proteases.
Isolated capillaries were homogenized with 10 ml of ice-cold Nuclei PURE lysis buffer using micro-homogenizers. The homogenate was mixed with 15 ml 1.8 M Nuclei PURE Sucrose Cushion Buffer and carefully layered on top of 2.5 ml 1.8 M Nuclei PURE Sucrose Cushion Buffer. Samples were centrifuged at 40,000 g for 2 hours at 4˚C (Beckman L8-55M ultracentrifuge). Supernatant was removed; nuclei pellets were resuspended in Nuclei PURE Storage Buffer and centrifuged at 500 g for 5 min at 4˚C (Beckman Allegra™ 21R centrifuge). After washing with Ca^{2+} and Mg^{2+}-free PBS, nuclei were resuspended in 100 µl nuclear extraction reagent. Samples were placed on ice and thoroughly vortexed every 10 min, for a total of 60 min. Samples were centrifuged at 16,000 g for 10 min at 4˚C. Supernatant (nuclear extract) was transferred to a pre-chilled tube and stored at -80˚C until use.

5.2.9 Bradford Protein Assay

(Bradford, 1976)

For the standard curve, BSA was diluted in 1N NaOH (0, 1, 2, 3, 4, 5 µg/µl). Samples were also diluted in 1N NaOH, vortexed and centrifuged. Per well, 10 µl standard or sample were pipetted (3 repeats of each). 200 µl freshly prepared Bradford reagent (1:5 in H_2O) was added and mixed thoroughly. NaOH was used as blank. The plate was read at λ = 595 nm in a VersaMax™ tunable micro-plate reader. Sample protein concentrations were calculated from the standard curve and obtained as mean concentration in µg/µl by SoftMax® Pro software program.

5.2.10 Western Blotting

(Bauer et al., 2004; Hartz et al., 2004; Laemmli, 1970)

Western blots were performed using the Invitrogen NuPage™ Bis-Tris electrophoresis system with pre-cast 4-12% Bis-Tris-gradient gels, NuPage® MOPS SDS running buffer and NuPage® transfer buffer under reducing conditions. Samples were prepared using NuPAGE® LDS sample buffer, NuPAGE® reducing agent and deionized water and diluted to the protein concentration needed (usually 1 µg/µl). Samples were heated (70°C) for 10 min, cooled down to room temperature, vortexed and loaded onto the gel. Full-Range Rainbow™ marker was used as molecular weight standard. The electrophoresis was run at 200 V (constant) for about 50-60 min. Gels were subsequently blotted on PVDF membranes. Transfer conditions were 30 V (constant) for 2 hours. After protein transfer, membranes were blocked with SuperBlock® blocking buffer containing 0.5% Surfact-Amps® 20 for 8 hours in the refrigerator. Membranes were incubated overnight with a primary antibody diluted in blocking buffer. Then, membranes were washed 7 times for 7 min while agitating on a rotary platform shaker with BupH™ Tris Buffered Saline containing 0.05% Tween® 20. Membranes were incubated with horseradish peroxidase-conjugated ImmunoPure® secondary antibody (1:10,000 - 1:20,000) for 1 hour at room temperature while shaking. After washing (7 times 7 min), proteins were detected using SuperSignal® West Pico Chemoluminescent Substrate and visualized with a BioRad Chemi Doc 2000™ gel documentation system.

5.2.11 *In Vitro* Induction Experiments

(Bauer et al., 2004)

Freshly isolated capillaries were exposed to modulators (dexamethasone, PCN, hyperforin and paclitaxel) in PBS for 6 hours at room temperature. Modulators in DMSO stock solutions were prepared in PBS. Control medium contained DMSO; the final DMSO concentration did not exceed 0.05%.

5.2.12 *In Vivo* Induction Experiments

(Bauer et al., 2004)

For *in vivo* induction, five animals per group were injected i.p. daily with PCN (10-50 mg/kg in corn oil, 3 days) or dexamethasone (1-50 mg/kg in corn oil, 3 days). Control animals were treated with corn oil only. The injection volume was 5 ml/kg. 24 hours after the last injection, rats were euthanized and decapitated; brains were taken immediately to isolate brain capillaries. Livers and kidneys were removed, snap-frozen in liquid nitrogen and stored at -80°C until use.

5.2.13 Total RNA Isolation

To avoid contamination with RNase, bench surfaces, pipettes and gloves were cleaned with RNaseZap™ prior to isolation. All steps were carefully performed and pipettes, reserved for RNA work only, were used with sterile RNase- and DNase-free pipet tips.
Total RNA was isolated using Trizol® reagent and further purified using the RNeasy® Mini Kit to obtain an optimal yield of high purity total RNA. 20-50 mg of tissue (isolated capillaries, brain, liver and kidney) were thoroughly homogenized in 1 ml Trizol® reagent using a micro-homogenizer. The homogenate was transferred into an RNase-free tube, 200 µl chloroform were added, then the samples were vortexed for 15 sec and incubated for 10 minutes at room temperature. For phase separation, samples were centrifuged at 12,000 g for 15 min at 4°C. The mixture separated into a lower red, phenol-chloroform phase, an inter-phase containing protein, and a colorless upper aqueous phase containing total RNA. The aqueous phase was transferred to a fresh tube and RNA was precipitated by adding 0.5 ml of 100% isopropyl alcohol. After 10 min incubation, samples were centrifuged at 12,000 g for 10 min at 4°C. The supernatant was removed, and the RNA pellet was washed with 1 ml ethanol (70%), followed by centrifugation (12,000 g, 5 min, 4°C). The supernatant was removed; the RNA pellet was air-dried and then dissolved in 100 µl DEPC-treated water. To further purify total RNA, the RNeasy® Mini Kit was used according to the manufacturer's protocol. Briefly, 350 µl RLT buffer containing 1% β-mercaptoethanol and 250 µl ethanol (100%) were added to 100 µl of total RNA and mixed thoroughly by pipetting. Samples were then applied to an RNeasy® mini column placed in a collection tube. Samples were centrifuged at 8,000 g for 30 sec; the flow-through was discarded. 350 µl RW1 wash buffer were pipetted into the column, which was then centrifuged for 1 min at 8,000 g. The flow-through was discarded. 80 µl DNase I incubation mix (10 µl DNase I stock solution + 70 µl RDD buffer) were applied directly onto the RNeasy® silica-gel membrane of the column and let incubate for 15-30 min at room temperature. 350 µl RW1 wash buffer were added and centrifuged at 8,000 g for 30 sec, the flow-through was discarded. Then, the column was washed 2 times with 500 µl RPE buffer and centrifuged at 8,000 g for 15 sec and 2 min, respectively. A new collection tube was applied and RNA was eluted with 10-30 µl RNase-free water. RNA yield and purity were determined by measuring optical density (OD). Only samples with an OD ratio 260 nm : 280 nm 1.8-2.0 were used.

5.2.14 Reverse Transcription

Reverse transcription (RT) was performed using the GeneAmp® RNA PCR kit. 1-5 µg total RNA, random hexamers, MuLV reverse transcriptase, dNTPs, RNase inhibitor, $MgCl_2$ and PCR buffer were mixed. The following thermocycler program was used:

25˚C	for	10 min
42˚C	for	90 min
95˚C	for	5 min
hold at 4˚C		

5.2.15 Touch-down PCR

Primers were designed either manually or by using Primer Express® software, Version 8.0. Complete mRNA sequences of the corresponding rat genes were obtained from PubMed. Primer specificity was confirmed by running the sequences through the PubMed BLAST database. Primers were then custom-synthesized by Qiagen.
For touch-down PCR, 1-5 µl RT product was mixed with forward and reverse primers. Then, Taq DNA polymerase, dNTPs, $MgCl_2$, PCR buffer and PCR-grade H_2O were added. PCR was run using the following thermocycler program:

95˚C	for	1 min	
95˚C	for	30 sec	1 cycle each
65-61˚C	for	30 sec	
72˚C	for	30 sec	
95˚C	for	30 sec	25-35 cycles
60˚C	for	30 sec	
72˚C	for	30 sec	
72˚C	for	3 min	
hold at 4˚C			

5.2.16 Electrophoresis

PCR products were electrophoresed on a freshly poured agarose gel (2-4%, 0.1 µg/ml ethidium bromide, Tris-borate-EDTA buffer). Samples were mixed with gel loading buffer and loaded into the wells. Running conditions were 100 V for 45-60 min. Bands were visualized under UV and imaged using the BioRad Chemi Doc 2000™ gel documentation system.

5.2.17 Cloning and Sequencing

(Bauer et al., 2004)

In order to clone and sequence the PCR product, first the PXR amplicon was extracted from the agarose gel, purified and cloned into the His-TOPO® vector, followed by transformation in One Shot® TOP10 chemically competent E. coli cells. Plasmid DNA was isolated using the UltraClean™ 6-minute plasmid kit; sequencing PCR was performed using the BigDye® DNA sequencing kit. Samples were purified on a spin column and sequenced on an ABI Prism 377 DNA sequencer.

Agarose Gel Extraction:

The 353 bp amplicon of rat PXR (GenBank Acc.No. AF151377) was electrophoresed on an agarose gel. The PCR product was extracted from the agarose gel using the QIAEX II agarose gel extraction kit according to the manufacturer's protocol. Briefly, DNA bands were excised from the gel. 3 volumes of QX1 buffer were added to 1 volume of gel. After adding 10 µl QIAEX II suspension, samples were incubated at 50˚C for 10 min while vortexing every 2 min.

After centrifugation (30 sec, 10,000 g), supernatant was removed and the pellets were washed once with 500 µl QX1 buffer and twice with 500 µl PE buffer. The pellets were air-dried for 10 min and resuspended in 20 µl PCR-grade H_2O. After centrifugation (30 sec, 10,000 g), supernatant containing purified DNA was transferred into a fresh tube.

Cloning:

The pcDNAA3.1/V5-His© TOPO® TA expression kit was used to clone the extracted PCR product. TOPO® Cloning reaction mixture containing sample, buffer and TOPO® vector was prepared according to the manufacturer's protocol, incubated for 5 min at room temperature and for an additional 5 min on ice.

Transformation:

Transformation in One Shot® TOP10 chemically competent E. coli cells was performed by gently mixing 4 µl of sample with One Shot® TOP10 chemically competent E. coli cells followed by 5 min incubation on ice. The cells were heat-shocked for 30 sec at 42˚C and immediately put back on ice. After adding 250 µl SOC medium, cells were plated on LB plates containing 100 µg/ml ampicillin and incubated overnight. 24 hours after plating, colonies were picked and cultured in Luria-Bertani Medium (100 µg/ml ampicillin) overnight at 37˚C.

Plasmid DNA isolation:

Plasmid DNA was isolated using the UltraClean™ 6 minute Mini Plasmid Prep kit according to the manufacturer's protocol. Briefly, 2 ml culture medium were added to the E. coli cells. Samples were centrifuged (1 min, 10,000 g), supernatant was removed and the cell pellets were resuspended in 50 µl Solution 1. 100 µl Solution 2 and 325 µl Solution 3 were added and the tubes were gently inverted to mix. After centrifugation (1 min, 10,000 g), the supernatant was pipetted into a spin filter and centrifuged (30 sec, 10,000 g). The flow through was discarded, 300 µl Solution 4 was added on the spin filter, which was centrifuged at 10,000 g for 30 sec. Plasmid DNA was eluted with 50 µl PCR-graded H_2O by centrifugation (10,000 g, 30 sec). Positive clones were selected by double-restriction digest with *Hind* III and *Xho* I restriction enzymes. 5 µl of the mixture for double restriction were added to 10 µl plasmid DNA and let incubate for 1 hour at 37˚C. Agarose gel electrophoresis was run to check the double-restriction.

Sequencing:

Sequencing was performed using the BigDye® Terminator Cycle Sequencing Kit and universal T7 and BGH primers. BigDye® Terminator master mix, sample and primers were mixed and the PCR reaction was performed using the following parameters:

96˚C	for	1 min	
96˚C	for	10 sec	25 cycles
50˚C	for	5 sec	
60˚C	for	4 min	
hold at 10˚C			

The PCR products were spin column purified using the DyeEx™ 2.0 Spin kit. Samples were transferred to the spin column and centrifuged for 3 min at 750 g. Samples were vacuum-dried and sequenced on an ABI Prism 377 DNA sequencer.

5.2.18 Transmission Electron Microscopy

Isolated rat brain capillaries were rinsed in 0.1 M sodium cacodylate buffer and centrifuged (300 g, 1 min, 4˚C). The pellet was resuspended in 3 ml fixative (modified Karnovsky's fixative: 2% para-formaldehyde/2.5% glutaraldehyde in 0.1 M sodium cacodylate buffer) and incubated for 10 min. After centrifugation at 15,000 g for 10 min, the pellet was overlaid with fresh fixative and incubated overnight. Then, the pellet was rinsed three times for 15 min in 0.1 M sodium cacodylate buffer, followed by 1-hour postfixation in 1% OsO_4. After three 15-min rinses with distilled H_2O, the pellet was dehydrated through a graded series of ethanol (50%, 70%, 95% and twice in 100% ethanol, 15 min each) followed by two 15-min rinses with propylene oxide.
The pellet was infiltrated overnight with a 1:1 mixture of propylene oxide and epoxy resin (containing 2 % DMP-30 as accelerator) in a desiccator containing Drierite® desiccant; specimen vials were left uncapped. The next day, the pellet was given two 4-hour changes in epoxy resin (2% DMP-30). For embedment of the pellet in a Beem™ embedding capsule, epoxy resin (2% DMP-30) was also used. Polymerization of the resin was conducted at 60˚C for 3 days. The Beem™ capsule was removed using a Beem™ capsule press. Semi- and ultra-thin sections (500 and 90 nm, respectively) were cut using a Leica Ultracut Ultramicrotome. Semi-thin sections were stained using 1% toluidine blue in 1% borate to locate areas with densest concentrations of well-preserved capillaries by light microscopy. Ultra-thin sections were placed on 150-mesh Formvar®/carbon-coated copper grids and stained with 5% uranyl acetate for 20 min at 60˚C and an additional 15 min at room temperature; numerous droplets of distilled water were used for rinsing. To further enhance contrast of the images, the grids were incubated for 15 min with Reynold's stain containing lead nitrate and sodium citrate followed by rinses with distilled water. Sections were examined in a FEI Tecnai™ G^2 12 electron microscope (operated at 80 kV) equipped with Mega View III Soft Imaging System software.

5.2.19 Statistics

F- and t-tests were performed using Microsoft® Excel 2002. Data are given as means ± SEM. Probability values (P) were calculated for $p < 0.05$ (*), $p < 0.01$ (**) and $p < 0.001$ (***) by use of the appropriate paired or unpaired t-test. Exponential efflux constants were obtained using non-linear regression and calculated using GraphPad Prism®, Version 4.00.

6 References

Abbott NJ, Hughes CC, Revest PA and Greenwood J (1992) Development and characterisation of a rat brain capillary endothelial culture: towards an in vitro blood-brain barrier. *J Cell Sci* **103 (Pt 1)**:23-37.

Achira M, Suzuki H, Ito K and Sugiyama Y (1999) Comparative studies to determine the selective inhibitors for P-glycoprotein and cytochrome P4503A4. *AAPS PharmSci* **1**:E18.

Adachi M, Reid G and Schuetz JD (2002) Therapeutic and biological importance of getting nucleotides out of cells: a case for the ABC transporters, MRP4 and 5. *Adv Drug Deliv Rev* **54**:1333-42.

Advani R, Fisher GA, Lum BL, Hausdorff J, Halsey J, Litchman M and Sikic BI (2001) A phase I trial of doxorubicin, paclitaxel, and valspodar (PSC 833), a modulator of multidrug resistance. *Clin Cancer Res* **7**:1221-9.

Allikmets R, Schriml LM, Hutchinson A, Romano-Spica V and Dean M (1998) A human placenta-specific ATP-binding cassette gene (ABCP) on chromosome 4q22 that is involved in multidrug resistance. *Cancer Res* **58**:5337-9.

Anderson JM (2001) Molecular structure of tight junctions and their role in epithelial transport. *News Physiol Sci* **16**:126-30.

Anderson RG (1998) The caveolae membrane system. *Annu Rev Biochem* **67**:199-225.

Aranda A and Pascual A (2001) Nuclear hormone receptors and gene expression. *Physiol Rev* **81**:1269-304.

Audus KL, Bartel RL, Hidalgo IJ and Borchardt RT (1990) The use of cultured epithelial and endothelial cells for drug transport and metabolism studies. *Pharm Res* **7**:435-51.

Avendano C and Menendez JC (2002) Inhibitors of multidrug resistance to antitumor agents (MDR). *Curr Med Chem* **9**:159-93.

Azzi A, Boscoboinik D and Hensey C (1992) The protein kinase C family. *Eur J Biochem* **208**:547-57.

Baas F and Borst P (1988) The tissue dependent expression of hamster P-glycoprotein genes. *FEBS Lett* **229**:329-32.

Bacic F, Uematsu S, McCarron RM and Spatz M (1992) Secretion of immunoreactive endothelin-1 by capillary and microvascular endothelium of human brain. *Neurochem Res* **17**:699-702.

Balda MS and Matter K (2000) Transmembrane proteins of tight junctions. *Semin Cell Dev Biol* **11**:281-9.

Banks WA (1999) Physiology and pathology of the blood-brain barrier: implications for microbial pathogenesis, drug delivery and neurodegenerative disorders. *J Neurovirol* **5**:538-55.

Bard SM, Bello SM, Hahn ME and Stegeman JJ (2002) Expression of P-glycoprotein in killifish (Fundulus heteroclitus) exposed to environmental xenobiotics. *Aquat Toxicol* **59**:237-51.

Barnes DM (2001) Expression of P-glycoprotein in the chicken. *Comp Biochem Physiol A Mol Integr Physiol* **130**:301-10.

Bauer B, Hartz AM, Fricker G and Miller DS (2004) Pregnane X receptor up-regulation of P-glycoprotein expression and transport function at the blood-brain barrier. *Mol Pharmacol* **66**:413-9.

Bauer B, Hartz AM, Fricker G and Miller DS (2005) Modulation of p-glycoprotein transport function at the blood-brain barrier. *Exp Biol Med (Maywood)* **230**:118-27.

Bauer B, Miller DS and Fricker G (2003) Compound profiling for P-glycoprotein at the blood-brain barrier using a microplate screening system. *Pharm Res* **20**:1170-6.

Bazzoni G and Dejana E (2004) Endothelial cell-to-cell junctions: molecular organization and role in vascular homeostasis. *Physiol Rev* **84**:869-901.

Beaulieu E, Demeule M, Ghitescu L and Beliveau R (1997) P-glycoprotein is strongly expressed in the luminal membranes of the endothelium of blood vessels in the brain. *Biochem J* **326 (Pt 2)**:539-44.

Begley DJ (2004a) ABC transporters and the blood-brain barrier. *Curr Pharm Des* **10**:1295-312.

Begley DJ (2004b) Delivery of therapeutic agents to the central nervous system: the problems and the possibilities. *Pharmacol Ther* **104**:29-45.

Begley DJ and Brightman MW (2003) Structural and functional aspects of the blood-brain barrier. *Prog Drug Res* **61**:39-78.

Belinsky MG, Bain LJ, Balsara BB, Testa JR and Kruh GD (1998) Characterization of MOAT-C and MOAT-D, new members of the MRP/cMOAT subfamily of transporter proteins. *J Natl Cancer Inst* **90**:1735-41.

Bertilsson G, Heidrich J, Svensson K, Asman M, Jendeberg L, Sydow-Backman M, Ohlsson R, Postlind H, Blomquist P and Berkenstam A (1998) Identification of a human nuclear receptor defines a new signaling pathway for CYP3A induction. *Proc Natl Acad Sci U S A* **95**:12208-13.

Betz AL (1986) Transport of ions across the blood-brain barrier. *Fed Proc* **45**:2050-4.

Betz AL, Firth JA and Goldstein GW (1980) Polarity of the blood-brain barrier: distribution of enzymes between the luminal and antiluminal membranes of brain capillary endothelial cells. *Brain Res* **192**:17-28.

Betz AL and Goldstein GW (1986) Specialized properties and solute transport in brain capillaries. *Annu Rev Physiol* **48**:241-50.

Biedler JL and Riehm H (1970) Cellular resistance to actinomycin D in Chinese hamster cells in vitro: cross-resistance, radioautographic, and cytogenetic studies. *Cancer Res* **30**:1174-84.

Biegel D, Spencer DD and Pachter JS (1995) Isolation and culture of human brain microvessel endothelial cells for the study of blood-brain barrier properties in vitro. *Brain Res* **692**:183-9.

Blumberg B, Sabbagh W, Jr., Juguilon H, Bolado J, Jr., van Meter CM, Ong ES and Evans RM (1998) SXR, a novel steroid and xenobiotic-sensing nuclear receptor. *Genes Dev* **12**:3195-205.

Boado RJ and Pardridge WM (1990) The brain-type glucose transporter mRNA is specifically expressed at the blood-brain barrier. *Biochem Biophys Res Commun* **166**:174-9.

Bodor M, Kelly EJ and Ho RJ (2004) Characterization of the Human MDR1 Gene. *The AAPS Journal 2004* **6**:1-5.

Bolz S, Farrell CL, Dietz K and Wolburg H (1996) Subcellular distribution of glucose transporter (GLUT-1) during development of the blood-brain barrier in rats. *Cell Tissue Res* **284**:355-65.

Bombardi C, Grandis A, Chiocchetti R, Lucchi ML, Callegari E and Bortolami R (2004) Membrane-transport systems in the fenestrated capillaries of the area postrema in rat and calf. *Anat Rec A Discov Mol Cell Evol Biol* **279**:664-70.

Bonfanti P, Colombo A and Camatini M (1998) Identification of a multixenobiotic resistance mechanism in Xenopus laevis embryos. *Chemosphere* **37**:2751-60.

Bosch I, Jackson GR, Jr., Croop JM and Cantiello HF (1996) Expression of Drosophila melanogaster P-glycoproteins is associated with ATP channel activity. *Am J Physiol* **271**:C1527-38.

Bradford MM (1976) A rapid and sensitive method for the quantitation of microgram quantities of protein utilizing the principle of protein-dye binding. *Anal Biochem* **72**:248-54.

Bremnes T, Paasche JD, Mehlum A, Sandberg C, Bremnes B and Attramadal H (2000) Regulation and intracellular trafficking pathways of the endothelin receptors. *J Biol Chem* **275**:17596-604.

Brightman MW and Reese TS (1969) Junctions between intimately apposed cell membranes in the vertebrate brain. *J Cell Biol* **40**:648-77.

Bruzzi I, Remuzzi G and Benigni A (1997) Endothelin: a mediator of renal disease progression. *J Nephrol* **10**:179-83.

Cardell LO, Uddman R and Edvinsson L (1994) Endothelins: a role in cerebrovascular disease? *Cephalalgia* **14**:259-65.

Castro AF, Horton JK, Vanoye CG and Altenberg GA (1999) Mechanism of inhibition of P-glycoprotein-mediated drug transport by protein kinase C blockers. *Biochem Pharmacol* **58**:1723-33.

Chambers TC, Chalikonda I and Eilon G (1990a) Correlation of protein kinase C translocation, P-glycoprotein phosphorylation and reduced drug accumulation in multidrug resistant human KB cells. *Biochem Biophys Res Commun* **169**:253-9.

Chambers TC, McAvoy EM, Jacobs JW and Eilon G (1990b) Protein kinase C phosphorylates P-glycoprotein in multidrug resistant human KB carcinoma cells. *J Biol Chem* **265**:7679-86.

Chambers TC, Zheng B and Kuo JF (1992) Regulation by phorbol ester and protein kinase C inhibitors, and by a protein phosphatase inhibitor (okadaic acid), of P-glycoprotein phosphorylation and relationship to drug accumulation in multidrug-resistant human KB cells. *Mol Pharmacol* **41**:1008-15.

Chan LM, Lowes S and Hirst BH (2004) The ABCs of drug transport in intestine and liver: efflux proteins limiting drug absorption and bioavailability. *Eur J Pharm Sci* **21**:25-51.

Chawla A, Repa JJ, Evans RM and Mangelsdorf DJ (2001) Nuclear receptors and lipid physiology: opening the X-files. *Science* **294**:1866-70.

Chen C and Klaassen CD (2004) Rat multidrug resistance protein 4 (Mrp4, Abcc4): molecular cloning, organ distribution, postnatal renal expression, and chemical inducibility. *Biochem Biophys Res Commun* **317**:46-53.

Chen C, Staudinger JL and Klaassen CD (2003) Nuclear receptor, pregname X receptor, is required for induction of UDP-glucuronosyltranferases in mouse liver by pregnenolone-16 alpha-carbonitrile. *Drug Metab Dispos* **31**:908-15.

Chen Y and Simon SM (2000) In situ biochemical demonstration that P-glycoprotein is a drug efflux pump with broad specificity. *J Cell Biol* **148**:863-70.

Chen ZS, Lee K and Kruh GD (2001) Transport of cyclic nucleotides and estradiol 17-beta-D-glucuronide by multidrug resistance protein 4. Resistance to 6-mercaptopurine and 6-thioguanine. *J Biol Chem* **276**:33747-54.

Chin JE, Soffir R, Noonan KE, Choi K and Roninson IB (1989) Structure and expression of the human MDR (P-glycoprotein) gene family. *Mol Cell Biol* **9**:3808-20.

Choi TB and Pardridge WM (1986) Phenylalanine transport at the human blood-brain barrier. Studies with isolated human brain capillaries. *J Biol Chem* **261**:6536-41.

Ciechanover A (1998) The ubiquitin-proteasome pathway: on protein death and cell life. *Embo J* **17**:7151-60.

Ciechanover A, Heller H, Elias S, Haas AL and Hershko A (1980) ATP-dependent conjugation of reticulocyte proteins with the polypeptide required for protein degradation. *Proc Natl Acad Sci U S A* **77**:1365-8.

Cisternino S, Mercier C, Bourasset F, Roux F and Scherrmann JM (2004) Expression, up-regulation, and transport activity of the multidrug-resistance protein Abcg2 at the mouse blood-brain barrier. *Cancer Res* **64**:3296-301.

Cisternino S, Rousselle C, Lorico A, Rappa G and Scherrmann JM (2003) Apparent lack of Mrp1-mediated efflux at the luminal side of mouse blood-brain barrier endothelial cells. *Pharm Res* **20**:904-9.

Clavell AL and Burnett JC, Jr. (1994) Physiologic and pathophysiologic roles of endothelin in the kidney. *Curr Opin Nephrol Hypertens* **3**:66-72.

Cole SP, Bhardwaj G, Gerlach JH, Mackie JE, Grant CE, Almquist KC, Stewart AJ, Kurz EU, Duncan AM and Deeley RG (1992) Overexpression of a transporter gene in a multidrug-resistant human lung cancer cell line. *Science* **258**:1650-4.

Cooray HC, Blackmore CG, Maskell L and Barrand MA (2002) Localisation of breast cancer resistance protein in microvessel endothelium of human brain. *Neuroreport* **13**:2059-63.

Cordon-Cardo C, O'Brien JP, Boccia J, Casals D, Bertino JR and Melamed MR (1990) Expression of the multidrug resistance gene product (P-glycoprotein) in human normal and tumor tissues. *J Histochem Cytochem* **38**:1277-87.

Cordon-Cardo C, O'Brien JP, Casals D, Rittman-Grauer L, Biedler JL, Melamed MR and Bertino JR (1989) Multidrug-resistance gene (P-glycoprotein) is expressed by endothelial cells at blood-brain barrier sites. *Proc Natl Acad Sci U S A* **86**:695-8.

Dallaire L, Tremblay L and Beliveau R (1991) Purification and characterization of metabolically active capillaries of the blood-brain barrier. *Biochem J* **276 (Pt 3)**:745-52.

Dallas S, Schlichter L and Bendayan R (2004) Multidrug resistance protein (MRP) 4- and MRP 5-mediated efflux of 9-(2-phosphonylmethoxyethyl)adenine by microglia. *J Pharmacol Exp Ther* **309**:1221-9.

Dallas S, Zhu X, Baruchel S, Schlichter L and Bendayan R (2003) Functional expression of the multidrug resistance protein 1 in microglia. *J Pharmacol Exp Ther* **307**:282-90.

Dano K (1973) Active outward transport of daunomycin in resistant Ehrlich ascites tumor cells. *Biochim Biophys Acta* **323**:466-83.

Demeule M, Jodoin J, Beaulieu E, Brossard M and Beliveau R (1999) Dexamethasone modulation of multidrug transporters in normal tissues. *FEBS Lett* **442**:208-14.

Dermietzel R and Krause D (1991) Molecular anatomy of the blood-brain barrier as defined by immunocytochemistry. *Int Rev Cytol* **127**:57-109.

Dey S, Patel J, Anand BS, Jain-Vakkalagadda B, Kaliki P, Pal D, Ganapathy V and Mitra AK (2003) Molecular evidence and functional expression of P-glycoprotein (MDR1) in human and rabbit cornea and corneal epithelial cell lines. *Invest Ophthalmol Vis Sci* **44**:2909-18.

Didier N, Banks WA, Creminon C, Dereuddre-Bosquet N and Mabondzo A (2002) HIV-1-induced production of endothelin-1 in an in vitro model of the human blood-brain barrier. *Neuroreport* **13**:1179-83.

Drewes LR (1999) What is the blood-brain barrier? A molecular perspective. Cerebral vascular biology. *Adv Exp Med Biol* **474**:111-22.

Durieu-Trautmann O, Federici C, Creminon C, Foignant-Chaverot N, Roux F, Claire M, Strosberg AD and Couraud PO (1993) Nitric oxide and endothelin secretion by brain microvessel endothelial cells: regulation by cyclic nucleotides. *J Cell Physiol* **155**:104-11.

Dussault I and Forman BM (2002) The nuclear receptor PXR: a master regulator of "homeland" defense. *Crit Rev Eukaryot Gene Expr* **12**:53-64.

Egidy G, Eberl LP, Valdenaire O, Irmler M, Majdi R, Diserens AC, Fontana A, Janzer RC, Pinet F and Juillerat-Jeanneret L (2000) The endothelin system in human glioblastoma. *Lab Invest* **80**:1681-9.

Ehrlich P (1885) Das Sauerstoff-Bedürfniss des Organismus. Eine farbenanalytische Studie. *Verlag von August Hischwald*:1-167.

Eisenblatter T and Galla HJ (2002) A new multidrug resistance protein at the blood-brain barrier. *Biochem Biophys Res Commun* **293**:1273-8.

Eloranta JJ and Kullak-Ublick GA (2005) Coordinate transcriptional regulation of bile acid homeostasis and drug metabolism. *Arch Biochem Biophys* **433**:397-412.

Erdlenbruch B, Alipour M, Fricker G, Miller DS, Kugler W, Eibl H and Lakomek M (2003) Alkylglycerol opening of the blood-brain barrier to small and large fluorescence markers in normal and C6 glioma-bearing rats and isolated rat brain capillaries. *Br J Pharmacol* **140**:1201-10.

Fannon SA, Vidaver RM and Marts SA (2001) An abridged history of sex steroid hormone receptor action. *J Appl Physiol* **91**:1854-9.

Farrell CL and Pardridge WM (1991) Blood-brain barrier glucose transporter is asymmetrically distributed on brain capillary endothelial lumenal and ablumenal membranes: an electron microscopic immunogold study. *Proc Natl Acad Sci U S A* **88**:5779-83.

Fellner S, Bauer B, Miller DS, Schaffrik M, Fankhanel M, Spruss T, Bernhardt G, Graeff C, Farber L, Gschaidmeier H, Buschauer A and Fricker G (2002) Transport of paclitaxel (Taxol) across the blood-brain barrier in vitro and in vivo. *J Clin Invest* **110**:1309-18.

Flens MJ, Zaman GJ, van der Valk P, Izquierdo MA, Schroeijers AB, Scheffer GL, van der Groep P, de Haas M, Meijer CJ and Scheper RJ (1996) Tissue distribution of the multidrug resistance protein. *Am J Pathol* **148**:1237-47.

Ford JM and Hait WN (1990) Pharmacology of drugs that alter multidrug resistance in cancer. *Pharmacol Rev* **42**:155-99.

Ford JM, Yang JM and Hait WN (1996) P-glycoprotein-mediated multidrug resistance: experimental and clinical strategies for its reversal. *Cancer Treat Res* **87**:3-38.

Fracasso PM, Westervelt P, Fears CL, Rosen DM, Zuhowski EG, Cazenave LA, Litchman M and Egorin MJ (2000) Phase I study of paclitaxel in combination with a multidrug resistance modulator, PSC 833 (Valspodar), in refractory malignancies. *J Clin Oncol* **18**:1124-34.

Fricker G, Nobmann S and Miller DS (2002) Permeability of porcine blood brain barrier to somatostatin analogues. *Br J Pharmacol* **135**:1308-14.

Fromm MF (2004) Importance of P-glycoprotein at blood-tissue barriers. *Trends Pharmacol Sci* **25**:423-9.

Furuse M, Fujita K, Hiiragi T, Fujimoto K and Tsukita S (1998) Claudin-1 and -2: novel integral membrane proteins localizing at tight junctions with no sequence similarity to occludin. *J Cell Biol* **141**:1539-50.

Furuse M, Hirase T, Itoh M, Nagafuchi A, Yonemura S and Tsukita S (1993) Occludin: a novel integral membrane protein localizing at tight junctions. *J Cell Biol* **123**:1777-88.

Gao B, Hagenbuch B, Kullak-Ublick GA, Benke D, Aguzzi A and Meier PJ (2000) Organic anion-transporting polypeptides mediate transport of opioid peptides across blood-brain barrier. *J Pharmacol Exp Ther* **294**:73-9.

Gao B, Stieger B, Noe B, Fritschy JM and Meier PJ (1999) Localization of the organic anion transporting polypeptide 2 (Oatp2) in capillary endothelium and choroid plexus epithelium of rat brain. *J Histochem Cytochem* **47**:1255-64.

Gao P and Shivers RR (2004) Correlation of the presence of blood-brain barrier tight junctions and expression of zonula occludens protein ZO-1 in vitro: a freeze-fracture and immunofluorescence study. *J Submicrosc Cytol Pathol* **36**:7-15.

Gatmaitan ZC, Nies AT and Arias IM (1997) Regulation and translocation of ATP-dependent apical membrane proteins in rat liver. *Am J Physiol* **272**:G1041-9.

Geick A, Eichelbaum M and Burk O (2001) Nuclear receptor response elements mediate induction of intestinal MDR1 by rifampin. *J Biol Chem* **276**:14581-7.

Germann UA, Chambers TC, Ambudkar SV, Pastan I and Gottesman MM (1995) Effects of phosphorylation of P-glycoprotein on multidrug resistance. *J Bioenerg Biomembr* **27**:53-61.

Glass CK (1994) Differential recognition of target genes by nuclear receptor monomers, dimers, and heterodimers. *Endocr Rev* **15**:391-407.

Goldmann EE (1909) Die äussere und innere Sekretion des gesunden und kranken Organismus im Lichte der "vitalen Färbung". *Beiträge zur klinischen Chirurgie* **64**:192-265.

Goldmann EE (1913) *Vitalfärbung am Zentralnervensystem. Beitrag zur Physio-Pathologie des Plexus Chorioideus und der Hirnhäute.* Verlag der königlichen Akademie der Wissenschaften, Berlin.

Goldstein GW and Betz AL (1983) Recent advances in understanding brain capillary function. *Ann Neurol* **14**:389-95.

Goldstein GW, Betz AL and Bowman PD (1984) Use of isolated brain capillaries and cultured endothelial cells to study the blood-brain barrier. *Fed Proc* **43**:191-5.

Goldstein GW, Wolinsky JS, Csejtey J and Diamond I (1975) Isolation of metabolically active capillaries from rat brain. *J Neurochem* **25**:715-7.

Goldstein MN, Slotnick IJ and Journey LJ (1960) In vitro studies with HeLa cell line sensitive and resistant to actinomycin D. *Ann N Y Acad Sci* **89**:474-83.

Grant GA, Abbott NJ and Janigro D (1998) Understanding the Physiology of the Blood-Brain Barrier: In Vitro Models. *News Physiol Sci* **13**:287-293.

Guo GL, Staudinger J, Ogura K and Klaassen CD (2002) Induction of rat organic anion transporting polypeptide 2 by pregnenolone-16 alpha-carbonitrile is via interaction with pregnane X receptor. *Molecular Pharmacology* **61**:832-839.

Handschin C and Meyer UA (2003) Induction of drug metabolism: the role of nuclear receptors. *Pharmacol Rev* **55**:649-73.

Hartley DP, Dai X, He YD, Carlini EJ, Wang B, Huskey SE, Ulrich RG, Rushmore TH, Evers R and Evans DC (2004) Activators of the rat pregnane X receptor differentially modulate hepatic and intestinal gene expression. *Mol Pharmacol* **65**:1159-71.

Hartz AM, Bauer B, Fricker G and Miller DS (2004) Rapid Regulation of P-Glycoprotein at the Blood-Brain Barrier by Endothelin-1. *Mol Pharmacol* **66**:387-394.

Henriksson G, Norlander T, Zheng X, Stierna P and Westrin KM (1997) Expression of P-glycoprotein 170 in nasal mucosa may be increased with topical steroids. *Am J Rhinol* **11**:317-21.

Hickey KA, Rubanyi G, Paul RJ and Highsmith RF (1985) Characterization of a coronary vasoconstrictor produced by cultured endothelial cells. *Am J Physiol* **248**:C550-6.

Highsmith RF (1998) *Endothelin - Molecular Biology, Physiology, and Pathology*. Humana Press.

Hocher B, Thone-Reineke C, Bauer C, Raschack M and Neumayer HH (1997) The paracrine endothelin system: pathophysiology and implications in clinical medicine. *Eur J Clin Chem Clin Biochem* **35**:175-89.

Hofmann J (2001) Modulation of protein kinase C in antitumor treatment. *Rev Physiol Biochem Pharmacol* **142**:1-96.

Honkakoski P, Sueyoshi T and Negishi M (2003) Drug-activated nuclear receptors CAR and PXR. *Ann Med* **35**:172-82.

Hori S, Ohtsuki S, Tachikawa M, Kimura N, Kondo T, Watanabe M, Nakashima E and Terasaki T (2004) Functional expression of rat ABCG2 on the luminal side of brain capillaries and its enhancement by astrocyte-derived soluble factor(s). *J Neurochem* **90**:526-36.

Howarth AG, Hughes MR and Stevenson BR (1992) Detection of the tight junction-associated protein ZO-1 in astrocytes and other nonepithelial cell types. *Am J Physiol* **262**:C461-9.

Hsu SI, Cohen D, Kirschner LS, Lothstein L, Hartstein M and Horwitz SB (1990) Structural analysis of the mouse mdr1a (P-glycoprotein) promoter reveals the basis for differential transcript heterogeneity in multidrug-resistant J774.2 cells. *Mol Cell Biol* **10**:3596-606.

Huber D, Balda MS and Matter K (2000) Occludin modulates transepithelial migration of neutrophils. *J Biol Chem* **275**:5773-8.

Huber JD, Egleton RD and Davis TP (2001) Molecular physiology and pathophysiology of tight junctions in the blood-brain barrier. *Trends Neurosci* **24**:719-25.

Hughes PM, Anthony DC, Ruddin M, Botham MS, Rankine EL, Sablone M, Baumann D, Mir AK and Perry VH (2003) Focal lesions in the rat central nervous system induced by endothelin-1. *J Neuropathol Exp Neurol* **62**:1276-86.

Idris I, Gray S and Donnelly R (2001) Protein kinase C activation: isozyme-specific effects on metabolism and cardiovascular complications in diabetes. *Diabetologia* **44**:659-73.

Jacobs MN, Dickins M and Lewis DF (2003) Homology modelling of the nuclear receptors: human oestrogen receptorbeta (hERbeta), the human pregnane-X-receptor (PXR), the Ah receptor (AhR) and the constitutive androstane receptor (CAR) ligand binding domains from the human oestrogen receptor alpha (hERalpha) crystal structure, and the human peroxisome proliferator activated receptor alpha (PPARalpha) ligand binding domain from the human PPARgamma crystal structure. *J Steroid Biochem Mol Biol* **84**:117-32.

Jedlitschky G, Tirschmann K, Lubenow LE, Nieuwenhuis HK, Akkerman JW, Greinacher A and Kroemer HK (2004) The nucleotide transporter MRP4 (ABCC4) is highly expressed in human platelets and present in dense granules, indicating a role in mediator storage. *Blood* **104**:3603-10.

Jette L and Beliveau R (1993) P-glycoprotein is strongly expressed in brain capillaries. *Adv Exp Med Biol* **331**:121-5.

Jette L, Tetu B and Beliveau R (1993) High levels of P-glycoprotein detected in isolated brain capillaries. *Biochim Biophys Acta* **1150**:147-54.

Jodoin J, Demeule M, Fenart L, Cecchelli R, Farmer S, Linton KJ, Higgins CF and Beliveau R (2003) P-glycoprotein in blood-brain barrier endothelial cells: interaction and oligomerization with caveolins. *J Neurochem* **87**:1010-23.

Johnstone RW, Ruefli AA and Smyth MJ (2000) Multiple physiological functions for multidrug transporter P-glycoprotein? *Trends Biochem Sci* **25**:1-6.

Jones PM and George AM (2000) Symmetry and structure in P-glycoprotein and ABC transporters what goes around comes around. *Eur J Biochem* **267**:5298-305.

Jones SA, Moore LB, Shenk JL, Wisely GB, Hamilton GA, McKee DD, Tomkinson NC, LeCluyse EL, Lambert MH, Willson TM, Kliewer SA and Moore JT (2000) The pregnane X receptor: a promiscuous xenobiotic receptor that has diverged during evolution. *Mol Endocrinol* **14**:27-39.

Jorajuria S, Dereuddre-Bosquet N, Naissant-Storck K, Dormont D and Clayette P (2004) Differential expression levels of MRP1, MRP4, and MRP5 in response to human immunodeficiency virus infection in human macrophages. *Antimicrob Agents Chemother* **48**:1889-91.

Juliano RL and Ling V (1976) A surface glycoprotein modulating drug permeability in Chinese hamster ovary cell mutants. *Biochim Biophys Acta* **455**:152-62.

Kast HR, Goodwin B, Tarr PT, Jones SA, Anisfeld AM, Stoltz CM, Tontonoz P, Kliewer S, Willson TM and Edwards PA (2002) Regulation of multidrug resistance-associated protein 2 (ABCC2) by the nuclear receptors pregnane X receptor, farnesoid X-activated receptor, and constitutive androstane receptor. *J Biol Chem* **277**:2908-15.

Kawai N, McCarron RM and Spatz M (1995a) Endothelins stimulate sodium uptake into rat brain capillary endothelial cells through endothelin A-like receptors. *Neurosci Lett* **190**:85-8.

Kawai N, Yamamoto T, Yamamoto H, McCarron RM and Spatz M (1995b) Endothelin 1 stimulates Na+,K(+)-ATPase and Na(+)-K(+)-Cl- cotransport through ETA receptors and protein kinase C-dependent pathway in cerebral capillary endothelium. *J Neurochem* **65**:1588-96.

Kedzierski RM and Yanagisawa M (2001) Endothelin system: the double-edged sword in health and disease. *Annu Rev Pharmacol Toxicol* **41**:851-76.

Kemper EM, Cleypool C, Boogerd W, Beijnen JH and Van Tellingen O (2004a) The influence of the P-glycoprotein inhibitor zosuquidar trihydrochloride (LY335979) on the brain penetration of paclitaxel in mice. *Cancer Chemother Pharmacol* **53**:173-8.

Kemper EM, van Zandbergen AE, Cleypool C, Mos HA, Boogerd W, Beijnen JH and van Tellingen O (2003) Increased penetration of paclitaxel into the brain by inhibition of P-Glycoprotein. *Clin Cancer Res* **9**:2849-55.

Kemper EM, Verheij M, Boogerd W, Beijnen JH and van Tellingen O (2004b) Improved penetration of docetaxel into the brain by co-administration of inhibitors of P-glycoprotein. *Eur J Cancer* **40**:1269-74.

Kermani F and McGuire S (2002) The outlook for CNS drug development. *Chiltern International*.

Kipp H and Arias IM (2002) Trafficking of canalicular ABC transporters in hepatocytes. *Annu Rev Physiol* **64**:595-608.

Kipp H, Pichetshote N and Arias IM (2001) Transporters on demand: intrahepatic pools of canalicular ATP binding cassette transporters in rat liver. *J Biol Chem* **276**:7218-24.

Kliewer SA, Goodwin B and Willson TM (2002) The nuclear pregnane X receptor: a key regulator of xenobiotic metabolism. *Endocr Rev* **23**:687-702.

Kliewer SA, Lehmann JM and Willson TM (1999) Orphan nuclear receptors: shifting endocrinology into reverse. *Science* **284**:757-60.

Kliewer SA, Moore JT, Wade L, Staudinger JL, Watson MA, Jones SA, McKee DD, Oliver BB, Willson TM, Zetterstrom RH, Perlmann T and Lehmann JM (1998) An orphan nuclear receptor activated by pregnanes defines a novel steroid signaling pathway. *Cell* **92**:73-82.

Kniesel U and Wolburg H (2000) Tight junctions of the blood-brain barrier. *Cell Mol Neurobiol* **20**:57-76.

Kobari M, Fukuuchi Y, Tomita M, Tanahashi N, Konno S and Takeda H (1994) Dilatation of cerebral microvessels mediated by endothelin ETB receptor and nitric oxide in cats. *Neurosci Lett* **176**:157-60.

Kool M, de Haas M, Scheffer GL, Scheper RJ, van Eijk MJ, Juijn JA, Baas F and Borst P (1997) Analysis of expression of cMOAT (MRP2), MRP3, MRP4, and MRP5, homologues of the multidrug resistance-associated protein gene (MRP1), in human cancer cell lines. *Cancer Res* **57**:3537-47.

Krogh A (1946) The active and passive exchanges of inorganic ions through the surfaces of living cells and through living membranes generally. *Proceedings of the Royal Society of London* **133**:140-200.

Kroll RA and Neuwelt EA (1998) Outwitting the blood-brain barrier for therapeutic purposes: osmotic opening and other means. *Neurosurgery* **42**:1083-99; discussion 1099-100.

Kullak-Ublick GA and Becker MB (2003) Regulation of drug and bile salt transporters in liver and intestine. *Drug Metab Rev* **35**:305-17.

Kusuhara H, Suzuki H, Naito M, Tsuruo T and Sugiyama Y (1998) Characterization of efflux transport of organic anions in a mouse brain capillary endothelial cell line. *J Pharmacol Exp Ther* **285**:1260-5.

Kusunoki N, Takara K, Tanigawara Y, Yamauchi A, Ueda K, Komada F, Ku Y, Kuroda Y, Saitoh Y and Okumura K (1998) Inhibitory effects of a cyclosporin derivative, SDZ PSC 833, on transport of doxorubicin and vinblastine via human P-glycoprotein. *Jpn J Cancer Res* **89**:1220-8.

Labialle S, Dayan G, Gayet L, Rigal D, Gambrelle J and Baggetto LG (2004) New invMED1 element cis-activates human multidrug-related MDR1 and MVP genes, involving the LRP130 protein. *Nucleic Acids Res* **32**:3864-76.

Labialle S, Gayet L, Marthinet E, Rigal D and Baggetto LG (2002) Transcriptional regulators of the human multidrug resistance 1 gene: recent views. *Biochem Pharmacol* **64**:943-8.

Laemmli UK (1970) Cleavage of structural proteins during the assembly of the head of bacteriophage T4. *Nature* **227**:680-5.

Lazar MA (2002) *Mechanism of Action of Hormones That Act on Nuclear Receptors*. Saunders.

Lee G, Dallas S, Hong M and Bendayan R (2001a) Drug transporters in the central nervous system: brain barriers and brain parenchyma considerations. *Pharmacol Rev* **53**:569-96.

Lee G, Schlichter L, Bendayan M and Bendayan R (2001b) Functional expression of P-glycoprotein in rat brain microglia. *J Pharmacol Exp Ther* **299**:204-12.

Lee ME, de la Monte SM, Ng SC, Bloch KD and Quertermous T (1990) Expression of the potent vasoconstrictor endothelin in the human central nervous system. *J Clin Invest* **86**:141-7.

Lee YJ, Kusuhara H, Jonker JW, Schinkel AH and Sugiyama Y (2005) Investigation of efflux transport of dehydroepiandrosterone sulfate and mitoxantrone at the mouse blood-brain barrier: a minor role of breast cancer resistance protein. *J Pharmacol Exp Ther* **312**:44-52.

Leggas M, Adachi M, Scheffer GL, Sun D, Wielinga P, Du G, Mercer KE, Zhuang Y, Panetta JC, Johnston B, Scheper RJ, Stewart CF and Schuetz JD (2004) Mrp4 confers resistance to topotecan and protects the brain from chemotherapy. *Mol Cell Biol* **24**:7612-21.

Lehmann JM, McKee DD, Watson MA, Willson TM, Moore JT and Kliewer SA (1998) The human orphan nuclear receptor PXR is activated by compounds that regulate CYP3A4 gene expression and cause drug interactions. *J Clin Invest* **102**:1016-23.

Leonard GD, Polgar O and Bates SE (2002) ABC transporters and inhibitors: new targets, new agents. *Curr Opin Investig Drugs* **3**:1652-9.

Levin ER (1995) Endothelins. *N Engl J Med* **333**:356-63.

Lewandowsky M (1900) Zur Lehre von der Cerebrospinalflüssigkeit. *Zeitschrift für Klinische Medicin* **40**:480-494.

Lin JH and Yamazaki M (2003) Role of P-glycoprotein in pharmacokinetics: clinical implications. *Clin Pharmacokinet* **42**:59-98.

Lippoldt A, Kniesel U, Liebner S, Kalbacher H, Kirsch T, Wolburg H and Haller H (2000) Structural alterations of tight junctions are associated with loss of polarity in stroke-prone spontaneously hypertensive rat blood-brain barrier endothelial cells. *Brain Res* **885**:251-61.

Loo TW, Bartlett MC and Clarke DM (2003) Substrate-induced conformational changes in the transmembrane segments of human P-glycoprotein. Direct evidence for the substrate-induced fit mechanism for drug binding. *J Biol Chem* **278**:13603-6.

Loo TW and Clarke DM (1999) The transmembrane domains of the human multidrug resistance P-glycoprotein are sufficient to mediate drug binding and trafficking to the cell surface. *J Biol Chem* **274**:24759-65.

Luker GD, Nilsson KR, Covey DF and Piwnica-Worms D (1999) Multidrug resistance (MDR1) P-glycoprotein enhances esterification of plasma membrane cholesterol. *J Biol Chem* **274**:6979-91.

Maglich JM, Sluder A, Guan X, Shi Y, McKee DD, Carrick K, Kamdar K, Willson TM and Moore JT (2001) Comparison of complete nuclear receptor sets from the human, Caenorhabditis elegans and Drosophila genomes. *Genome Biol* **2**:RESEARCH0029.

Maliepaard M, Scheffer GL, Faneyte IF, van Gastelen MA, Pijnenborg AC, Schinkel AH, van De Vijver MJ, Scheper RJ and Schellens JH (2001) Subcellular localization and distribution of the breast cancer resistance protein transporter in normal human tissues. *Cancer Res* **61**:3458-64.

Mangelsdorf DJ, Thummel C, Beato M, Herrlich P, Schutz G, Umesono K, Blumberg B, Kastner P, Mark M, Chambon P and et al. (1995) The nuclear receptor superfamily: the second decade. *Cell* **83**:835-9.

Martin-Padura I, Lostaglio S, Schneemann M, Williams L, Romano M, Fruscella P, Panzeri C, Stoppacciaro A, Ruco L, Villa A, Simmons D and Dejana E (1998) Junctional adhesion molecule, a novel member of the immunoglobulin superfamily that distributes at intercellular junctions and modulates monocyte transmigration. *J Cell Biol* **142**:117-27.

Masereeuw R, Terlouw SA, van Aubel RA, Russel FG and Miller DS (2000) Endothelin B receptor-mediated regulation of ATP-driven drug secretion in renal proximal tubule. *Mol Pharmacol* **57**:59-67.

Matsuoka Y, Okazaki M, Kitamura Y and Taniguchi T (1999) Developmental expression of P-glycoprotein (multidrug resistance gene product) in the rat brain. *J Neurobiol* **39**:383-92.

Matter K and Balda MS (2003a) Holey barrier: claudins and the regulation of brain endothelial permeability. *J Cell Biol* **161**:459-60.

Matter K and Balda MS (2003b) Signalling to and from tight junctions. *Nat Rev Mol Cell Biol* **4**:225-36.

Mayer U, Wagenaar E, Dorobek B, Beijnen JH, Borst P and Schinkel AH (1997) Full blockade of intestinal P-glycoprotein and extensive inhibition of blood-brain barrier P-glycoprotein by oral treatment of mice with PSC833. *J Clin Invest* **100**:2430-6.

McRae MP, Brouwer KL and Kashuba AD (2003) Cytokine regulation of P-glycoprotein. *Drug Metab Rev* **35**:19-33.

Melaine N, Lienard MO, Dorval I, Le Goascogne C, Lejeune H and Jegou B (2002) Multidrug resistance genes and p-glycoprotein in the testis of the rat, mouse, Guinea pig, and human. *Biol Reprod* **67**:1699-707.

Miller DS (2002) Xenobiotic export pumps, endothelin signaling, and tubular nephrotoxicants--a case of molecular hijacking. *J Biochem Mol Toxicol* **16**:121-7.

Miller DS (2003) Confocal imaging of xenobiotic transport across the blood-brain barrier. *J Exp Zoolog Part A Comp Exp Biol* **300**:84-90.

Miller DS, Graeff C, Droulle L, Fricker S and Fricker G (2002a) Xenobiotic efflux pumps in isolated fish brain capillaries. *Am J Physiol Regul Integr Comp Physiol* **282**:R191-8.

Miller DS, Masereeuw R and Karnaky KJ, Jr. (2002b) Regulation of MRP2-mediated transport in shark rectal salt gland tubules. *Am J Physiol Regul Integr Comp Physiol* **282**:R774-81.

Miller DS, Nobmann SN, Gutmann H, Toeroek M, Drewe J and Fricker G (2000) Xenobiotic transport across isolated brain microvessels studied by confocal microscopy. *Mol Pharmacol* **58**:1357-67.

Miller DS, Sussman CR and Renfro JL (1998) Protein kinase C regulation of p-glycoprotein-mediated xenobiotic secretion in renal proximal tubule. *Am J Physiol* **275**:F785-95.

Miller RD, Monsul NT, Vender JR and Lehmann JC (1996) NMDA- and endothelin-1-induced increases in blood-brain barrier permeability quantitated with Lucifer yellow. *J Neurol Sci* **136**:37-40.

Minami M, Kimura M, Iwamoto N and Arai H (1995) Endothelin-1-like immunoreactivity in cerebral cortex of Alzheimer-type dementia. *Prog Neuropsychopharmacol Biol Psychiatry* **19**:509-13.

Moore LB, Goodwin B, Jones SA, Wisely GB, Serabjit-Singh CJ, Willson TM, Collins JL and Kliewer SA (2000a) St. John's wort induces hepatic drug metabolism through activation of the pregnane X receptor. *Proc Natl Acad Sci U S A* **97**:7500-2.

Moore LB, Parks DJ, Jones SA, Bledsoe RK, Consler TG, Stimmel JB, Goodwin B, Liddle C, Blanchard SG, Willson TM, Collins JL and Kliewer SA (2000b) Orphan nuclear receptors constitutive androstane receptor and pregnane X receptor share xenobiotic and steroid ligands. *J Biol Chem* **275**:15122-7.

Morita K, Sasaki H, Furuse M and Tsukita S (1999) Endothelial claudin: claudin-5/TMVCF constitutes tight junction strands in endothelial cells. *J Cell Biol* **147**:185-94.

Nag S (2003) Morphology and molecular properties of cellular components of normal cerebral vessels. *Methods Mol Med* **89**:3-36.

Nagy Z, Peters H and Huttner I (1984) Fracture faces of cell junctions in cerebral endothelium during normal and hyperosmotic conditions. *Lab Invest* **50**:313-22.

Narushima I, Kita T, Kubo K, Yonetani Y, Momochi C, Yoshikawa I, Ohno N and Nakashima T (2003) Highly enhanced permeability of blood-brain barrier induced by repeated administration of endothelin-1 in dogs and rats. *Pharmacol Toxicol* **92**:21-6.

Narushima I, Kita T, Kubo K, Yonetani Y, Momochi C, Yoshikawa I, Shimada K and Nakashima T (1999) Contribution of endothelin-1 to disruption of blood-brain barrier permeability in dogs. *Naunyn Schmiedebergs Arch Pharmacol* **360**:639-45.

Nie XJ and Olsson Y (1996) Endothelin peptides in brain diseases. *Rev Neurosci* **7**:177-86.

Nies AT, Jedlitschky G, Konig J, Herold-Mende C, Steiner HH, Schmitt HP and Keppler D (2004) Expression and immunolocalization of the multidrug resistance proteins, MRP1-MRP6 (ABCC1-ABCC6), in human brain. *Neuroscience* **129**:349-60.

Nitta T, Hata M, Gotoh S, Seo Y, Sasaki H, Hashimoto N, Furuse M and Tsukita S (2003) Size-selective loosening of the blood-brain barrier in claudin-5-deficient mice. *J Cell Biol* **161**:653-60.

Nobmann S, Bauer B and Fricker G (2001) Ivermectin excretion by isolated functionally intact brain endothelial capillaries. *Br J Pharmacol* **132**:722-8.

Notenboom S, Miller DS, Smits P, Russel FG and Masereeuw R (2002) Role of NO in endothelin-regulated drug transport in the renal proximal tubule. *Am J Physiol Renal Physiol* **282**:F458-64.

Offermanns (2004) *Encyclopedic Reference of Molecular Pharmacology*.

Ogawa Y, Nakao K, Arai H, Nakagawa O, Hosoda K, Suga S, Nakanishi S and Imura H (1991) Molecular cloning of a non-isopeptide-selective human endothelin receptor. *Biochem Biophys Res Commun* **178**:248-55.

Ohtsuki S, Asaba H, Takanaga H, Deguchi T, Hosoya K, Otagiri M and Terasaki T (2002) Role of blood-brain barrier organic anion transporter 3 (OAT3) in the efflux of indoxyl sulfate, a uremic toxin: its involvement in neurotransmitter metabolite clearance from the brain. *J Neurochem* **83**:57-66.

Okamoto T, Schlegel A, Scherer PE and Lisanti MP (1998) Caveolins, a family of scaffolding proteins for organizing "preassembled signaling complexes" at the plasma membrane. *J Biol Chem* **273**:5419-22.

Omidi Y, Campbell L, Barar J, Connell D, Akhtar S and Gumbleton M (2003) Evaluation of the immortalised mouse brain capillary endothelial cell line, b.End3, as an in vitro blood-brain barrier model for drug uptake and transport studies. *Brain Res* **990**:95-112.

Orte C, Lawrenson JG, Finn TM, Reid AR and Allt G (1999) A comparison of blood-brain barrier and blood-nerve barrier endothelial cell markers. *Anat Embryol (Berl)* **199**:509-17.

Palade G (1953) Fine structure of blood capillaries. *Journal of Applied Physics* **24**:1424.

Pardridge WM (1998) *Introduction to the Blood-Brain Barrier. Methodology, Biology and Pathology*. Cambridge University Press, Cambridge; UK.

Pardridge WM (2001) BBB-Genomics: creating new openings for brain-drug targeting. *Drug Discov Today* **6**:381-383.

Pardridge WM (2002) Why is the global CNS pharmaceutical market so under-penetrated? *Drug Discov Today* **7**:5-7.

Pardridge WM (2003a) Blood-brain barrier drug targeting: the future of brain drug development. *Mol Interv* **3**:90-105, 51.

Pardridge WM (2003b) Blood-brain barrier genomics and the use of endogenous transporters to cause drug penetration into the brain. *Curr Opin Drug Discov Devel* **6**:683-91.

Pardridge WM, Boado RJ and Farrell CR (1990a) Brain-type glucose transporter (GLUT-1) is selectively localized to the blood-brain barrier. Studies with quantitative western blotting and in situ hybridization. *J Biol Chem* **265**:18035-40.

Pardridge WM, Eisenberg J and Yamada T (1985) Rapid sequestration and degradation of somatostatin analogues by isolated brain microvessels. *J Neurochem* **44**:1178-84.

Pardridge WM, Golden PL, Kang YS and Bickel U (1997) Brain microvascular and astrocyte localization of P-glycoprotein. *J Neurochem* **68**:1278-85.

Pardridge WM, Triguero D, Yang J and Cancilla PA (1990b) Comparison of in vitro and in vivo models of drug transcytosis through the blood-brain barrier. *J Pharmacol Exp Ther* **253**:884-91.

Pascussi JM, Drocourt L, Gerbal-Chaloin S, Fabre JM, Maurel P and Vilarem MJ (2001) Dual effect of dexamethasone on CYP3A4 gene expression in human hepatocytes. Sequential role of glucocorticoid receptor and pregnane X receptor. *Eur J Biochem* **268**:6346-58.

Peters A, Schweiger U, Pellerin L, Hubold C, Oltmanns KM, Conrad M, Schultes B, Born J and Fehm HL (2004) The selfish brain: competition for energy resources. *Neurosci Biobehav Rev* **28**:143-80.

Pleban K and Ecker GF (2005) Inhibitors of p-glycoprotein--lead identification and optimisation. *Mini Rev Med Chem* **5**:153-63.

Potschka H, Fedrowitz M and Loscher W (2003) Multidrug resistance protein MRP2 contributes to blood-brain barrier function and restricts antiepileptic drug activity. *J Pharmacol Exp Ther* **306**:124-31.

Rang HP (1999) *Pharmacology*. Churchill Livingstone.

Rao VV, Dahlheimer JL, Bardgett ME, Snyder AZ, Finch RA, Sartorelli AC and Piwnica-Worms D (1999) Choroid plexus epithelial expression of MDR1 P glycoprotein and multidrug resistance-associated protein contribute to the blood-cerebrospinal-fluid drug-permeability barrier. *Proc Natl Acad Sci U S A* **96**:3900-5.

Reese TS and Karnovsky MJ (1967) Fine structural localization of a blood-brain barrier to exogenous peroxidase. *J Cell Biol* **34**:207-17.

Regina A, Koman A, Piciotti M, El Hafny B, Center MS, Bergmann R, Couraud PO and Roux F (1998) Mrp1 multidrug resistance-associated protein and P-glycoprotein expression in rat brain microvessel endothelial cells. *J Neurochem* **71**:705-15.

Renes J, de Vries EG, Jansen PL and Muller M (2000) The (patho)physiological functions of the MRP family. *Drug Resist Updat* **3**:289-302.

Richaud-Patin Y, Soto-Vega E, Jakez-Ocampo J and Llorente L (2004) P-glycoprotein in autoimmune diseases. *Autoimmun Rev* **3**:188-92.

Risau W and Wolburg H (1990) Development of the blood-brain barrier. *Trends Neurosci* **13**:174-8.

Rodriguez-Baeza A, Reina-de la Torre F, Poca A, Marti M and Garnacho A (2003) Morphological features in human cortical brain microvessels after head injury: a three-dimensional and immunocytochemical study. *Anat Rec A Discov Mol Cell Evol Biol* **273**:583-93.

Rosenberg MF, Callaghan R, Ford RC and Higgins CF (1997) Structure of the multidrug resistance P-glycoprotein to 2.5 nm resolution determined by electron microscopy and image analysis. *J Biol Chem* **272**:10685-94.

Rosenfeld JM, Vargas R, Jr., Xie W and Evans RM (2003) Genetic profiling defines the xenobiotic gene network controlled by the nuclear receptor pregnane X receptor. *Mol Endocrinol* **17**:1268-82.

Rubanyi GM and Polokoff MA (1994) Endothelins: molecular biology, biochemistry, pharmacology, physiology, and pathophysiology. *Pharmacol Rev* **46**:325-415.

Sachs CW, Chambers TC and Fine RL (1999) Differential phosphorylation of sites in the linker region of P-glycoprotein by protein kinase C isozymes alpha, betaI, betaII, gamma, delta, epsilon, eta, and zeta. *Biochem Pharmacol* **58**:1587-92.

Saeki T, Ueda K, Tanigawara Y, Hori R and Komano T (1993) Human P-glycoprotein transports cyclosporin A and FK506. *J Biol Chem* **268**:6077-80.

Sai Y, Nies AT and Arias IM (1999) Bile acid secretion and direct targeting of mdr1-green fluorescent protein from Golgi to the canalicular membrane in polarized WIF-B cells. *J Cell Sci* **112 (Pt 24)**:4535-45.

Saikotos (1969) Isolation of highly purified human and bovine brain endothelial calls and nuclei and theri phospholipid composition. *Lipids* **4**:234-42.

Salphati L and Benet LZ (1998) Modulation of P-glycoprotein expression by cytochrome P450 3A inducers in male and female rat livers. *Biochem Pharmacol* **55**:387-95.

Sarkadi B, Ozvegy-Laczka C, Nemet K and Varadi A (2004) ABCG2 -- a transporter for all seasons. *FEBS Lett* **567**:116-20.

Schinkel AH (1999) P-Glycoprotein, a gatekeeper in the blood-brain barrier. *Adv Drug Deliv Rev* **36**:179-194.

Schinkel AH (2001) The roles of P-glycoprotein and MRP1 in the blood-brain and blood-cerebrospinal fluid barriers. *Adv Exp Med Biol* **500**:365-72.

Schinkel AH, Wagenaar E, Mol CA and van Deemter L (1996) P-glycoprotein in the blood-brain barrier of mice influences the brain penetration and pharmacological activity of many drugs. *J Clin Invest* **97**:2517-24.

Schlachetzki F and Pardridge WM (2003) P-glycoprotein and caveolin-1alpha in endothelium and astrocytes of primate brain. *Neuroreport* **14**:2041-6.

Schmuth M (2003) Beyond glucocorticoids, retinoids and vitamin D - the evolution of nuclear hormone type transcription factor targeting in the skin. *JDDG*:352-362.

Schramm U, Fricker G, Wenger R and Miller DS (1995) P-glycoprotein-mediated secretion of a fluorescent cyclosporin analogue by teleost renal proximal tubules. *Am J Physiol* **268**:F46-52.

Schuetz E and Strom S (2001) Promiscuous regulator of xenobiotic removal. *Nat Med* **7**:536-7.

Sharom FJ (1997) The P-glycoprotein efflux pump: how does it transport drugs? *J Membr Biol* **160**:161-75.

Shirai A, Naito M, Tatsuta T, Dong J, Hanaoka K, Mikami K, Oh-hara T and Tsuruo T (1994) Transport of cyclosporin A across the brain capillary endothelial cell monolayer by P-glycoprotein. *Biochim Biophys Acta* **1222**:400-4.

Shivers RR, Betz AL and Goldstein GW (1984) Isolated rat brain capillaries possess intact, structurally complex, interendothelial tight junctions; freeze-fracture verification of tight junction integrity. *Brain Res* **324**:313-22.

Siakotos (1969) Isolation of highly purified human and bovine brain endothelial cells and nuclei and their phospholipid composition. *Lipids* **4**:234-42.

Smit JJ, Schinkel AH, Oude Elferink RP, Groen AK, Wagenaar E, van Deemter L, Mol CA, Ottenhoff R, van der Lugt NM, van Roon MA and et al. (1993) Homozygous disruption of the murine mdr2 P-glycoprotein gene leads to a complete absence of phospholipid from bile and to liver disease. *Cell* **75**:451-62.

Sonoda J, Rosenfeld JM, Xu L, Evans RM and Xie W (2003) A nuclear receptor-mediated xenobiotic response and its implication in drug metabolism and host protection. *Current Drug Metabolism* **4**:59-72.

Spatz H (1933) Die Bedeutung der vitalen Färbung für die Lehre vom Stoffaustausch zwischen dem Zentralnervensystem und dem übrigen Körper. *Archiv für Phsychiatrie* **101**:267-358.

Speciale L, Sarasella M, Ruzzante S, Caputo D, Mancuso R, Calvo MG, Guerini FR and Ferrante P (2000) Endothelin and nitric oxide levels in cerebrospinal fluid of patients with multiple sclerosis. *J Neurovirol* **6 Suppl 2**:S62-6.

Staddon JM, Herrenknecht K, Schulze C, Smales C and Rubin LL (1995) Signal transduction at the blood-brain barrier. *Biochem Soc Trans* **23**:475-9.

Stanimirovic DB, Yamamoto T, Uematsu S and Spatz M (1994) Endothelin-1 receptor binding and cellular signal transduction in cultured human brain endothelial cells. *J Neurochem* **62**:592-601.

Stevenson BR, Siliciano JD, Mooseker MS and Goodenough DA (1986) Identification of ZO-1: a high molecular weight polypeptide associated with the tight junction (zonula occludens) in a variety of epithelia. *J Cell Biol* **103**:755-66.

Stewart PA, Beliveau R and Rogers KA (1996) Cellular localization of P-glycoprotein in brain versus gonadal capillaries. *J Histochem Cytochem* **44**:679-85.

Stewart PA, Hayakawa K and Farrell CL (1994) Quantitation of blood-brain barrier ultrastructure. *Microsc Res Tech* **27**:516-27.

Sugawara I (1990) Expression and functions of P-glycoprotein (mdr1 gene product) in normal and malignant tissues. *Acta Pathol Jpn* **40**:545-53.

Sugawara I, Kataoka I, Morishita Y, Hamada H, Tsuruo T, Itoyama S and Mori S (1988) Tissue distribution of P-glycoprotein encoded by a multidrug-resistant gene as revealed by a monoclonal antibody, MRK 16. *Cancer Res* **48**:1926-9.

Sugiyama D, Kusuhara H, Lee YJ and Sugiyama Y (2003a) Involvement of multidrug resistance associated protein 1 (Mrp1) in the efflux transport of 17beta estradiol-D-17beta-glucuronide (E217betaG) across the blood-brain barrier. *Pharm Res* **20**:1394-400.

Sugiyama D, Kusuhara H, Taniguchi H, Ishikawa S, Nozaki Y, Aburatani H and Sugiyama Y (2003b) Functional characterization of rat brain-specific organic anion transporter (Oatp14) at the blood-brain barrier: high affinity transporter for thyroxine. *J Biol Chem* **278**:43489-95.

Synold TW, Dussault I and Forman BM (2001) The orphan nuclear receptor SXR coordinately regulates drug metabolism and efflux. *Nat Med* **7**:584-90.

Taipalensuu J, Tornblom H, Lindberg G, Einarsson C, Sjoqvist F, Melhus H, Garberg P, Sjostrom B, Lundgren B and Artursson P (2001) Correlation of gene expression of ten drug efflux proteins of the ATP-binding cassette transporter family in normal human jejunum and in human intestinal epithelial Caco-2 cell monolayers. *J Pharmacol Exp Ther* **299**:164-70.

Tan B, Piwnica-Worms D and Ratner L (2000) Multidrug resistance transporters and modulation. *Curr Opin Oncol* **12**:450-8.

Tanaka Y, Abe Y, Tsugu A, Takamiya Y, Akatsuka A, Tsuruo T, Yamazaki H, Ueyama Y, Sato O, Tamaoki N and et al. (1994) Ultrastructural localization of P-glycoprotein on capillary endothelial cells in human gliomas. *Virchows Arch* **425**:133-8.

Teng S, Jekerle V and Piquette-Miller M (2003) Induction of ABCC3 (MRP3) by pregnane X receptor activators. *Drug Metab Dispos* **31**:1296-9.

Terlouw SA, Masereeuw R, Russel FG and Miller DS (2001) Nephrotoxicants induce endothelin release and signaling in renal proximal tubules: effect on drug efflux. *Mol Pharmacol* **59**:1433-40.

Thiebaut F, Tsuruo T, Hamada H, Gottesman MM, Pastan I and Willingham MC (1987) Cellular localization of the multidrug-resistance gene product P-glycoprotein in normal human tissues. *Proc Natl Acad Sci U S A* **84**:7735-8.

Thiebaut F, Tsuruo T, Hamada H, Gottesman MM, Pastan I and Willingham MC (1989) Immunohistochemical localization in normal tissues of different epitopes in the multidrug transport protein P170: evidence for localization in brain capillaries and crossreactivity of one antibody with a muscle protein. *J Histochem Cytochem* **37**:159-64.

Tirona RG, Leake BF, Podust LM and Kim RB (2004) Identification of amino acids in rat pregnane X receptor that determine species-specific activation. *Mol Pharmacol* **65**:36-44.

Tohyama K, Kusuhara H and Sugiyama Y (2004) Involvement of multispecific organic anion transporter, Oatp14 (Slc21a14), in the transport of thyroxine across the blood-brain barrier. *Endocrinology* **145**:4384-91.

Tsai CE, Daood MJ, Lane RH, Hansen TW, Gruetzmacher EM and Watchko JF (2002) P-glycoprotein expression in mouse brain increases with maturation. *Biol Neonate* **81**:58-64.

Tsuji A, Terasaki T, Takabatake Y, Tenda Y, Tamai I, Yamashima T, Moritani S, Tsuruo T and Yamashita J (1992) P-glycoprotein as the drug efflux pump in primary cultured bovine brain capillary endothelial cells. *Life Sci* **51**:1427-37.

Tsuruo T, Iida H, Tsukagoshi S and Sakurai Y (1981) Overcoming of vincristine resistance in P388 leukemia in vivo and in vitro through enhanced cytotoxicity of vincristine and vinblastine by verapamil. *Cancer Res* **41**:1967-72.

Turksen K and Troy TC (2004) Barriers built on claudins. *J Cell Sci* **117**:2435-47.

Twentyman PR (1992) Cyclosporins as drug resistance modifiers. *Biochem Pharmacol* **43**:109-17.

U.S. Department of Health EaW (1985) NIH Guide for the Use and Care of Laboratory Animals, NIH Publication No. 85-23. *http://www.nyu.edu/uawc/Forms/Guide-excerpts.pdf*.

Ueda K, Cornwell MM, Gottesman MM, Pastan I, Roninson IB, Ling V and Riordan JR (1986) The mdr1 gene, responsible for multidrug-resistance, codes for P-glycoprotein. *Biochem Biophys Res Commun* **141**:956-62.

Uematsu T, Yamaoka M, Matsuura T, Doto R, Hotomi H, Yamada A, Hasumi-Nakayama Y and Kayamoto D (2001) P-glycoprotein expression in human major and minor salivary glands. *Arch Oral Biol* **46**:521-7.

Valverde MA, Diaz M, Sepulveda FV, Gill DR, Hyde SC and Higgins CF (1992) Volume-regulated chloride channels associated with the human multidrug-resistance P-glycoprotein. *Nature* **355**:830-3.

van Aubel RA, Smeets PH, Peters JG, Bindels RJ and Russel FG (2002) The MRP4/ABCC4 gene encodes a novel apical organic anion transporter in human kidney proximal tubules: putative efflux pump for urinary cAMP and cGMP. *J Am Soc Nephrol* **13**:595-603.

van der Bliek AM, Kooiman PM, Schneider C and Borst P (1988) Sequence of mdr3 cDNA encoding a human P-glycoprotein. *Gene* **71**:401-11.

van Zuylen L, Sparreboom A, van der Gaast A, van der Burg ME, van Beurden V, Bol CJ, Woestenborghs R, Palmer PA and Verweij J (2000) The orally administered P-glycoprotein inhibitor R101933 does not alter the plasma pharmacokinetics of docetaxel. *Clin Cancer Res* **6**:1365-71.

Virgintino D, Errede M, Robertson D, Capobianco C, Girolamo F, Vimercati A, Bertossi M and Roncali L (2004) Immunolocalization of tight junction proteins in the adult and developing human brain. *Histochem Cell Biol* **122**:51-9.

Vorbrodt AW and Dobrogowska DH (2003) Molecular anatomy of intercellular junctions in brain endothelial and epithelial barriers: electron microscopist's view. *Brain Res Brain Res Rev* **42**:221-42.

Vorbrodt AW and Dobrogowska DH (2004) Molecular anatomy of interendothelial junctions in human blood-brain barrier microvessels. *Folia Histochem Cytobiol* **42**:67-75.

Wakayama K, Ohtsuki S, Takanaga H, Hosoya K and Terasaki T (2002) Localization of norepinephrine and serotonin transporter in mouse brain capillary endothelial cells. *Neurosci Res* **44**:173-80.

Walker J, Martin C and Callaghan R (2004) Inhibition of P-glycoprotein function by XR9576 in a solid tumour model can restore anticancer drug efficacy. *Eur J Cancer* **40**:594-605.

Watanabe T, Tsuge H, Oh-Hara T, Naito M and Tsuruo T (1995) Comparative study on reversal efficacy of SDZ PSC 833, cyclosporin A and verapamil on multidrug resistance in vitro and in vivo. *Acta Oncol* **34**:235-41.

Watkins RE, Davis-Searles PR, Lambert MH and Redinbo MR (2003a) Coactivator binding promotes the specific interaction between ligand and the pregnane X receptor. *J Mol Biol* **331**:815-28.

Watkins RE, Maglich JM, Moore LB, Wisely GB, Noble SM, Davis-Searles PR, Lambert MH, Kliewer SA and Redinbo MR (2003b) 2.1 A crystal structure of human PXR in complex with the St. John's wort compound hyperforin. *Biochemistry* **42**:1430-8.

Watkins RE, Noble SM and Redinbo MR (2002) Structural insights into the promiscuity and function of the human pregnane X receptor. *Curr Opin Drug Discov Devel* **5**:150-8.

Watkins RE, Wisely GB, Moore LB, Collins JL, Lambert MH, Williams SP, Willson TM, Kliewer SA and Redinbo MR (2001) The human nuclear xenobiotic receptor PXR: structural determinants of directed promiscuity. *Science* **292**:2329-33.

Webb DJ (1997) Endothelin: from molecule to man. *Br J Clin Pharmacol* **44**:9-20.

Wentworth JM, Agostini M, Love J, Schwabe JW and Chatterjee VK (2000) St John's wort, a herbal antidepressant, activates the steroid X receptor. *J Endocrinol* **166**:R11-6.

WHO (2001) Mental Health: New Understanding, New Hope. *The Wold Health Report*.

Wijnholds J (2002) Drug resistance caused by multidrug resistance-associated proteins. *Novartis Found Symp* **243**:69-79; discussion 80-2, 180-5.

Willette RNF, G.Z.; Barone, F.C. (1995) Endothelin Receptors: From the Gene to the Human, in *Endothelin in the Central Nervous System* pp 187-206.

Wolburg H and Lippoldt A (2002) Tight junctions of the blood-brain barrier: development, composition and regulation. *Vascul Pharmacol* **38**:323-37.

Xie W, Uppal H, Saini SP, Mu Y, Little JM, Radominska-Pandya A and Zemaitis MA (2004) Orphan nuclear receptor-mediated xenobiotic regulation in drug metabolism. *Drug Discov Today* **9**:442-9.

Yakubu MA and Leffler CW (1999) Regulation of ET-1 biosynthesis in cerebral microvascular endothelial cells by vasoactive agents and PKC. *Am J Physiol* **276**:C300-5.

Yanagisawa M, Inoue A, Ishikawa T, Kasuya Y, Kimura S, Kumagaye S, Nakajima K, Watanabe TX, Sakakibara S, Goto K and et al. (1988a) Primary structure, synthesis, and biological activity of rat endothelin, an endothelium-derived vasoconstrictor peptide. *Proc Natl Acad Sci U S A* **85**:6964-7.

Yanagisawa M, Kurihara H, Kimura S, Tomobe Y, Kobayashi M, Mitsui Y, Yazaki Y, Goto K and Masaki T (1988b) A novel potent vasoconstrictor peptide produced by vascular endothelial cells. *Nature* **332**:411-5.

Yoshimoto S, Ishizaki Y, Kurihara H, Sasaki T, Yoshizumi M, Yanagisawa M, Yazaki Y, Masaki T, Takakura K and Murota S (1990) Cerebral microvessel endothelium is producing endothelin. *Brain Res* **508**:283-5.

Zhang H, LeCulyse E, Liu L, Hu M, Matoney L, Zhu W and Yan B (1999) Rat pregnane X receptor: molecular cloning, tissue distribution, and xenobiotic regulation. *Arch Biochem Biophys* **368**:14-22.

Zhang W, Mojsilovic-Petrovic J, Andrade MF, Zhang H, Ball M and Stanimirovic DB (2003a) The expression and functional characterization of ABCG2 in brain endothelial cells and vessels. *Faseb J* **17**:2085-7.

Zhang W, Purchio A, Chen K, Burns SM, Contag CH and Contag PR (2003b) In vivo activation of the human CYP3A4 promoter in mouse liver and regulation by pregnane X receptors. *Biochem Pharmacol* **65**:1889-96.

Zhang Y, Han H, Elmquist WF and Miller DW (2000) Expression of various multidrug resistance-associated protein (MRP) homologues in brain microvessel endothelial cells. *Brain Res* **876**:148-53.

Zhang Y, Schuetz JD, Elmquist WF and Miller DW (2004a) Plasma Membrane Localization of Multidrug Resistance-Associated Protein (MRP) Homologues in Brain Capillary Endothelial Cells. *J Pharmacol Exp Ther*.

Zhang Z, Burch PE, Cooney AJ, Lanz RB, Pereira FA, Wu J, Gibbs RA, Weinstock G and Wheeler DA (2004b) Genomic analysis of the nuclear receptor family: new insights into structure, regulation, and evolution from the rat genome. *Genome Res* **14**:580-90.

Zhang Z, Wu JY, Hait WN and Yang JM (2004c) Regulation of the stability of P-glycoprotein by ubiquitination. *Mol Pharmacol* **66**:395-403.

Zlokovic BV and Apuzzo ML (1998) Strategies to circumvent vascular barriers of the central nervous system. *Neurosurgery* **43**:877-8.

Zlokovic BV, Mackic JB, Wang L, McComb JG and McDonough A (1993) Differential expression of Na,K-ATPase alpha and beta subunit isoforms at the blood-brain barrier and the choroid plexus. *J Biol Chem* **268**:8019-25.